Phytochemistry of natural polyamines and their analogues

Alnajadat, Rami

Award date:
2019

Awarding institution:
University of Bath

Phytochemistry of natural polyamines and their analogues

Rami Mahmood Alnajadat

A thesis submitted for the degree of Doctor of Philosophy

University of Bath

Department of Pharmacy and Pharmacology

October 2018

Signed ……

Date …….

ABSTRACT

Biofilm formation is a significant mechanism by which pathogens are able to evade the human immune system and to be unresponsive to antimicrobial treatments. Indeed, biofilm formation is a major contributor to antimicrobial resistance (AMR), a current and growing clinical problem around the world. Herein, the synthesis of linear and cyclic polyamines containing different spatial distances between the amino groups were designed on the basis of the chemical structures of certain naturally occurring polyamines. The complete reduction of aliphatic nitrile functional groups to primary amines can be performed via catalytic hydrogenation using Raney nickel catalyst under 1 atm pressure of hydrogen and in basic media. The NMR spectroscopic data of the synthesised polyamines that have not been fully assigned, or indeed are mis-assigned in the literature, were fully and typically unambiguously assigned. Then their biological activities in preventing biofilm formation and for the dispersal of existing biofilms, with and without combination with the antibiotic vancomycin, were investigated. Two novel polyamines **33** and **35** show activity in preventing biofilm formation in NCTC 6571 and MSSA 15981 strains. In the NCTC 6571 strain, each of these two polyamines shows high activity when used in combination with vancomycin achieving higher activity in the killing of bacterial cells inside preformed biofilms than the use of vancomycin alone. Polyamine **49** shows antibacterial activity and prevents biofilm formation in the above two *S. aureus* strains and in the MRSA 252 strain, and shows high activity in the killing of bacterial cells within preformed NCTC 6571 biofilms in combination with vancomycin. These results are a contribution to the fight against AMR. Whilst simple linear polyamines do not exhibit the biological activity some have claimed in this research area, these three polyamines **33**, **35**, and **49** certainly do show potential, at least in a bacterial strain dependent manner.

DEDICATION

For my Parents

ACKNOWLEDGEMENTS

I gratefully thank my parents and my family for their unlimited support all the way. Nothing could be achieved without their constant encouragement.

I sincerely thank my supervisors Dr. Ian S. Blagbrough and Dr. Albert Bolhuis for their advice, guidance, understanding, patience, kind encouragement and continuous support throughout my PhD.

I sincerely thank Al Isra University, Amman, Jordan, for funding my PhD scholarship. I also thank Catalent, Swindon, UK for generously funding the writing-up period.

My deep thanks to Prof. Mohammad Amin Mohammad (Al Isra University and later at the University of Bath) and Prof. Feras Q. Alali (Jordan University of Science and Technology, Jordan) for their support before and during my PhD.

I also thank all my laboratory colleagues in both 5W3.14 and 7W2.9 for their help and for the friendly working environment. I thank all the students in the PhD office for fun chats that made my time in Bath enjoyable. I thank Yuan Ji and Alexandria Holland for their help in microbiology experiments. I thank Dr. Ulrich Hintermair, Department of Chemistry, University of Bath, for his generous assistance. I also thank all the Technical Staff in the Department of Pharmacy and Pharmacology, University of Bath, for all their assistance.

ABBREVIATIONS

^{13}C-NMR	Carbon nuclear magnetic resonance
^{1}H-NMR	Proton nuclear magnetic resonance
Agr	Accessory gene regulatory
AHL	Acyl homoserine lactone
AIP	Autoinducing peptide
AMR	Anti-microbial resistance
br	Broad
c-di-AMP	Cyclic di-adenylate monophosphate
c-di-GMP	Cyclic dimeric guanosine monophosphate
CFU	Colony Forming Unit
CLSM	Confocal Laser Scanning Microscopy
dsDNA	double stranded DNA
EPS	Extracellular Polymeric Substance
eq	equivalent
ESI	electrospray ionisation
g	gram
HR TOF	High resolution time-of-flight
HRMS	High resolution mass spectrometry
HSQC-NMR	Heteronuclear single quantum correlation NMR
Hz	Hertz
IR	Infra-red
J	Coupling constant
M	molar (mole per litre)
m	multiplet

MHz	MegaHertz
mm	millimetre
mmol	millimole
MRSA	Meticillin-resistant *Staphylococcus aureus*
MSSA	Meticillin-sensitive *Staphylococcus aureus*
NCTC	National Collection of Type Cultures
NS	Norspermine
NSD	Norspermidine
O.D.	Optical density
PBS	Phosphate buffered saline
ppGpp	Guanosine tetraphosphate
ppm	parts per million
pppGpp	Guanosine pentaphosphate
q	quartet
QS	Quorum sensing
R_f	Retention factor
rpm	revolutions per minute
s	singlet
t	triplet
TLC	Thin layer chromatography
TSB	Tryptone soya broth
UV	Ultraviolet
v/v	volume/volume
v/v/v	volume/volume/volume
v/v/v/v	volume/volume/volume/volume
WHO	World Health Organization

CONTENTS

LIST OF FIGURES

Chapter 1

Chapter 2

Chapter 3

LIST OF TABLES

Chapter 2

Chapter 3

Chapter 1

Introduction

1.1 Introduction and Literature Review

Natural products have played important roles in treating and even in preventing diseases for thousands of years. The closely associated development of pharmacology is, in part, based on structural modification of lead molecules derived from natural products. Drugs developed from natural sources mainly come from plants and also from microorganisms, marine life, vertebrates and invertebrates.

Increasing bacterial resistance is creating a great challenge to global health (Tse et al., 2017). *Staphylococcus aureus* is a major cause of bacterial infections in the community and infections associated with health facilities (Archer and Climo, 2001). Patients infected with meticillin resistant *S. aureus* (MRSA) are estimated to have a 64% higher mortality rate than patients who are infected with the sensitive form of the bacteria, meticillin sensitive *S. aureus* (MSSA) (WHO, report 2018). This ever growing threat gives rise to the need to discover new strategies in the treatment of bacterial infections.

Bacterial cells live in two styles: as free planktonic cells and in aggregation clusters called biofilms. These aggregations were described in 1978 by Costerton as a glycocalyx film formed by bacteria that can stick to biotic surfaces such as teeth and lungs (Costerton et al., 1978). Biofilms are a major source of the problem of anti-microbial resistance (AMR) (Costerton et al., 1999), and about 80% of human bacterial infections are biofilm-related (Worthington et al., 2012; Barsoumian et al., 2015). Biofilms are multicellular communities of bacterial cells that are embedded in an

extracellular matrix of polymeric substances (Costerton et al., 1999). These extracellular polymeric substances (EPS) are generally composed of polysaccharides, proteins, and DNA (Oppenheimer-Shaanan et al., 2013). The matrix mass can represent more than 90% of the biofilm dry mass, while bacterial cells may represent less than 10% of the total weight (Flemming and Wingender, 2010).

In *Staphylococcal* biofilms, the extracellular matrix of polymeric substances may contain the polysaccharide β(1-6)-N-acetylglucosamine, proteins, and/or extracellular DNA (Arciola et al., 2015). The synthesis of this intercellular adhesion polysaccharide depends on the expression of the gene *ica*ADBC, the expression of which depends on environmental stimuli such as anaerobic conditions, high osmolality, and subinhibitory concentrations of antibiotics (Valle et al., 2003).

Enzymes secreted by bacteria supply bacterial cells with nutrients by digesting polymers which could be derived from e.g., dead cells, some of the EPS components or other nutrient sources that are trapped in the biofilm matrix. The hydrophilicity of exopolysaccharide components of the EPS can retain water within the biofilm. The presence of water channels provides bacterial cells deep in the biofilm with nutrients. Overall, the biofilm matrix represents a hydrated and nutrient rich environment for bacteria (Flemming and Wingender, 2010).

Several factors determine the composition of biofilms, including the type of bacteria forming the biofilm, the nature of the surface, nutrients, and temperature. This variation in EPS constituents affects biofilm response to external effects such as antibacterial agents (Naik et al., 2018; Wang et al., 2018). Therefore, it is important to

know accurately the constituents of a biofilm as this will significantly affect the methods and approaches by which biofilm disruptors can be designed.

Biofilms play an important role in the environment. For example, a defensive technique for some plants to protect themselves from pathogens is by biofilms formed *Bacillus subtilis* in soil. Biofilms could be found anywhere in the environment, like soil, industrial places, waste water pipes, medical devices, and teeth surfaces (Beauregard et al., 2013; Mack et al., 2006).

Biofilms are formed in three steps: attachment to a surface, formation of micro colonies, and maturation to biofilm (Boles and Horswill, 2011). Biofilms are formed initially by the adherence of planktonic bacteria to a surface. Bacterial cells can attach to biotic or abiotic surfaces or even form aggregations at liquid/air interfaces (Costerton et al., 1999; Tan and Darby, 2004). Then bacteria irreversibly attach to the surface. At this step bacteria cannot be washed off by gentle washing (Donlan, 2002). Hydrophobicity, smoothness of the surface, and quorum sensing (QS) play important roles in this step (Lv et al., 2014; Mack et al., 2006). Cell wall associated proteins are involved in the attachment of *Staphylococcus* bacteria to polymeric surfaces (Mack et al., 2006). The composition of bacterial cell surface and the medium properties significantly influence the attachment step (Donlan, 2002). Bacterial cells start to anchor to each other driven by changes in gene expression that are dependent on QS and the formation of primary colonies (Figure 1).

Biofilms mature by cell growth and division in different architectural forms that vary in roughness, shape, and degrees of porosity. This process is to some degree controlled by QS which is a phenomenon by which bacterial cells are able to communicate.

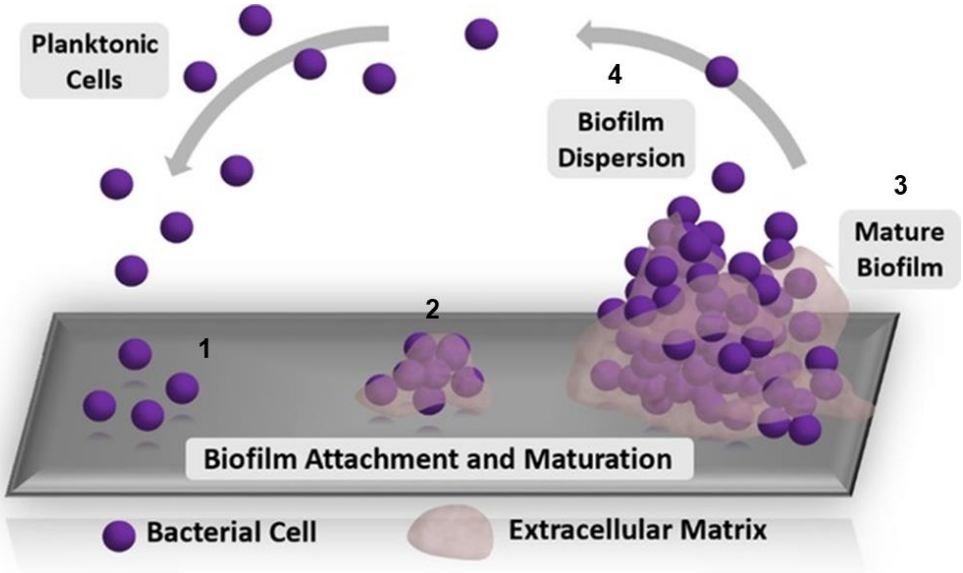

Figure 1: Stages of biofilm formation: 1. Free planktonic cells attach to a surface. 2. Under QS, bacterial cells start to anchor to each other forming small colonies and start to secrete EPS. 3. The biofilms mature by cell growth and division. 4. Biofilm may disperse allowing bacterial cells to form new biofilms. Adapted from Abouelhassan et al., 2017.

Bacterial cells produce signalling molecules that are used in cell-to-cell communication, e.g. peptides in *S. aureus* (Kavanaugh and Horswill, 2016). At low concentrations, these signalling molecules are inactive, but when the population of bacteria increases, the concentration of signalling molecules reaches a certain threshold and activates gene expression in bacterial cells leading to secretion of EPS. The EPS matrix protects bacterial cells against the immune system and antibacterial agents, and provides nutrients by trapping digestive enzymes within the biofilm which generates an external digestive system able to supply bacterial cells with essential nutrients. The presence of minerals, like calcium ions, strengthens biofilms by forming cross linking bridges between acidic groups of exopolysaccharides chains (Flemming and Wingender, 2010). Finally, biofilms may disperse allowing bacterial cells to move to other nutrient rich places and form new biofilms.

Biofilms and bacterial resistance. The presence of bacterial cells within the biofilm provides them with protection from antimicrobial agents and the human immune defence system, such as phagocytes and antibodies. Bacterial biofilms are very tolerant to the body's defence system and resist phagocytosis and antibiotics (Costerton et al., 1999; Mah and O'Toole, 2001).

Biofilms are up to 1000-times more resistant to antibiotics than planktonic cells (Hoiby et al., 2010), but resistance mechanisms such as modifying enzymes and target mutation are not specifically responsible for bacterial biofilm resistance. Three main hypothetical mechanisms by which biofilms resist antimicrobial agents have been proposed (Stewart and Costerton, 2001). The first hypothesis is that the biofilm matrix decreases antibiotic permeability into the biofilm. Positively charged antibiotics such as aminoglycosides may be adsorbed by negatively charged EPS leading to slower penetration of these antibiotics through a biofilm matrix. The second hypothesis is that the chemical environmental conditions inside the biofilm e.g., oxygen depletion and pH gradients inactivate some antibiotics. In anaerobic conditions, aminoglycosides are much less active against the same organism compared to under aerobic conditions (Stewart and Costerton, 2001). The third hypothesis is that some bacterial cells in biofilms differentiate into a spore-like or semi-dormant state. In this state, bacterial cells have a lower growth rate in the centre of the biofilm and are highly resistant to antibiotics which may explain the inactivity of antibiotics even if they reach high concentrations within the biofilm. Biofilms are involved in many serious infections e.g. cystic fibrosis, wound infections, and device-related infections such as valves and catheters (Donlan and Costerton, 2002; O'Neill et al., 2007; Percival et al., 2012). *S. aureus* and *S. epidermidis* are among the major causes of biofilm related infections

found clinically in Hickman catheters, central venous catheters, mechanical heart valves, vascular grafts, and orthopedic devices (Cha et al., 2013; Costerton et al., 1999). This, combined with the high level of resistance, makes biofilms a serious healthcare problem for which better solutions urgently need to be found.

Several compounds have been proposed and some tested for their ability to disrupt biofilms, mainly QS modifying molecules, amino acids, and polyamines (Bottcher et al., 2013; De la Fuente-Nunez et al., 2014; De la Fuente-Nunez et al., 2015; Hochbaum et al., 2011; Kavanaugh and Horswill, 2016; Kolodkin-Gal et al., 2010; Konai et al., 2015; Nesse et al., 2015; Oppenheimer-Shaanan et al., 2013; Ramon-Perez et al., 2015; Sarkar and Pires, 2015; Si et al., 2015; Wu et al., 2016). Different classes of biofilm-disrupting agents are discussed in more detail below.

Quorum sensing modifying molecules. Acyl homoserine lactones (AHLs) (Figure 2) are signalling molecules for QS in Gram negative bacteria. Modified AHL molecules were able to block QS in *P. aeruginosa* and thereby inhibit biofilm formation (Worthington et al., 2012). Several *Bacillus* species produce the enzyme acyl homoserine lactonase which hydrolyses AHL, preventing cell communication by QS in Gram negative bacteria and thus preventing biofilm formation (Oppenheimer-Shaanan et al., 2013). This approach is limited in its ability to prevent biofilm formation and it has limited effect on already formed biofilms. A second limitation for this method is that biofilm dispersion itself is thought to be a QS dependent process (Kavanaugh and Horswill, 2016; Yarwood et al., 2004) and therefore deactivation of QS could be unbeneficial. Hyper-activation of QS was proposed to disperse already (pre)formed biofilms (Oppenheimer-Shaanan et al., 2013).

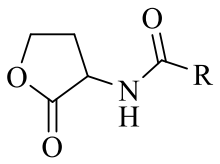

Figure 2: Acyl homoserine lactones (AHL), R: Alkyl chain.

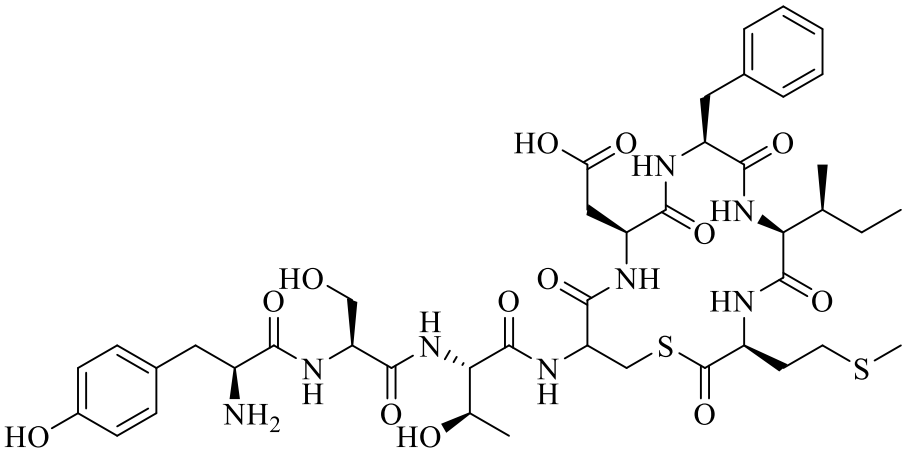

Figure 3: Autoinducing peptide type I (AIP-I).

Autoinducing peptides (AIPs) (Figure 3) are part of the QS system and regulate the secretion of matrix degrading enzymes by targeting accessory gene regulatory (*agr*) system in *S. aureus*. Via the *agr* system, AIPs activate multiple proteases and small pore-forming toxins leading to biofilm disassembly (Oppenheimer-Shaanan et al., 2013). AIPs and their derivatives are promising molecules in disrupting biofilms (Sakoulas, et al. 2003; Vuong et al., 2004). However, their specificity to certain bacterial strains may limit their activity.

The second messenger nucleotides guanosine tetraphosphate (ppGpp) and guanosine pentaphosphate (pppGpp) (Figure 4) are also involved in biofilm formation in e.g., *S. aureus* (De la Fuente-Nunez et al., 2014). D-Enantiomeric peptides were reported to inhibit biofilm formation and disperse existing biofilms by degrading (p)ppGpp second messengers (De la Fuente-Nunez et al., 2015). The second messenger cyclic dimeric

guanosine monophosphate (c-di-GMP) is an intracellular signalling molecule that regulates the conversion of bacterial cells from the planktonic into the biofilm state and vice versa (Ha et al., 2015). Biofilm formation is associated with a high level of c-di-GMP, while a low level of c-di-GMP is associated with the higher motility of different bacterial species (Simm, et al., 2004). Both second messengers, (p)ppGpp and (c-di-GMP), are involved in the regulation of biofilm formation and other functions such as virulence and quorum sensing (QS) (Gupta et al., 2015). The second messenger cyclic di-adenylate monophosphate (c-di-AMP) was recently reported to be involved in biofilm formation in certain bacterial species by increasing the production of the EPS (Peng et al., 2016; Townsley et al., 2018).

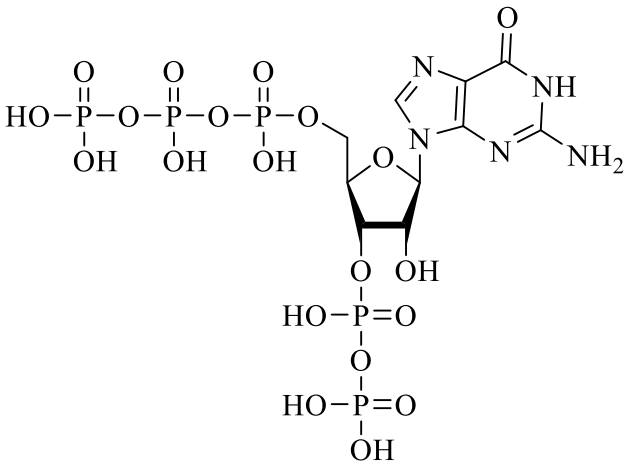

Figure 4: Guanosine pentaphosphate (pppGpp).

Amino acids. Amino acids are constituents of the peptidoglycans of Gram-positive cells, where a short peptide chain of amino acids is bound to the sugar polymer of the peptidoglycans. This peptide chain may play a role in cell-cell contact (Oppenheimer-Shaanan et al., 2013). Amyloid fibres are aggregates of protein that attach to the bacterial cell wall and strengthen the structural integrity of *B. subtilis* biofilms (Romero et al., 2011). This attachment can be interrupted by introducing noncanonical D-amino acids that may not be a part of the peptidoglycan's peptide chain amino acids leading to the prevention of biofilm maturation. Potentially this could disrupt

preformed biofilms in *B. subtilis* and prevent biofilm maturation in *S. aureus* (Hochbaum et al., 2011; Kolodkin-Gal et al., 2010). In contrast to these results of Kolodkin-Gal et al. (2010), recent studies show that D-amino acids do not inhibit biofilm formation in *S. aureus* or *B. subtilis* (Sarkar and Pires, 2015), but this may possibly be due to the different strains used in both studies.

Polyamines. Polyamines are found in high concentrations in cells, concentrations which increase in rapidly growing cells (Tabor and Tabor, 1984). Linear polyamines incorporate 1,3-diaminopropane **1** and 1,4-diaminobutane **2** (putrescine). They play vital functions in almost all life including plants, mammals, and bacteria (Cohen, 1998; Oshima, 2010). Norspermidine **3** (caldine, 3.3) and norspermine **6** (thermine, 3.3.3) were first discovered in *Thermus thermophilus* as part of the many elegant studies in naturally occurring polyamines by Professor Oshima (Oshima, 1975, Oshima, 1978). *T. thermophilus* is an extreme thermophile, an aerobic Gram negative bacterium that lives at high temperatures 47-85º C with optimum temperature for growth between 65º C and 72ºC (Oshima and Imahori, 1971, 1974). Several linear polyamines have been isolated from *T. thermophilus*, including homospermidine **5**, spermine **7**, thermospermine **8**, homospermine **9**, caldopentamine **10**, thermopent-amine **11**, homocaldopentamine **12**, caldohexamine **13**, and homocaldohexamine **14** (Figure 5). They can stabilize double stranded DNA (dsDNA) at high temperatures which is vital for the thermophilic life of such bacteria (Oshima, 1975; Oshima, 1978; Oshima, 1979; Oshima, 1983; Oshima, 2010; Oshima et al., 1987; Oshima and Imahori, 1971, 1974). Spermidine **4**, among other naturally occurring polyamines, works as a growth factor and regulates the synthesis of nucleic acids and proteins (Jansson et al., 2000; Yoshida et al., 2001). Longer and more complex polyamines can stabilize the structure of nucleic acids at high temperature (Terui et al., 2005).

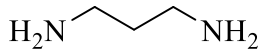

1

1,3-Diaminopropane 3

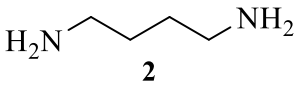

2

Putrescine 4

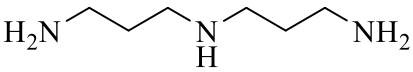

3

Norspermidine 3.3

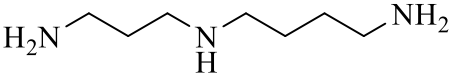

4

Spermidine 3.4

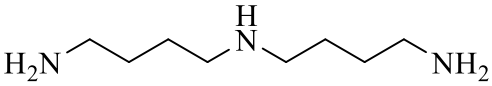

5

Homospermidine 4.4

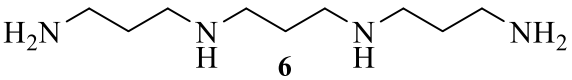

6

Norspermine (Thermine) 3.3.3

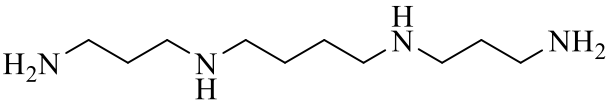

7

Spermine 3.4.3

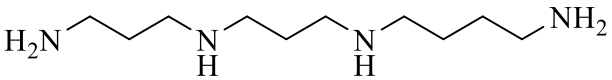

8

Thermospermine 3.3.4

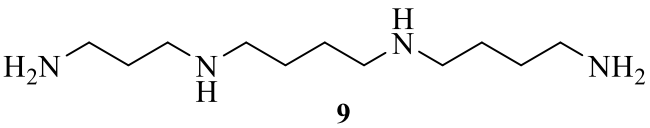

9

Homospermine 3.4.4

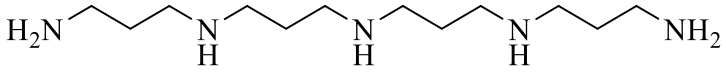

10

Caldopentamine 3.3.3.3

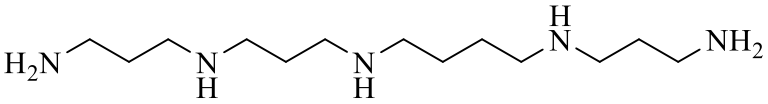

11

Thermopentamine 3.3.4.3

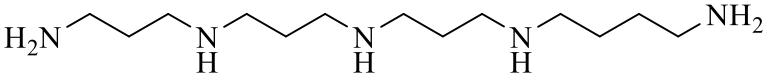

12

Homocaldopentamine 3.3.3.4

13

Caldohexamine 3.3.3.3.3

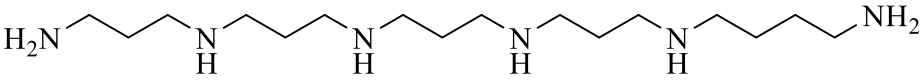

14

Homocaldohexamine 3.3.3.3.4

Figure 5: Polyamines isolated from *T. thermophilus*. The numbers after the polyamine names indicate the number of methylene groups between the amino groups.

The activity of polyamines against biofilms varies among bacterial strains. Spermidine was reported to inhibit biofilm formation in *Vibrio cholerae* (Karatan et al., 2005). Norspermidine was required for biofilm formation in *Vibrio cholerae* (Burrell, et al., 2010). These polyamines exert their different biological activities via multiple pathways including both QS and transport systems (Burrell et al., 2010; Karatan et al., 2005; McGinnis et al., 2009). In contrast, norspermidine and norspermidine-structurally related compounds (guanidine and biguanidine adducts) were reported to have a biofilm disrupting activity by preventing biofilm formation and dispersing existing biofilms in *B. subtilis* and *S. aureus* (Figure 6) (Bottcher et al., 2013; Oppenheimer-Shaanan et al., 2013), while spermidine or other polyamines were essential for biofilm formation in *B. subtilis* (Burrell et al., 2010). Recently, norspermidine was reported to have the ability to prevent biofilm formation in combination with copper ions (Lee et al., 2017). The exact mechanism of action of polyamines is still not fully understood.

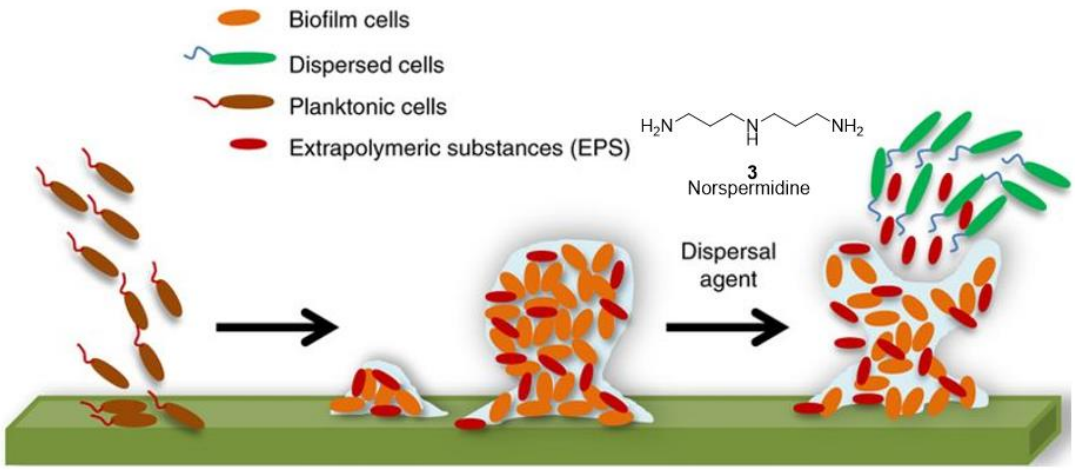

Figure 6: Certain polyamines, norspermidine and norspermine, have the ability to disperse existing biofilms liberating bacterial cells from within the biofilm matrix where they will be vulnerable to the body's defences (the immune system) and also become accessible to antibacterial agents. Adapted from Chua et al., 2015.

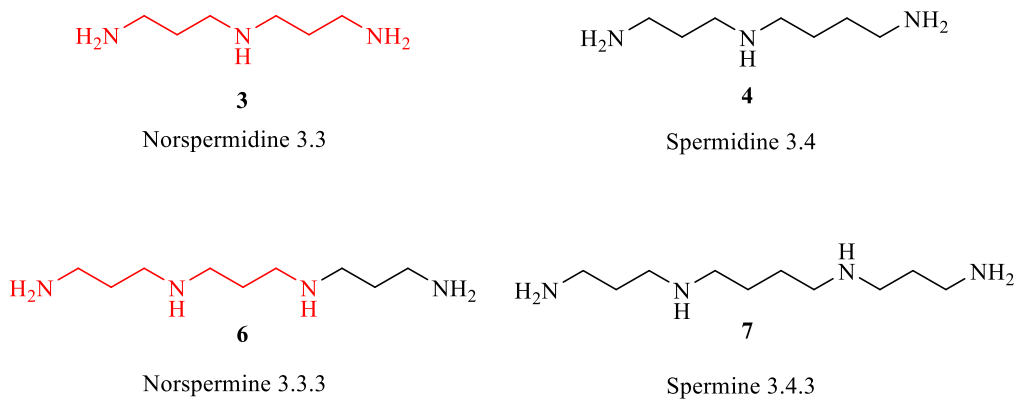

Figure 7: Some naturally occurring polyamines. The two compounds on the left, norspermidine and norspermine, have the common motif of two adjacent three methylene groups separated and flanked by three amino groups. The two compounds on the right, spermidine and spermine, do not have this motif.

The polyamines active against bacteria have a common component of two adjacent three methylene groups separated and flanked by three amino groups in their structure. Figure 7 shows the structure of four naturally occurring polyamines used in this study, where norspermidine (3.3) and norspermine (3.3.3) have a structural motif in common. Spermidine (3.4) and spermine (3.4.3) have an extra methylene group and so do not have the common motif in their structures. The numbers after the polyamine names indicate the number of methylene groups between the amino groups.

A hypothesis was suggested by Kolodkin-Gal et al. (2012) to explain the structure-activity relationship (SAR) of polyamines. However, it should be noted that this hypothesis was published in a *Cell* paper that has now been retracted. The authors of this paper claimed that norspermidine is biosynthesized by *B. subtilis* and is found in biofilms. In addition, they claimed that low concentrations of norspermidine inhibits biofilm formation in *B. subtilis* at concentration = 25 µM via an exopolysaccharide dependent pathway.

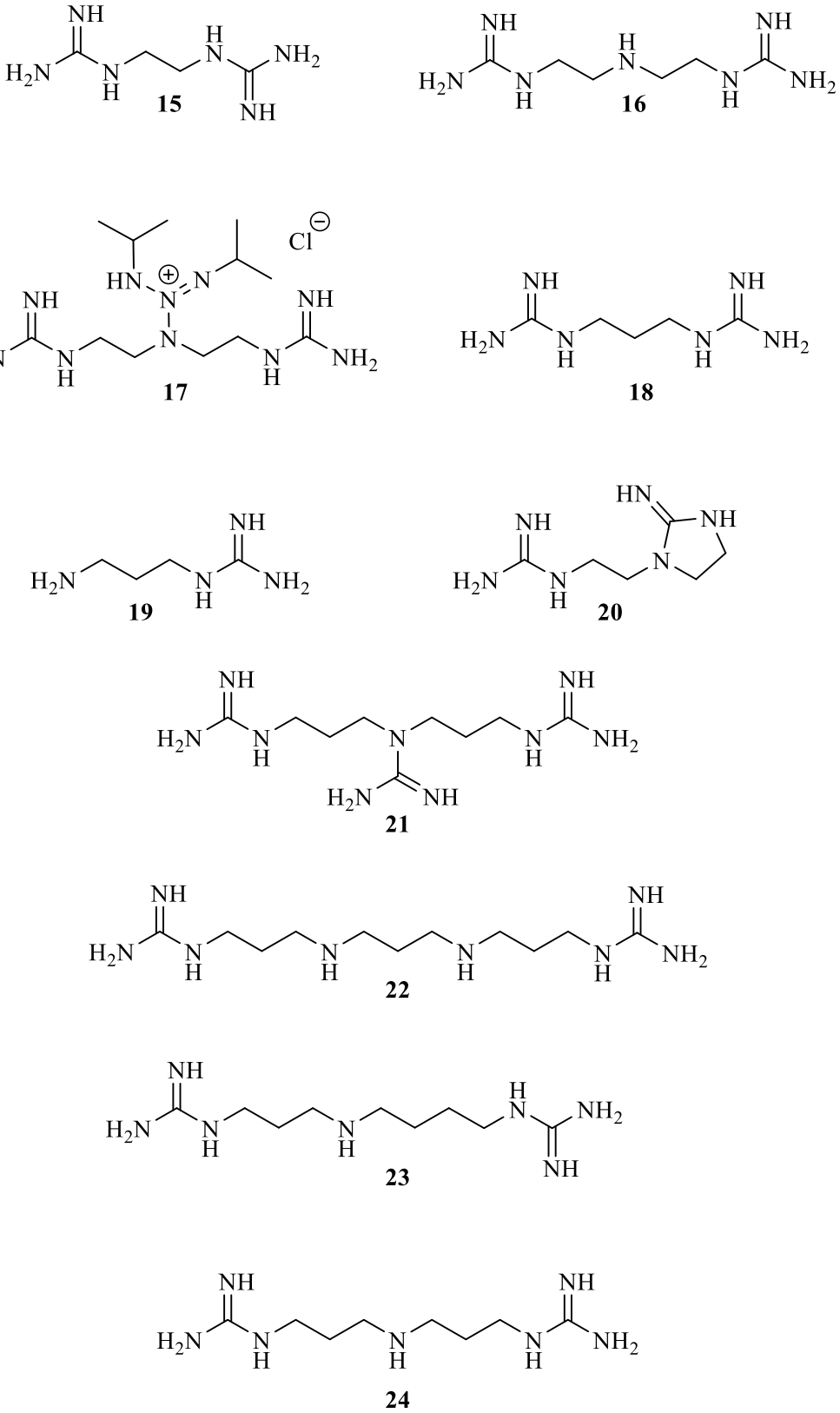

Figure 8: Some guanidine derivatives of polyamines.

It was also suggested by Kolodkin-Gal et al. that the positively charged amino groups of polyamines bind to negatively charged acidic (or neutral) groups of the exopolysaccharide, breaking hydrogen bonds between them and collapsing the exopolysaccharide network that holds the biofilm matrix together. Norspermidine (3.3) amino groups aligned well with the carboxyl groups of exopolysaccharide (or polar groups of neutral exopolysaccharide), while the spacing of the amino groups of spermidine (3.4) did not match the symmetric pattern. In contrast, another *Cell* paper reported that wild-type *B. subtilis* biofilms are norspermidine free throughout all the biofilm (Hobley et al., 2014). Moreover, the authors of this paper found that the activity of norspermidine depends on its concentration; at low concentrations up to 200 μM it promotes biofilm formation, but at higher concentrations norspermidine prevents biofilm formation via an exopolysaccharide independent pathway.

Kolodkin-Gal et al. also reported, in *J. Am. Chem. Soc*., that the activity of some polyamines and their guanidine (Figure 8) and biguanide adducts in inhibiting biofilm formation in *S. aureus* and *B. subtilis* generally increased at high protonation state in these compounds, while inactive compounds did not respond to changes in protonation (Bottcher et al., 2013). Indeed, both charge and the spacing between such positively charged functional groups affect biological activity. Understanding the SAR of polyamines will help to determine the active functional groups and the chemical structure of biologically active compounds, and thus the development of novel polyamines with anti-biofilm activity.

Norspermidine and a combination of norspermidine with silver ions were reported to disrupt and disinfect multispecies wastewater biofilms (Si et al., 2015; Wu et al., 2016). Among two naturally occurring polyamines (norspermidine, spermidine) and the two diamines, putrescine (1,4-diaminobutane) and cadaverine (1,5-diaminopentane), only norspermidine has the ability to inhibit biofilm formation in *S. epidermidis* (Ramon-Perez et al., 2015). However, not all polyamines are active against all bacterial strains, and those that are active demonstrate no clear mechanism of action. Some recent publications suggest that norspermidine acts by interfering with the QS process in bacteria (Cardile et al., 2017; Ou and Ling, 2017).

Biofilm disruption makes the bacterial cells more vulnerable to antimicrobial agents, thereby potentially breathing new life into old drugs. These research studies will have impact and economic significance in many countries, especially if an understanding is developed of how polyamines and their conjugates or analogues could be used in order to overcome biofilm formation and disperse existing biofilms. This may also work in combination with antimicrobial agents as coatings of medical devices, in wastewater treatment, and in industries which use microorganisms. It is therefore important that new medicines are discovered and developed better to treat biofilm related infections. Polyamines and especially novel polyamines are compounds with potential in preventing and dispersing existing biofilms, because they can be active on several bacterial species and display their biological activity even at low (μM) concentrations. Alone or in combination with antibiotics, polyamines could have the advantage to eradicate many serious infections where biofilms are involved in mediating resistance. Therefore, the design and synthesis of some analogues of naturally occurring polyamines has been undertaken.

1.2 Aims and Objectives

The aims of the research described in this thesis are to develop novel polyamines that can prevent biofilm formation and/or disrupt existing biofilms which will be of great importance for the treatment of bacterial infections. Such biofilm disruption will enhance the conventional activity of antibiotics against bacteria in pre-formed biofilms. A combination of antibiotics and polyamines together in a novel formulation could demonstrate exceptional synergistic activity in the therapy of bacterial infections. The mechanisms of action of polyamines against biofilms will also be investigated.

These aims will be achieved by means of the following objectives:

- Target polyamines will be synthesized by reacting selected natural polyamines with paraformaldehyde to form hexahydropyrimidines. These products will then be elongated with three carbons and amino groups by reacting with acrylonitrile followed by reduction of the nitrile groups to primary amines.
- The activity of target products to prevent biofilm formation and disperse existing biofilms will be tested against three *S. aureus* strains using crystal violet and Miles-Misra assays.
- The activity of target products to prevent biofilm formation and disperse existing biofilms in combination with the antibiotic vancomycin will be tested and assayed using confocal laser scanning microscopy.
- The mechanisms of action will be investigated by testing the effects of micro-biologically active polyamines on bacterial growth and bacterial attachment.

References (in the style of *Phytochemistry*)

Abouelhassan, Y., Basak, A., Yousaf, H., Huigens, R. W. 3rd., 2017. Identification of N-arylated NH125 analogues as rapid eradicating agents against MRSA persister cells and potent biofilm Killers of gram-positive pathogens. Chembiochem. 18, 352-357.

Archer, G. L., Climo, M. W., 2001. *Staphylococcus aureus* bacteremia-consider of source. N. Engl. J. Med. 344, 55-56.

Arciola, C. R., Campoccia, D., Ravaioli, S., Montanaro, L. 2015. Polysaccharide intercellular adhesin in biofilm: structural and regulatory aspects. Front. Cell. Infect. Microbiol. 5: 7.

Barsoumian, A. E., Mende, K., Sanchez, C. J.,Beckius, M. L., Wenke, J. C., Murray, C. K., Akers, K. S., 2015. Clinical infectious outcomes associated with biofilm-related bacterial infections: a retrospective chart review. BMC Infect. Dis. 15:223

Beauregard, P. B., Chai, Y., Vlamakis, H., Losick, R., Kolter, R., 2013. *Bacillus subtilis* biofilm induction by plant polysaccharides. Proc. Natl. Acad. Sci. U S A 110, E1621-1630.

Boles, B. R., Horswill, A. R., 2011. *Staphylococcal* biofilm disassembly. Trends Microbiol. 19, 449-455.

Bottcher, T., Kolodkin-Gal, I., Kolter, R., Losick, R., Clardy, J., 2013. Synthesis and activity of biomimetic biofilm disruptors. J. Am. Chem. Soc. 135, 2927-2930.

Burrell, M., Hanfrey, C. C., Murray, E. J., Stanley-Wall, N. R., Michael, A. J., 2010. Evolution and multiplicity of arginine decarboxylases in polyamine biosynthesis and essential role in *Bacillus subtilis* biofilm formation. J. Biol. Chem. 285, 39224-39238.

Cardile, A. P., Woodbury, R. L., Sanchez, C. J., Becerra, S. C., Garcia, R. A., Mende, K., Wenke, J. C., Akers, K. S., 2017. Activity of norspermidine on bacterial biofilms of multidrug-resistant clinical isolates associated with persistent extremity wound infections. Adv. Exp. Med. Biol. 973, 53-70.

Cha, J. O., Yoo, J. I., Yoo, J. S., Chung, H. S., Park, S. H., Kim, H. S., Lee, Y. S., Chung, G. T., 2013. Investigation of biofilm formation and its association with the molecular and

clinical characteristics of methicillin-resistant *Staphylococcus aureus*. Osong. Public Health Res. Perspect. 4, 225-232.

Chua, S. L., Hultqvist, L. D., Yuan, M., Rybtke, M., Nielsen, T. E., Givskov, M., Tolker-Nielsen, T., Yang, L., 2015. In vitro and in vivo generation and characterization of *Pseudomonas aeruginosa* biofilm-dispersed cells via c-di-GMP manipulationNat. Protoc. 10,1165-1180.

Cohen, S. S., 1998. A guide to the polyamines. Oxford University Press, New York.

Costerton, J. W., Geesey, G. G., Cheng, K. J., 1978. How bacteria stick. Sci. Am. 238, 86-95.

Costerton, J. W., Stewart, P. S., Greenberg, E. P., 1999. Bacterial biofilms: A common cause of persistent infections. Science 284, 1318-1322.

De la Fuente-Nunez, C., Reffuveille, F., Haney, E. F., Straus, S. K., Hancock, R. E., 2014. Broad-spectrum anti-biofilm peptide that targets a cellular stress response. PLOS Pathog. 10, e1004152.

De la Fuente-Nunez, C., Reffuveille, F., Mansour, S. C., Reckseidler-Zenteno, S. L., Hernandez, D., Brackman, G., Coenye, T., Hancock, R. E., 2015. D-enantiomeric peptides that eradicate wild-type and multidrug-resistant biofilms and protect against lethal *pseudomonas aeruginosa* infections. Chem. Biol. 22, 196-205.

Donlan, R. M., 2002. Biofilms: Microbial life on surfaces. Emerg. Infect. Dis. 8, 881-890.

Donlan, R. M., Costerton, J. W., 2002. Biofilms: Survival mechanisms of clinically relevant microorganisms. Clin. Microbiol. Rev. 15, 167-193.

Flemming, H. C., Wingender, J., 2010. The biofilm matrix. Nat. Rev. Microbiol. 8, 623-633.

Hobley, L., Kim, S. H., Maezato, Y., Wyllie, S., Fairlamb, A. H., Stanley-Wall, N. R., Michael, A. J., 2014. Norspermidine is not a self-produced trigger for biofilm disassembly. Cell 156, 844-854.

Ha, D. G., O'Toole, G. A., 2015. c-di-GMP and its effects on biofilm formation and dispersion: a *Pseudomonas aeruginosa* review. Microbiol. Spectr. 3: 2.

Hochbaum, A. I., Kolodkin-Gal, I., Foulston, L., Kolter, R., Aizenberg, J., Losick, R., 2011. Inhibitory effects of D-amino acids on *Staphylococcus aureus* biofilm development. J. Bacteriol. 193, 5616-5622.

Hoiby, N., Bjarnsholt, T., Givskov, M., Molin, S., Ciofu, O., 2010. Antibiotic resistance of bacterial biofilms. Int. J. Antimicrob. Agents. 35, 322-332.

Gupta, K. R., Kasetty S., Chatterji D., 2015. Novel functions of (p)ppGpp and cyclic di-GMP in mycobacterial physiology revealed by phenotype microarray analysis of wild-type and isogenic strains of *Mycobacterium smegmatis* Appl. Environ. Microbiol. 81: 7.

Jansson, B. P., Malandrin, L., Johansson, H. E., 2000. Cell cycle arrest in archaea by the hypusination inhibitor n(1)-guanyl-1,7-diaminoheptane. J Bacteriol 182, 1158-1161.

Karatan, E., Duncan, T. R., Watnick, P. I., 2005. Nsps, a predicted polyamine sensor, mediates activation of vibrio cholerae biofilm formation by norspermidine. J. Bacteriol. 187, 7434-7443.

Kavanaugh, J. S., Horswill, A. R., 2016. Impact of environmental cues on *Staphylococcal* quorum sensing and biofilm development. J. Biol. Chem. 291, 12556-12564.

Kolodkin-Gal, I., Cao, S., Chai, L., Bottcher, T., Kolter, R., Clardy, J., Losick, R., 2012. A self-produced trigger for biofilm disassembly that targets exopolysaccharide. Cell 149, 684-692.

Kolodkin-Gal, I., Romero, D., Cao, S., Clardy, J., Kolter, R., Losick, R., 2010. D-Amino acids trigger biofilm disassembly. Science 328, 627-629.

Konai, M. M., Adhikary, U., Samaddar, S., Ghosh, C., Haldar, J., 2015. Structure-activity relationship of amino acid tunable lipidated norspermidine conjugates: Disrupting biofilms with potent activity against bacterial persisters. Bioconjug. Chem. 26, 2442-2453.

Lee, H. J., Seo, J., Kim, M. S., Lee, C., 2017. Inactivation of biofilms on ro membranes by copper ion in combination with norspermidine. Desalination 424, 95-101.

Lv, J., Wang, Y., Zhong, C., Li, Y., Hao, W., Zhu, J., 2014. The microbial attachment potential and quorum sensing measurement of aerobic granular activated sludge and flocculent activated sludge. Bioresour. Technol. 151, 291-296.

Mack, D., Rohde, H., Harris, L. G., Davies, A. P., Horstkotte, M. A., Knobloch, J. K. M., 2006. Biofilm formation in medical device-related infection. Int. J. Artif. Organs 29, 343-359.

Mah, T.-F. C., O'Toole, G. A., 2001. Mechanisms of biofilm resistance to antimicrobial agents. Trends Microbiol. 9, 34-39.

McGinnis, M. W., Parker, Z. M., Walter, N. E., Rutkovsky, A. C., Cartaya-Marin, C., Karatan, E., 2009. Spermidine regulates *Vibrio cholerae* biofilm formation via transport and signaling pathways. FEMS Microbiol. Lett. 299, 166-174.

Naik, M. M., Naik, S. P., Dubey, S. K., Bhat, C., Charya, L. S., 2018. Enhanced exopolysaccharide production and biofilm forming ability in methicillin resistant *Staphylococcus sciuri* isolated from dairy in response to acyl homoserine lactone (AHL). J. Food Sci. Technol. 55, 2087-2094.

Nesse, L. L., Berg, K., Vestby, L. K., 2015. Effects of norspermidine and spermidine on biofilm formation by potentially pathogenic *Escherichia coli* and *Salmonella enterica* wild-type strains. Appl. Environ. Microbiol. 81, 2226-2232.

O'Neill, E., Pozzi, C., Houston, P., Smyth, D., Humphreys, H., Robinson, D. A., O'Gara, J. P., 2007. Association between methicillin susceptibility and biofilm regulation in *Staphylococcus aureus* isolates from device-related infections. J. Clin. Microbiol. 45, 1379-1388.

Oppenheimer-Shaanan, Y., Steinberg, N., Kolodkin-Gal, I., 2013. Small molecules are natural triggers for the disassembly of biofilms. Trends Microbiol. 21, 594-601.

Oshima, T., 1975. Thermine: A new polyamine from an extreme thermophile. Biochim. Biophys. Res. Commun. 63, 1093-1098.

Oshima, T., 1978. Novel polyamines of extremely thermophilic bacteria. In: Friedman, S. M. (Ed.), Biochemistry of thermophily. Academic Press, pp. 211-220.

Oshima, T., 1979. A new polyamine, thermospermine, 1,12-diamino-4,8-diazadodecane, from an extreme thermophile. J. Biol. Chem. 254, 8720-8722.

Oshima, T., 1983. Novel polyamines in *Thermus thermophilus*: Isolation, identification, and chemical synthesis. Methods in enzymology, vol. 94. Academic Press, pp. 401-411.

Oshima, T., 2010. Enigmas of biosyntheses of unusual polyamines in an extreme thermophile, *thermus thermophilus*. Plant Physiol. Biochem. 48, 521-526.

Oshima, T., Hamasaki, N., Senshu, M., Kakinuma, K., Kuwajima, I., 1987. A new naturally occurring polyamine containing a quaternary ammonium nitrogen. J. Biol. Chem. 262, 11979-11981.

Oshima, T., Imahori, K., 1971. Isolation of an extreme thermophile and thermostability of its transfer ribonucleic acid and ribosomes. J. Gen. Appl. Microbiol. 17, 513-517.

Oshima, T., Imahori, K., 1974. Description of *Thermus thermophilus* (Yoshida and Oshima) comb. nov., a nonsporulating thermophilic bacterium from a Japanese thermal spa. Int. J. Syst. Bacteriol. 24, 102-112.

Ou, M. Z., Ling, J. Q., 2017. Norspermidine changes the basic structure of *S. mutans* biofilm. Mol. Med. Rep. 15, 210-220.

Peng, X., Zhang, Y., Bai, G., Zhou, X., Wu, H.,2016. Cyclic di-AMP mediates biofilm formation. Mol**.** Microbiol. **99,** 945-59.

Percival, S. L., Hill, K. E., Williams, D. W., Hooper, S. J., Thomas, D. W., Costerton, J. W., 2012. A review of the scientific evidence for biofilms in wounds. Wound Repair Regen. 20, 647-657.

Ramon-Perez, M. L., Diaz-Cedillo, F., Contreras-Rodriguez, A., Betanzos-Cabrera, G., Peralta, H., Rodriguez-Martinez, S., Cancino-Diaz, M. E., Jan-Roblero, J., Cancino Diaz, J. C., 2015. Different sensitivity levels to norspermidine on biofilm formation in clinical and commensal *Staphylococcus epidermidis* strains. Microb. Pathog. 79, 8-16.

Romero, D., Vlamakis, H., Losick, R., Kolter, R., 2011. An accessory protein required for anchoring and assembly of amyloid fibres in *B. subtilis* biofilms. Mol. Microbiol. 80, 1155-1168.

Sakoulas, G., Eliopoulos, G. M., Moellering, Jr. R. C., Novick, R. P., Venkataraman, L., Wennersten, C., DeGirolami, P. C., Schwaber, M. J., Gold, H. S. 2003. *Staphylococcus*

aureus accessory gene regulator (*agr*) group II: Is there a relationship to the development of intermediate-level glycopeptide resistance? J. Infect. Dis. 187, 929-938.

Sarkar, S., Pires, M. M., 2015. D-amino acids do not inhibit biofilm formation in *Staphylococcus aureus*. PLoS One 10, e0117613.

Si, X., Quan, X., Wu, Y., 2015. A small-molecule norspermidine and norspermidine-hosting polyelectrolyte coatings inhibit biofilm formation by multi-species wastewater culture. Appl. Microbiol. Biotechnol. 99, 10861-10870.

Stewart, P. S., Costerton, J. W., 2001. Antibiotic resistance of bacteria in biofilms. Lancet 358, 135-138.

Tabor, C. W., Tabor, H., 1984. Polyamines. Annu. Rev. Biochem. 53, 749-790.

Tan, L., Darby, C., 2004. A movable surface: Formation of *Yersinia* sp. biofilms on motile *Caenorhabditis elegans*. J. Bacteriol. 186, 5087-5092.

Terui, Y., Ohnuma, M., Hiraga, K., Kawashima, E., Oshima, T., 2005. Stabilization of nucleic acids by unusual polyamines produced by an extreme thermophile, *Thermus thermophilus*. Biochem. J. 388, 427-433.

Townsley, L., Yannarell, S. M., Huynh, T. N., Woodward, J. J., Shank, E. A. 2018. Cyclic di-AMP acts as an extracellular signal that impacts *Bacillus subtilis* biofilm formation and plant attachment. MBio. 9: 18.

Tse, B. N., Adalja, A. A., Houchens, C., Larsen, J., Inglesby, T. V., Hatchett, R., 2017. Challenges and opportunities of nontraditional approaches to treating bacterial infections. Clin. Infect. Dis. 56, 495-500.

Valle, J., Toledo-Arana, A., Berasain, C., Ghigo, J. M., Amorena, B., Penadés, J. R., Lasa, I. 2003. SarA and not sigmaB is essential for biofilm development by *Staphylococcus aureus*. Mol. Microbiol. 48, 1075-1087.

Vuong, C., Dürr, M., Carmody, A. B., Peschel, A., Klebanoff, S. J., Otto, M., 2004. Regulated expression of pathogen-associated molecular pattern molecules in *Staphylococcus*

epidermidis: quorum-sensing determines pro-inflammatory capacity and production of phenol-soluble modulins. Cell. Microbiol. 6, 753-759.

Wang, L. F., Li, Y., Wang, L. , Zhang, H. J., Zhu, M. J., Zhang, P. S., Zhu, X. X., 2018. Extracellular polymeric substances affect the response of multi-species biofilms in the presence of sulfamethizole. Environ. Pollut. 235, 283-292.

World Health Organization, 2018. Antimicrobial resistance. Accessed 3 September 2018. http://www.who.int/en/news-room/fact-sheets/detail/antimicrobial-resistance

Worthington, R. J., Richards, J. J., Melander, C., 2012. Small molecule control of bacterial biofilms. Org. Biomol. Chem. 10, 7457-7474.

Wu, Y., Quan, X., Si, X., Wang, X., 2016. A small molecule norspermidine in combination with silver ion enhances dispersal and disinfection of multi-species wastewater biofilms. Appl. Microbiol. Biotechnol. 100, 5619-5629.

Yarwood, J. M., Bartels, D. J., Volper, E. M., Greenberg, E. P., 2004. Quorum sensing in *Staphylococcus aureus* biofilms. J. Bacteriol. 186, 1838-1850.

Yoshida, M., Kashiwagi, K., Kawai, G., Ishihama, A., Igarashi, K., 2001. Polyamine enhancement of the synthesis of adenylate cyclase at the translational level and the consequential stimulation of the synthesis of the RNA polymerase sigma 28 subunit. J. Biol. Chem. 276, 16289-16295.

Chapter 2

Medicinal chemistry of polyamines

2.1 Introduction

As highlighted in Chapter 1, polyamines can prevent biofilm formation and disperse existing biofilms in some bacterial strains. In order to design novel compounds, four naturally occurring polyamines, spermidine (**4**, 3.4), spermine (**7**, 3.4.3), norspermidine (**3**, 3.3), and norspermine (**6**, 3.3.3), were selected as starting materials. They vary in the number of amino groups and the distance between the amino groups.

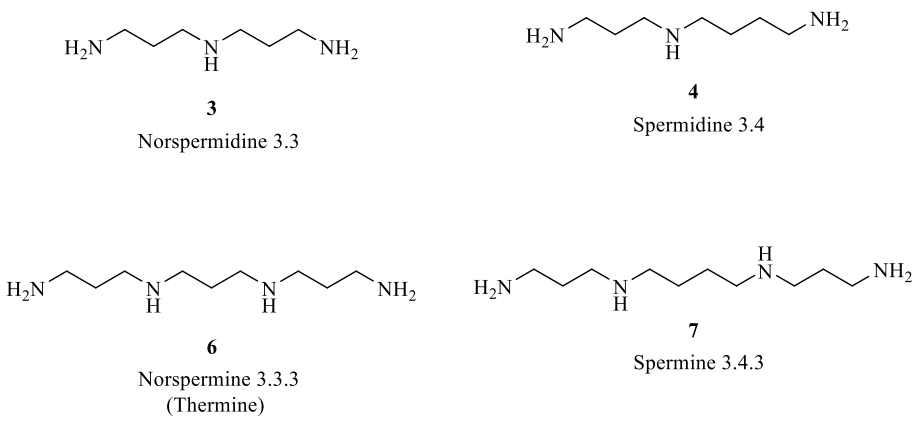

Figure 1: Homologous naturally occurring polyamines.

Norspermine (thermine) **6** and norspermidine **3** have three methylene groups between each amino group. This will make the linear distance between each two amino groups three-carbon atoms as methylene groups. In comparison, spermine **7** and spermidine **4** have an extra methylene group, which will increase the linear distance between some amino groups. Spermine **7** and norspermine **6** have four amino groups, but spermidine **4** and norspermidine **3** have three amino groups in their chemical structures. This will therefore increase the number of positive charges that spermine and norspermine bear under the physiological range of pH likely to be present in biofilms (Figure 1).

2.2 Design and synthesis of analogues of naturally occurring polyamines

Two factors were central in the polyamine compounds designed in this thesis: the first was to add more amine groups, the second was making the charge spacing between certain amino groups, in an extended conformation, to be three methylenes. The difference between norspermidine and spermidine is an additional methylene group in the latter, and so spermidine potentially has a longer distance between amine groups, while norspermidine has a three methylene bridge between each two amine groups,. Spermine potentially has a longer distance between amine groups, while norspermine has a three methylene bridge between each two amine groups. However, spermidine can rearrange by free rotation of C-C bonds to have the same distance between the amino groups as found in norspermidine (Figure 2) although conformational analysis of these highly flexible linear polyamines is virtually unprecedented (Haworth et al., 1991; Menger and D'Angelo, 1991; Maruyoshi et al., 2004).

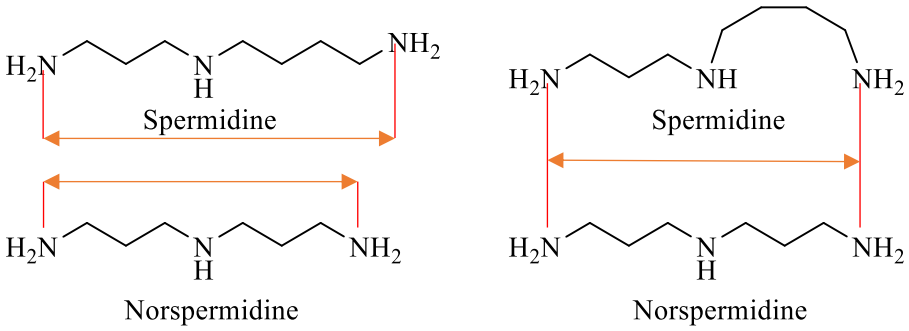

Figure 2: Spermidine can freely rotate (conformational isomerism) to have the same distance between the amino groups as is found in norspermidine.

The second factor in the designed compounds was the number of amine groups. Additional positive charges on polyamines were reported to increase the activity of polyamines in preventing biofilm formation (Bottcher et al., 2013). The designed polyamines have additional amino groups with three methylene spacers between these amino groups which might give them more anti-biofilm activity.

2.3 Results and discussion

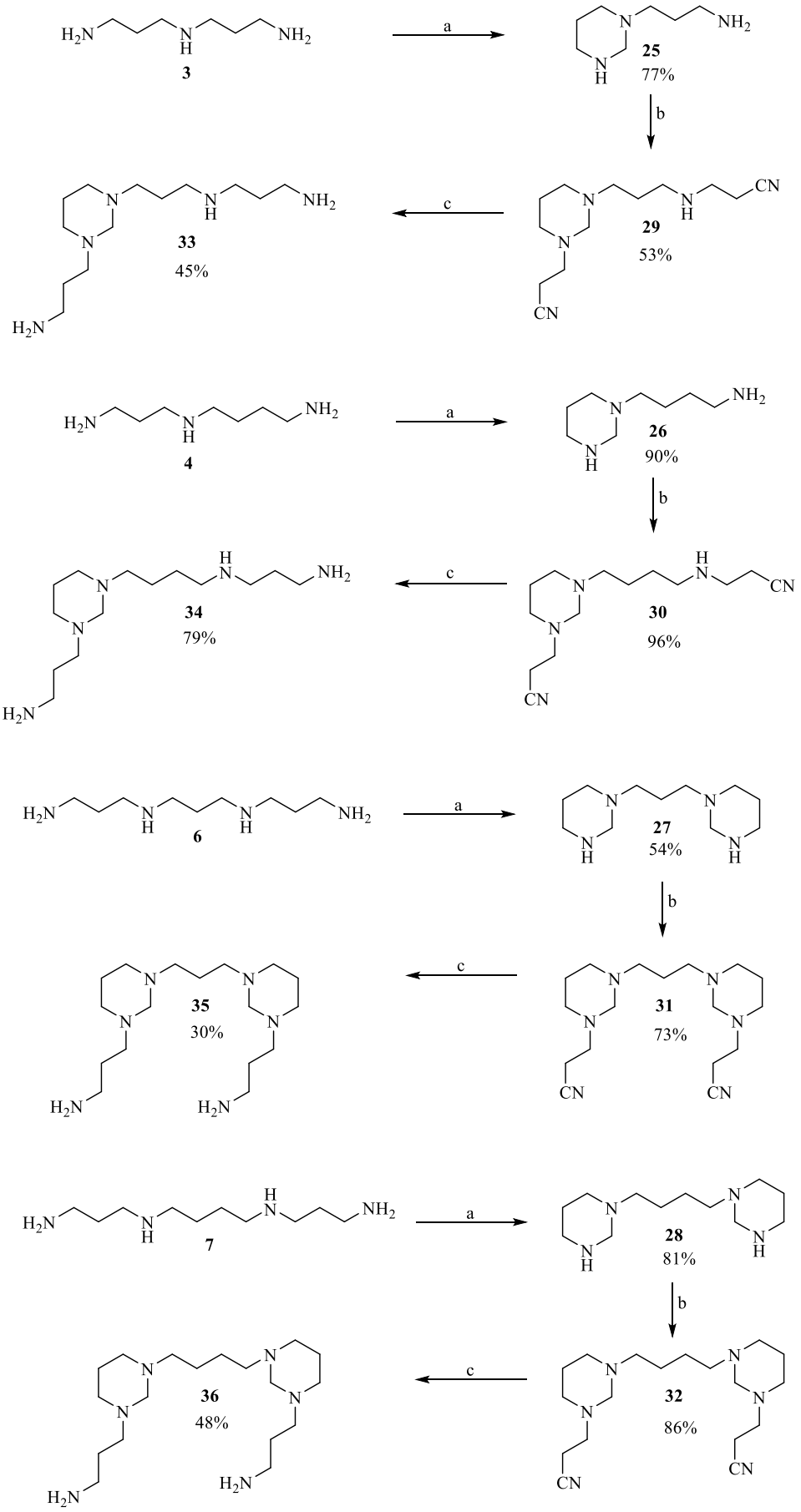

Figure 3: Synthetic scheme of **33-36** from norspermidine **3,** spermidine **4**, norspermine **6** and spermine **7**, respectively. Reagents and conditions: (a) (i) H_2O, cooling to 5°C, (ii) paraformaldehyde, 1 h; (b) (i) acrylonitrile, N_2, anhydrous methanol, 15 h, (ii) acrylonitrile, N_2, 9 h; (c) ethanol 95%, NaOH, H_2 20 bar, Raney nickel, 20 h.

The cyclic hexahydropyrimidine adducts **25-28** (Figure 3) were synthesised by the addition of solid paraformaldehyde to a cold aqueous solution of the starting polyamine (Ganem, 1982). This reaction is an example of a Mannich reaction where the formation of a Schiff base on one the primary amino groups is followed by a nucleophilic attack of another amino group on the formed Schiff base and the formation of a cycle. The reaction favours the formation of the stable six membered ring (Figure 4).

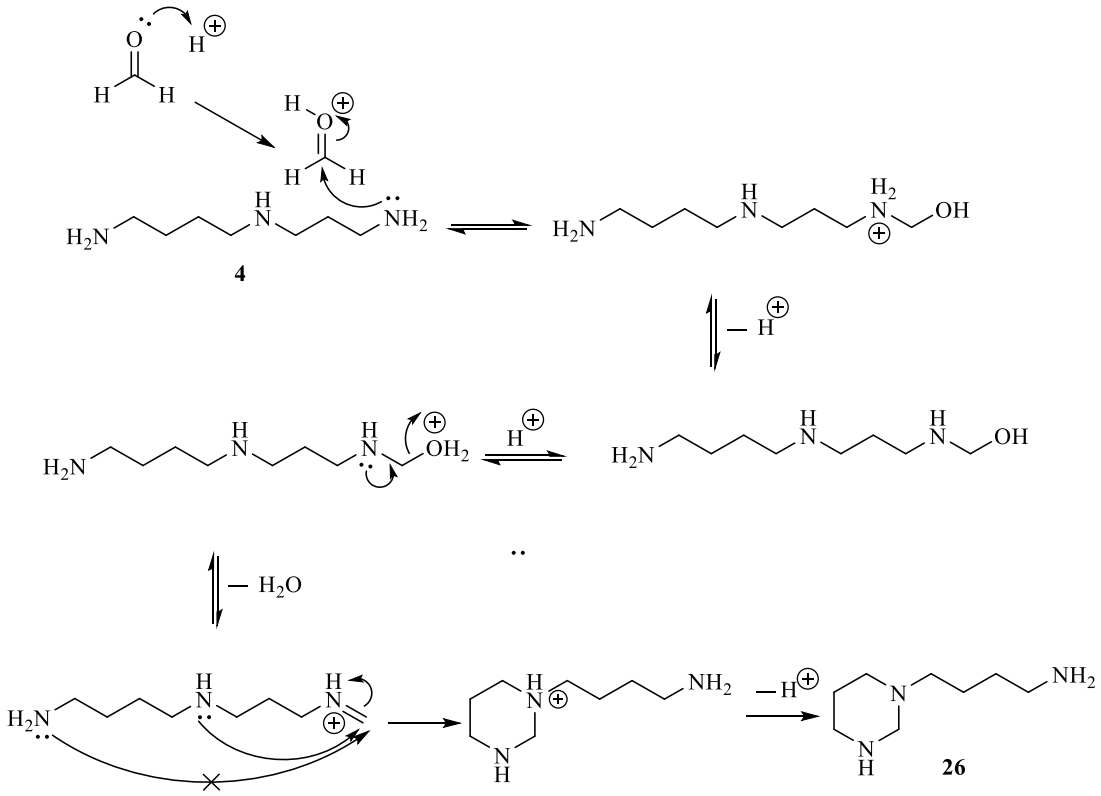

Figure 4: Reaction mechanism for synthesis of **26**.

The product of this reaction is obtained from the aqueous reaction mixture by thoroughly extracting with chloroform. However, the high polarity of such polyamine products often decreases the isolated yield. This low yield was overcome by saturating the reaction mixture with sodium hydroxide until an oily layer of the product appeared. The product layer was removed and the reaction mixture was thoroughly extracted with chloroform. This process increased the isolated yield up to 90% for compound **26**. The yields for compounds **25**-**28** were 77%, 90%, 54%, and 81% respectively.

The potential for free rotation about bonds in a linear polyamine chain prompted the design of conformationally restricted targets by incorporating two neighbouring amines into a hexahydropyrimidine. The addition of more amino groups separated by three methylene bridges to the hexahydropyrimidines was obtained by the 1,4-Michael addition of two equivalents of acrylonitrile to the hexahydropyrimidine adducts **25**-**28** to form **29**-**32**, respectively. This reaction did not always go to completion. Therefore, more acrylonitrile was added to the reaction mixture in order to achieve the desired products **29**-**32** having reacted with two equivalents of acrylonitrile. The yields for compounds **29**-**32** were 53%, 96%, 73%, and 86% respectively. None of these nitrile products has been previously reported except compound **29**. The spectral data obtained for compound **29** are in agreement with those reported (Frydman et al., 2004) except that $[M + H]^+$ is 250 not 249. Compound **29** has the chemical formula $C_{13}H_{23}N_5$. So, the required mass for $[M+H]^+$ which has the chemical formula $C_{13}H_{24}N_5$ is equal to 250.2032. Frydman et al. (2004) reported the mass for $[M+H]^+ = 249$ for this compound. Our result shows the observed mass for $[M+H]^+$ to be 250.2046 which is in agreement with the required value.

In order to reduce nitrile compounds **29-32** to their corresponding target polyamines **33-36** (Figure 3), several methods were tried. Firstly, catalytic hydrogenation using palladium. Palladium on carbon (Pd/C) is reported to reduce nitrile groups (Vilches-Herrera et al., 2014). Catalytic hydrogenation using a hydrogen balloon as a hydrogen source and Pd/C (10%) as a catalyst in order to reduce compound **29** to **33** has been tried, but there was no reaction. TLC analysis showed a major spot of the starting material and several minor spots which could be from partial reduction. Replacing Pd/C with Pearlman's catalyst (palladium hydroxide 20% on activated charcoal) gave the same result as the previous reaction. Increasing the hydrogen pressure to 20 bar resulted in a mixture of several products which could not be purified to homogeneity.

A mild procedure to reduce nitrile groups to amines was reported using potassium borohydride (KBH_4) as a reducing agent, Raney nickel as a catalyst and ethanol as a solvent (Wu et al., 2008). TLC analysis of the reaction following this procedure showed a major spot of the starting material and a few minor spots, possibly for partially reduced products. Lithium aluminium hydride ($LiAlH_4$) has been reported to reduce some nitrile groups to primary amines (Bagal and Bhanage, 2015). Compound **29** was dissolved in anhydrous tetrahydrofuran and added dropwise to $LiAlH_4$ in anhydrous tetrahydrofuran heated under reflux. After quenching with saturated aqueous Na_2SO_4 and then neutralising with dilute sulfuric acid, the product was extracted with ether. In the experiments using $LiAlH_4$, the starting material disappeared, but the product could not be extracted from the reaction mixture. Apparently, the amine product formed complexes with the metallic ions of lithium and / or aluminium in the reaction mixture. Another system has been published for reducing nitrile groups to primary amines by transfer hydrogenation using isopropanol as a hydrogen donor and a solvent and Raney

nickel as a catalyst (Mebane et al., 2003). Following this method, reactions showed the presence of a mixture of several products.

In 2004, Frydman et al. reported that using ammonia as a co-catalyst with Raney nickel reduced the amount of secondary amine by-products in the reduction of nitriles to primary amines (Frydman et al., 2004). Following this procedure for compound **29** resulted in a mixture of several products. In 1984, Bergeron and Garlich reported a method to reduce nitrile groups to primary amines using Raney nickel as a catalyst and sodium hydroxide as a co-catalyst under a hydrogen pressure of 2.7 bar (Bergeron and Garlich, 1984). Following this method at 20 bar of hydrogen pressure, the reaction was finally successful. Sodium hydroxide was dissolved in ethanol and added to compound **29**, Raney nickel was added to the mixture and the mixture was introduced into a Parr hydrogenator under 20 bar of hydrogen pressure for 20 h, the Parr hydrogenator was purged twice with hydrogen, the reduction afforded **33** in 45% yield. Repeating this reaction under 2.7 bar (Bergeron and Garlich, 1984) and even under 1 bar (Nazih et al., 1999) of hydrogen pressure were also successful. It appeared that the use of sodium hydroxide as a co-catalyst was the key factor in the reduction of aliphatic nitrile groups to primary amines, at least in our hands.

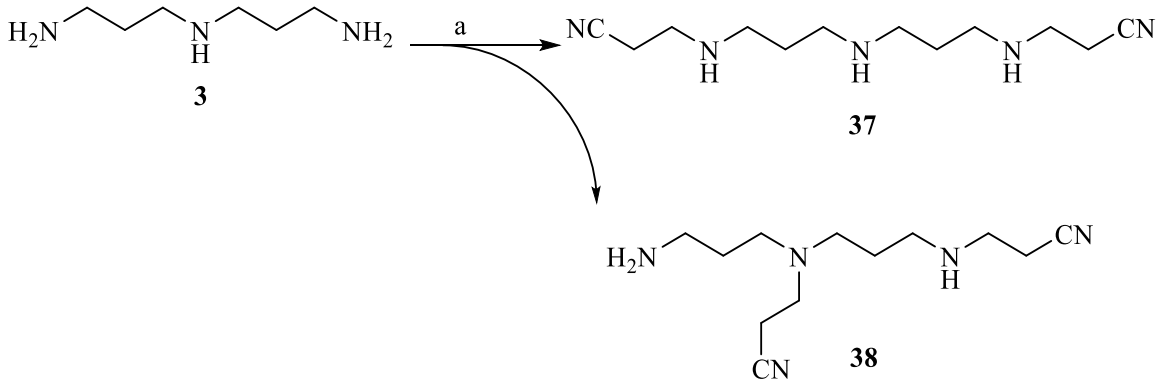

Figure 5: Synthetic scheme of **37** and **38** from norspermidine **3**.

Reagents and conditions: (a) acrylonitrile (2 eq), N_2, ethanol, 24 h.

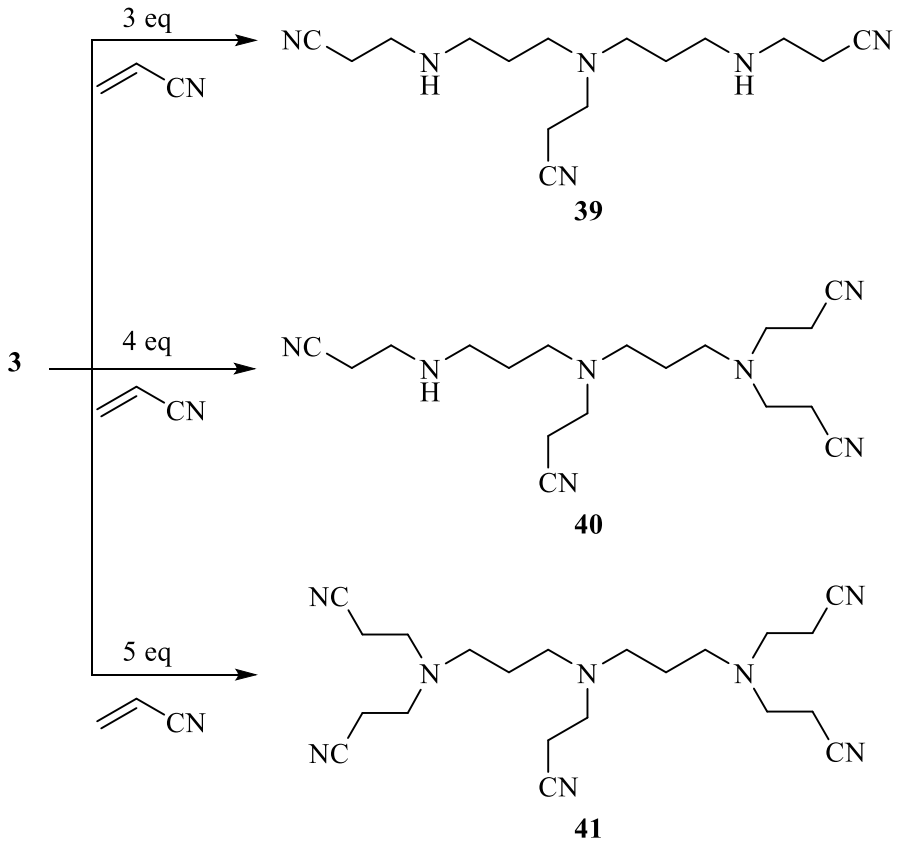

Figure 6: Synthetic scheme of **39**, **40** and **41** from norspermidine **3**.

Reagents and conditions: acrylonitrile (4 eq), N_2, ethanol, 72 h.

Compounds **37**-**41** (Figures 5 and 6) were designed to test the effect of branched polyamines compared to linear polyamines after reducing these nitrile adducts **37**-**41** to their corresponding target amines. Compound **38** was formed as a by-product from the synthesis of its linear structural isomer **37.** Both of them have the same chemical formula $C_{12}H_{24}N_5$, which requires 238.2026 $[M+H]^+$, found 238.2079 for **37** and 238.2033 for **38**. They cannot be differentiated using mass spectrometry only. However, NMR spectroscopic analysis showed interesting results. Figure 7 shows the chemical shifts of carbon atoms for **37** and **38**. Although the two compounds are isomers, **37** possesses a mirror plane of symmetry and therefore half of its carbons are equivalent to the other half. While in **38**, all carbons have different chemical shifts, giving 6 peaks for **37** and 12 peaks for **38**.

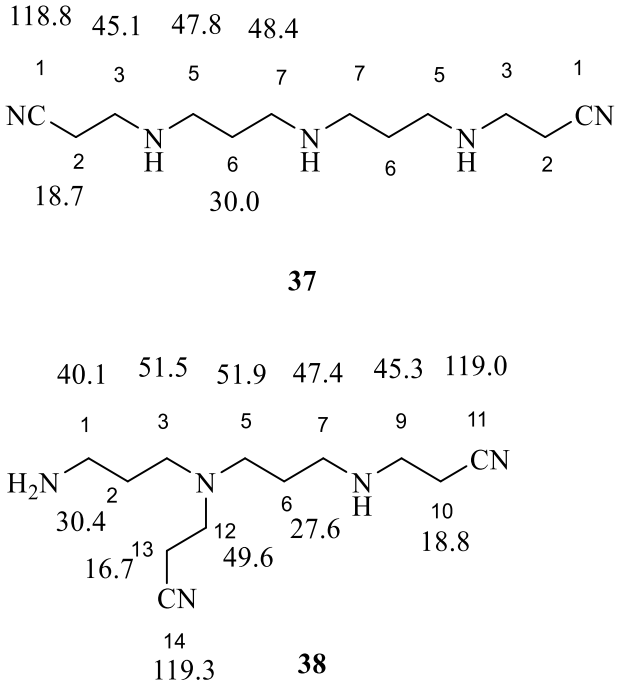

Figure 7: ^{13}C NMR (125 MHz) chemical shifts of **37** and **38** in ppm.

Figures 8 and 9 show the ^{13}C-NMR spectra and assignment of both compounds **37** and **38**. The peak at 18.7 ppm in **37** represents the two equivalent carbons C-2 attached directly to nitrile groups, while in the spectrum of **38**, there are two signals at 16.7 and 18.8 ppm for C-13 and C-10, respectively. C-10 in **38** has a similar magnetic environment to the two equivalent carbons C-2 in **37** and has a similar chemical shift. C-13 in **38** is affected by the presence of one additional alkyl substitution at both γ- and δ-positions compared to C-10, which resulted in chemical shifts lower by a value of 2.2 ppm than C-10. The calculated values of chemical shifts for C-10 and C-13 are in agreement with the observed value (Williams and Fleming, 2008). The peak at 30.0 ppm in **37** is assigned to the equivalent carbons C-6, while in **38** there are two peaks at 27.6 and 30.4 ppm and they are assigned to C-6 and C-2, respectively. C-6 in **38** is shielded by one more γ-alkyl substitution compared to C-2 and is expected to appear

in a more upfield position than C-2, so the peak at 27.5 ppm is assigned to C-6 and the peak at 30.3 ppm is assigned to C-2. The downfield low-intensity peak at 118.8 ppm in **37** is assigned to the equivalent carbons C-1 de-shielded by the CN triple bond, while in **38** low-intensity peaks at 119.0 and 119.3 ppm are assigned to C-11 and C-14, respectively. These assignments follow because C-14 has one more δ-alkyl substitution compared to C-11 and is expected to appear in a more downfield position than C-11 by a value of 0.3 ppm (Williams and Fleming, 2008). So the peak at 119.0 ppm is assigned to C-11 and the peak at 119.3 ppm is assigned to C-14. However, other signals (45.1, 47.8 and 48.4 in **37** and 45.3, 47.4, 48.6, 51.5 and 51.9 in **38**) are α- to nitrogen with similar alkyl substitutions and can be less securely assigned due to their close chemical shifts which overlap in both ^{1}H and ^{13}C NMR spectroscopy over a narrow range in the spectra.

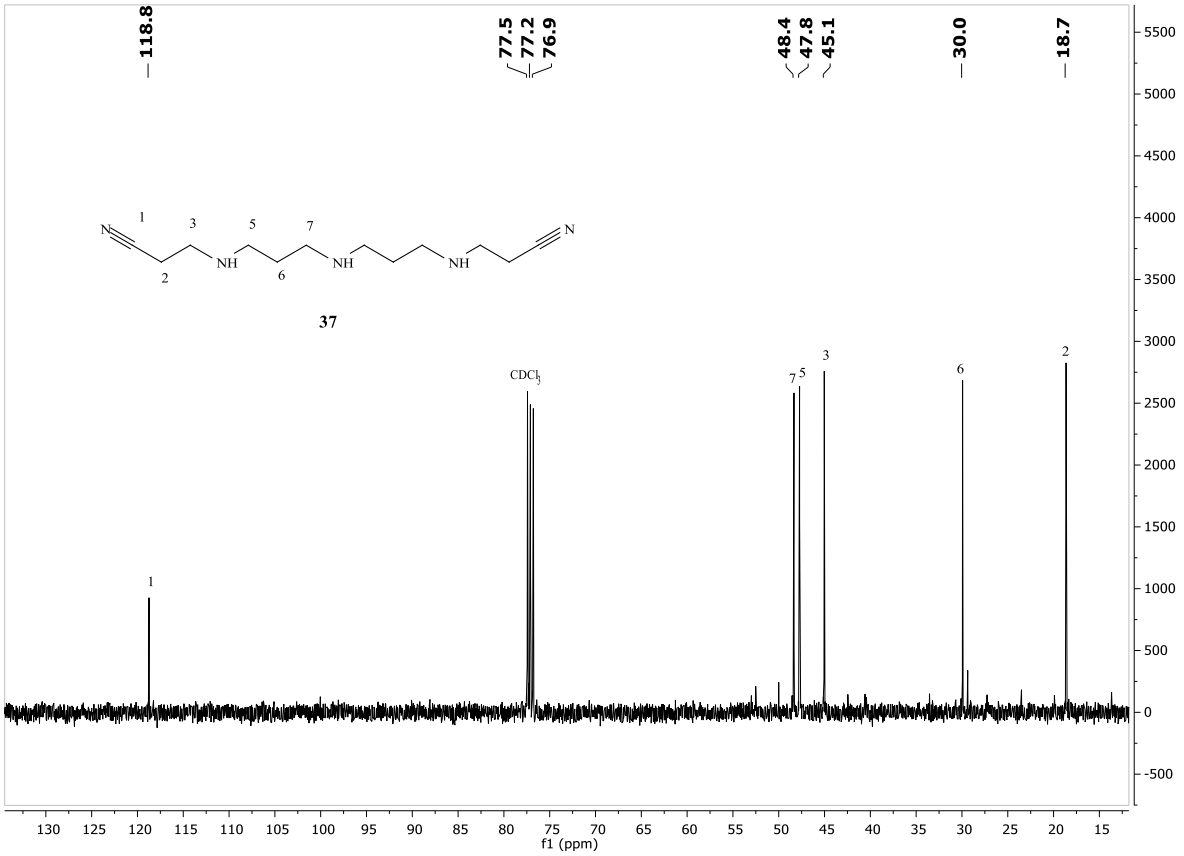

Figure 8: ^{13}C-NMR (125 MHz) spectrum of compound **37**.

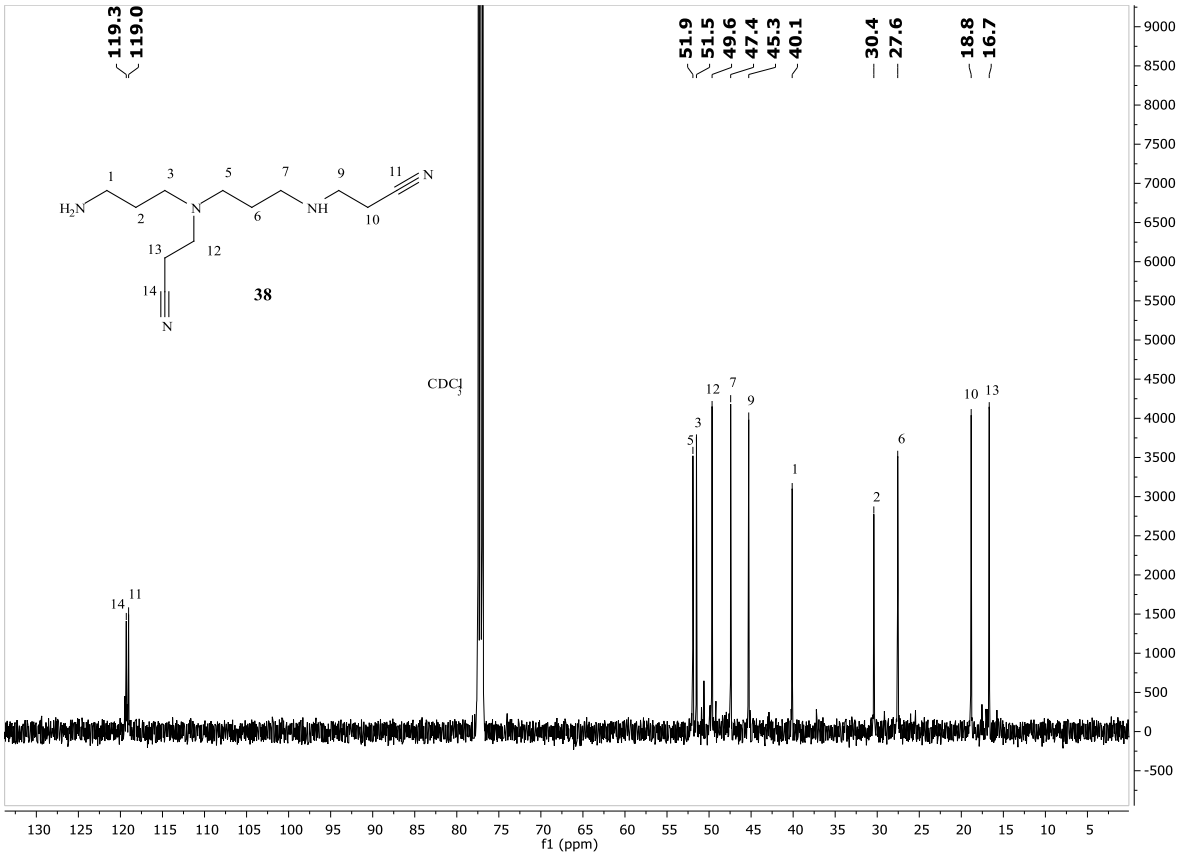

Figure 9: ^{13}C-NMR (125 MHz) spectrum of compound **38**.

As an example of ^{1}H NMR data, Figure 10 shows the chemical shifts of protons for **37** and **38**. Protons of C-2, C-3, C-5 and C-6 in **37** have similar magnetic environments to protons of C-10, C-9, C-7 and C-6 in **38** and have similar chemical shifts, while other protons in **38** are affected by the presence of the nitrile side-chain and the primary amine.

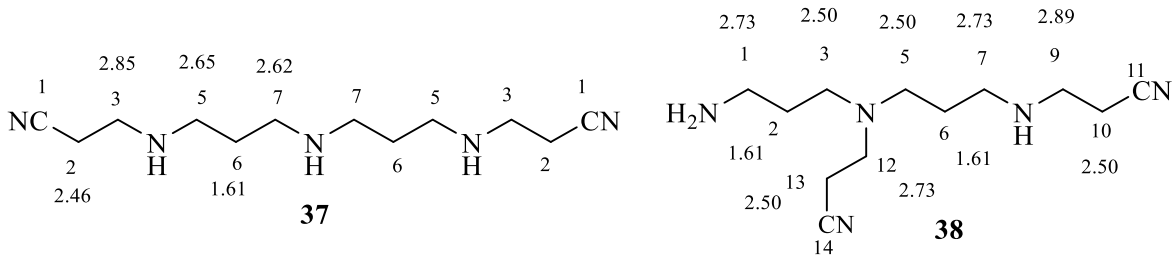

Figure 10: ^{1}H-NMR (500 MHz) chemical shifts of **37** and **38** in ppm.

Figures 11 and 12 show the ^{1}H-NMR spectra and assignments of **37** and **38** respectively. Protons were assigned according to matching with their corresponding ^{13}C signals depending on their HSQC-NMR spectrum (Figures 13 and 14).

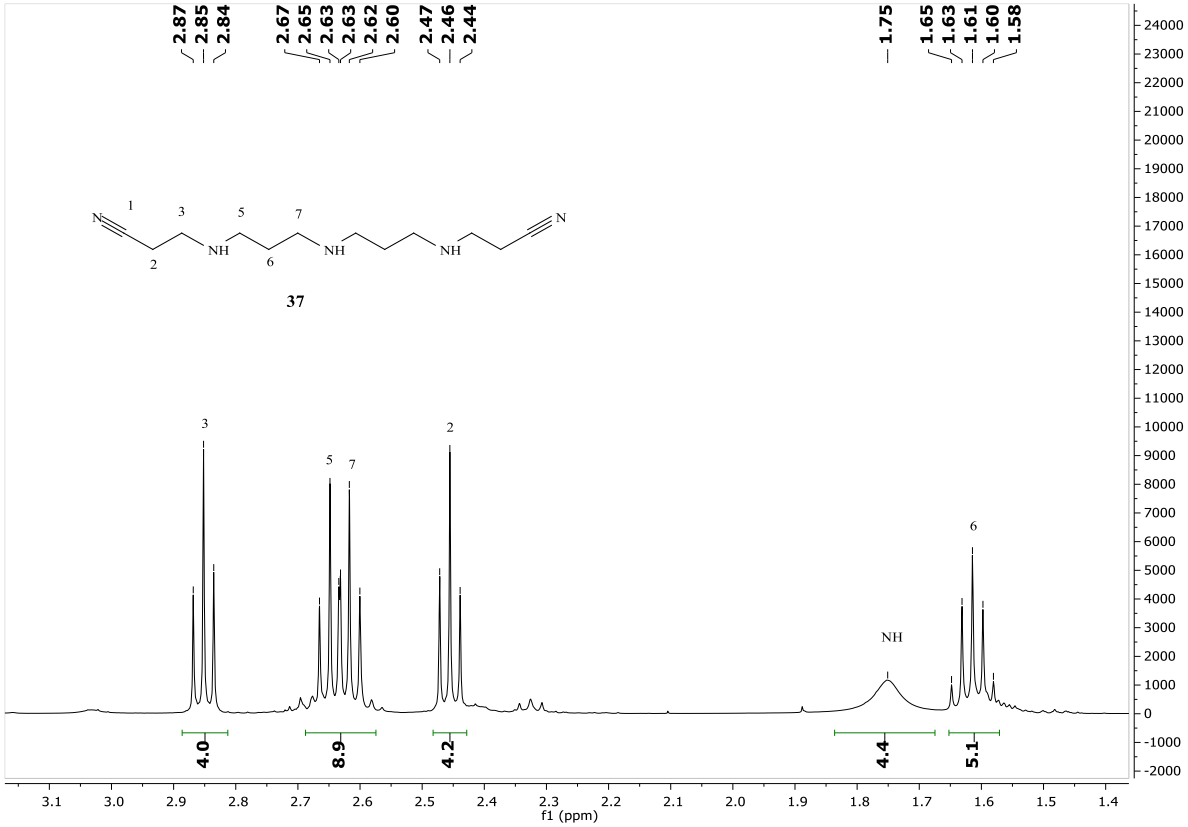

Figure 11: ^{1}H-NMR (500 MHz) spectrum of compound **37**.

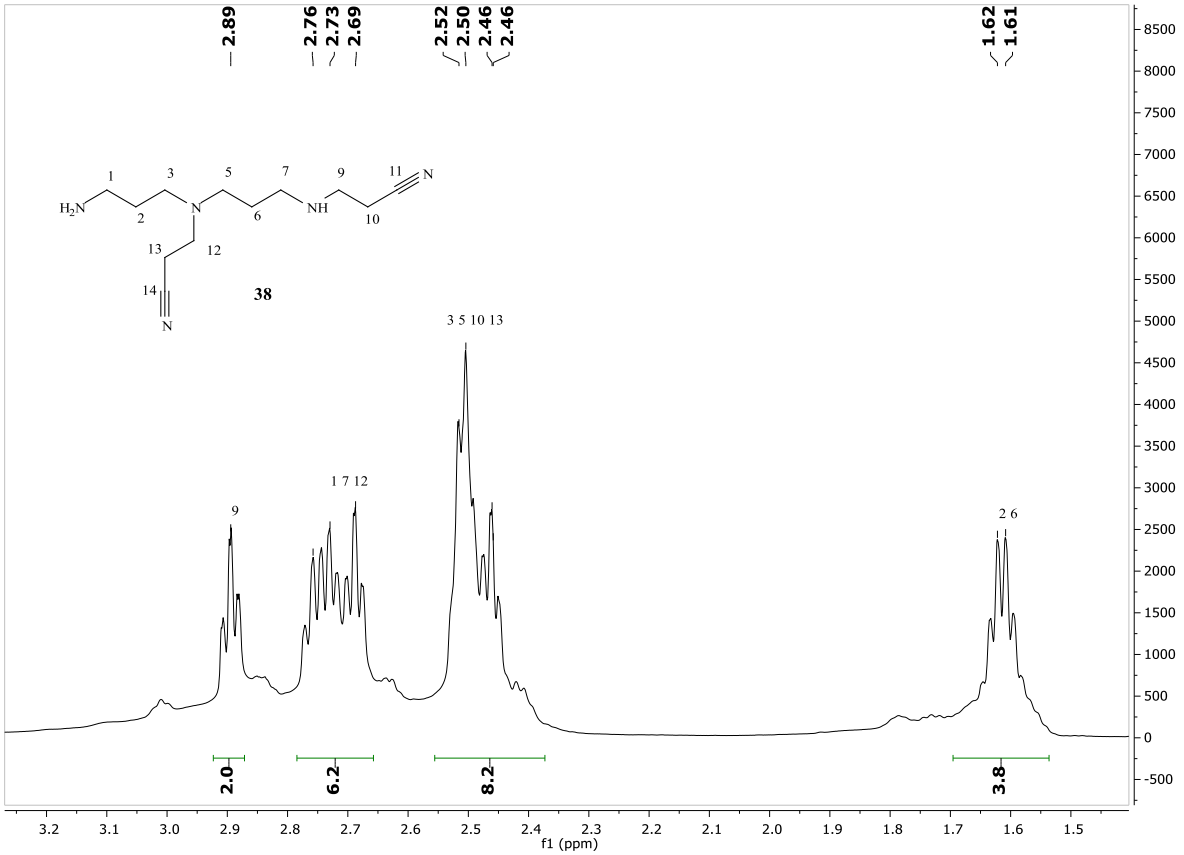

Figure 12: ^{1}H-NMR (500 MHz) spectrum of compound **38**.

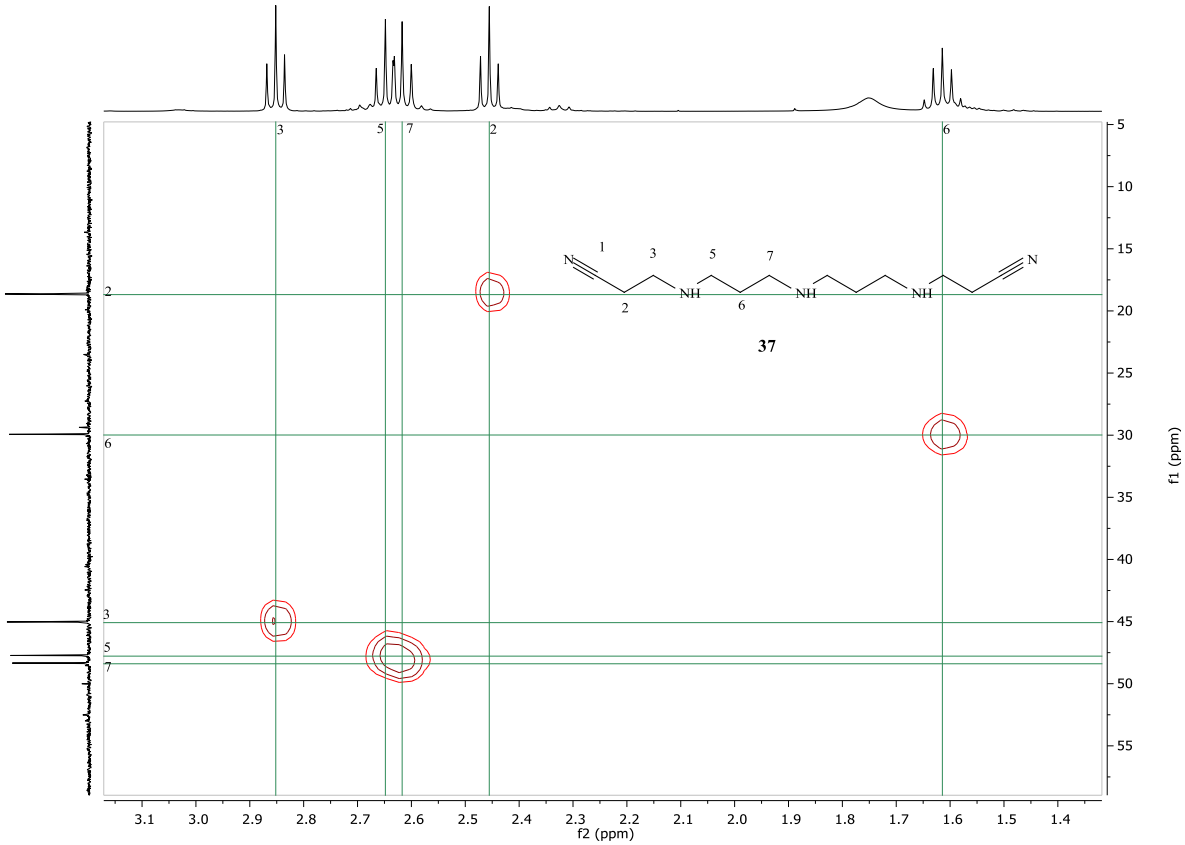

Figure 13: HSQC-NMR (500 MHz) spectrum of compound **37**.

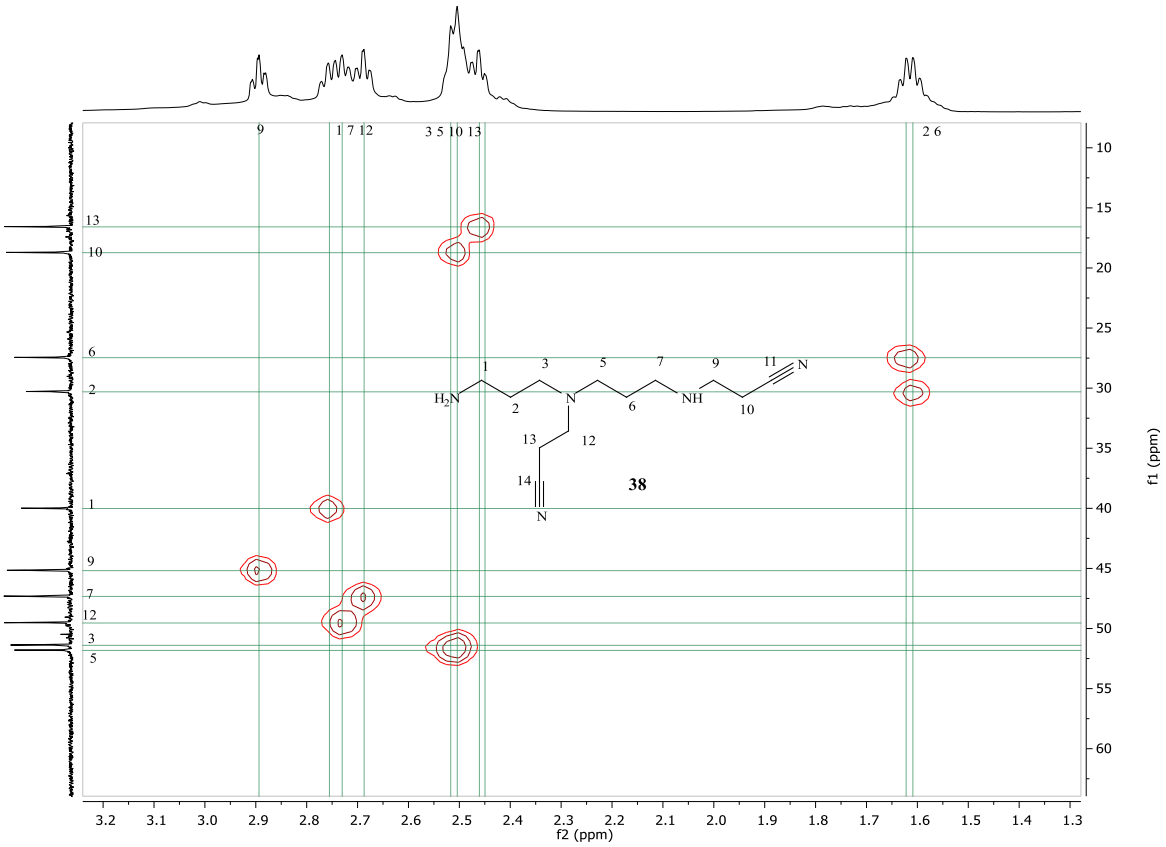

Figure 14: HSQC-NMR (500 MHz) spectrum of compound **38**.

Figure 15 shows the chemical shifts of carbon atoms for **39**. This compound is symmetrical about the central tertiary nitrogen atom and its side-chain.

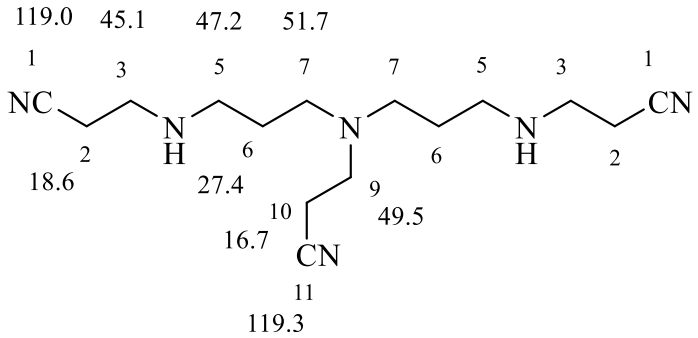

39

Figure 15: ^{13}C NMR (100 MHz) chemical shift of **39** in ppm.

Figure 16 shows the ^{13}C-NMR spectrum and assignment of **39**. The spectrum shows 9 signals, the two downfield low intense signals at 119.3 and 119.0 ppm are assigned to C-11 and C-1 nitrile carbons, respectively. These assignments are based upon the relative intensities of the two signals, 119.0 ppm being significantly higher in intensity than that resonating at 119.3 ppm (Figure 17). The next 4 signals at 51.8, 49.6, 47.3 and 45.2 ppm are assigned to NCH_2 carbons C-7, C-9, C-5 and C-3 de-shielded by nitrogen. However, the assignment of these 4 signals is secured only for C-9 at 49.6 ppm due to its lower relative intensity. The next 3 upfield signals at 27.5, 18.7 and 16.7 ppm are assigned to carbons C-5, C-2 and C-10, respectively, in the same manner of the calculations used to assign the spectral data of **38**. The peak at 16.7 ppm is assigned to C-10 due to its lower relative intensity compared to the peak at 18.7 ppm, and the effect of the presence of one additional alkyl substitution at γ- and δ-positions compared to the equivalent carbons C-2. So, the signal at 16.7 ppm is assigned to C-10 and the signal at 18.7 ppm is assigned to C-2.

Compound **39** has been previously synthesized (Balczewski et al., 2009) in order to make neurotoxins. The authors reported the spectral data for **39** but with one extra carbon signal. Compound **39** has 15 carbons and one point of symmetry in its chemical structure. Six (C-1, C-2, C-3, C-5, C-6, and C-7) have an equivalent six carbons, while three (C-9, C-10, and C-11) have no equivalent carbons (Figure 15). Therefore, its ^{13}C NMR spectrum should show 9 signals. Balczewski et al. reported compound **39** with 10 carbon signals; our ^{13}C NMR spectra show only 9 carbon signals (Figure 16) as anticipated.

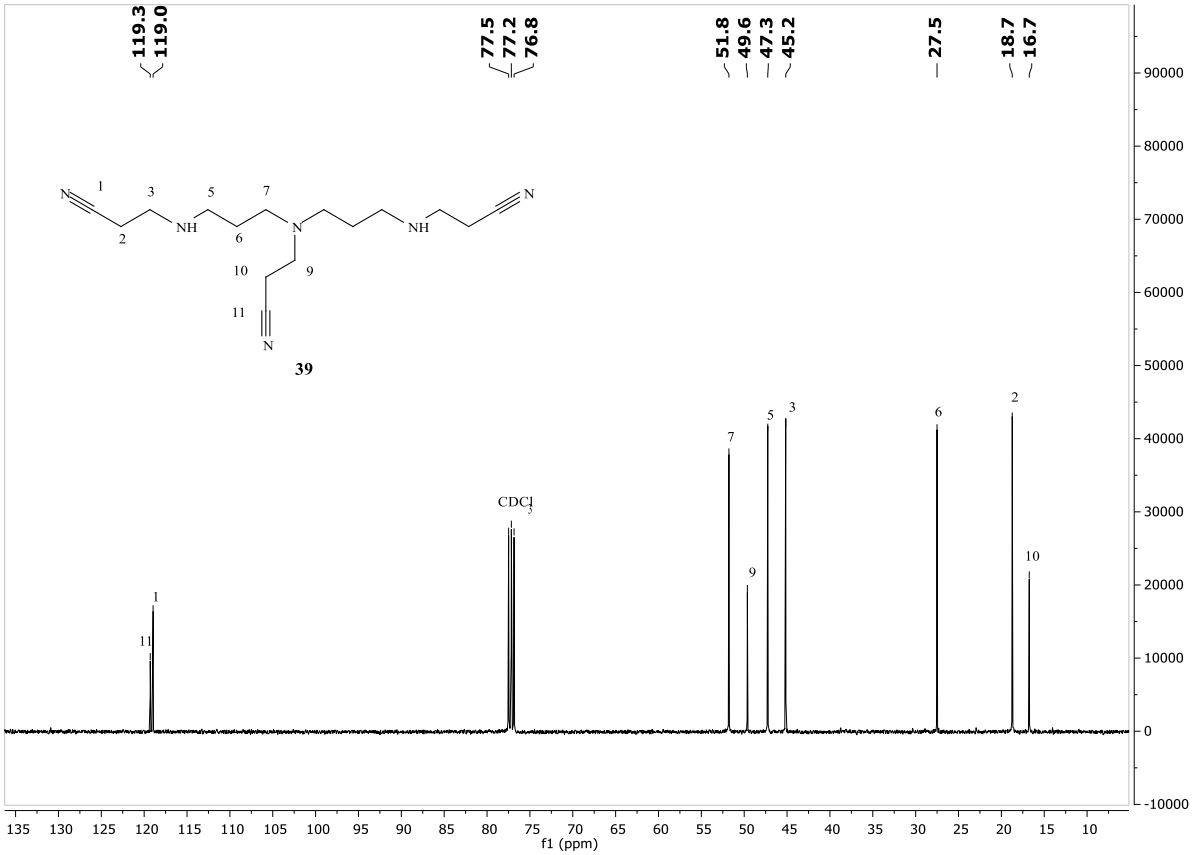

Figure 16: ^{13}C-NMR (100 MHz) spectrum of compound **39**.

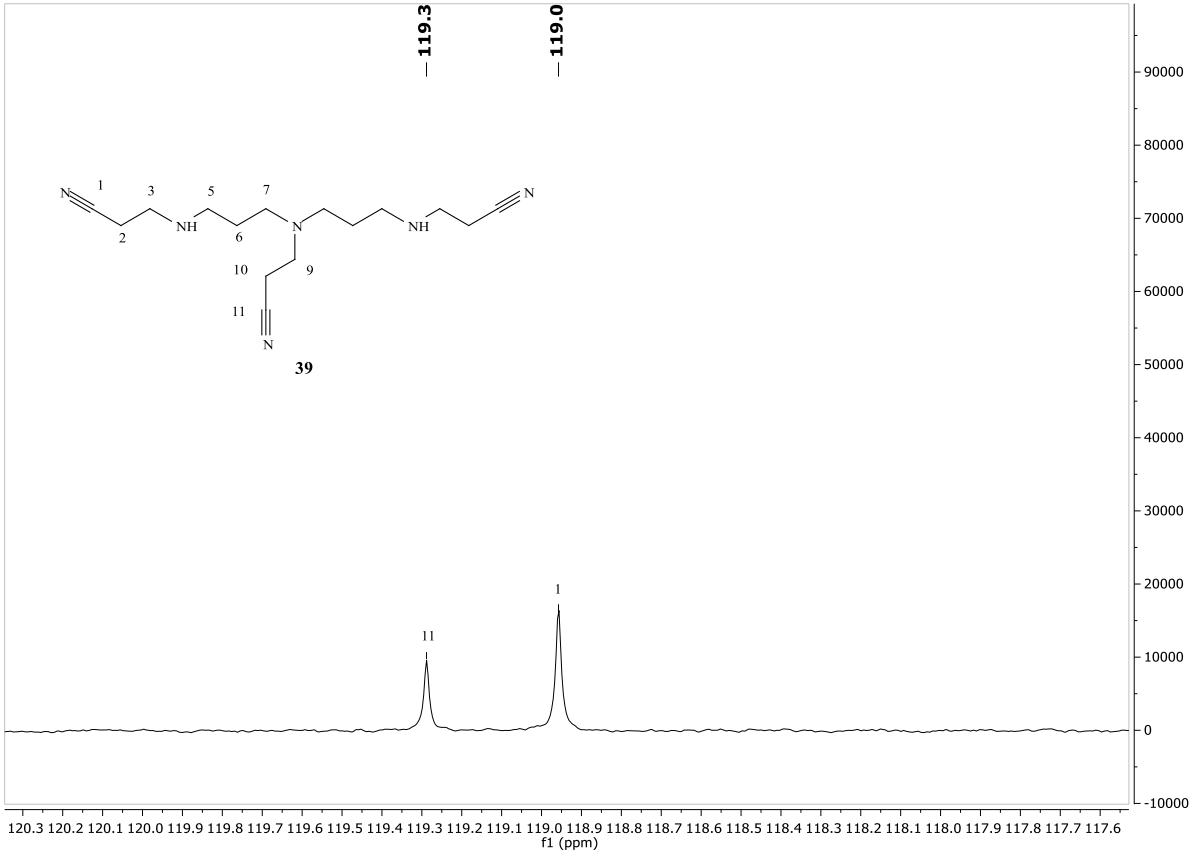

Figure 17: Expanded ^{13}C-NMR (125 MHz) spectrum of compound **39**.

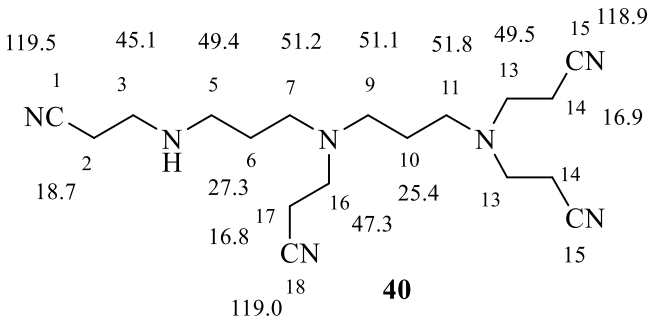

Figure 18: ^{13}C NMR (125 MHz) chemical shifts of **40** in ppm.

Figure 18 shows the chemical shifts of carbon atoms for **40**. Carbons C-13, C-14 and C-15 are equivalent. Figures 19 to 22 show the ^{13}C-NMR spectrum and its expansions leading to the assignment of **40**. The spectrum shows 15 signals. The three downfield low intense signals at 119.5, 119.0 and 118.9 ppm are assigned to C-1, C-18 and C-15 nitrile carbons, the assignment of these 4 signals is secured only for the equivalent C-15 at 118.9 ppm due to its higher relative intensity (Figure 20). The next 7 signals at 51.8, 51.2, 51.1, 49.5, 49.4, 47.3 and 45.1 ppm are assigned to NCH_2 carbons C-9, C-7, C-11, C-5, C-13, C-16 and C-3 de-shielded by nitrogen. However, the assignment of these 7 signals is secured only for the equivalent carbons C-13 at 49.5 ppm due to its higher relative intensity (Figure 21). The next two signals at 27.4 and 25.5 ppm are assigned to carbons C-6 and C-10, respectively. C-10 is affected by the presence of one additional alkyl substitution at γ- and δ-positions compared to C-6 which resulted in a chemical shift lower than C-6. The next 3 upfield signals at 18.8, 17.0 and 16.8 ppm are assigned to carbons C-2, C-14 and C-17. C-2 is affected by the presence of one less alkyl substitution at γ- and δ-positions compared to C-14 and C-17 which resulted in a chemical shift lower than C-14 and C-17, so the signal at 18.8 ppm is assigned to C-2. The signal at 17.0 ppm is assigned to the two equivalent carbons C-14 due to its higher relative intensity, and the signal at 16.8 ppm is therefore assigned to C-17 (Figure 22).

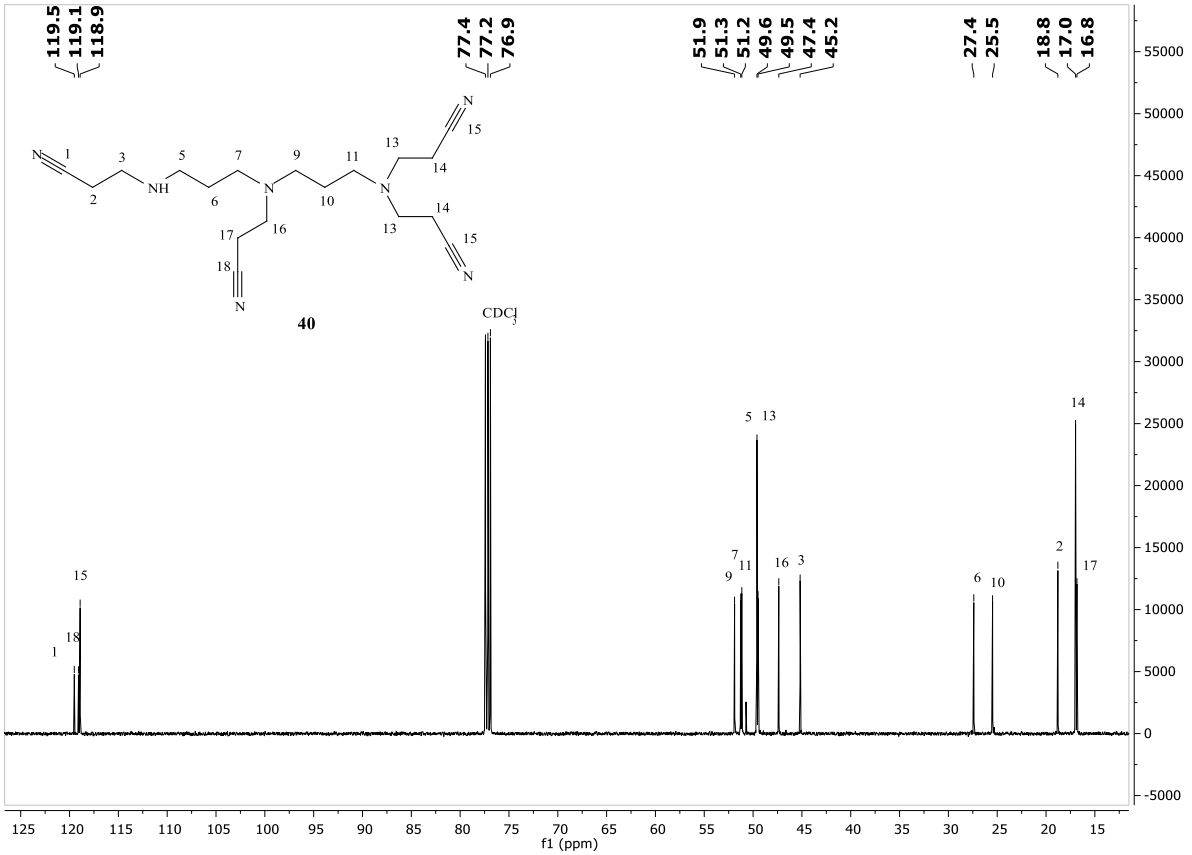

Figure 19: ^{13}C-NMR (125 MHz) spectrum of compound **40**.

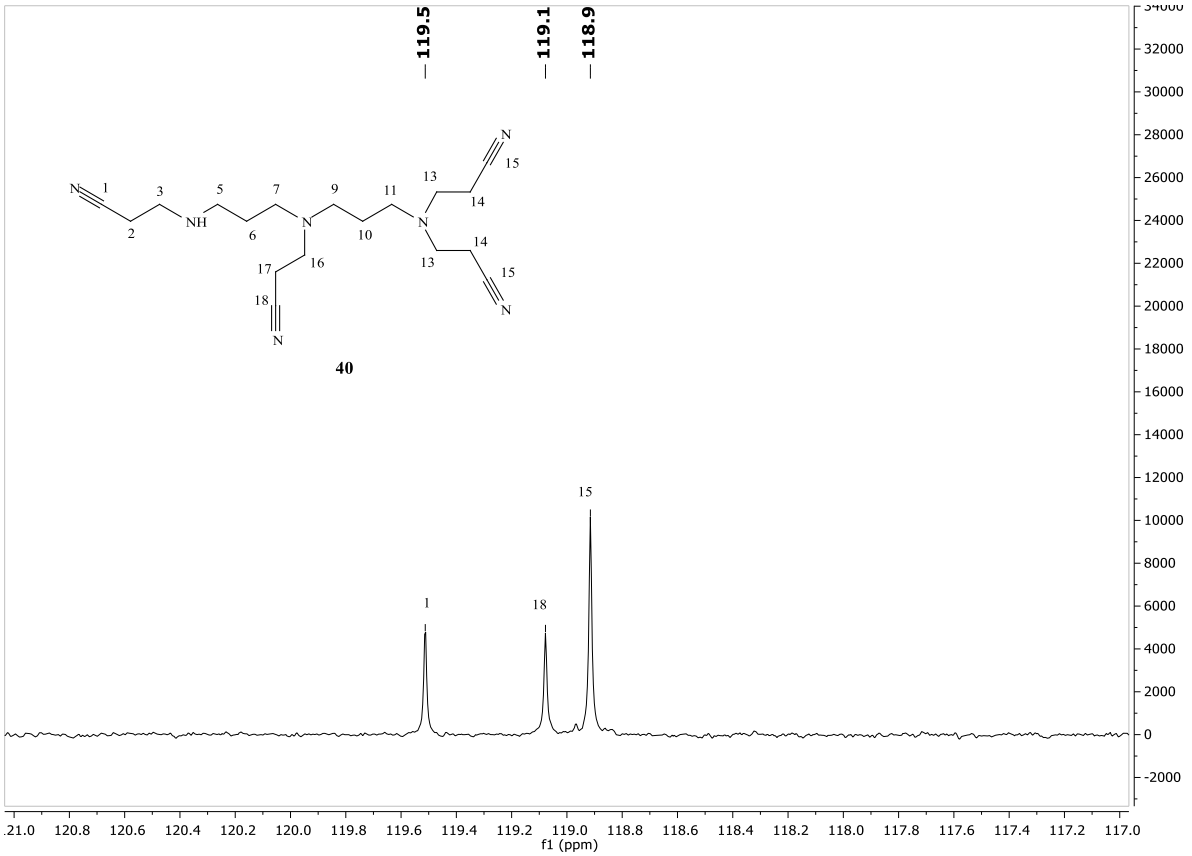

Figure 20: Expanded ^{13}C-NMR (125 MHz) spectrum of compound **40**.

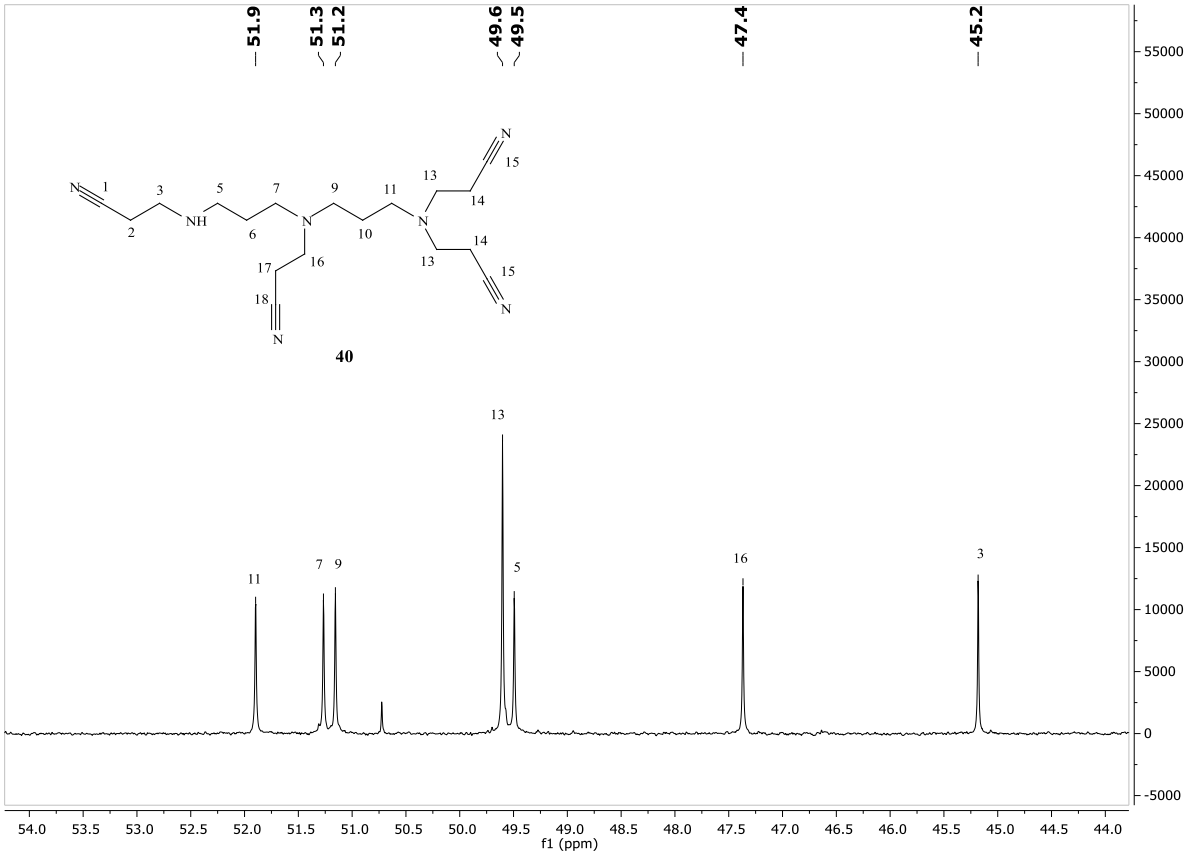

Figure 21: Expanded ^{13}C-NMR (125 MHz) spectrum of compound **40**.

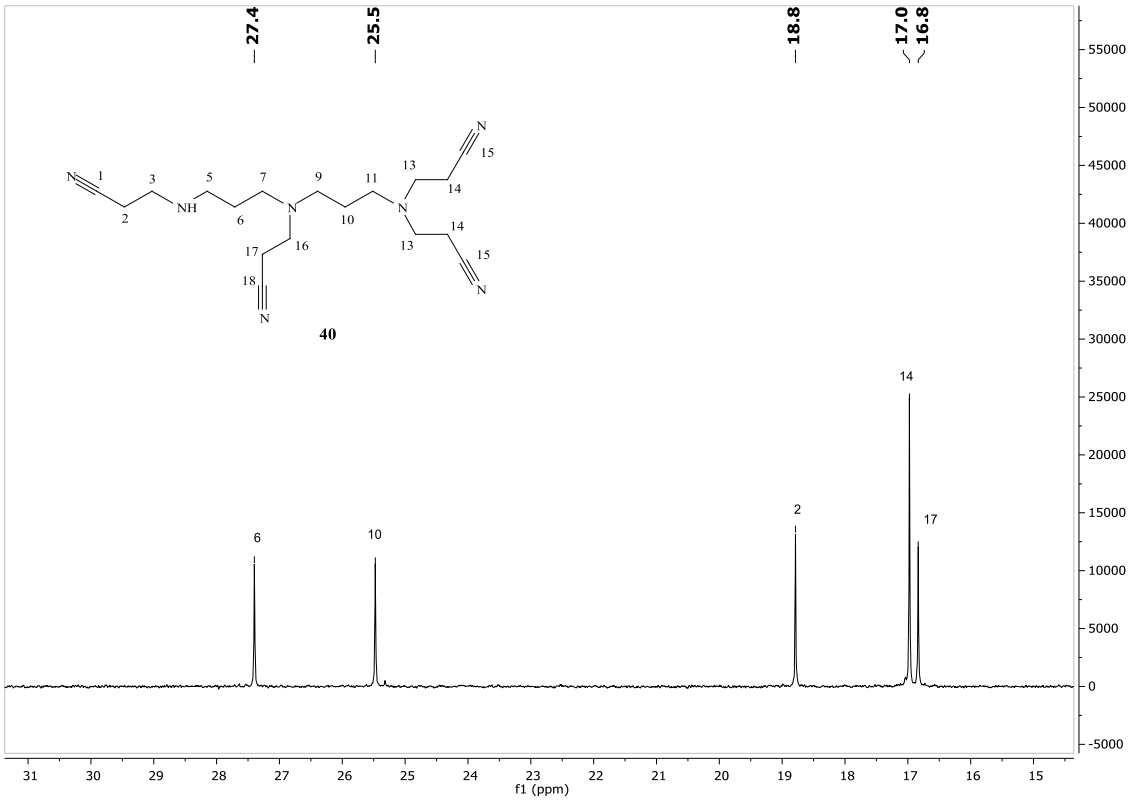

Figure 22: Expanded ^{13}C-NMR (125 MHz) spectrum of compound **40**.

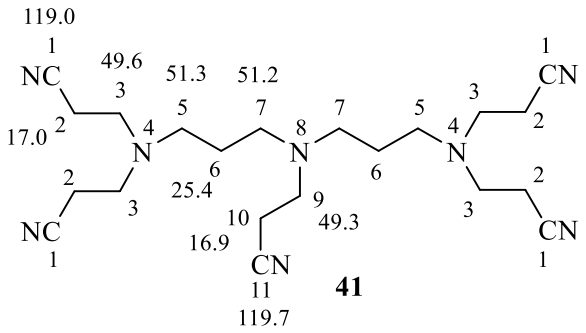

Figure 23: ^{13}C NMR (125 MHz) chemical shift of **41** in ppm.

Figure 23 shows the chemical shifts of carbon atoms in **41**. This compound is symmetrical about the central nitrogen N-8 and also about the two N-4 nitrogens. Figures 24 to 26 show the ^{13}C-NMR spectrum and assignments of **41**. The spectrum shows 9 signals, the two downfield low intense signals at 119.7 and 119.0 ppm are assigned to C-11 and C-1 nitrile carbons. The signal at 119.7 ppm is assigned to C-11 and the signal at 119.0 ppm is assigned to four equivalent carbons C-1 due to its higher relative intensity. The next four signals resonating at 51.3, 51.2, 49.6 and 49.3 ppm are assigned to NCH_2 carbons C-7, C-5, C-3 and C-9 de-shielded by nitrogen. C-5 and C-7 have the same α-, β- and γ-substitution, but C-5 is affected by the presence of one δ-alkyl and two δ-CN substitution, while C-7 is affected by the presence of three δ-alkyl and one δ-CN substitution, which makes the calculated chemical shift for C-5 to be 1.1 ppm lower than C-7, so the peak at 51.3 ppm is assigned to the two equivalent carbons C-5, the peak at 51.2 ppm is assigned to the two equivalent carbons C-7. However, due to the close chemical shift for these carbons, it is not secure enough to depend on this low difference for assignment. The signal at 49.6 ppm is assigned to the four equivalent carbons C-3 due to its higher relative intensity, while the signal at 49.3 ppm is assigned to C-9 due to its lower relative intensity (Figure 25). The peak at 25.4 ppm is assigned to the two equivalent carbons C-6. The next peak at 17.0 ppm is assigned to the four equivalent carbons C-2 due to its higher relative intensity, while the peak at 16.9 ppm is assigned to C-10 due to its lower relative intensity (Figure 26).

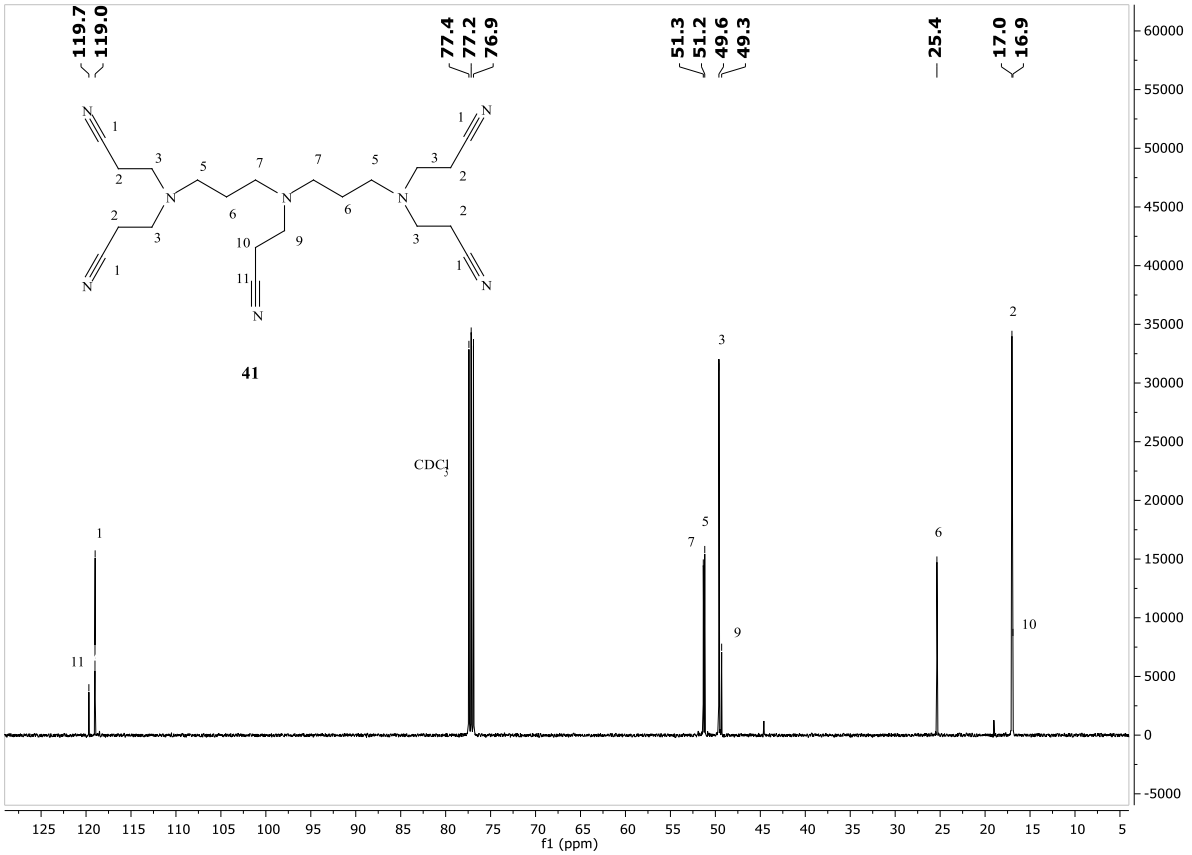

Figure 24: ^{13}C-NMR (125 MHz) spectrum of compounds **41**.

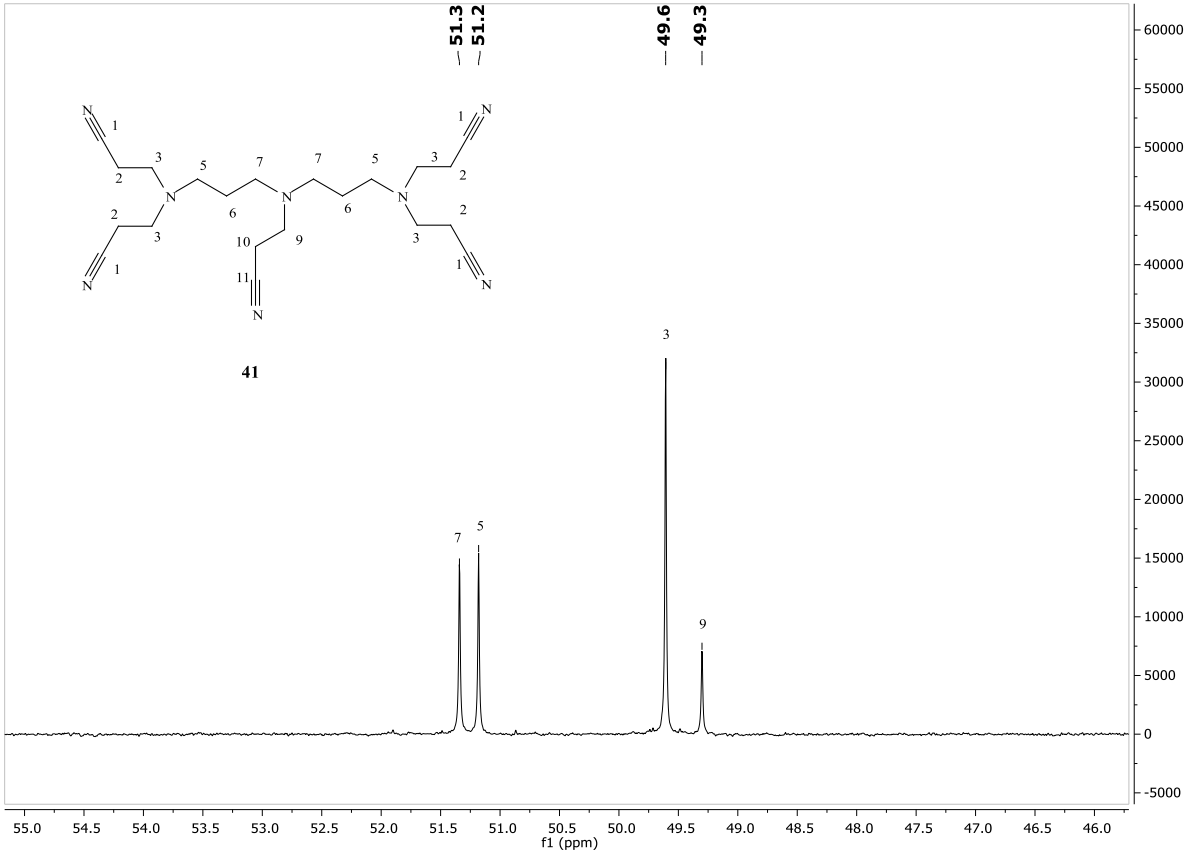

Figure 25: Expanded ^{13}C-NMR (125 MHz) spectrum of compound **41**.

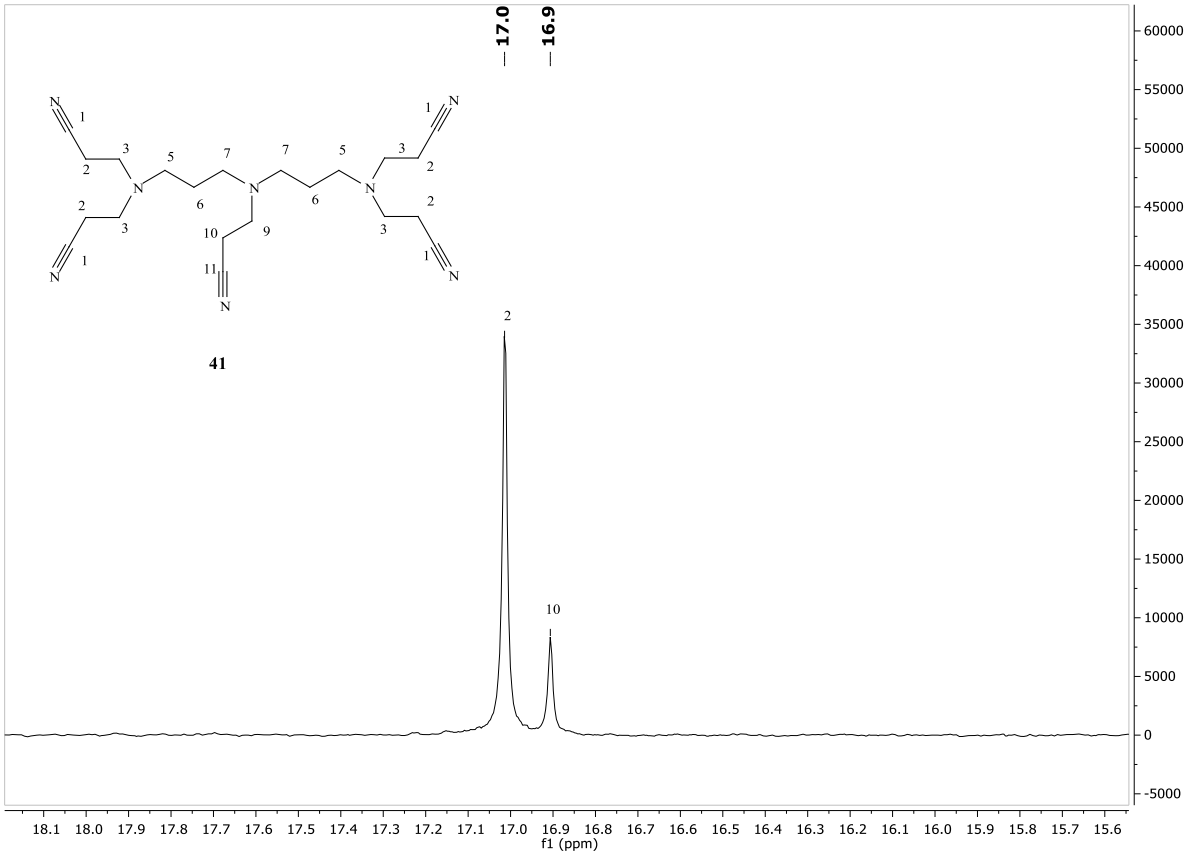

Figure 26: Expanded ^{13}C-NMR (125 MHz) spectrum of compound **41**.

The purpose of designing compounds **37**-**41** was to reduce these nitrile adducts to their corresponding branched polyamines and compare their activity against bacterial biofilms with linear polyamines. However, the reduction of these compounds following the procedure mentioned above for the reduction of compound **29** was not successful. The products could not be extracted from the reaction mixture. Most likely, the high polarity of the products made it hard to extract these products from the aqueous sodium hydroxide solution. Compounds **33**-**36** were successfully obtained following this procedure by the reduction of compounds **29**-**32**, respectively. The presence of hexahydropyrimidine rings in compounds **33**-**36** slightly decreased their polarity, compared with free linear polyamines, enough to be extracted from the aqueous sodium hydroxide solution with a mixture of chloroform: methanol (85: 15 v/v).

Whilst these experiments were underway, a paper published by Hoque and co-workers (Hoque et al., 2016) showed the activity of diamino-diamide-substituted molecules to prevent biofilm formation and even to eradicate established biofilms. Some of their bactericidal molecules share a common structural feature having a hydrocarbon chain flanked by positively charged moieties, quaternised amines, as illustrated (Figure 27):

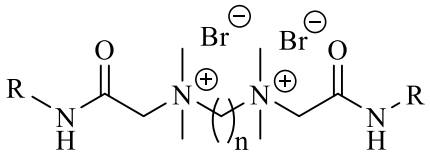

n = 6, 8, 10, 12
R = C_6H_{13}, C_8H_{17}

Figure 27: Cationic molecules which are both antibacterial and antibiofilm in their activities.

Their most active molecules **64**-**67** (Figure 34) are discussed in more detail in Chapter 3. They contain a hydrocarbon chain of 6- to 12-methylene spacers between amine groups. By varying the length of the hydrophobic spacers between the ammonium positive charges, they synthesised cationic molecules that demonstrated both antibacterial and antibiofilm activity with low toxicity. Studying the SAR of these active compounds prompted the design of molecules **46**-**49** (Figure 28). Compounds **46**-**49** are therefore expected to have biological activity against biofilms as they have two amine functional groups (ammonium ions) separated by methylene bridges of 7, 8, 10, and 12 carbons and flanked by another three methylenes each terminating in primary amine groups.

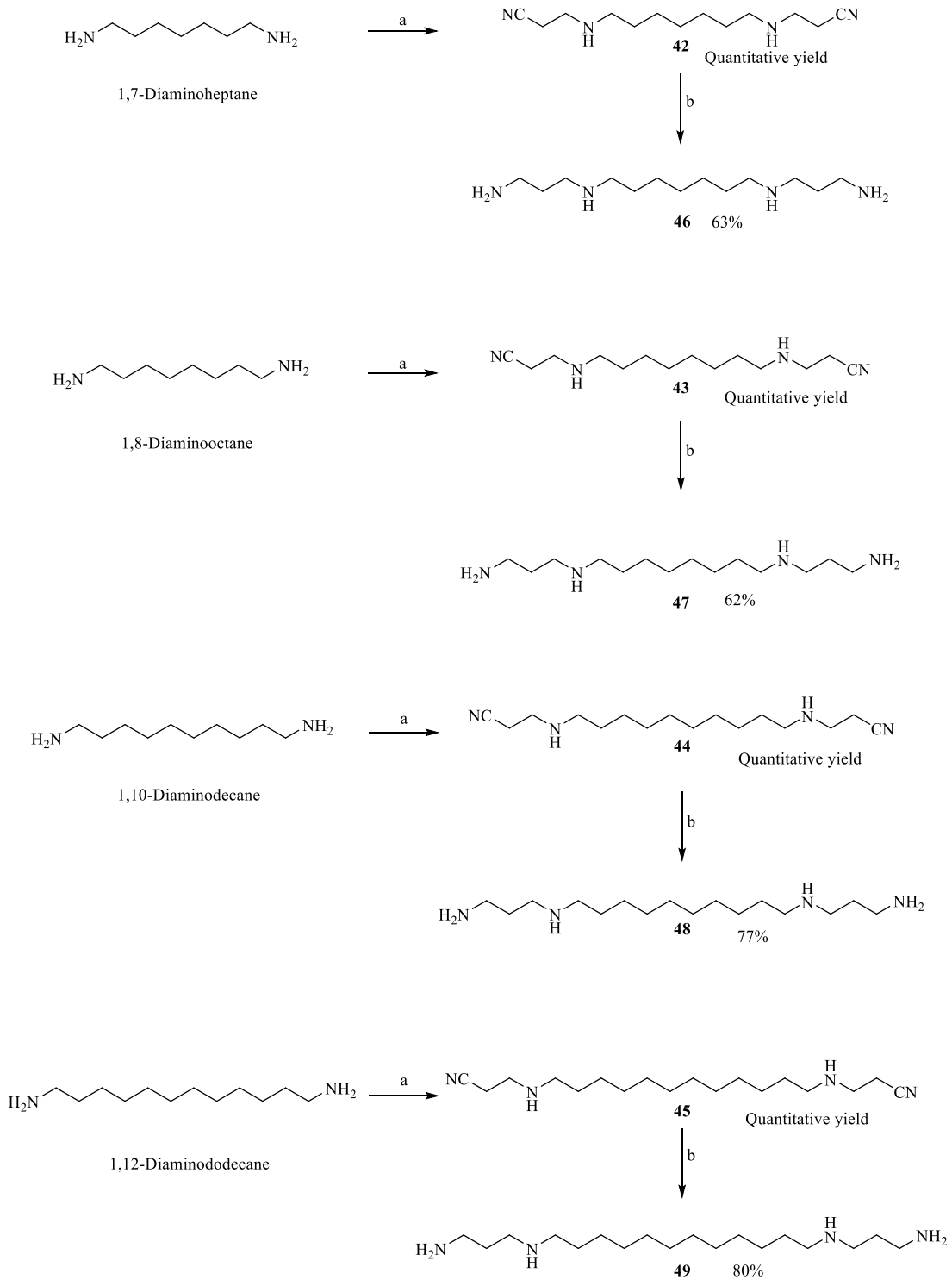

Figure 28: Synthetic scheme of **46**-**49**.

Reagents and conditions: (a) (i) acrylonitrile, N_2, anhydrous methanol, 15 h, (ii) acrylonitrile, N_2, 9 h; (b) ethanol 95%, NaOH, H_2, Raney nickel, 20 h.

Compounds **46**-**49** were synthesized by the addition of two equivalents of acrylonitrile to the starting materials to produce **42**-**45** respectively, followed by the reduction of nitrile groups to primary amines. Compounds **37**-**45** (Figure 28) have been reported (Balczewski et al., 2009; Frydman et al., 2004; Jahromi et al., 2013; Klenke et al., 2001; Liew et al., 2013; Pearce et al., 2017; Sharma et al., 2010), but either without spectral data or the spectral data were not fully assigned. Therefore, the spectral data were fully assigned for these compounds supported by the calculated values of their chemical shifts. Proton signals were assigned according to their carbon connectivities in the corresponding HSQC-NMR spectra. Figures 29-36 show the assigned ^{13}C, ^{1}H and HSQC-NMR spectra for compounds **42**-**45** supported by the calculated values compared to the observed ones (Tables 1-9). The calculations are made using the ^{13}C equation and the associated data tables in Williams and Fleming (2008):

$\delta_C = -2.3 + \Sigma z + \Sigma S + \Sigma K$

where -2.3 ppm is the ^{13}C chemical shift for methane (ppm), z is the substituent constant, S is a "steric" correction, and K is a conformational increment for γ-substituents.

Figure 29 shows the chemical shifts of proton and carbon atoms for **42**, this molecule is symmetrical around C-8.

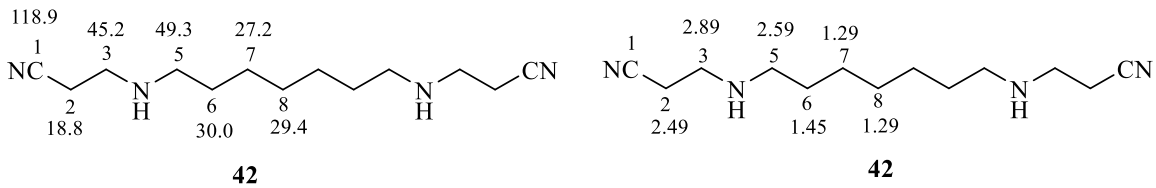

Figure 29: ^{13}C-NMR (left) and ^{1}H-NMR (right) chemical shifts of **42** in ppm.

Figures 30 to 32 show the ^{13}C, ^{1}H and HSQC-NMR spectrum and assignment of **42**. The ^{13}C-NMR spectrum (Figure 32) shows 7 signals, the downfield low intense signal at 118.9 ppm are assigned to C-1 nitrile carbons. The next 2 signals at 49.3 and 45.2 ppm are assigned to NCH_2 carbons C-5, C-3, respectively de-shielded by nitrogen. The next 3 signals at 30.0, 29.4 and 27.2 ppm are assigned to carbons C-6, C-8 and C-7, respectively. The signal at 29.4 is assigned to carbon C-8 due to its lower relative intensity only occurring once in this symmetrical molecule **42**. The upfield peak at 18.8 ppm is assigned to C-2.

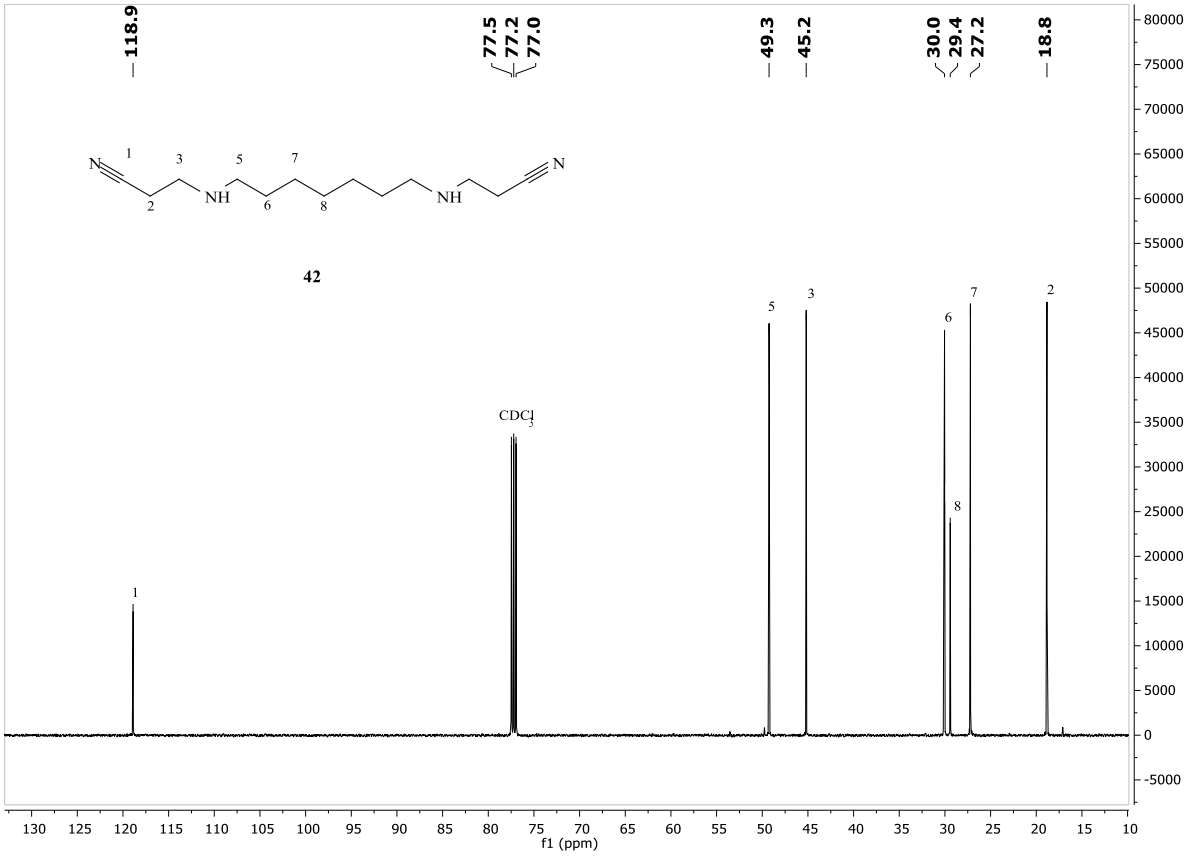

Figure 30: ^{13}C-NMR (125 MHz) spectrum of compound **42**.

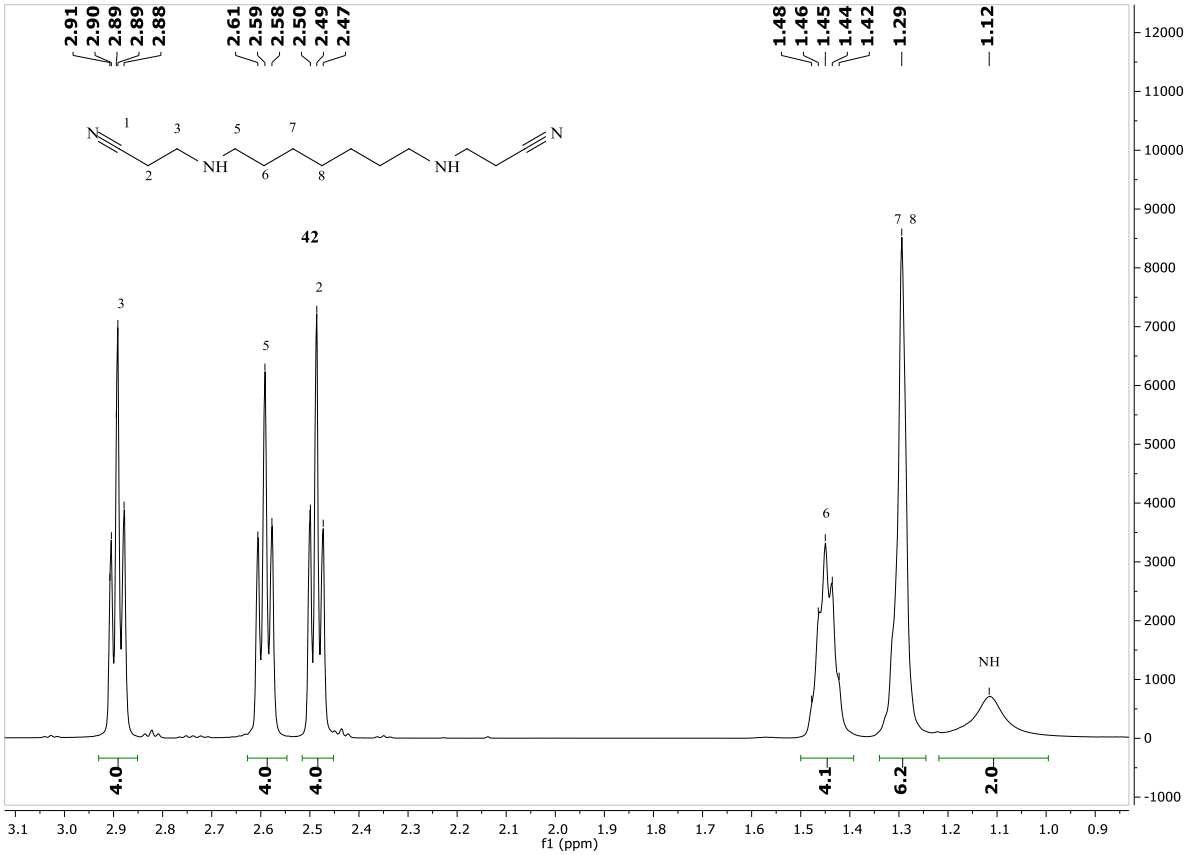

Figure 31: ^{1}H-NMR (500 MHz) spectrum of compound **42**.

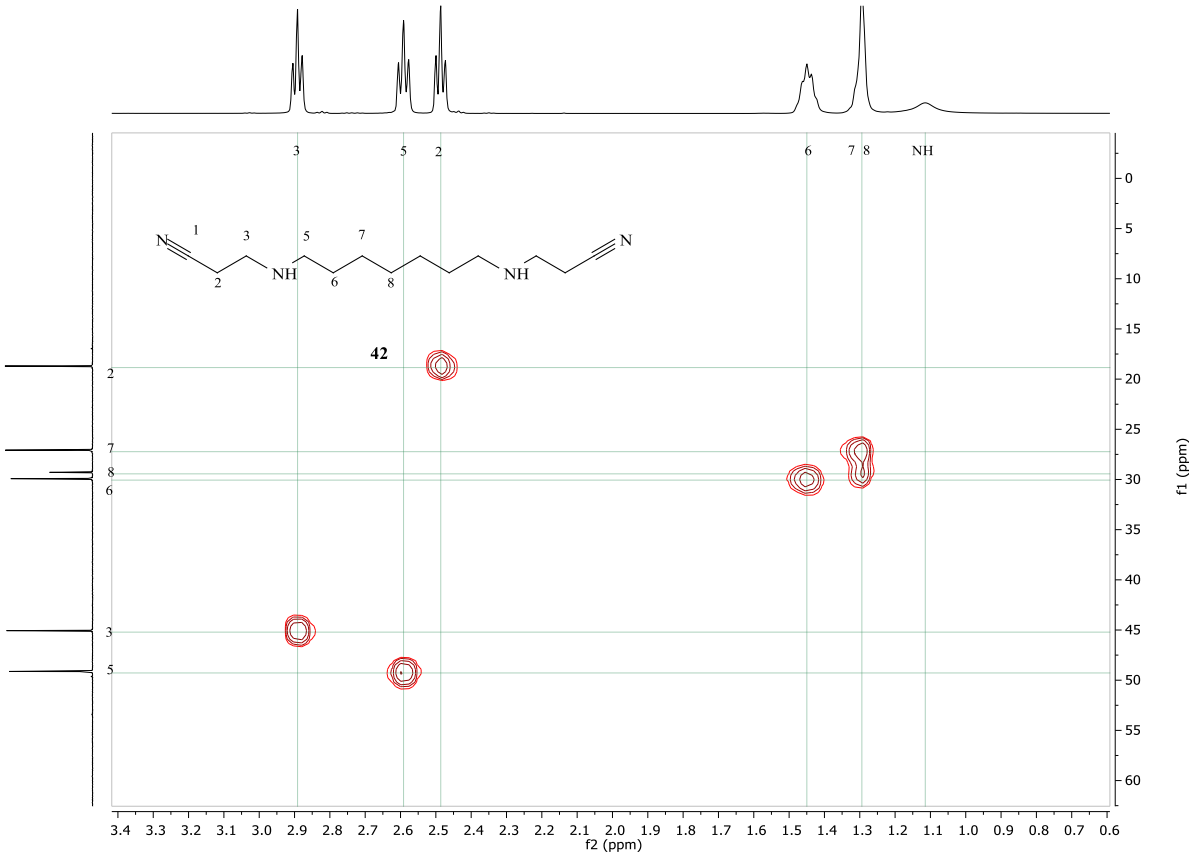

Figure 32: HSQC-NMR spectrum of compound **42**.

Figure 33 shows the chemical shifts of all the carbon and proton atoms in **43**.

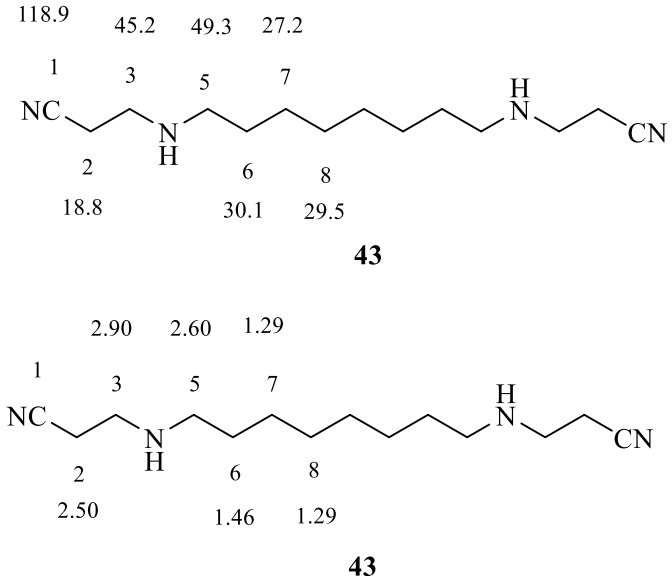

Figure 33: ^{13}C-NMR (upper) and ^{1}H-NMR (lower) chemical shifts of **43** in ppm.

Figures 34 to 36 show the ^{13}C, ^{1}H and HSQC-NMR spectrum and assignment of **43**. The ^{13}C-NMR spectrum (Figure 34) shows 7 signals, the downfield low intense signal at 118.9 ppm is assigned to C-1 nitrile carbons. The next 2 signals at 49.3 and 45.2 ppm are assigned to NCH_2 carbons C-5 and C-3, respectively, deshielded by nitrogen. The next 3 signals at 30.1, 29.5 and 27.2 ppm are assigned to carbons C-6, C-8 and C-7, respectively. The signal at 29.5 is assigned to carbons C-8 which have higher relative intensity compared to C-8 in compound **42**, as it represents two equivalent carbons in **43** while it represents only one carbon in **42**. The upfield peak at 18.8 ppm is assigned to C-2. Compound **43** has been previously synthesized (Liew et al., 2013) in order to make antimalarial polyamines. The authors reported the spectral data for compound **43**. It appears that using DMSO-d_6 as the solvent, they mistakenly swapped the assignment of the carbon signals for methylene groups at 14.4 and 42.0 ppm to C-3 and C-2, respectively (Liew et al., 2013), but these have been corrected in this thesis.

Here, carbon signals at 18.8 and 45.2 ppm were assigned to C-2 and C-3, respectively (Figure 34). C-3 is α-position to amino group and should appear in an upfield region, while C-2 is α-position to nitrile group and β-position to amino group. Nitrile group have low effect on de-shielding adjacent carbons and increase their chemical shift only by 3.1 ppm, therefore, C-2 should appear in a downfield region. The calculated value for C-2 and C-3 signals are 19.0 and 44.7 ppm, respectively (Williams and Fleming, 2008). Our results are in agreement with the calculated values. We performed our experiment in $CDCl_3$ solvent. To overcome the effect on NMR signals that may derived from using a different solvent, the NMR measurements were made using DMSO-d_6 where C-2 and C-3 appeared at 17.8 and 44.9 ppm respectively, in agreement with our $CDCl_3$ and calculated values (Table 7).

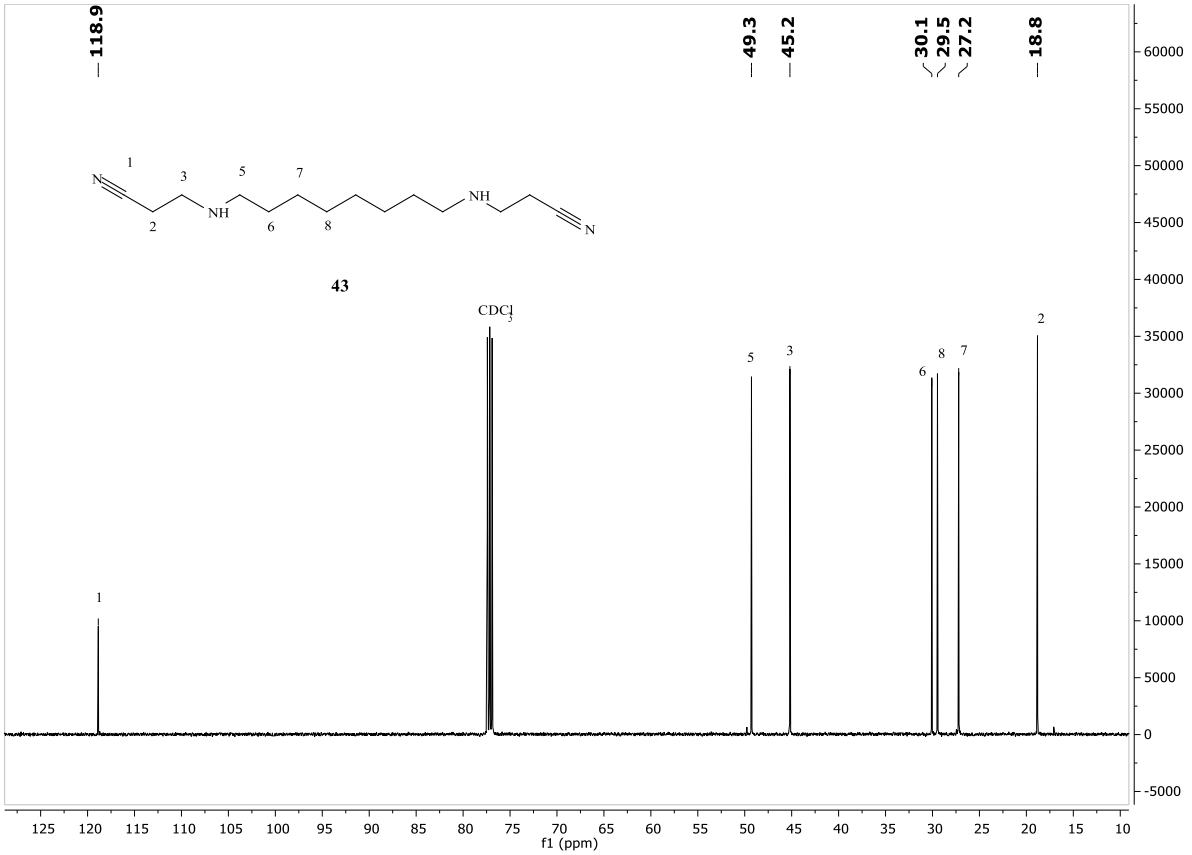

Figure 34: ^{13}C-NMR (125MHz) spectrum of compound **43**.

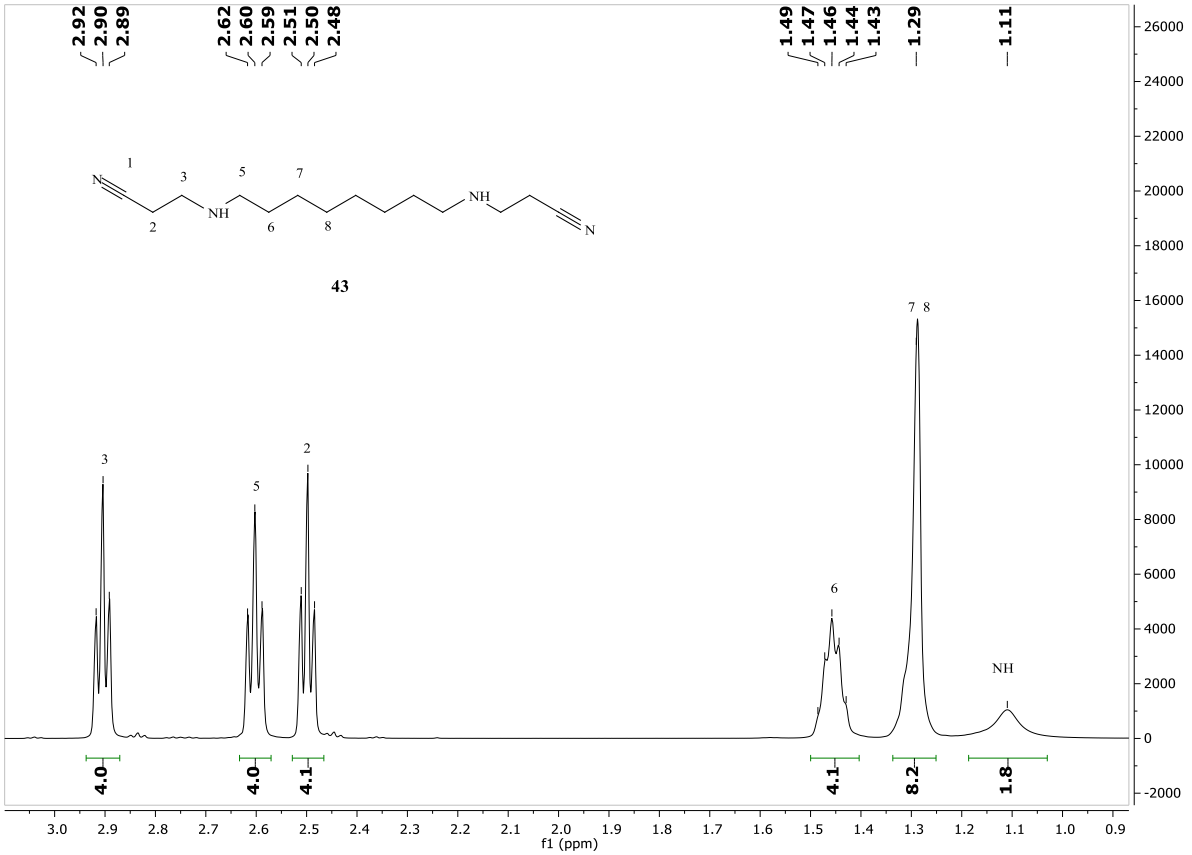

Figure 35: ^{1}H-NMR (500 MHz) spectrum of compound **43**.

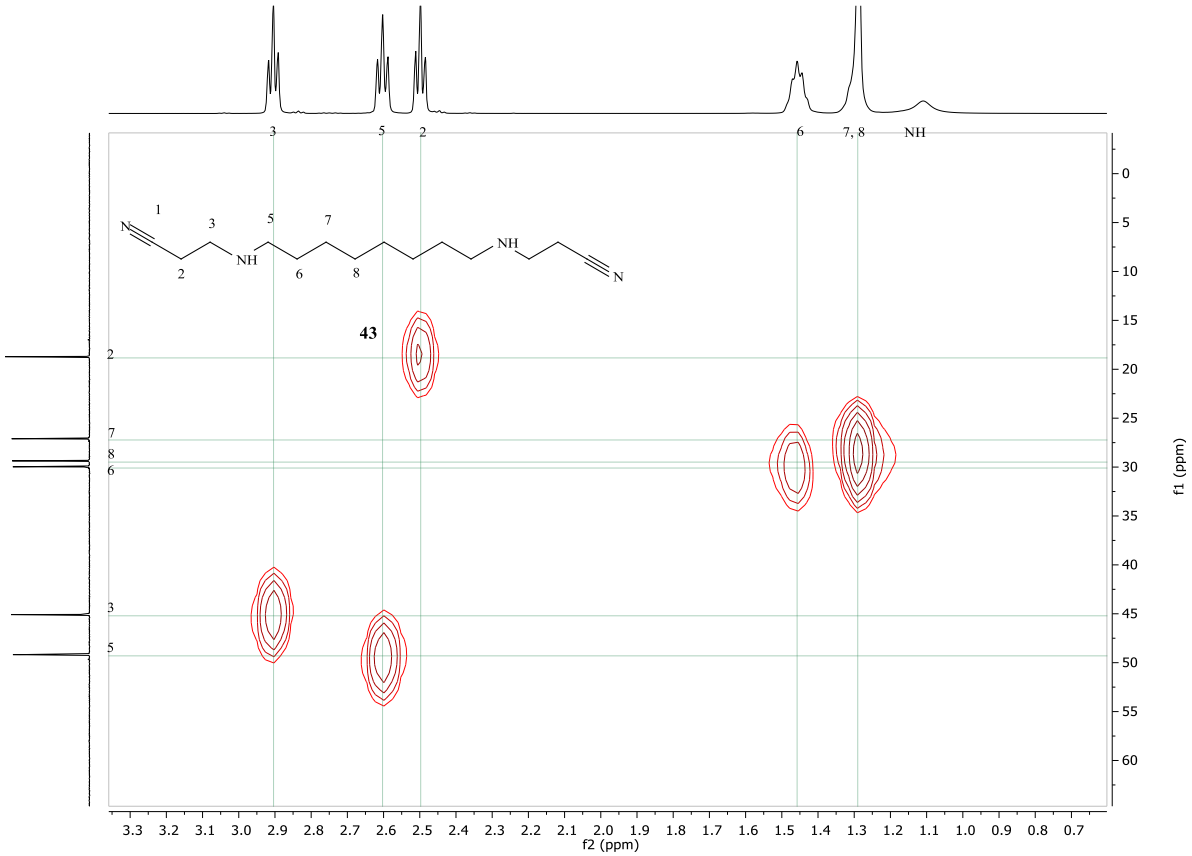

Figure 36: HSQC-NMR spectrum of compound **43**.

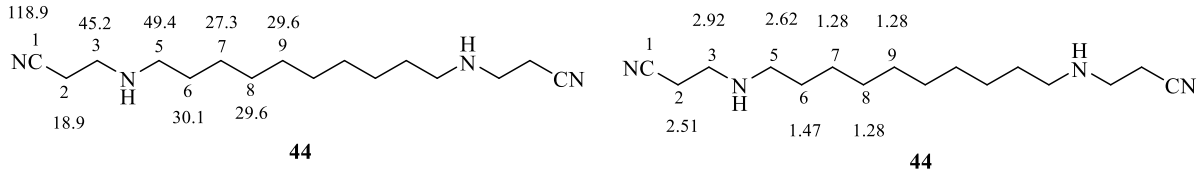

Figure 37: ^{13}C-NMR (Left) and ^{1}H-NMR (right) chemical shifts of **44** in ppm.

Figure 37 shows the chemical shifts of proton and carbon atoms in **44**. Figures 38 to 40 show the ^{13}C, ^{1}H and HSQC-NMR spectrum and assignment of **44**. The ^{13}C-NMR spectrum (Figure 38) shows 7 signals, the downfield low intensity signal at 118.9 ppm is assigned to both C-1 nitrile carbons. The next 2 signals at 49.4 and 45.2 ppm are assigned to NCH_2 carbons C-5 and C-3, respectively, de-shielded by nitrogen. The next 3 signals at 30.1, 29.6 and 27.3 ppm are assigned to carbons C-6, C-8 and C-9, and C-7, respectively. The signal at 29.6 is assigned to two carbons, C-8 and C-9, due to its higher relative intensity. The upfield peak at 18.9 ppm is assigned to C-2.

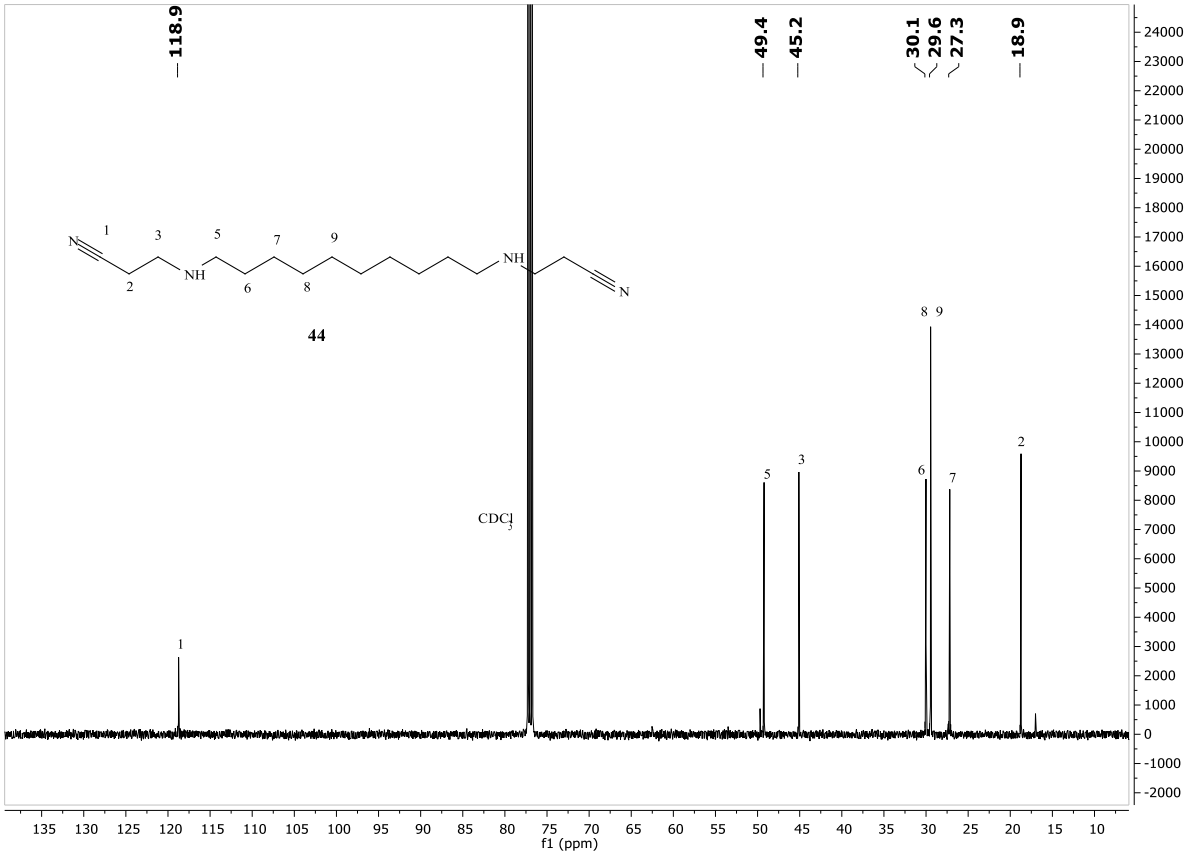

Figure 38: ^{13}C-NMR (125 MHz) spectrum of compound **44**.

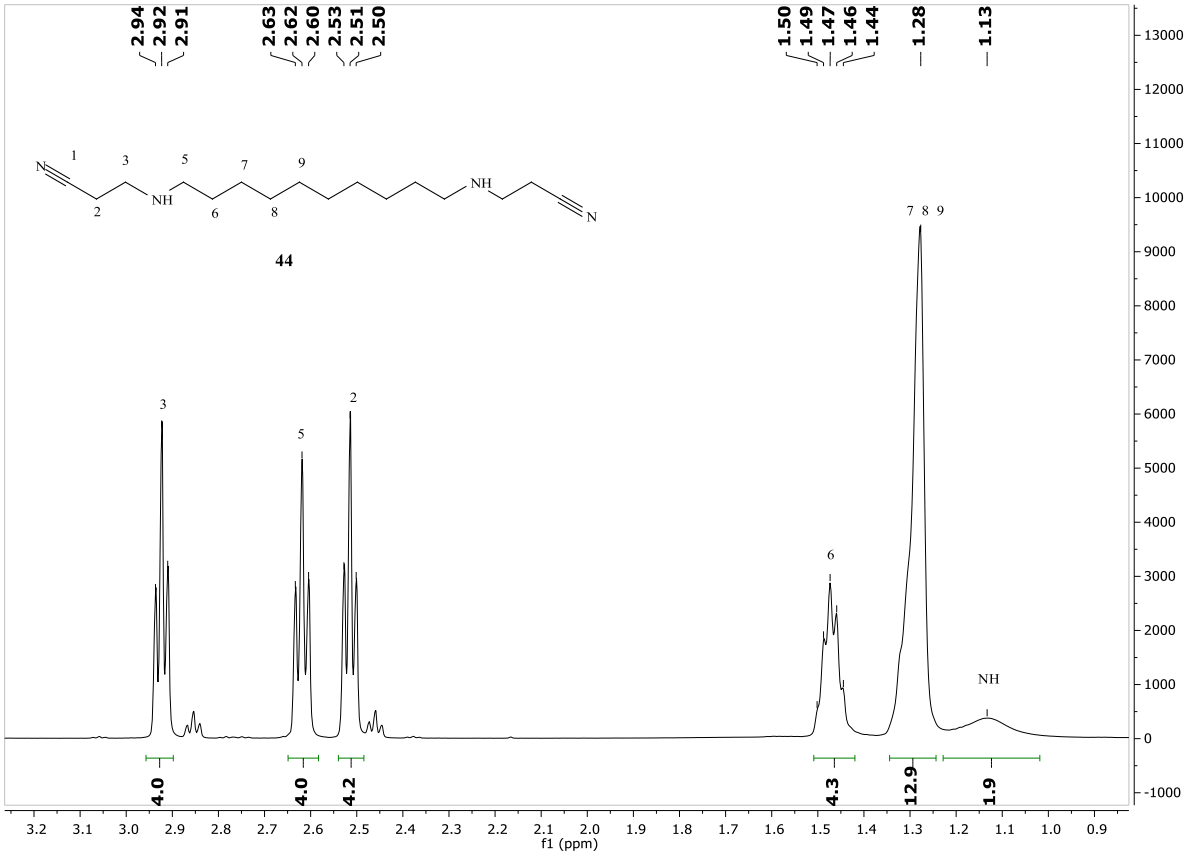

Figure 39: ^{1}H-NMR (500 MHz) spectrum of compound **44**.

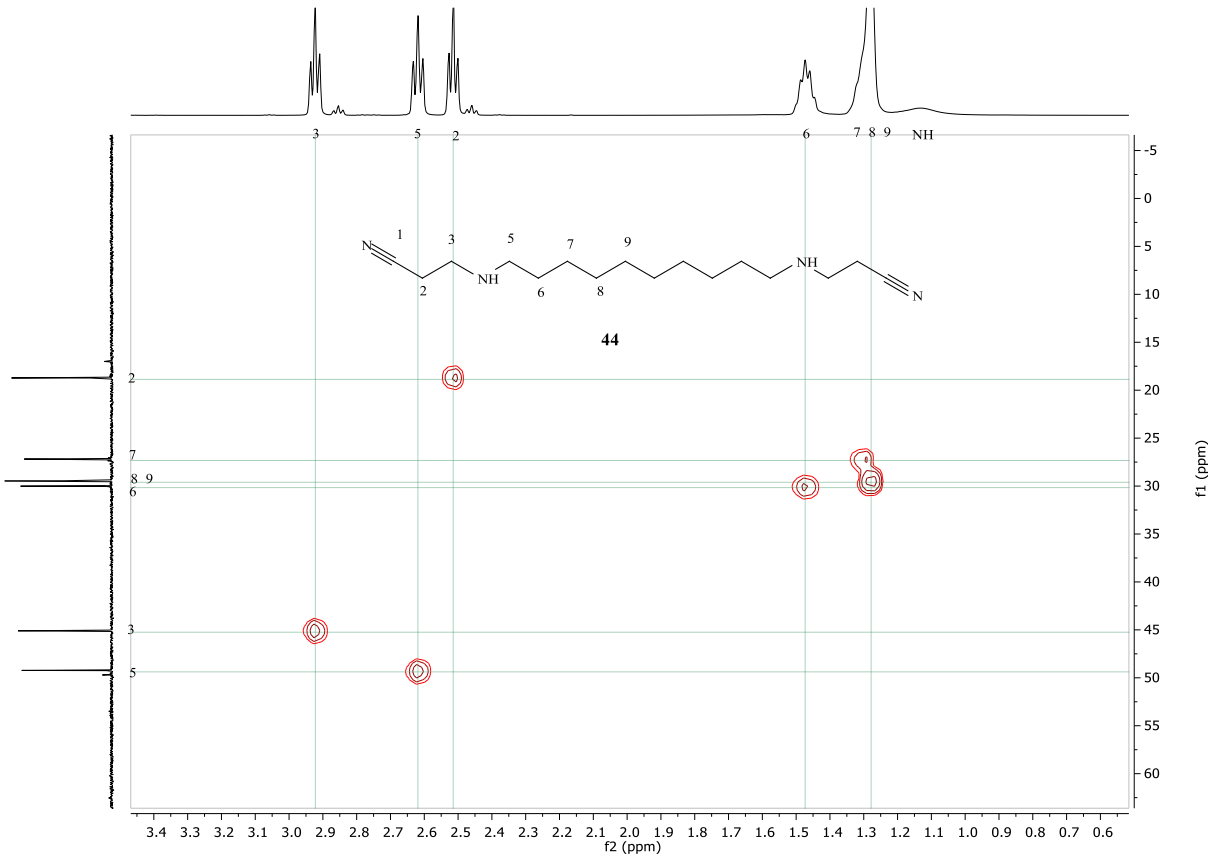

Figure 40: HSQC-NMR spectrum of compound **44**.

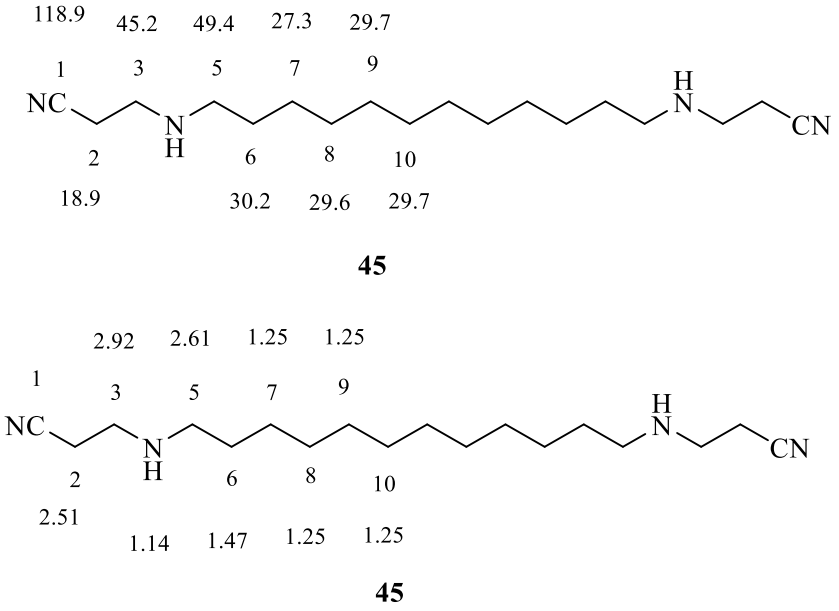

Figure 41: ^{13}C-NMR (upper) and ^{1}H-NMR (lower) chemical shifts of **45** in ppm.

Figure 41 shows the chemical shifts of the proton and carbon atoms in **45**.

Figures 42 to 44 show the ^{13}C, ^{1}H and HSQC-NMR spectrum and assignment of **45**. The ^{13}C-NMR spectrum (Figure 42) shows 9 signals, the downfield low intense signal at 118.9 ppm is assigned to C-1 nitrile carbons. The next 2 signals at 49.4 and 45.2 ppm are assigned to NCH_2 carbons C-5 and C-3, respectively, de-shielded by nitrogen. The next 5 signals at 30.2, 29.7, 29.7, 29.6 and 27.3 ppm are assigned to carbons C-6, C-8, C-9, C-10 and C-7, respectively. The upfield peak at 18.9 ppm is assigned to C-2.

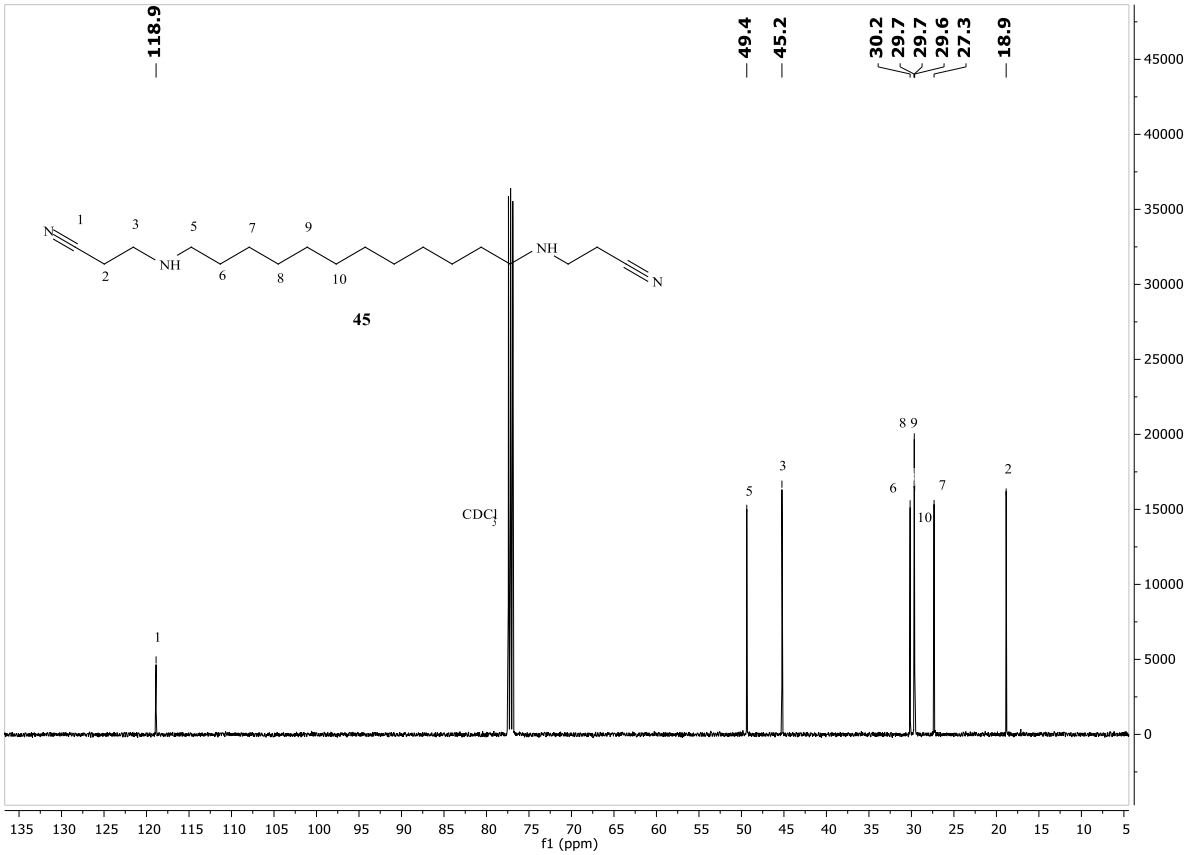

Figure 42: ^{13}C-NMR (125 MHz) spectrum of compound **45**.

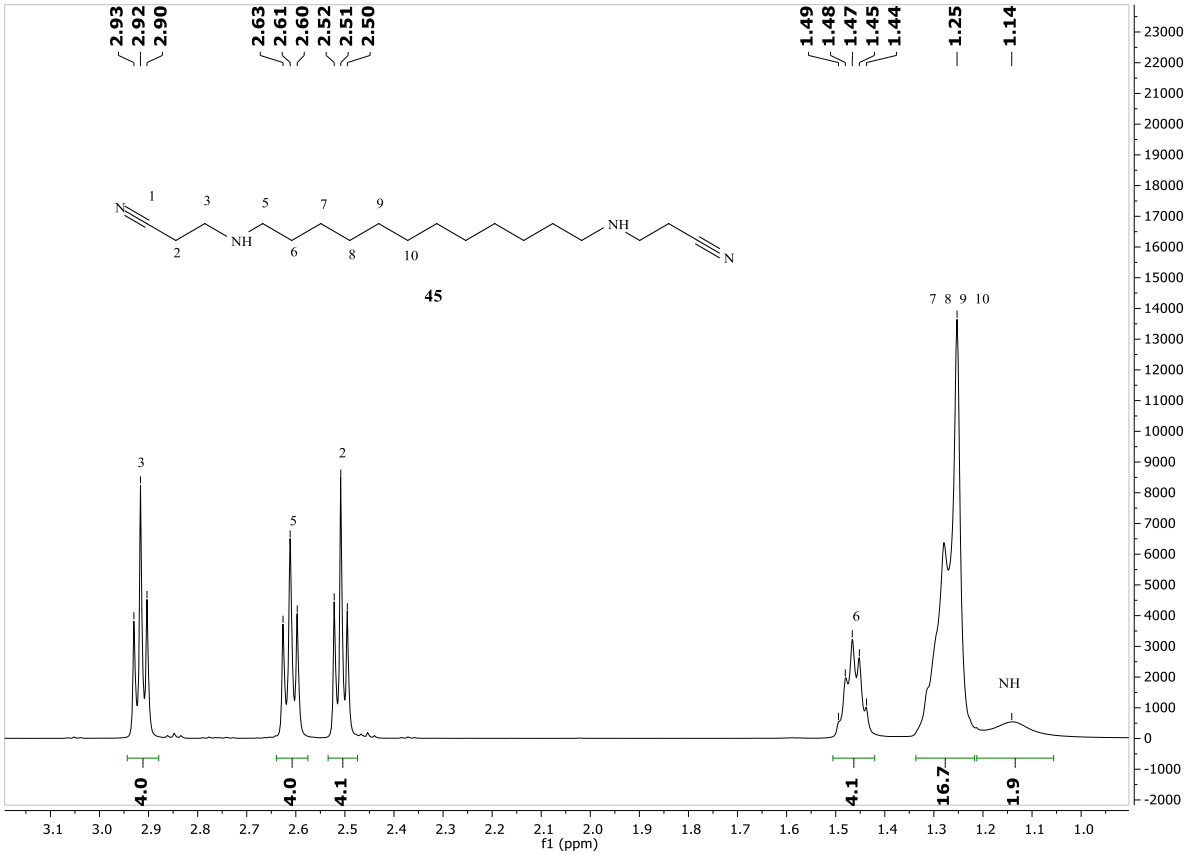

Figure 43: ^{1}H-NMR (500 MHz) spectrum of compound **45**.

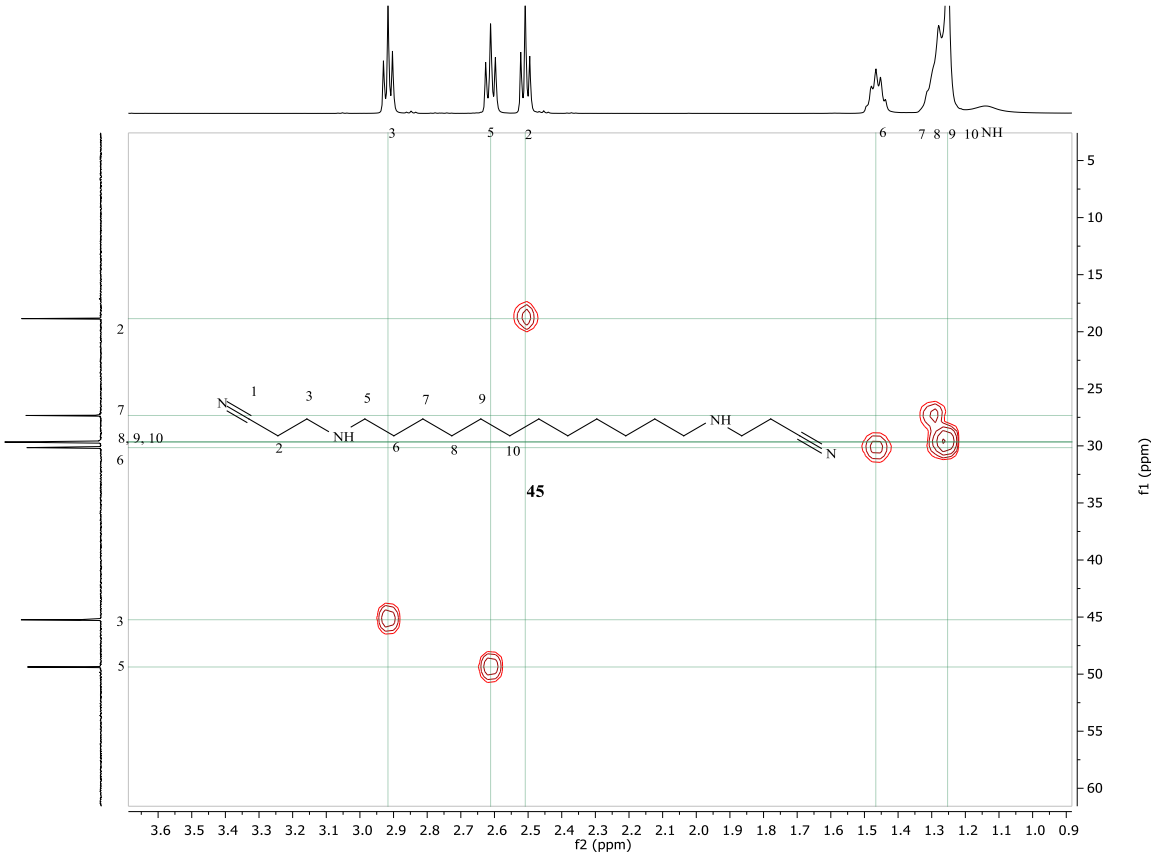

Figure 44: HSQC-NMR spectrum of compound **45**.

As discussed above, all the polyamine conjugate spectral data were fully assigned for these compounds supported by the calculated values of their chemical shifts. Tables 1-9 show the calculated ^{13}C-NMR chemical shifts for compounds **37**-**45** using the equation given by Williams and Fleming (2008); the observed values are all in agreement with the calculated values. These are significant data as is often the case with phytochemistry and the spectroscopic analysis of natural products where the unambiguous assignment allows the correct chemical structure to be confirmed.

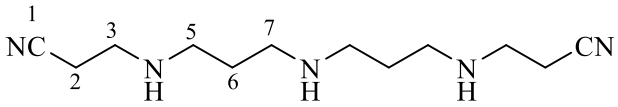

37

Table 1: The calculated ^{13}C-NMR chemical shifts for compound **37** are in agreement with the observed.

	Base value	α-alkyl	α-CN	β-N	γ-alkyl	δ-alkyl			Total	Observed
C2	-2.3	9.1	3.1	11.3	-2.5	0.3			19.0	18.7
		α-alkyl	α-N	β-alkyl	β-CN	γ-alkyl	δ-alkyl			
C3	-2.3	9.1	28.3	9.4	2.4	-2.5	0.3		44.7	45.1
		α-alkyl	α-N	2β-alkyl	γ-N	γ-alkyl	δ-alkyl	δ-CN		
C5	-2.3	9.1	28.3	18.8	-5.1	-2.5	0.3	-0.5	46.1	47.8
		α-alkyl	2β- N	2γ-alkyl	2δ-alkyl					
C6	-2.3	18.2	22.6	-5	0.6				34.1	30.0
		α-alkyl	α-N	2β-alkyl	γ-N	γ-alkyl	2 δ-alkyl			
C7	-2.3	9.1	28.3	18.8	-5.1	-2.5	0.6		46.9	48.4

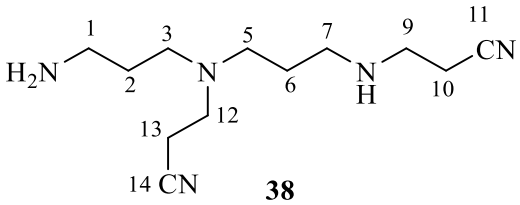

38

Table 2: The calculated ^{13}C-NMR chemical shifts for compound **38** are in agreement with the observed.

	Base value	α-alkyl	α-N	β-alkyl	γ-N	δ-alkyl		Total	Observed
C1	-2.3	9.1	28.3	9.4	-5.1	0.6		40.0	40.1
		2α-alkyl	2β-N	2γ-alkyl	2δ-alkyl				
C2	-2.3	18.2	22.6	-5	0.6			34.1	30.3
		α-alkyl	α-N	3β-alkyl	γ-N	2γ-alkyl	δ-alkyl		
C3	-2.3	9.1	28.3	28.2	-5.1	-5	0.3	53.5	51.4
		α-alkyl	α-N	3β-alkyl	γ-N	2γ-alkyl	2δ-alkyl		
C5	-2.3	9.1	28.3	28.2	-5.1	-5	0.6	53.8	51.8
		2α-alkyl	2β-N	3γ-alkyl	2δ -alkyl				
C6	-2.3	18.2	22.6	-7.5	0.9			31.9	27.4
		α-alkyl	α-N	2β-alkyl	γ-N	γ-alkyl	2δ-alkyl		
C7	-2.3	9.1	28.3	18.8	-5.1	-2.5	0.6	46.9	47.3
		α-alkyl	α-N	β-alkyl	β-CN	γ-alkyl	δ-alkyl		
C9	-2.3	9.1	28.3	9.4	2.4	-2.5	0.3	44.7	45.2
		α-alkyl	α-CN	β-N	γ-alkyl	δ-alkyl			
C10	-2.3	9.1	3.1	11.3	-2.5	0.3		19.0	18.7
		α-alkyl	α-N	2β-alkyl	β-CN	2γ-alkyl	2δ-alkyl		
C12	-2.3	9.1	28.3	18.8	2.4	-5	0.6	51.9	49.5
		α-alkyl	α-CN	β-N	2γ-alkyl	2δ-alkyl			
C13	-2.3	9.1	3.1	11.3	-5	0.6		16.8	16.6

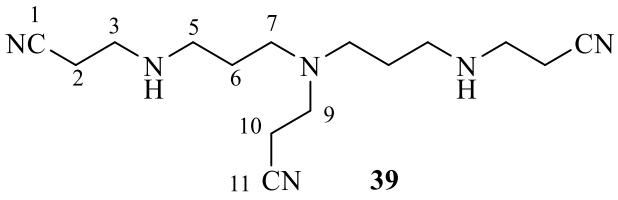

39

Table 3: The calculated ^{13}C-NMR chemical shifts for compound **39** are in agreement with the observed.

	Base value	α-alkyl	α-CN	β-N	γ-alkyl	δ-alkyl			Total	Observed
C2	-2.3	9.1	3.1	11.3	-2.5	0.3			19.0	18.6
		α-alkyl	α-N	β-alkyl	β-CN	γ-alkyl	δ-alkyl			
C3	-2.3	9.1	28.3	9.4	2.4	-2.5	0.3		44.7	45.1
		α-alkyl	α-N	2β-alkyl	γ-N	γ-alkyl	2δ-alkyl			
C5	-2.3	9.1	28.3	18.8	-5.1	-2.5	0.6		46.9	47.2
		2α-alkyl	2β-N	3γ-alkyl	3δ-alkyl					
C6	-2.3	18.2	22.6	-7.5	0.9				31.9	27.4
		α-alkyl	α-N	3β-alkyl	γ-N	2γ-alkyl	2δ-alkyl	S		
C7	-2.3	9.1	28.3	28.2	-5.1	-5	0.6	-2.5	51.3	51.7
		α-alkyl	α-N	2β-alkyl	β-CN	2γ-alkyl	2δ-alkyl			
C9	-2.3	9.1	28.3	18.8	2.4	-5	0.6	-2.5	47.0	49.5
		α-alkyl	α-CN	β-N	2γ-alkyl	δ-alkyl				
C10	-2.3	9.1	3.1	11.3	-5	0.6			16.8	16.7

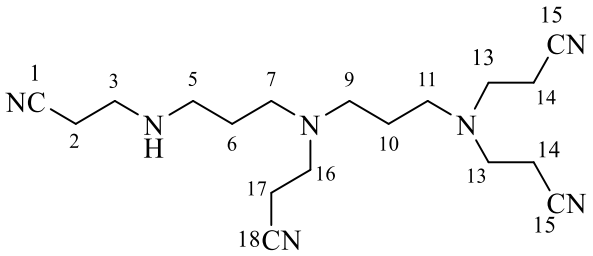

40

Table 4: The calculated ^{13}C-NMR chemical shifts for compound **40** are in agreement with the observed.

	Base value	α-alkyl	α-CN	β-N	γ-alkyl	δ-alkyl			Total	Observed
C2	-2.3	9.1	3.1	11.3	-2.5	0.3			19.0	18.7
		α-alkyl	α-N	β-alkyl	β-CN	γ-alkyl	δ-alkyl			
C3	-2.3	9.1	28.3	9.4	2.4	-2.5	0.3		44.7	45.1
		α-alkyl	α-N	2β-alkyl	γ-N	γ-alkyl	2δ-alkyl			
C5	-2.3	9.1	28.3	18.8	-5.1	-2.5	0.6		46.9	49.4
		2α-alkyl	2β-N	3γ-alkyl	2δ-alkyl					
C6	-2.3	18.2	22.6	-7.5	0.9				31.9	27.3
		α-alkyl	α-N	3β-alkyl	γ-N	2γ-alkyl	2γ-alkyl	S		
C7	-2.3	9.1	28.3	28.2	-5.1	-5	0.6	-2.5	51.3	51.2
		α-alkyl	α-N	3β-alkyl	γ-N	2γ-alkyl	3δ-alkyl	S		
C9	-2.3	9.1	28.3	28.2	-5.1	-5	0.9	-2.5	51.6	51.1
		2α-alkyl	2β-N	4γ-alkyl	4δ-alkyl					
10	-2.3	18.2	22.6	-10	1.2				29.7	25.4

		α-alkyl	α-N	3β-alkyl	γ-N	2γ-alkyl	2δ-alkyl	S		
C11	-2.3	9.1	28.3	28.2	-5.1	-5	0.6	-2.5	51.3	51.8
		α-alkyl	α-N	2β-alkyl	β-CN	2γ-alkyl	δ-alkyl	S		
C13	-2.3	9.1	28.3	18.4	2.4	-5	0.3	-2.5	49.1	49.5
		α-alkyl	α-CN	β-N	2γ-alkyl	2δ-alkyl				
C14	-2.3	9.1	3.1	11.3	-5	0.6			16.8	16.9
		α-alkyl	α-N	2β-alkyl	β-CN	2γ-alkyl	2δ-alkyl			
C16	-2.3	9.1	28.3	18.8	2.4	-5	0.6	-2.5	47.0	47.3
		α-alkyl	α-CN	β-N	2γ-alkyl	δ-alkyl				
C17	-2.3	9.1	3.1	11.3	-5	0.6			16.8	16.8

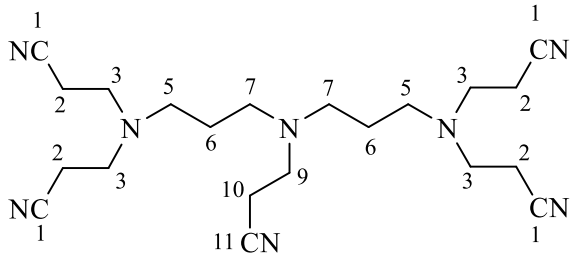

41

Table 5: The calculated ^{13}C-NMR chemical shifts for compound **41** are in agreement with the observed.

	Base value	α-alkyl	α-CN	β-N	2γ-alkyl	2δ-alkyl			Total	Observed
C2	-2.3	9.1	3.1	11.3	-5	0.6			16.8	17.0
		α-alkyl	α-N	2β-alkyl	β-CN	2γ-alkyl	δ-alkyl	S		
C3	-2.3	9.1	28.3	18.8	2.4	-5	0.3	-2.5	49.1	49.6

		α-alkyl	α-N	2β-alkyl	γ-N	2γ-alkyl	2δ-alkyl	S		
C5	-2.3	9.1	28.3	28.2	-5.1	-5	0.6	-2.5	51.3	51.3
		2α-alkyl	2β-N	3γ-alkyl	2δ-alkyl					
C6	-2.3	18.2	22.6	-10	1.2				29.7	25.4
		α-alkyl	α-N	3β-alkyl	γ-N	2γ-alkyl	3 δ-alkyl	S		
C7	-2.3	9.1	28.3	28.2	-5.1	-5	0.9	-2.5	51.6	51.2
		α-alkyl	α-N	2β-alkyl	β-CN	2γ-alkyl	2δ-alkyl			
C9	-2.3	9.1	28.3	18.8	2.4	-5	0.6	-2.5	47.0	49.3
		α-alkyl	α-CN	β-N	2γ-alkyl	δ-alkyl				
C10	-2.3	9.1	3.1	11.3	-5	0.6			16.8	16.9

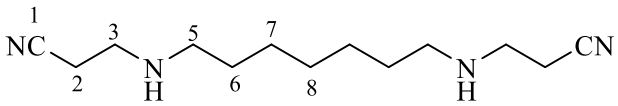

42

Table 6: The calculated ^{13}C-NMR chemical shifts for compound **42** are in agreement with the observed.

	Base value	α-alkyl	α-CN	β-N	γ-alkyl	δ-alkyl		Total	Observed
C2	-2.3	9.1	3.1	11.3	-2.5	0.3		19.0	18.8
		α-alkyl	α-N	β-alkyl	β-CN	γ-alkyl	δ-alkyl		
C3	-2.3	9.1	28.3	9.4	2.4	-2.5	0.3	44.7	45.2
		α-alkyl	α-N	2β-alkyl	β-CN	2γ-alkyl	2δ-alkyl		
C5	-2.3	9.1	28.3	18.8	2.4	-5	0.6	48.7	49.3

		α-alkyl	β-N	β-alkyl	2γ-alkyl	2δ-alkyl			
C6	-2.3	9.1, 9.1	11.3	9.4	-5	0.6		32.2	30.0
		α-alkyl	2β-alkyl	γ-N	γ-alkyl	2δ-alkyl			
C7	-2.3	9.1, 9.1	18.8	-5.1	-2.5	0.6		27.7	27.2
		2α-alkyl	2β-alkyl	2γ-alkyl					
C8	-2.3	18.2	18.8	-5				29.7	29.4

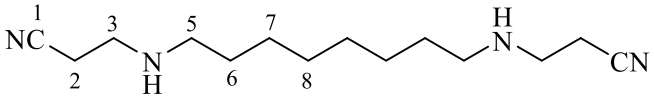

43

Table 7: The calculated ^{13}C-NMR chemical shifts for compound **43** are in agreement with the observed.

	Base value	α-alkyl	α-CN	β-N	γ-alkyl	δ-alkyl		Total	Observed
C2	-2.3	9.1	3.1	11.3	-2.5	0.3		19.0	18.8
		α-alkyl	α-N	β-alkyl	β-CN	γ-alkyl	δ-alkyl		
C3	-2.3	9.1	28.3	9.4	2.4	-2.5	0.3	44.7	45.2
		α-alkyl	α-N	2β-alkyl	β-CN	2γ-alkyl	2δ-alkyl		
C5	-2.3	9.1	28.3	18.8	2.4	-5	0.6	48.7	49.3
		2α-alkyl	β-N	β-alkyl	2γ-alkyl	2δ-alkyl			
C6	-2.3	18.2	11.3	9.4	-5	0.6		32.2	30.1
		2α-alkyl	2β-alkyl	γ- N	γ-alkyl	2δ-alkyl			
C7	-2.3	18.2	18.8	-5.1	-2.5	0.6		27.7	27.2

		2α-alkyl	2β-alkyl	2γ-alkyl	δ-alkyl				
C8	-2.3	18.2	18.8	-5	0.3			30.0	29.5

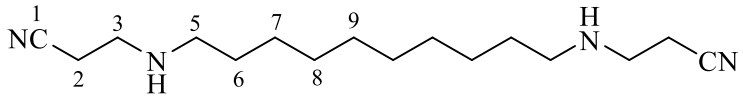

44

Table 8: The calculated ^{13}C-NMR chemical shifts for compound **44** are in agreement with the observed.

	Base value	α-alkyl	α-CN	β-N	γ-alkyl	δ-alkyl		Total	Observed
C2	-2.3	9.1	3.1	11.3	-2.5	0.3		19.0	18.9
		α-alkyl	α-N	β-alkyl	β-CN	γ-alkyl	δ-alkyl		
C3	-2.3	9.1	28.3	9.4	2.4	-2.5	0.3	44.7	45.2
		α-alkyl	α-N	2β-alkyl	β-CN	2γ-alkyl	2δ-alkyl		
C5	-2.3	9.1	28.3	18.8	2.4	-5	0.6	48.7	49.4
		2α-alkyl	β-N	β-alkyl	2γ-alkyl	2δ-alkyl			
C6	-2.3	18.2	11.3	9.4	-5	0.6		32.2	30.1
		2α-alkyl	2β-alkyl	γ-N	γ-alkyl	2δ-alkyl			
C7	-2.3	18.2	18.8	-5.1	-2.5	0.6		27.7	27.3
		2α-alkyl	2β-alkyl	2γ-alkyl	δ-alkyl				
C8	-2.3	18.2	18.8	-5	0.3			30.0	29.6
		2α-alkyl	2β-alkyl	2γ-alkyl	δ-alkyl				
C9	-2.3	18.2	18.8	-5	0.3			30.3	29.6

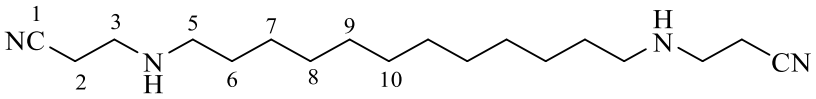

45

Table 9: The calculated ^{13}C-NMR chemical shifts for compound **45** are in agreement with the observed.

	Base value	α-alkyl	α-CN	β-N	γ-alkyl	δ-alkyl		Total	Observed
C2	-2.3	9.1	3.1	11.3	-2.5	0.3		19.0	18.9
		α-alkyl	α-N	β-alkyl	β-CN	γ-alkyl	δ-alkyl		
C3	-2.3	9.1	28.3	9.4	2.4	-2.5	0.3	44.7	45.2
		α-alkyl	α-N	2β-alkyl	β-CN	2γ-alkyl	2δ-alkyl		
C5	-2.3	9.1	28.3	18.8	2.4	-5	0.6	48.7	49.4
		2α-alkyl	β-N	β-alkyl	2γ-alkyl	2δ-alkyl			
C6	-2.3	18.2	11.3	9.4	-5	0.6		32.2	30.2
		α-alkyl	2β-alkyl	γ-N	γ-alkyl	2δ-alkyl			
C7	-2.3	9.1, 9.1	18.8	-5.1	-2.5	0.6		27.7	27.3
		2α-alkyl	2β-alkyl	2γ-alkyl	δ-alkyl				
C8	-2.3	18.2	18.8	-5	0.3			30.0	29.6
		2α-alkyl	2β-alkyl	2γ-alkyl	δ-alkyl				
C9	-2.3	18.2	18.8	-5	0.3			30.3	29.7
		2α-alkyl	2β-alkyl	2γ-alkyl	δ-alkyl				
C10	-2.3	18.2	18.8	-5	0.3			30.3	29.7

2.4 Experimental

Materials

Norspermidine, norspermine, spermidine, spermine, paraformaldehyde, acrylonitrile, and Raney nickel were purchased from Sigma-Aldrich. Anhydrous sodium sulfate and Celite were purchased from Fisher Scientific. Anhydrous methanol, methanol, ethanol, acetone, chloroform, dichloromethane, ethyl acetate, and ammonia were purchased from VWR. $CDCl_3$, DMSO-d_6 and deuterium oxide were purchased from Goss Scientific. All chemicals and solvents were used in reactions directly as obtained, without further purification.

Thin-Layer Chromatography (TLC) was carried out on aluminium-backed silica gel F_{254} plates 20 x 20 cm purchased from Merck (Darmstadt, Germany). Reaction mixtures and products were separated using the following mobile phases: $CHCl_3$: EtOH: NH_4OH (5:10:12, v/v/v); $CHCl_3$: EtOH: NH_4OH (5:5:1, v/v/v); $CHCl_3$: EtOH: NH_4OH (7:3:1, v/v/v); CH_2Cl_2: EtOH: EtOAc: NH_4OH (3:3:3:0.5, v/v/v/v). After drying, the TLC eluted chromatograms were developed by spraying with Dragendorff's reagent which was prepared by mixing two solutions A and B. Solution A contains bismuth nitrate (0.17 g) in glacial acetic acid (2 mL) and H_2O (8 mL). Solution B contains KI (4 g) in glacial acetic acid (10 mL) and H_2O (20 mL). Solutions A and B were mixed and then diluted to 100 mL with H_2O (Bisen, 2014). An alternative TLC spray reagent for amines is ninhydrin reagent (0.2 g of ninhydrin in 100 mL ethanol). Column chromatography was performed on silica gel 60-120 mesh (purchased from Sigma-Aldrich) using different ratios of ethanol, methanol, chloroform, and concentrated aqueous ammonia (NH_4OH) as eluents.

Instrumentation

NMR spectroscopic analysis (^{1}H, ^{13}C, and HSQC) was carried out by dissolving samples (about 15 mg) in $CDCl_3$, DMSO-d_6 or D_2O (0.6 mL). IR spectroscopic analysis used a Perkin-Elmer 65 FT-IR spectrometer with solid samples prepared as KBr discs and liquid samples examined as thin films on NaCl plates. High Resolution Time-of-Flight (HR TOF) mass spectra were obtained on a Bruker Daltonics "micrOTOF" mass spectrometer using positive-ion mode electrospray ionisation (ESI).

General procedure for analogue synthesis.

Compounds **25**-**28** were prepared as previously described by the Blagbrough research group (Ashton et al., 1995) with the exception that paraformaldehyde was used instead of formalin. Briefly, each polyamine (1 g each of spermidine, spermine, norspermidine, or norspermine) was dissolved in water (30 mL). The aqueous solution was then cooled to 5 °C and paraformaldehyde (1 or 2 eq. depending upon the starting material) was added. The mixture was stirred for 1 h at 20 °C and then thoroughly extracted with chloroform (8 x), dried (Na_2SO_4), filtered and the solvent was then removed under reduced pressure. Compounds (**29**-**32** and **37**-**41**) were synthesized as previously described (Frydman et al., 2004) with the exception that anhydrous methanol was used instead of ethanol. The formaldehyde adducts were dissolved in anhydrous methanol followed by the dropwise addition of acrylonitrile with stirring under N_2. After 15 h, more acrylonitrile was added because not all of the starting material was reacted (TLC analysis) and stirring was continued for a further 9 h. The resulting mixture was then concentrated under reduced pressure. Compounds **33**-**36** and **46**-**49** were prepared as previously described (Bergeron and Garlich, 1984). Products were purified to homogeneity by column chromatography, and characterised by HR-MS, IR, and ^{1}H, ^{13}C and HSQC NMR spectroscopy.

*2.4.1 Synthesis of 3-(hexahydropyrimidin-1(2H)-yl)propan-1-amine (**25**).*

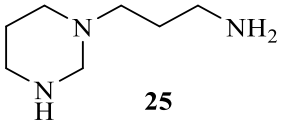

25

Method A: this compound was prepared as previously described (Ashton et al., 1995) except that solid paraformaldehyde was used instead of aqueous formalin solution. To norspermidine **3** (1.00 g, 7.62 mmol) in distilled water (30 mL), cooled to 5 °C, was added paraformaldehyde (0.229 g, 7.62 mmol, 1 eq.). After stirring for 1 h at 20 °C the resulting mixture was then thoroughly extracted with chloroform (8 x 10 mL). The combined organic extracts were dried (Na_2SO_4), filtered and the solvent was removed under reduced pressure to give a colourless oil (0.280 g, 26%).

IR: 3303 (NH), 2938, 2805 (CH_2) cm^{-1};

HRMS: found 144.1477, $C_7H_{18}N_3$ requires 144.1495 $[M+H]^+$;

^1H NMR (400 MHz; $CDCl_3$): 1.48-1.56 (m, 4 H, $2CH_2$), 1.78 (br s, 3 H, NH and NH_2), 2.20 (t, *J* = 7.6 Hz, 2 H, NCH_2), 2.47 (br s, 2 H, NCH_2), 2.64 (t, *J* = 6.8 Hz, 2 H, NCH_2), 2.71 (t, *J* = 5.6 Hz, 2H, NCH_2), 3.28 (s, 2 H, NCH_2N);

^{13}C NMR (100 MHz; $CDCl_3$): 27.0, 30.4 (CH_2), 40.6, 45.1, 53.0, 53.1 (NCH_2), 69.9 (NCH_2N).

The spectral data are in agreement with those reported (Houen et al., 2005).

The above reaction was repeated under different conditions to increase the yield.

Method B: to norspermidine (1.00 g, 7.62 mmol) in methanol (15 mL, 0.01M NaOH) cooled to 5 °C was added paraformaldehyde (0.229 g, 7.62 mmol, 1 eq.). After stirring for 1 h at 20 °C the TLC analysis showed several spots.

To norspermidine (10.00 g, 76.2 mmol) in distilled water (60 mL) cooled to 5 °C was added paraformaldehyde (2.29 g, 76.2 mmol, 1 eq.). After stirring for 1 h at 20 °C, TLC

analysis showed one spot (R_f = 0.4, ethanol: $CHCl_3$: NH_4OH, 5: 5: 1 v/v/v). Sodium hydroxide pellets were added until a second layer appeared. The organic layer was removed and dissolved in chloroform. The aqueous layer was thoroughly extracted with chloroform (8 x 10 mL). The combined chloroform fractions were dried (Na_2SO_4), filtered and the solvent was removed under reduced pressure to give a colourless oil (8.39 g, 77%) that was used in the next step without further purification.

*2.4.2 Synthesis 4-(hexahydropyrimidin-1(2H)-yl)butan-1-amine (**26**).*

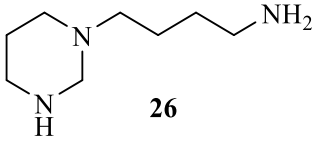

26

Method A: this compound was prepared by the same procedure as described for **25**. To spermidine (1.00 g, 6.89 mmol) in distilled water (30 mL), cooled to 5 °C, paraformaldehyde (0.207 g, 6.89 mmol, 1 eq.) was added. After stirring for 1 h at 20 °C, the resulting mixture was thoroughly extracted with chloroform (8 x 10 mL). The combined chloroform fractions were dried (Na_2SO_4), filtered and the solvent was removed under reduced pressure to give a colourless oil (0.65 g, 60%).

IR: 3343 (NH), 2940 and 2861 (CH_2) cm^{-1};

HRMS: Found 158.1645, $C_8H_{19}N_4$ requires 158.1652 $[M+H]^+$;

^{1}H NMR (400 MHz): 1.37-1.55 (m, 4 H, 2CH_2), 1.57 (quin, *J* = 5.5 Hz, 2 H, CH_2), 2.19-2.22 (m, 2 H, NCH_2), 2.53 (br s, 2 H, NCH_2), 2.66 (t, *J* = 6.4 Hz, 2 H, NCH_2), 2.77 (t, *J* = 5.5 Hz, 2 H, NCH_2), 3.34 (s, 2 H, NCH_2N);

^{13}C NMR (100 MHz): 24.2, 27.0, 31.7 (CH_2), 41.9, 45.1, 53.0, 55.3 (NCH_2), 69.8 (NCH_2N).

The spectral data are in agreement with those reported (Siddiqui et al., 1999).

The above reaction was repeated with different conditions to increase the yield.

Method B: to spermidine (5.00 g, 34.4 mmol) in distilled water (75 mL) cooled to 5 °C was added paraformaldehyde (1.083 g, 36.1 mmol, 1.05 eq.). After stirring for 1 h at 20 °C the TLC analysis showed one spot (R_f = 0.3, ethanol: $CHCl_3$: NH_4OH, 5: 5: 1 v/v/v). Sodium hydroxide pellets were added until a second layer appeared. The upper organic layer was removed and dissolved in chloroform. The aqueous layer was thoroughly extracted with chloroform (8 x 10 mL). The combined chloroform fractions were dried (Na_2SO_4), filtered and the solvent was removed under reduced pressure to give a colourless oil (4.90 g, 90%).

*2.4.3 Synthesis of 1,3-bis(hexahydropyrimidin-1(2H)-yl)propane (**27**).*

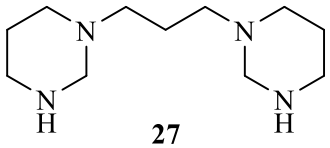

27

This compound was prepared following the same procedure described for **25**. To norspermine (1.00 g, 5.31 mmol) in distilled water (30 mL) cooled to 5 °C was added paraformaldehyde (0.318 g, 10.62 mmol, 2 eq.). After stirring for 1 h at 20 °C, the resulting mixture was then thoroughly extracted with chloroform (8 x 10 mL). The combined chloroform fractions were dried (Na_2SO_4), filtered and the solvent was removed under reduced pressure to give a colourless oil (0.61 g, 54%).

IR: 3263 (NH), 2937 and 2793 (CH_2) cm^{-1};

HRMS: Found 213.2100, $C_{11}H_{25}N_4$ requires 213.2074 $[M+H]^+$;

^{1}H NMR (400 MHz): 1.55-1.66 (m, 8 H, 3CH_2, 2NH), 2.23 (t, *J* = 7.6 Hz, 4 H, 2NCH_2), 2.54 (br s, 4 H, 2NCH_2), 2.78 (t, *J* = 6.0 Hz, 4 H, 2NCH_2), 3.35 (s, 4 H, 2NCH_2N)

^{13}C NMR: (100 MHz): 24.3, 27.1 (3 x CH_2), 45.2, 53.1, 53.6 (6 x NCH_2), 70.0 (2 x NCH_2N).

This compound has not been previously reported.

*2.4.4 Synthesis 1,4-bis(hexahydropyrimidin-1(2H)-yl)butane (**28**).*

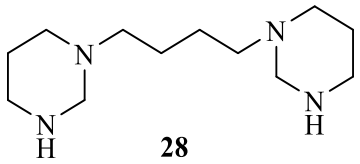

28

Method A: to spermine (1.00 g, 4.94 mmol) in distilled water (30 mL), cooled to 5 °C, was added paraformaldehyde (0.297 g, 9.88 mmol, 2 eq.) After stirring for 1 h at 20 °C, the resulting mixture was then thoroughly extracted with chloroform (8 x 10 mL). The combined chloroform fractions were dried (Na_2SO_4), filtered and the solvent was removed under reduced pressure to give a colourless oil (0.38 g, 34%).

IR: 3348 (NH), 2934 (CH_2) cm^{-1};

HRMS: Found 227.2273, $C_{12}H_{27}N_4$ requires 227.2230 $[M + H]^+$;

^{1}H NMR (400 MHz): 1.41-1.50 (m, 4 H, 2CH_2), 1.55-1.65 (m, 6 H, 2NH and 2CH_2), 2.21 (br s, 4 H, 2NCH_2), 2.53 (br s, 4 H, 2NCH_2), 2.78 (t, *J* = 6.0 Hz, 4 H, 2NCH_2), 3.34 (s, 4 H, 2NCH_2N);

^{13}C NMR (100 MHz): 25.0, 27.2 (4 x CH_2), 45.2, 53.1, 55.4 (6 x NCH_2), 70.0 (2 x NCH_2N).

This compound was previously reported, but without any spectral data (Ganem, 1982).

Method B: the above reaction was repeated with different conditions in order to increase the yield. To spermine (5.00 g, 24.7 mmol) in distilled water (75 mL), cooled to 5 °C, was added paraformaldehyde (1.558 g, 51.9 mmol, 2.05 eq.). After stirring for 1 h at 20 °C the TLC analysis showed one spot (R_f = 0.6, ethanol: $CHCl_3$: NH_4OH, 5: 5: 1 v/v/v). Sodium hydroxide pellets were added until a second layer appeared. The upper organic layer was removed and dissolved in chloroform. The aqueous layer was thoroughly extracted with chloroform (8 x 10 mL). The combined chloroform fractions were dried (Na_2SO_4), filtered and the solvent was removed under reduced pressure to give a colourless oil (4.50 g, 81%).

*2.4.5 Synthesis of 3-(3-(3-((2-cyanoethyl)amino)propyl)hexahydropyrimidin-1(2H)-yl)propanenitrile (**29**).*

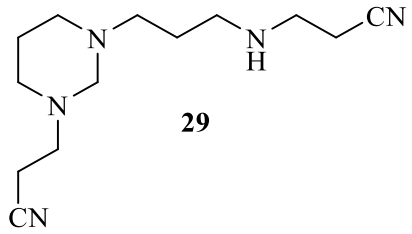

29

This compound was prepared as previously described (Frydman et al., 2004) with the exception that anhydrous methanol was used instead of ethanol. To **25** (1.00 g, 6.98 mmol) in anhydrous methanol (15 mL) was added acrylonitrile (0.91 mL, d = 0.81 g/mL, 0.741 g, 13.96 mmol, 2 eq.) and the solution was stirred at 20 °C under N_2 for 15 h. TLC analysis showed that the reaction had not gone to completion by the presence of two spots (R_f = 0.1, 0.6, ethanol: ethyl acetate: CH_2Cl_2: NH_4OH, 3: 3: 3: 0.5 v/v/v/v). Therefore, an excess of acrylonitrile (0.46 mL, d = 0.81 g/mL, 0.37 g, 6.98 mmol, 1 equivalent) was added and stirring continued for a further 7 h and then the excess of acrylonitrile and the solvent were removed under reduced pressure to give a colourless oil (1.18 g, 53%).

IR: 3306, (NH), 2940 and 2818 (CH_2), 2249 (CN) cm^{-1};

HRMS: Found 250.2046, $C_{13}H_{24}N_5$ requires 250.2032 $[M+H]^+$;

^{1}H NMR (400 MHz; $CDCl_3$): 1.55-1.63 (m, 4 H), 2.34 (t, *J* = 7.2 Hz, 2 H), 2.42-2.47 (m, 6 H), 2.53-2.56 (m, 2 H), 2.61 (t, *J* = 6.8 Hz, 2 H), 2.69 (t, *J* = 6.8 Hz, 2 H), 2.84 (t, *J* = 6.4 Hz, 2 H) (10 CH_2), 3.15 (s, 2 H, NCH_2N).

^{13}C NMR (100 MHz; $CDCl_3$): 16.6, 18.5, 22.7, 27.0 (4 x CH_2), 45.0, 47.6, 50.0, 51.8, 52.3, 53.0 (6 x CH_2), 75.2 (NCH_2N), 118.8, 118.9 (2 x CN).

The spectral data are in agreement with those reported (Frydman et al., 2004) except that $[M + H]^+$ is 250 not 249.

2.4.6 Synthesis of *3-(3-(4-((2-cyanoethyl)amino)butyl)hexahydropyrimidin-1(2H)-yl)-propanenitrile (**30**).*

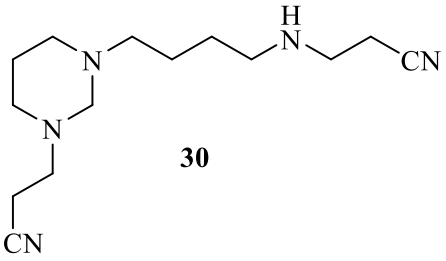

30

Method A: this compound was prepared by the same procedure as described for **29**. To **26** (1.00 g, 6.36 mmol) in anhydrous methanol (15 mL) was added acrylonitrile (0.84 mL, d = 0.81 g/mL, 0.68 g, 12.72 mmol, 2 eq.) and the solution was stirred at 20 °C under N_2 for 15 h. TLC analysis showed that the reaction had not gone to completion by the presence of two spots (R_f = 0.1, 0.7, ethanol: ethyl acetate: CH_2Cl_2: NH_4OH, 3: 3: 3: 0.5 v/v/v/v). Therefore, an excess of acrylonitrile (0.42 mL, d = 0.81 g/mL, 0.34 g, 6.36 mmol, 1 equivalent) was added and stirring continued for a further 7 h and then the excess of acrylonitrile and the solvent were removed under reduced pressure to give a colourless oil (1.61 g, 96%).

IR: 3352 (NH), 2937 and 2815 (CH_2), 2247 (CN) cm^{-1};

HRMS: Found 264.2190, $C_{14}H_{26}N_5$ requires 264.2183 $[M + H]^+$;

^{1}H NMR (400 MHz): 1.37-1.50 (m, 4 H), 1.58-1.63 (m, 2 H), 2.24-2.31 (m, 2 H), 2.39-2.47 (m, 6 H), 2.51-2.61 (m, 4 H), 2.69 (t, *J* = 7.2 Hz, 2 H), 2.85 (t, *J* = 6.8 Hz, 2 H) (11 CH_2), 3.15 (s, 2 H, NCH_2N);

^{13}C NMR (100 MHz): 16.6, 18.7, 22.8, 24.8, 27.9 (5 x CH_2), 45.0, 48.9, 50.1, 51.9, 52.2, 54.7 (6 x NCH_2), 75.4 (NCH_2N), 118.6, 118.8 (2 x CN).

This compound has not been previously reported.

Method B: the above reaction was repeated with different conditions in order to increase the scale.

To 4-(hexahydropyrimidin-1(2H)-yl)butan-1-amine (4.9 g, 31.2 mmol) in anhydrous methanol (25 mL) was added acrylonitrile (4.1 mL, d = 0.81 g/mL, 3.32 g, 62.6 mmol, 2 eq.) dissolved in methanol (15 mL) dropwise over 10 min, and the solution was stirred at 20 °C under N_2 for 15 h. TLC analysis showed the presence of two spots (R_f = 0.1, 0.7, ethanol: ethyl acetate: CH_2Cl_2: NH_4OH, 3: 3: 3: 0.5 v/v/v/v). However the NMR analysis showed high purity, the second spot was only a minor impurity. The excess of acrylonitrile and the solvent were removed under reduced pressure to give a colourless oil (7.847 g, 96%).

*2.4.7 Synthesis of 3,3'-(propane-1,3-diylbis(hexahydropyrimidine-3,1(2H)-diyl))-di-propanenitrile (**31**).*

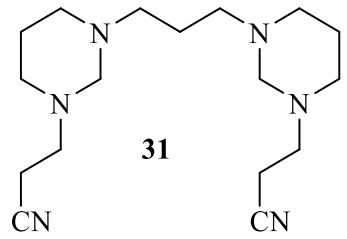

31

This compound was prepared using the same procedure as described for **29**. To **27** (1.00 g, 4.71 mmol) in anhydrous methanol (15 mL) was added acrylonitrile (0.62 mL, d = 0.81 g/mL, 0.450 g, 9.42 mmol, 2 eq.) and the solution was stirred at 20 °C under N_2 for 15 h. TLC analysis showed that the reaction had not gone to completion by the presence of two spots (R_f = 0.1, 0.8, ethanol: ethyl acetate: CH_2Cl_2: NH_4OH, 3: 3: 3: 0.5 v/v/v/v). Therefore, an excess of acrylonitrile (0.31 mL, d = 0.81 g/mL, 0.225 g, 4.71 mmol, 1 equivalent) was added and stirring continued for a further 7 h and then the excess of acrylonitrile and the solvent were removed under reduced pressure to give a pale yellow liquid (1.4 g), which was subjected to chromatography over silica gel column and eluted with CH_2Cl_2: methanol: NH_4OH (85: 14: 1 v/v/v) to give a clear yellow oil (1.09 g, 73%). This compound has not been previously reported.

IR: 3371 (NH), 2941and 2805 (CH_2), 2249 (CN) cm^{-1};

HRMS: Found 319.2644, $C_{17}H_{31}N_6$ requires 319.2605 $[M + H]^+$;

^1H NMR (400 MHz): 1.53-1.65 (m, 6 H), 2.31 (t, *J* = 7.2 Hz, 4 H), 2.40-2.46 (m, 8 H), 2.55 (t, *J* = 5.2 Hz, 4 H), 2.70 (t, *J* = 6.8 Hz, 4 H), (13 CH_2), 3.15 (s, 4 H, NCH_2N);

^{13}C NMR (100 MHz): 16.6, 22.8, 24.8 (5 x CH_2), 50.1, 51.9, 52.2, 52.9 (8 x NCH_2), 75.4 (2 x NCH_2N), 118.8 (2 x CN).

*2.4.8 Synthesis of 3,3'-(butane-1,4-diylbis(hexahydropyrimidine-3,1(2H)-diyl))-di-propanenitrile (**32**).*

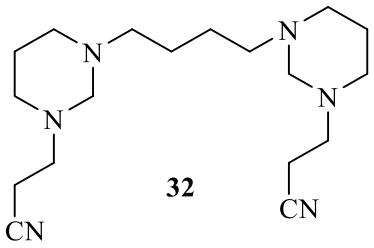

32

Method A: this compound was prepared using the same procedure as described for **29**. To **28** (1.00 g, 4.42 mmol) in anhydrous methanol (15 mL) was added acrylonitrile (0.58 mL, d = 0.81 g/mL, 0.47 g, 8.84 mmol, 2 eq.) and the solution was stirred at 20 °C under N_2 for 15 h. TLC analysis showed that the reaction had not gone to completion by the presence of two spots (R_f = 0.1, 0.8, ethanol: ethyl acetate: CH_2Cl_2: NH_4OH, 3: 3: 3: 0.5 v/v/v/v). Therefore, an excess of acrylonitrile (0.29 mL, d = 0.81 g/mL, 0.24 g, 4.42 mmol, 1 equivalent) was added and stirring continued for a further 7 h, and then the excess of acrylonitrile and the solvent were removed under reduced pressure to give a colourless oil (1.26 g, 86%).

IR: 3371 (NH), 3939, 2859 (CH_2), 2244 (CN) cm^{-1};

HRMS: Found 333.2809, $C_{18}H_{33}N_6$ requires 333.2761 $[M+H]^+$;

^1H NMR (400 MHz): 1.38-1.46 (m, 2 H), 1.57-1.65 (m, 2 H), 2.23-2.30 (m, 2 H), 2.40-2.47 (m, 4 H), 2.50-2.85 (m, 2 H), 2.67-2.73 (m, 2 H) (7 CH_2), 3.14 (s, 2 H, NCH_2N);

^{13}C NMR (100 MHz): 16.6, 22.8, 25.1 (6 x CH_2), 50.1, 51.9, 52.2, 54.9 (8 x CH_2), 75.4 (2 x NCH_2N), 118.8 (2 x CN). This compound has not been previously reported.

Method B: the above reaction was repeated with different conditions on a larger scale. To 1,4-bis(hexahydropyrimidin-1(2H)-yl)butane (2.673 g, 11.81 mmol) in methanol (25 mL) was added acrylonitrile (1.55 mL, d = 0.81 g/mL, 1.25 g, 23.62 mmol, 2 eq.) dropwise over 1 h, and the solution was stirred at 20 °C under N_2 for 2 h. TLC analysis showed that the reaction had not gone to completion by the presence of two spots (R_f = 0.1, 0.8, ethanol: ethyl acetate: CH_2Cl_2: NH_4OH, 3: 3: 3: 0.5 v/v/v/v). Therefore, an excess of acrylonitrile (1 mL, d = 0.81 g/mL, 0.81 g, 15.26 mmol, 1.3 eq.) was added and stirring continued for 15 h under N_2 and then the excess of acrylonitrile and the solvent were removed under reduced pressure to give a colourless oil (3.378 g, 86%).

*2.4.9 Synthesis of N1-(3-(3-(3-aminopropyl)hexahydropyrimidin-1(2H)-yl)propyl)propane-1,3-diamine (**33**).*

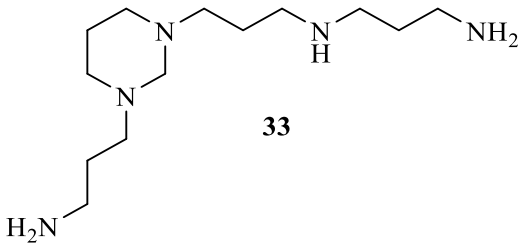

33

Method A: $LiAlH_4$ (1.22 g, 32.1 mmol, 4 eq) was dissolved in anhydrous tetrahydrofuran (20 mL) and heated under reflux. Compound **29** (2.00 g, 8.02 mmol) was dissolved in tetrahydrofuran (50 mL) and added dropwise slowly, under nitrogen, to the mixture without affecting the reflux. The reaction was heated under reflux for 10 minutes then cooled to 20 °C. Saturated aqueous Na_2SO_4 solution was cautiously added to the reaction mixture, then quenched with 10% aqueous sulfuric acid (95 mL). The reaction mixture was then extracted with ether (3 x 30 mL). The combined organic

fractions were dried (Na_2SO_4), filtered and the solvent was removed under reduced pressure. TLC analysis showed that the starting material disappeared, but the product could not be extracted from the reaction mixture. Apparently, the amine product formed complexes with the metallic ions of lithium and/or aluminium in the reaction mixture.

Method B: this compound was prepared as previously described (Bergeron and Garlich, 1984). Compound **29** (2.00 g, 8.02 mmol) was dissolved in anhydrous ethanol (50 mL) that was previously saturated with ammonia gas and introduced into a Parr hydrogenator. Raney nickel (~ 3 g) was activated by heating in NaOH solution (6 M) for 90 minutes, 60 °C and washed 6 times with anhydrous ethanol (20 mL) and was added to the Parr hydrogenator. The Parr hydrogenator was purged twice with H_2 and the reaction was carried out at room temperature for 2 h at H_2 pressure of 50 bar. After 2 h, the pressure did not fall down suggesting that the hydrogen was not consumed and the reaction had not finished, so the reaction left for another 15 h. After 15 h, the pressure did not fall down so the temperature was elevated to 60 °C at H_2 pressure of 50 bar. After 6 h the pressure fell down to lower than 20 bar suggesting that either the reaction had finished or the hydrogen was leaking. The reaction mixture was filtered through Celite with ethanol, the residue was washed with ethanol (2 x 5 mL) and the combined filtrates were removed under reduced pressure. The resulting mixture was then thoroughly extracted with a mixture of chloroform: methanol (85: 15 v/v, 8 x 10 mL). The combined organic fractions were dried (Na_2SO_4), filtered and the solvent was removed under reduced pressure to give colourless oil. However, TLC analysis showed that the reaction had not gone to completion by the presence of several spots (ethanol: NH_4OH, 2: 1 v/v).

HRMS: showed several peaks of a mixture of products unrelated to the desired product.

^{1}H NMR analysis showed overlapped and broad peaks that could not be assigned.

^{13}C NMR analysis showed the disappearance of nitrile signals at 118.7 and 118.8 and the appearance of several new peaks in the aliphatic carbons region.

The above reaction was therefore attempted under different conditions.

Method C: the compound **29** (2.00 g, 8.02 mmol) was added to a solution of sodium hydroxide (0.74 g, 18.50 mmol) in 95% ethanol (15 mL). Raney nickel (~ 0.3 g) was added to the mixture and introduced into a Parr hydrogenator. The Parr hydrogenator was purged twice with H_2 and the reaction was carried out at 30 °C for 20 h at H_2 pressure of 20 bar. After 20 h the pressure fell down to lower than 5 bar suggesting that the hydrogen was consumed. The reaction mixture was filtered through Celite with ethanol and the filtrate was removed under reduced pressure. The resulting mixture was then thoroughly extracted with a mixture of chloroform: methanol (85: 15 v/v, 8 x 10 mL). The combined organic fractions were dried (Na_2SO_4), filtered and the solvent was removed under reduced pressure to give a pale yellow oil (0.920 g, 45%). TLC analysis showed a major spot (R_f = 0.1, ethanol: NH_4OH, 2: 1 v/v).

IR: 3280, (NH), 2930, 2858 (CH_2) cm^{-1};

HRMS: Found 258.2658, $C_{13}H_{32}N_5$ requires 258.2652 $[M+H]^+$;

^{1}H NMR (500 MHz): 1.45-1.61 (m, 8 H, 4CH_2), 2.26-2.35 (m, 4 H, 2NCH_2), 2.38-2.54 (m, 12 H, 6NCH_2), 3.1 (s, 2 H, NCH_2N);

^{13}C NMR (125 MHz): 21.2, 25.7, 28.9, 31.6 (4 x CH_2), 38.6, 39.0, 46.2, 46.8, 51.9, 52.2 (6 x NCH_2), 51.4 (2 x NCH_2), 73.1 (NCH_2N).

This compound has not been previously reported.

*2.4.10 Synthesis of N1-(4-(3-(3-aminopropyl)hexahydropyrimidin-1(2H)-yl)butyl)-propane-1,3-diamine (**34**).*

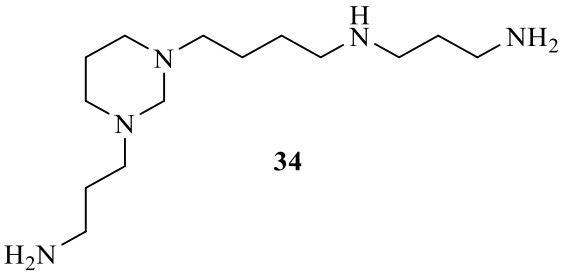

34

This compound was prepared by the same procedure described for **34**. The nitrile compound **30** (1.00 g, 3.80 mmol) was added to a solution of sodium hydroxide (0.74 g, 18.50 mmol) in 95% ethanol (15 mL). Raney nickel (~ 0.3 g) was added to the mixture and introduced into a Parr hydrogenator. The Parr hydrogenator was purged twice with H_2 and the reaction was carried out at 30 °C for 20 h at H_2 pressure of 20 bar. After 20 h the pressure fell down to lower than 5 bar suggesting that the hydrogen was consumed. The reaction mixture was centrifuged and the supernatant liquid was filtered through Celite and the filtrate was removed under reduced pressure. The resulting mixture was then thoroughly extracted with a mixture of chloroform: methanol (85: 15 v/v, 8 x 10 mL). The combined organic fractions were dried (Na_2SO_4), filtered and the solvent was removed under reduced pressure to give a pale yellow oil (0.815 g, 79%). TLC analysis showed a major spot (R_f = 0.1, ethanol: NH_4OH, 2: 1 v/v).

IR: 3329, (NH), 2930, 2858 (CH_2) cm^{-1};

HRMS: Found 272.2832, $C_{14}H_{33}N_5$ requires 272.2809 $[M+H]^+$;

^{1}H NMR (500 MHz): 1.41-1.53 (m, 4 H, $2CH_2$), 1.57-1.68 (m, 6 H, $3CH_2$), 2.26-2.39 (m, 4H, $2NCH_2$), 2.40-2.50 (m, 4 H, $2NCH_2$), 2.54-2.60 (m, 2 H, NCH_2), 2.63 (t, *J* = 7.0 Hz, 2 H, NCH_2), 2.67-2.77 (m, 4 H, $2NCH_2$), 3.08 (s, 2 H, NCH_2N);

^{13}C NMR (125 MHz): 23.8, 25.2, 28.3, 31.0, 34.0 (5 x CH_2), 40.5, 40.6, 47.9, 50.1, 52.6, 52.7, 53.2, 55.4 (8 x NCH_2), 76.8 (NCH_2N).

This compound has not been previously reported.

*2.4.11 Synthesis of 3,3'-(propane-1,3-diylbis(hexahydropyrimidine-3,1(2H)-diyl))bis-(propan-1-amine) (**35**).*

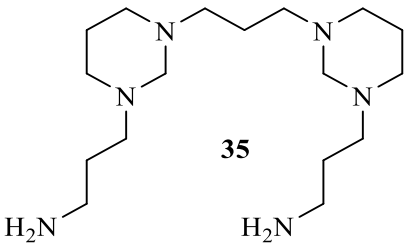

Following the procedure described for **35**. The nitrile compound **20** (1.00 g, 3.14 mmol) was added to a solution of sodium hydroxide (0.74 g, 18.50 mmol) in 95% ethanol (15 mL). Raney nickel (~ 0.3 g) was added to the mixture and introduced into a Parr hydrogenator. The Parr hydrogenator was purged twice with H_2 and the reaction was carried out at 30 °C for 20 h at H_2 pressure of 20 bar. After 20 h, the pressure fell down to lower than 5 bar suggesting that the hydrogen was consumed. The reaction mixture was centrifuged and the supernatant liquid was filtered through Celite using ethanol and the filtrate was removed under reduced pressure. The resulting mixture was then thoroughly extracted with a mixture of chloroform: methanol (85: 15 v/v, 8 x 10 mL). The combined organic fractions were dried (Na_2SO_4), filtered and the solvent was removed under reduced pressure to give a pale yellow oil (0.313 g, 30%). TLC analysis showed a major spot (R_f = 0.3, ethanol: NH_4OH, 2: 1 v/v).

IR: 3329 (NH), 2941, 2790 (CH_2) cm^{-1};

HRMS: Found 327.3252, $C_{17}H_{38}N_6$ requires 327.3231 $[M+H]^+$;

^{1}H NMR (500 MHz): 1.54-1.69 (m, 12 H, 6CH_2), 2.29-2.38 (m, 8 H, 4NCH_2), 2.39-2.51 (m, 8 H, 4NCH_2), 2.7 (t, *J* = 7.0 Hz, 4 H, 2NCH_2), 3.06 (s, 4 H, 2NCH_2N);

^{13}C NMR (125 MHz): 23.8 (2 x CH_2), 25.1 (CH_2), 31.0 (2 x CH_2), 40.6, 52.6, 52.7, 53.2, 53.6 (10 x NCH_2), 76.7 (2 x NCH_2N).

This compound has not been previously reported.

*2.4.12 Synthesis of 3,3'-(butane-1,4-diylbis(hexahydropyrimidine-3,1(2H)-diyl))-bis-(propan-1-amine) (**36**).*

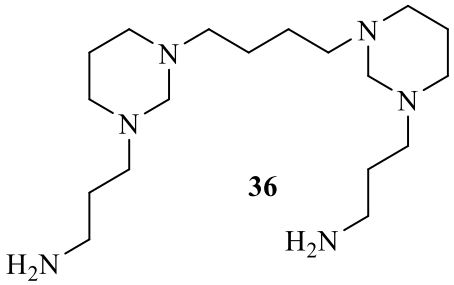

36

Following the procedure described for **33**, nitrile **32** (1.00 g, 3.01 mmol) was added to a solution of sodium hydroxide (0.74 g, 18.50 mmol) in 95% ethanol (15 mL). Raney nickel (~ 0.3 g) was added to the mixture and introduced into a Parr hydrogenator. The Parr hydrogenator was purged twice with H_2 and the reaction was carried out at 30 °C for 20 h at H_2 pressure of 20 bar. After 20 h, the pressure fell down to lower than 5 bar suggesting that the hydrogen was consumed. The reaction mixture was filtered through Celite and the filtrate was removed under reduced pressure. The resulting mixture was then thoroughly extracted with a mixture of chloroform: methanol (85: 15 v/v, 8 x 10 mL). The combined organic fractions were dried (Na_2SO_4), filtered and the solvent was removed under reduced pressure to give a white solid (0.487 g, 48%). TLC analysis showed a major spot (R_f = 0.3, ethanol: NH_4OH, 2: 1 v/v).

IR: 3354, (NH), 2940 and 2799 (CH_2) cm^{-1};

HRMS: Found 341.3403, $C_{18}H_{41}N6$ requires 341.3387 $[M+H]^+$;

^1H NMR (500 MHz): 1.34-1.38 (m, 4 H, $2CH_2$), 1.47-1.57 (m, 8 H, $4CH_2$), 2.16-2.23 (m, 4 H, $2NCH_2$), 2.26 (t, *J* = 7.0 Hz, 4 H, $2NCH_2$), 2.28-2.43 (m, 8 H, $4NCH_2$), 2.62 (t, *J* = 7.0 Hz, 4 H, $2NCH_2$), 2.97 (s, 4 H, $2NCH_2N$);

^{13}C NMR (125 MHz): 23.5 (2 x CH_2), 25.2 (2 x CH_2), 30.8 (2 x CH_2), 40.6, 52.4, 52.5, 52.9, 55.2 (10 x NCH_2), 76.5 (2 x NCH_2N).

This compound has not been previously reported.

*2.4.13 Synthesis of 3,3'-((azanediylbis(propane-3,1-diyl))bis(azanediyl)-)dipropane-nitrile (**37**).*

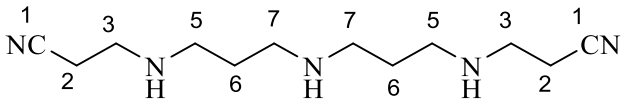

37

This compound was prepared as previously described (Frydman et al., 2004). To norspermidine (2.00 g, 15.24 mmol) in ethanol (20 mL) was added acrylonitrile (2 mL, d = 0.81 g/mL, 1.60 g, 30.48 mmol, 2 eq.) and the solution was stirred at 20 °C under N_2 for 24 h. TLC analysis showed the presence of two close spots (R_f = 0.4, 0.4, ethanol: ethyl acetate: CH_2Cl_2: NH_4OH, 3: 3: 3: 0.5 v/v/v/v). Then the solution was removed under reduced pressure to give a clear pale yellow liquid (3.6 g) which was subjected to chromatography over silica gel column and eluted with methanol: CH_2Cl_2: NH_4OH (14: 85: 1 v/v/v) to give a clear yellow oil **37** (0.4 g, 11%) and a clear pale yellow oil **38** (0.2 g, 6%).

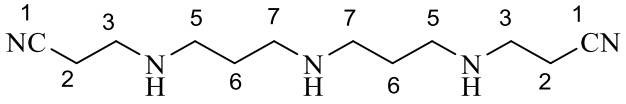

37

IR: 3308 (NH), 2947 and 2832 (CH_2), 2248 (CN);

HRMS: Found 238.2079, $C_{12}H_{24}N_5$ requires 238.2026 $[M + H]^+$;

^{1}H NMR (500 MHz): 1.61 (q, *J* = 6.8 Hz, 4 H, H-6), 2.46 (t, *J* = 6.8 Hz, 4 H, H-2), 2.59-2.68 (m, 8 H, H-5, H-7), 2.85 (t, *J* = 6.4 Hz, 2 H, H-3);

^{13}C NMR (100 MHz): 18.7 (2x C-2), 30.0 (2x C-6), 45.1, 47.8, 48.4 (2x C-3, 2x C-5, 2x C-7), 118.8 (2x C-1).

The spectral data are in good agreement with those reported (Frydman et al., 2004).

*2.4.14 Synthesis of 3-((3-((3-aminopropyl)(2-cyanoethyl)amino)propyl)amino)-propanenitrile (**38**).*

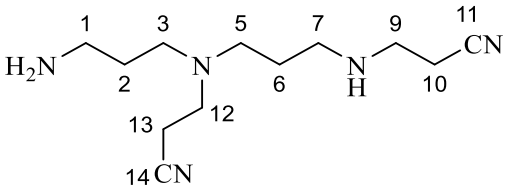

38

IR: 3300 (NH), 2937 and 2828 (CH_2), 2246 (CN);

HRMS: Found 238.2033, $C_{12}H_{24}N_5$ requires 238.2026 $[M+H]^+$;

^{1}H NMR (500 MHz; $CDCl_3$): 1.61-1.68 (m, 4 H, H-2, H-7), 2.48-2.56 (m, 8 H, H-3, H-5. H-10, H-13), 2.66-2.78 (m, 6 H, H-1, H-7, H-12), 2.89 (t, *J* = 7.0 Hz, 2 H, H-9);

^{13}C NMR (125 MHz; $CDCl_3$): 16.7 (C-13), 18.8 (C-10), 27.6 (C-6), 30.4 (C-2), 40.1 (C-1), 45.3 (C-9), 47.4 (C-7), 49.6 (C-12), 51.5(C-3), 51.9 (C-5), 119.0 (C-11), 119.3 (C-14).

This compound has been reported, but without spectral data (Balczewski et al., 2009)

*2.4.15 Synthesis of 3,3'-((((2-cyanoethyl)azanediyl)bis(propane-3,1-diyl))bis-(azanediyl))dipropanenitrile (**39**).*

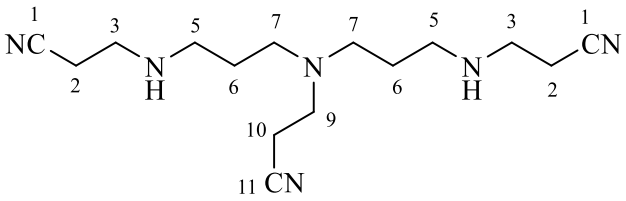

39

This compound was prepared as previously described (Frydman et al., 2004). To norspermidine (2.00 g, 15.24 mmol) in ethanol (20 mL) was added acrylonitrile (4 mL, d = 0.81 g/mL, 3.2 g, 60.96 mmol, 4 eq.) and the solution was stirred at 20 °C under N_2 for 72 h. TLC analysis showed the presence of several spots. Then the solution was removed under reduced pressure to give a clear yellow liquid which was subjected to

chromatography over silica gel column and eluted with two mobile phases (CH_2Cl_2: methanol: NH_4OH, 95: 4.75: 0.25 v/v/v) and (CH_2Cl_2: methanol: NH_4OH, 90: 9.5: 0.5 v/v/v) to give a clear yellow oil **39** (0.64 g, 15%), a clear yellow oil **40** (0.975 g, 19%) and a clear yellow oil **41** (0.24 g, 4%).

IR: 3299, (NH), 2939, 2831 (CH_2), 2247 (CN) cm^{-1};

HRMS: Found 291.2300, $C_{15}H_{27}N_6$ requires 291.2292 $[M+H]^+$;

^1H NMR (500 MHz): 1.61-1.68 (m, 4 H, H-6, 2NH), 2.45-2.56 (m, 10 H, 2x H-2, 2x H-7, H-10), 2.69-2.76 (m, 6 H, 2 x H-5, H-9), 2.92 (t, *J* = 7.0 Hz, 4 H, 2 x H-3);

^{13}C NMR (125 MHz): 16.7 (C-10), 18.7 (2 x C-2), 27.5 (2 x C-6), 45.1 (2 x C-3), 47.3 (2 x C-5), 49.6 (C-9), 51.8 (2 x C-7), 119.0 (2 x C-1), 119.3 (C-11).

The spectral data are in good agreement with those reported (Balczewski et al., 2009) with the exception that they reported an extra carbon in the NMR ^{13}C data. This issue is discussed in the results section of compound **39** (Figure 16).

*2.4.16 Synthesis of 3,3'-((3-((2-cyanoethyl)(3-((2-cyanoethyl)amino)propyl)amino)-propyl)azanediyl)dipropanenitrile (**40**).*

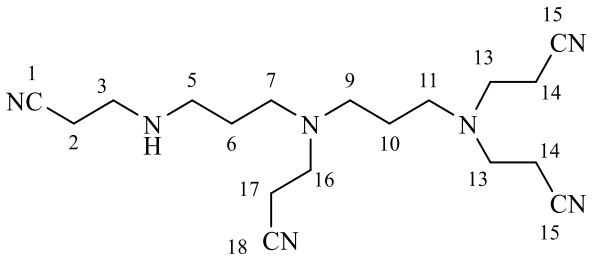

40

IR: 3340, (NH), 2943, 2830 (CH_2), 2247 (CN) cm^{-1};

HRMS: Found 344.2615, $C_{18}H_{30}N_7$ requires 344.2557 $[M+H]^+$;

^{1}H NMR (500 MHz; $CDCl_3$): 1.61-1.68 (m, 4 H, C-6, C-10), 2.48-2.56 (m, 12 H, H-2, H-7, H-11, 2x H-14, H-17), 2.62 (t, *J* = 7.0 Hz, 2 H, H-9), 2.69-2.76 (m, 4 H, H-5, H-16), 2.86 (t, *J* = 6.5 Hz, 4 H, 2x H-13), 2.92 (t, *J* = 6.5 Hz, 2 H, H-3);

^{13}C NMR (125 MHz; $CDCl_3$): 16.8 (C-17), 17.0 (2x C-14), 18.8 (C-2), 25.5 (C-10), 27.4 (C-6), 45.2 (C-3), 47.4 (C-16), 49.5 (C-5), 49.6 (2x C-13), 51.2 (C-9), 51.3 (C-7), 51.9 (C-11), 118.9 (2x C-15), 119.1 (C-18), 119.5 (C-1).

This compound has not been previously reported.

*2.4.17 Synthesis of 3,3'-((3-((2-cyanoethyl)(3-((2-cyanoethyl)(2-isocyanoethyl)-amino)propyl)amino)propyl)-azanediyl)dipropanenitrile (**41**).*

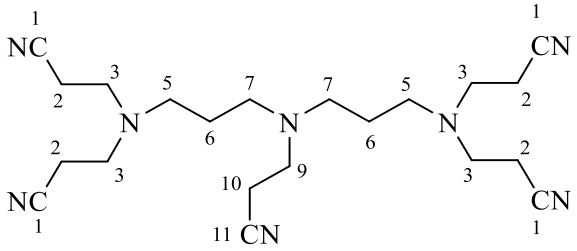

41

IR: 3620, (NH), 2945, 2833 (CH_2), 2247 (CN) cm^{-1};

HRMS: Found 397.2861, $C_{21}H_{33}N_8$ requires 397.2823 $[M+H]^+$;

^{1}H NMR (400 MHz): 1.64 (q, *J* = 7.0 Hz, 4 H, 2x H-6), 2.47-2.53 (m, 10 H, 4x H-2, H-10), 2.55 (t, *J* = 7.0 Hz, 4 H, 2 x H-5), 2.62 (t, *J* = 7.0 Hz, 4 H, 2x H-7), 2.74 (t, *J* = 6.5 Hz, 2 H, H-9), 2.86 (t, *J* = 7.0 Hz, 8 H, 4 x H-3);

^{13}C NMR (100 MHz): 16.9 (C-10), 17.0 (4 x C-2), 25.4 (2 x C-6), 49.3 (C-9), 49.6 (4 x C-3), 51.2 (2 x C-5), 51.3 (2 x C-7), 119.0 (4 x C-1), 119.7 (C-11).

The spectral data are in good agreement with those reported (Balczewski et al., 2009).

*2.4.18 Synthesis of 3,3'-(heptane-1,7-diylbis(azanediyl))dipropanenitrile (**42**).*

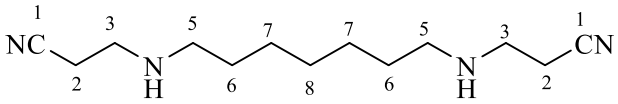

42

To heptane-1,7-diamine (1.00 g, 8.68 mmol) in ethanol (30 mL) was added acrylonitrile (1 mL, d = 0.81 g/mL, 0.815 g, 15.35 mmol, 2 eq.) dropwise and the solution was stirred at 20 °C under N_2 for 15 h. TLC analysis showed that the reaction had not gone to completion by the presence of two spots (R_f = 0.1, 0.5, ethanol: ethyl acetate: CH_2Cl_2: NH_4OH, 3: 3: 3: 0.5 v/v/v/v). Therefore, an excess of acrylonitrile (0.25 mL, d = 0.81 g/mL, 0.225 g, 3.8 mmol, 0.4 equivalent) was added and stirring continued for a further 7 h and then the excess acrylonitrile and the solvent were removed under reduced pressure to give a colourless liquid in quantitative yield. This compound has been previously reported (Sharma et al., 2010).

IR: 3312 (NH), 2929 and 2855 (CH_2), 2248 (CN) cm^{-1};

HRMS: Found 237.2109, $C_{13}H_{25}N_4$ requires 237.2074 $[M+H]^+$;

^{1}H NMR (500 MHz; $CDCl_3$): 1-1.2 (br, 2 H) (NH), 1.25-1.34 (m, 6 H, H-7, H-8), 1.45 (q, *J* = 7.0 Hz, *J* = 7.0 Hz, 4 H, H-6), 2.49 (t, *J* = 7.0 Hz, 4 H, H-2), 2.59 (t, *J* = 7.0 Hz, 4 H, H-5), 2.89 (t, *J* = 7.0 Hz, 4 H, H-3);

^{13}C NMR (125 MHz; $CDCl_3$): 18.8 (2 x C-2), 27.2 (2 x C-7), 29.4 (C-8), 30.0 (2 x C-6), 45.2 (2 x C-3), 49.3 (2 x C-5). 118.9 (2 x C-1).

*2.4.19 Synthesis of N,N'-bis(2-cyanoethyl)-1,8-octanediamine (**43**).*

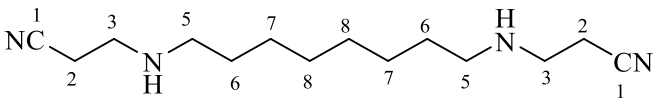

43

This compound was prepared as previously described for **29**. To 1,8-octanediamine (1.00 g, 6.93 mmol) in ethanol (30 mL) was added acrylonitrile (0.91 mL, d = 0.81 g/mL, 0.74 g, 13.86 mmol, 2 eq.) dropwise and the solution was stirred at 20 °C under N_2 for 15 h. TLC analysis showed that the reaction had not gone to completion by the presence of two spots (R_f = 0.1, 0.6, ethanol: ethyl acetate: CH_2Cl_2: NH_4OH, 3: 3: 3: 0.5 v/v/v/v). Therefore, an excess of acrylonitrile (0.2 mL, d = 0.81 g/mL, 0.162 g, 2.7 mmol, 0.4 equivalent) was added and stirring continued for 7 h and then the excess of acrylonitrile and the solvent were removed under reduced pressure to give a white solid in quantitative yield. The spectral data are in agreement with those previously reported (Jahromi et al., 2013; Liew et al., 2013).

IR: 3312 (NH), 2925 and 2853 (CH_2), 2248 (CN) cm^{-1};

HRMS: Found 251.2262, $C_{14}H_{27}N_4$ requires 251.2230 $[M+H]^+$;

^{1}H NMR (500 MHz; $CDCl_3$): 1.11 (br, 2 H, 2 x NH), 1.25-1.34 (m, 8 H, H-7, H-8), 1.46 (q, *J* = 7.0 Hz, *J* = 7.0 Hz, 4 H, H-6), 2.50 (t, *J* = 7.0 Hz, 4 H, H-2), 2.60 (t, *J* = 7.0 Hz, 4 H, H-5), 2.90 (t, 4 H, *J* = 7.0 Hz, H-3);

^{13}C NMR (125 MHz; $CDCl_3$): 18.8 (C-2), 27.2 (C-7), 29.5 (C-8), 30.1 (C-6), 45.2 (C-3), 49.3 (C-5). 118.9 (C-1).

*2.4.20 Synthesis of 3,3'-(decane-1,10-diylbis(azanediyl))dipropanenitrile (**44**).*

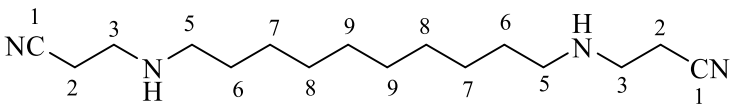

44

This compound was prepared as previously described for **29**. To decane-1,10-diamine (1.00 g, 5.80 mmol) in ethanol (30 mL) was added acrylonitrile (0.76 mL, d = 0.81 g/mL, 0.616 g, 11.61 mmol, 2 eq.) dropwise and the solution was stirred at 20 °C under N_2 for 15 h. TLC analysis showed that the reaction had not gone to completion by the

presence of two spots (R_f = 0.1, 0.6, ethanol: ethyl acetate: CH_2Cl_2: NH_4OH, 3: 3: 3: 0.5 v/v/v/v). Therefore, an excess of acrylonitrile (0.2 mL, d = 0.81 g/mL, 0.162 g, 2.7 mmol, 0.5 equivalent) was added and stirring continued for a further 7 h and then the excess acrylonitrile and the solvent were removed under reduced pressure to give a white solid in quantitative yield. The spectral data are in agreement with those previously reported (Pearce et al., 2017).

IR: 3314 (NH), 2921 and 2847 (CH_2), 2248 (CN) cm^{-1};

HRMS: Found 279.2560, $C_{16}H_{31}N_4$ requires 279.2543 $[M+H]^+$;

^1H NMR (500 MHz; $CDCl_3$): 1.13 (br, 2 H) (NH), 1.24-1.34 (m, 12 H, H-7, H-8, H-9), 1.47 (q, *J* = 7.0 Hz, *J* = 7.0 Hz, 4 H, H-6), 2.51 (t, *J* = 7.0 Hz, 4 H, H-2), 2.62 (t, *J* = 7.0 Hz, 4 H, H-5), 2.92 (t, *J* = 7.0 Hz, 4 H, H-3);

^{13}C NMR (125 MHz; $CDCl_3$): 18.9 (C-2), 27.3 (C-7), 29.6 (C-8), 29.6 (C-9), 30.1 (C-6), 45.2 (C-3), 49.4 (C-5). 118.9 (C-1).

*2.4.21 Synthesis of 3-(12-[(2-cyanoethyl)amino]dodecylamino)propanenitrile (**45**).*

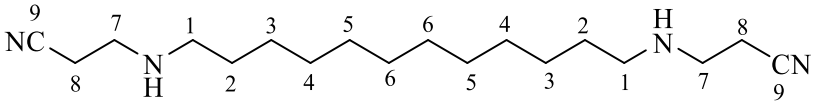

45

This compound was prepared as previously described for **29**. To 1,12-diaminododecane (1.00 g, 4.99 mmol) in ethanol (30 mL) was added acrylonitrile (0.65 mL, d = 0.81 g/mL, 0.53 g, 9.98 mmol, 2 eq.) dropwise and the solution was stirred at 20 °C under N_2 for 15 h. TLC analysis showed that the reaction had not gone to completion by the presence of two spots (R_f = 0.1, 0.7, ethanol: ethyl acetate: CH_2Cl_2: NH_4OH, 3: 3: 3: 0.5 v/v/v/v). Therefore, an excess of acrylonitrile (0.2 mL, d = 0.81 g/mL, 0.162 g, 2.7 mmol, 1 equivalent) was added and stirring continued for 7 h and then the excess acrylonitrile and the solvent were removed under reduced pressure to give a white solid

in quantitative yield. The spectral data are in agreement with those previously reported (Klenke et al., 2001).

IR: 3289 (NH), 2919 and 2851 (CH_2), 2260 (CN) cm^{-1};

HRMS: Found 307.2791, $C_{16}H_{31}N_4$ requires 307.2856 $[M+H]^+$;

^{1}H-NMR (500 MHz; $CDCl_3$): 1.14 (br, 2 H, NH), 1.22-1.33 (m, 16 H, H-7, H-8, H-9, H-10), 1.47 (q, *J* = 7.0 Hz, 4 H, H-6), 2.51 (t, *J* = 7.0 Hz, 4 H, H-2), 2.61 (t, *J* = 7.0 Hz, 4 H, H-5), 2.92 (t, *J* = 6.5 Hz, 4 H, H-3);

^{13}C-NMR (125 MHz; $CDCl_3$): 18.9 (C-2), 27.3 (C-7), 29.6 (C-10), 29.7 (C-8), 29.7 (C-9), 30.2 (C-6), 45.2 (C-3), 49.4 (C-5). 118.9 (C-1).

*2.4.22 Synthesis of N1,N1'-(heptane-1,7-diyl)bis(propane-1,3-diamine) (**46**).*

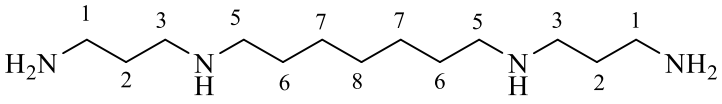

46

This compound was prepared by the same procedure as described for **34.** The nitrile compound **42** (2.00 g, 8.02 mmol) was added to a solution of sodium hydroxide (0.74 g, 18.50 mmol) in 95% ethanol (3 mL). Raney nickel (~ 0.3 g) was added to the mixture and introduced into a Parr hydrogenator. The Parr hydrogenator was purged twice with H_2 and the reaction was carried out at 30 °C for 20 h at H_2 pressure of 20 bar. After 20 h the pressure fell down to lower than 5 bar suggesting that the hydrogen was consumed. The reaction mixture was filtered through Celite and the filtrate was evaporated under vacuum. The resulting mixture was then thoroughly extracted with a mixture of chloroform: methanol (85: 15 v/v, 8 x 10 mL). The combined organic fractions were dried (Na_2SO_4), filtered and the solvent was removed under reduced pressure to give a white solid (1.30 g, 63%). TLC analysis showed a major spot (R_f = 0.1, ethanol: NH_4OH, 2: 1 v/v).

IR: 3263 cm^{-1}, (NH), 2922 cm^{-1}, 2849 cm^{-1} (CH_2);

HRMS: Found 245.2750, $C_{13}H_{33}N_4$ requires 245.2700 $[M+H]^+$;

^1H NMR (500 MHz; $CDCl_3$): 0.91-1.22 (br, 6 H) (NH, NH_2), 1.22-1.33 (m, 6 H, H-7, H-8), 1.39-1.48 (m, 4 H, H-6), 1.54-1.66 (m, 4 H, H-2), 2.51-2.59 (m, 4 H, H-5), 2.59-2.68 (m, 4 H, H-3), 2.68-2.77 (m, 4 H, H-1);

^{13}C NMR (125 MHz; $CDCl_3$): 27.5 (2 x C-7), 29.6 (C-8), 30.3 (2 x C-6), 34.2 (2 x C-2), 40.7 (2 x C-1), 48.1 (2 x C-3). 50.3 (2 x C-5).

The spectral data for this compound have been previously reported including mass and ^1H NMR data, but not ^{13}C NMR data (Edwards et al., 1991). Our spectral data are in agreement with the reported data.

*2.4.23 Synthesis of N1,N1'-(octane-1,8-diyl)bis(propane-1,3-diamine) (**47**).*

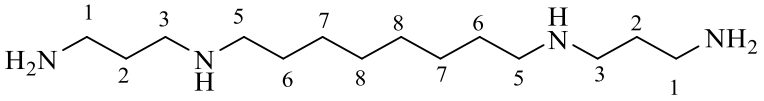

47

This compound was prepared by the same procedure as described for **34**. The nitrile compound **43** (2.00 g, 7.99 mmol) was added to a solution of sodium hydroxide (0.74 g, 18.50 mmol) in 95% ethanol (3 mL). Raney nickel (~ 0.3 g) was added to the mixture and introduced into a Parr hydrogenator. The Parr hydrogenator was purged twice with H_2 and the reaction was carried out at 30 °C for 20 h at H_2 pressure of 20 bar. After 20 h, the pressure fell down to lower than 5 bar suggesting that the hydrogen was consumed. The reaction mixture was filtered through Celite and the filtrate was evaporated under vacuum. The resulting mixture was then thoroughly extracted with a mixture of chloroform: methanol (85: 15 v/v, 8 x 10 mL). The combined organic fractions were dried (Na_2SO_4), filtered and the solvent was removed under reduced

pressure to give a white solid (1.28 g, 62%). TLC analysis showed a major spot (R_f = 0.1, ethanol: NH_4OH, 2: 1 v/v).

IR: 3264 cm^{-1}, (NH), 2924 cm^{-1}, 2848 cm^{-1} (CH_2);

HRMS: Found 259.2919, $C_{14}H_{35}N_4$ requires 259.2856 $[M+H]^+$;

^1H NMR (500 MHz; $CDCl_3$): 0.93-1.24 (br, 6 H) (NH, NH_2), 1.24-1.33 (m, 8 H, H-7, H-8), 1.40-1.51 (m, 4 H, H-6), 1.57-1.68 (m, 4 H, H-2), 2.51-2.61 (m, 4 H, H-5), 2.61-2.69 (m, 4 H, H-3), 2.70-2.80 (m, 4 H, H-1);

^{13}C NMR (125 MHz; $CDCl_3$): 27.5 (2 x C-7), 29.6 (C-8), 30.3 (2 x C-6), 34.2 (2 x C-2), 40.7 (2 x C-1), 48.1 (2 x C-3). 50.4 (2 x C-5).

This compound has been previously reported, but without spectral data (Edwards et al., 1991).

*2.4.24 Synthesis of N1,N1'-(decane-1,10-diyl)bis(propane-1,3-diamine) (**48**).*

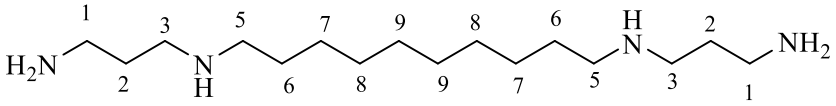

48

This compound was prepared by the same procedure as described for **34**. The nitrile compound **44** (2.00 g, 7.18 mmol) was added to a solution of sodium hydroxide (0.74 g, 18.50 mmol) in 95% ethanol (3 mL). Raney nickel (~ 0.3 g) was added to the mixture and introduced into a Parr hydrogenator. The Parr hydrogenator was purged twice with H_2 and the reaction was carried out at 30 °C for 20 h at H_2 pressure of 20 bar. After 20 h, the pressure fell down to lower than 5 bar suggesting that the hydrogen was consumed. The reaction mixture was filtered through Celite and the filtrate was evaporated under vacuum. The resulting mixture was then thoroughly extracted with a mixture of chloroform: methanol (85: 15 v/v, 8 x 10 mL). The combined organic fractions were dried (Na_2SO_4), filtered and the solvent was removed under reduced

pressure to give a white solid (1.58 g, 77%). TLC analysis showed a major spot (R_f = 0.2, ethanol: NH_4OH, 2: 1 v/v).

IR: 3227 cm^{-1}, (NH), 2893 cm^{-1}, 2824 cm^{-1} (CH_2);

HRMS: Found 287.3252, $C_{16}H_{39}N_4$ requires 287.3169 $[M+H]^+$;

^1H NMR (500 MHz; $CDCl_3$): 0.94-1.17 (br, 6 H) (NH, NH_2), 1.22-1.31 (m, 12 H, H-7, H-8, H-9), 1.45 (q, *J* = 7.0 Hz, *J* = 7.0 Hz, 4 H, H-6), 1.62 (t, *J* = 7.0 Hz, 4 H, H-2), 2.57 (t, *J* = 7.0 Hz, 4 H, H-5), 2.65 (t, *J* = 7.0 Hz, 4 H, H-3), 2.74 (t, *J* = 7.0 Hz, 4 H, H-1);

^{13}C NMR (125 MHz; $CDCl_3$): 27.5 (2 x C-7), 29.7 (2 x C-8), 29.7 (2 x C-9) 30.3 (2 x C-6), 34.2 (2 x C-2), 40.7 (2 x C-1), 48.1 (2 x C-3). 50.4 (2 x C-5).

The spectral data are in good agreement with those reported (Bradley et al., 1997).

*2.4.25 Synthesis of N1,N1'-(dodecane-1,12-diyl)bis(propane-1,3-diamine) (**49**).*

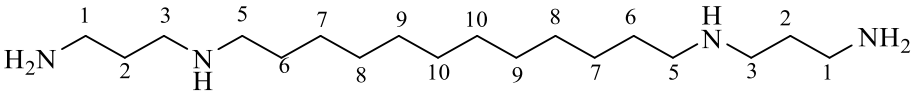

49

This compound was prepared by the same procedure as described for **34**. The nitrile compound **45** (2.00 g, 6.52 mmol) was added to a solution of sodium hydroxide (0.74 g, 18.50 mmol) in 95% ethanol (3 mL). Raney nickel (~ 0.3 g) was added to the mixture and introduced into a Parr hydrogenator. The Parr hydrogenator was purged twice with H_2 and the reaction was carried out at 30 °C for 20 h at H_2 pressure of 20 bar. After 20 h, the pressure fell down to lower than 5 bar suggesting that the hydrogen was consumed. The reaction mixture was filtered through Celite and the filtrate was evaporated under vacuum. The resulting mixture was then thoroughly extracted with a mixture of chloroform: methanol (85: 15 v/v, 8 x 10 mL). The combined organic fractions were dried (Na_2SO_4), filtered and the solvent was removed under reduced

pressure to give a white solid (1.64 g, 80%). TLC analysis showed a major spot (R_f = 0.2, ethanol: NH_4OH, 2: 1 v/v).

IR: 3263 cm^{-1}, (NH), 2922 cm^{-1}, 2849 cm^{-1} (CH_2);

HRMS: Found 315.3581, $C_{18}H_{43}N_4$ requires 315.3482 $[M+H]^+$;

^1H NMR (500 MHz; $CDCl_3$): 0.94-1.17 (br, 22 H, H-7, H-8, H-9, H-10) (NH, NH_2), 1.46 (q, *J* = 7.0 Hz, *J* = 7.0 Hz, 4 H, H-6), 1.62 (t, *J* = 7.0 Hz, 4 H, H-2), 2.57 (t, *J* = 7.0 Hz, 4 H, H-5), 2.65 (t, *J* = 7.0 Hz, 4 H, H-3), 2.75 (t, *J* = 7.0 Hz, 4 H, H-1);

^{13}C NMR (125 MHz; $CDCl_3$): 27.6 (2 x C-7), 29.7 (2 x C-8), 29.7 (4 x C-9, C-10), 30.3 (2 x C-6), 34.2 (2 x C-2), 40.7 (2 x C-1), 48.1 (2 x C-3). 50.4 (2 x C-5).

The spectral data previously reported for this compound are ^1H NMR data only (Bradley et al., 1997). Our ^1H NMR spectral data are in agreement with those data.

References (in the style of *Phytochemistry*)

Ashton, M. R., Moya, E., Blagbrough, I. S., 1995. Total synthesis of modified JSTX toxins: Reductive alkylation is a practical route to hexahydropyrimidine polyamine amides. Tetrahedron Lett. 36, 9397-9400.

Bagal, D. B., Bhanage, B. M., 2015. Recent advances in transition metal-catalyzed hydrogenation of nitriles. Adv. Synth. Catal. 357, 883-900.

Balczewski, P., Zurawinski, R., Mikina, M., Dudzinski, B., 2009. Synthesis of polyamino nitriles, en route to acylpolyamine neurotoxins, via the regioselective Michael cyanoethylation of unprotected polyamines. Unusual behaviour of 1-(2-aminoethyl)-piperazine. Tetrahedron 65, 8727-8732.

Bergeron, R. J., Garlich, J. R., 1984. Amines and polyamines from nitriles. Synthesis. 782-784.

Bisen, P. S., 2014. Laboratory protocols in applied life sciences, 1st ed. CRC Press.

Bottcher, T., Kolodkin-Gal, I., Kolter, R., Losick, R., Clardy, J., 2013. Synthesis and activity of biomimetic biofilm disruptors. J. Am. Chem. Soc. 135, 2927-2930.

Bradley, J. C., Vigneron, J. P., Lehn, J. M., 1997. A rapid and efficient preparation of linear and macrocyclic polyamine bolaphiles. Synth. Commun. 27, 2833-2845.

Edwards, M. L., Stemerick, D. M., Bitonti, A. J., Dumont, J. A., McCann, P. P., Bey, P., Sjoerdsma, A., 1991. Antimalarial polyamine analogs. J. Med. Chem. 34, 569-574.

Frydman, B., Bhattacharya, S., Sarkar, A., Drandarov, K., Chesnov, S., Guggisberg, A., Popaj, K., Sergeyev, S., Yurdakul, A., Hesse, M., Basu, H. S., Marton, L. J., 2004. Macrocyclic polyamines deplete cellular ATP levels and inhibit cell growth in human prostate cancer cells. J. Med. Chem. 47, 1051-1059.

Ganem, B., 1982. New chemistry of naturally-occurring polyamines. Acc. Chem. Res. 15, 290-298.

Haworth, I. S., Rodger, A., Richards, W. G., 1991. A molecular mechanics study of spermine complexation to DNA: a new model for spermine-poly(dG-dC) binding. Proc. Roy. Soc. Lond. B, 244, 107-116. **DOI:** 10.1098/rspb.1991.0058

Hoque, J., Konai, M. M., Sequeira, S. S., Samaddar, S., Haldar, J., 2016. Antibacterial and antibiofilm activity of cationic small molecules with spatial positioning of hydrophobicity: An in vitro and in vivo evaluation. J. Med. Chem. 59, 10750-10762.

Houen, G., Struve, C., Sondergaard, R., Friis, T., Anthoni, U., Nielsen, P. H., Christophersen, C., Petersen, B. O., Duus, J. O., 2005. Substrate specificity of the bovine serum amine oxidase and in situ characterisation of aminoaldehydes by NMR spectroscopy. Bioorg. Med. Chem. 13, 3783-3796.

Jahromi, A. H., Fu, Y., Miller, K. A., Lien, N., Luu, L. M., Baranger, A. M., Zimmerman, S. C., 2013. Developing bivalent ligands to target cug triplet repeats, the causative agent of myotonic dystrophy type 1. J. Med. Chem. 56, 9471-9481.

Klenke, B., Stewart, M., Barrett, M. P., Brun, R., Gilbert, I. H., 2001. Synthesis and biological evaluation of s-triazine substituted polyamines as potential new anti-trypanosomal drugs. J. Med. Chem. 44, 3440-3452.

Liew, L. P. P., Pearce, A. N., Kaiser, M., Copp, B. R., 2013. Synthesis and in vitro and in vivo evaluation of antimalarial polyamines. Eur. J. Med. Chem. 69, 22-31.

Maruyoshi, K., Demura, T., Sagane, T., Matsumori, N., Oishi, T., Murata, M., 2004. Synthesis and conformation of deuterated spermidine for investigating weak interaction with polyanionic biomolecules. Tetrahedron 60, 5163-5170.

Mebane, R. C., Jensen, D. R., Rickerd, K. R., Gross, B. H., 2003. Transfer hydrogenation of nitriles with 2-propanol and Raney® nickel. Synth. Commun. 33, 3373-3379.

Menger, F. M., D'Angelo, L. L., 1991. Conformation of DNA-bound spermidine by double C-13 labeling. J. Org. Chem. 56, 3467-3468.

Nazih, A., Cordier, Y., Bischoff, R., Kolbe, H. V. J., Heissler, D., 1999. Synthesis and stability study of the new pentammonio lipid pcTG90, a gene transfer agent. Tetrahedron Lett. 40, 8089-8091.

Pearce, A. N., Kaiser, M., Copp, B. R., 2017. Synthesis and antimalarial evaluation of artesunate-polyamine and trioxolane-polyamine conjugates. Eur. J. Med. Chem. 140, 595-603.

Sharma, S. K., Wu, Y., Steinbergs, N., Crowley, M. L., Hanson, A. S., Casero, R. A., Jr., Woster, P. M., 2010. (Bis)urea and (bis)thiourea inhibitors of lysine-specific demethylase 1 as epigenetic modulators. J. Med. Chem. 53, 5197-5212.

Siddiqui, A. Q., Merson-Davies, L., Cullis, P. M., 1999. The synthesis of novel polyamine-nitroimidazole conjugates designed to probe the structural specificities of the polyamine uptake system in A549 lung carcinoma cells. J. Chem. Soc., Perkin Trans. 1., 3243-3252.

Vilches-Herrera, M., Werkmeister, S., Junge, K., Borner, A., Beller, M., 2014. Selective catalytic transfer hydrogenation of nitriles to primary amines using pd/c. Catal. Sci. Technol. 4, 629-632.

Valle, J., Toledo-Arana, A., Berasain, C., Ghigo, J. M., Amorena, B., Penadés, J. R., Lasa, I. 2003. SarA and not sigmaB is essential for biofilm development by *Staphylococcus aureus*. Mol. Microbiol. 48, 1075-1087.

Williams, D. H., Fleming, I., 2008. Spectroscopic methods in organic chemistry, 6th edn. McGraw-Hill, London.

Wu, B., Zhang, J., Yang, M., Yue, Y., Ma, L.-J., Yu, X.-Q., 2008. Raney Ni/KBH_4: An efficient and mild system for the reduction of nitriles to amines. Arkivoc, 95-102.

Chapter 3

Microbiological activities of polyamines

3.1 Introduction

Increasing bacterial resistance is a great challenge to global health. Anti-microbial resistance (AMR) is spreading globally, decreasing the ability to fight epidemic infections and creating an ever more significant challenge to global health. Biofilms are a major source of the problem of AMR. About 80% of human bacterial infections are biofilm-related (Worthington et al., 2012, Barsoumian et al., 2015). It is much worse where the bacteria form biofilms because such biofilms are very tolerant to the body's defence system and resist antibodies, phagocytosis, and antibiotics as biofilms represent a physical and diffusional barrier restricting their access to the bacteria in the biofilm. Bacterial cells within the biofilms are up to 1000-times more resistant to antibiotics than free floating planktonic cells (Hoiby et al., 2010). These biofilms are formed in clinical isolates and therefore the future of operations in hospitals (which typically all require antibiotic treatments) requires a solution to this AMR problem.

Having synthesized designed polyamines as described in chapter 2, their biological activities against biofilms were evaluated. Polyamine starting materials and synthesized analogues were initially tested for their activity to prevent biofilm formation in 96-well plate assays using crystal violet staining method on three chosen *S. aureus* strains (Alhusein et al., 2015; Phuong et al., 2017). The first, MRSA 252, is a clinical isolate that was isolated in 1997 (Holden et al., 2004). This strain is resistant to several antibiotics including erythromycin, meticillin, and ciprofloxacin, and it was

responsible for the death of three patients due to septicaemia from this strain after a miniature outbreak (Holden et al., 2004). The second strain, *S. aureus* MSSA 15981, was isolated in the University Clinics of Navarra, Spain (Valle et al., 2003). It is able to produce strong, thick biofilms. The third strain, *S. aureus* NCTC6571 is a commonly used reference strain that was first described by Heatley (1944). For biofilms of MSSA 15981 the EPS has been analysed and was shown to contain the extracellular polysaccharide N-acetylglucoseamine, decreasing the production N-acetylglucoseamine completely prevented biofilm formation (Valle et al., 2003). The biofilm composition of these three strains were examined to see if there is a relationship between the activity of the polyamines and the biofilm composition.

Compounds showing activity in preventing biofilm formation were then tested for their activity to disperse existing biofilm in 96-well plates by quantifying the amount of biofilm formed using crystal violet. In this, biomass (cells and EPS) are stained with an 0.1% crystal violet solution, after which the crystal violet is dissolved in 30% acetic acid and the visible absorbance measured using a UV-visible plate reader at $\lambda = 595$ nm. Crystal violet stains live and dead cells and some components of the extracellular matrix of the biofilm, which gives information about the whole biofilm mass, but not viable counts within the biofilm. So, the active compounds were tested for their activity to prevent biofilm formation using the Miles-Misra method (Alhusein et al., 2015), which gives clear information about the viable counts within the biofilm. Moreover, these active compounds were also tested for their activity to prevent biofilm formation and disperse preformed biofilms using Live/Dead stains by a confocal microscopy technique, which provides more information about the thickness of the biofilm and the spread of live and dead cells through each biofilm. Commonly used methods to quantify biofilms have been evaluated (Doll et al., 2016). The authors

concluded that LIVE/DEAD staining combined with the confocal laser-scanning microscopy (CSLM) method is favoured for detailed analysis of mature biofilms and initial adhesion, but its demanding time and cost make it unsuitable for rapid high-throughput screening. sSimpler methods such as resazurin and crystal violet are time and cost effective and therefore preferred for rapid high-throughput screening. Crystal violet is not applicable for experiments detecting the antimicrobial activity, as dead bacterial cells are embedded within non-degraded biofilms (Doll et al., 2016).

As previously discussed in chapter 1, the mechanism of action of polyamines is not yet well-established. In this thesis, the most active compounds were tested for their activity to prevent bacterial attachment to a surface, the very first step of biofilm formation. This test shows if the activity of polyamines is affecting the EPS component of the biofilm after the maturation of the biofilm or an earlier step. Active compounds were also tested for their effect on bacterial growth curve compared to control bacteria. This test will show if the biofilm inhibition refers to polyamine toxicity by inhibiting bacterial growth or to the inhibition of biofilm formation. In order to test the ability of polyamines to prevent biofilm formation, four naturally occurring polyamines, spermidine, spermine, norspermidine, and norspermine, known to be biologically active molecules (Cohen, 1998) were therefore selected as potentially microbiologically active natural products as the starting point in these studies.

Norspermine (NS, 3.3.3) and norspermidine (NSD, 3.3) have 3-carbon atoms distance between each pair of amino-groups, while spermine and spermidine have an extra carbon atom as a methylene group. Spermine (S, 3.4.3) and norspermine (NS, 3.3.3) have four amino groups (two primary and two secondary amines) and are symmetrical molecules. They carry four positive charges at mammalian physiological pH.

Norspermidine (3.3) and spermidine (3.4) each have three amino groups (two primary amines and one secondary) and they each carry three positive charges at pH = 7.4. At such a pH, these linear polyamines are essentially fully charged. This follows from the Henderson-Hasselbalch equation which describes the relationship between pK_a, pH, and the ratio of ionized to unionized species. Spermine for example carries 3.8 net positive charges at physiological pH on its four amino groups, following from its pK_a values of 10.9, 10.1, 8.9, and 8.1 (potentiometry). Similarly, spermidine carries 2.9 net positive charges at pH = 7.4 on its three amino groups following from its pK_a values of 10.8, 9.9, and 8.4 (potentiometry) (Blagbrough et al., 2011).

The microbiological infections which are the targets of this research are growing on or in the host at the typical mammalian blood physiological pH = 7.4. *S. aureus* bacteria have cytoplasmic pH values in the range of 7.5 to 8.0 (Booth, 1985). Clearly, if the net charge is calculated at pH = 7.4, this will be comparable with the charge at pH = 7.5. Therefore, if polyamines enter microbiological cells, they will display a similar net positive charge and fold to adopt similar structures. Even in the slightly more basic bacterial milieu of pH = 8.0, they will be similarly charged. The distribution of positive charges on such poly-cationic molecules is important for their biological activity by affecting their interactions with macromolecular components of the cell surface or within the cell, e.g. in the cytoplasm or the nucleus.

3.2 Results and discussion

3.2.1 Effect of polyamines on biofilm formation

The microbiological activities of these four selected naturally occurring polyamines to prevent biofilm formation were measured on the three *S. aureus* strains: one MRSA (MRSA 252) and two MSSA strains (NCTC 6571 and MSSA 15981).

In Figure 1 and in many subsequent figures, the control data are from untreated bacteria, normalised as a negative control. Figure 1a shows the activity of these selected polyamines in preventing biofilm formation in MRSA 252. All tested polyamines show low activity in MRSA 252 biofilms, the most active one was spermine at concentration = 0.3 mM with activity of only around 20% in preventing biofilm formation. Figure 1b shows their activity to prevent biofilm formation in *S. aureus* NCTC 6571, an MSSA strain. Spermine and spermidine were inactive against NCTC 6571 biofilm, but norspermidine and norspermine were active and prevented biofilm formation. The most active was norspermine at concentration = 0.5 mM which reduced biofilm by 85%. These results are in agreement with results previously reported (Kolodkin-Gal et al., 2012). It should be noted that this *Cell* paper has been retracted. However, the reason for the retraction was not related to the activity of polyamines on biofilms. The active polyamines (norspermidine and norspermine) have 3-methylene groups distance between all amino groups while the inactive polyamines (spermidine and spermine) have an extra methylene group in their chemical structure. From this SAR, it may be concluded that repeating the 3-carbon atoms distance between the amino groups in polyamines may be necessary for such anti-biofilm activity.

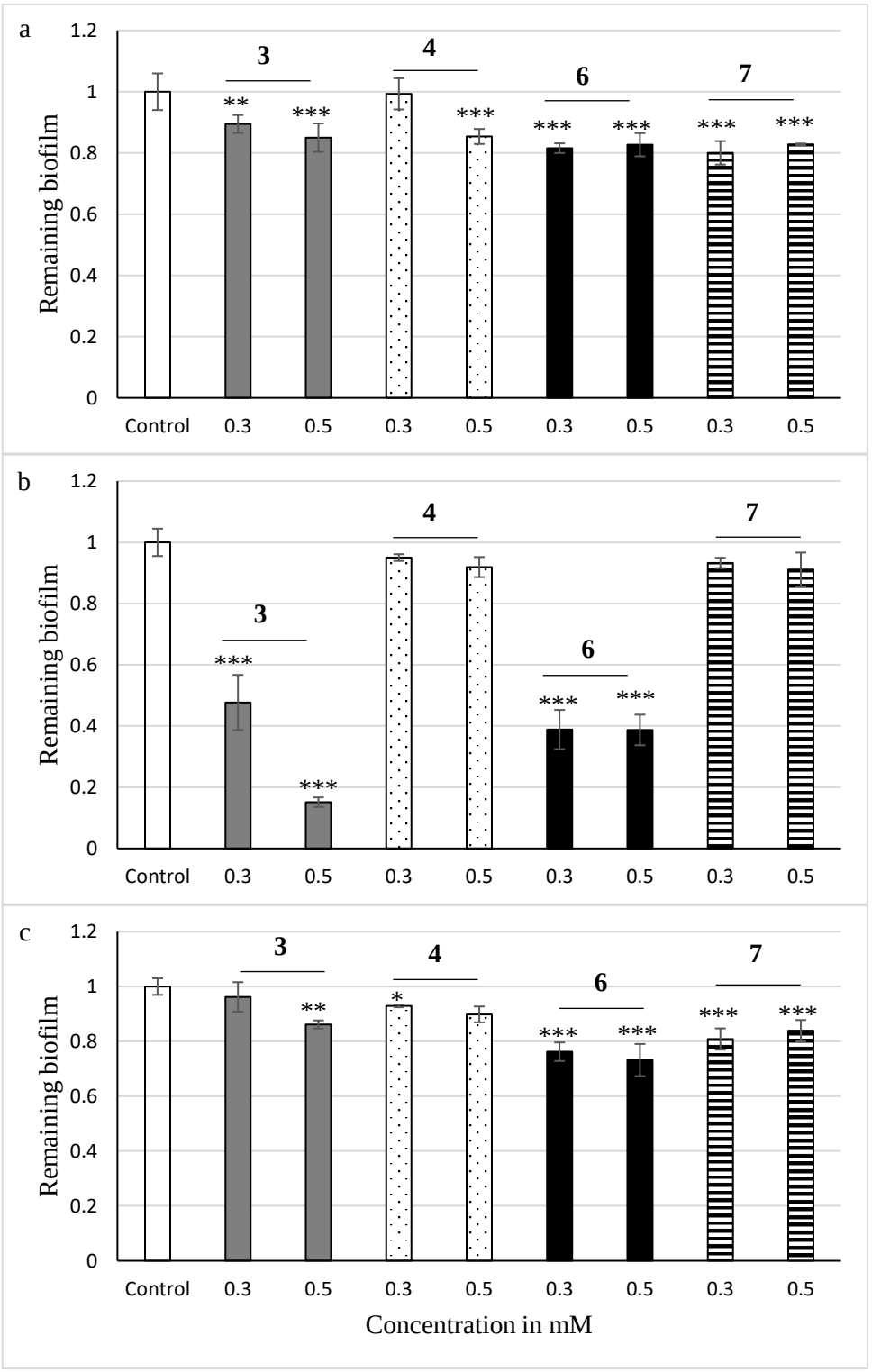

Figure 1: The effects of norspermidine **3**, spermidine **4**, norspermine **6**, and spermine **7** on biofilm formation in a) MRSA 252, b) NCTC 6571, c) MSSA 15981. The results are the average of three independent experiments, with each one replicated in 8 wells and normalised against Control (untreated bacteria). The error bars indicate the standard deviation. * $p < 0.05$, ** $p < 0.01$, *** $p < 0.001$. Crystal violet assay.

Figure 1c shows spermidine, spermine, norspermidine, and norspermine activity in preventing biofilm formation in MSSA 15981 strain. All tested polyamines show low activity in MSSA 15981 biofilms, the most active one was norspermine, which only resulted in 27% reduction of biofilm formation at concentration = 0.5 mM. Norspermidine and norspermine showed higher activity against NCTC 6571 strain comparing to this strain MSSA 15981. This variation in polyamine microbiological activities suggested the importance of an analysis of the composition of these bacterial strains biofilms, which could explain these laboratory observed variations.

3.2.2 Biofilm composition studies

The variance in polyamine activity between different bacterial strains may be due to the different biofilm compositions. The major components of biofilms can be identified by using a variety of substances. For example, in terms of the extracellular matrix, polysaccharide-based biofilms can be oxidised by sodium periodate, protein-based biofilms can be hydrolysed by enzymes such as proteinase K, and DNA-based biofilms can be hydrolysed by DNases such as DNase I.

Sodium periodate ($NaIO_4$, Figure 2) is an inorganic salt used to cleave the carbon-carbon bond in certain sugars in which two the carbons constitute a vicinal diol (Xiu et al., 2010). This oxidation of the two secondary alcohol functional groups to two aldehydes occurs with carbohydrate ring cleavage. Sodium periodate salt can exist in two forms: sodium metaperiodate, which has the formula $NaIO_4$, and sodium orthoperiodate, which has the formula $Na_2H_3IO_6$. Both salts can be used as oxidising agents. Sodium metaperiodate was exclusively used in these experiments (Phuong et al., 2017).

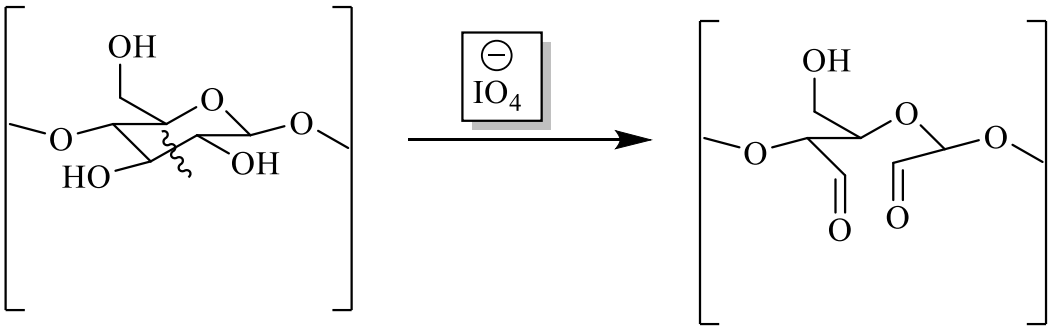

Figure 2: Cleavage of a polysaccharide 1,2 diol-by sodium metaperiodate.

Proteinase K is a protease (Figure 3). It was isolated from an extract of the fungus *Tritirachium album Limber* and named after its ability to digest keratin in hair (Morihara and Tsuzuki, 1975). Proteinase K is an extracellular serine endopeptidase that has a broad-spectrum of activity against proteins and can work catalytically at a wide range of pH and temperature (Yang et al., 2016). This broad-spectrum makes it suitable for digesting the wide range of amino acid sequences comprising the proteins that might be found in different bacterial biofilms.

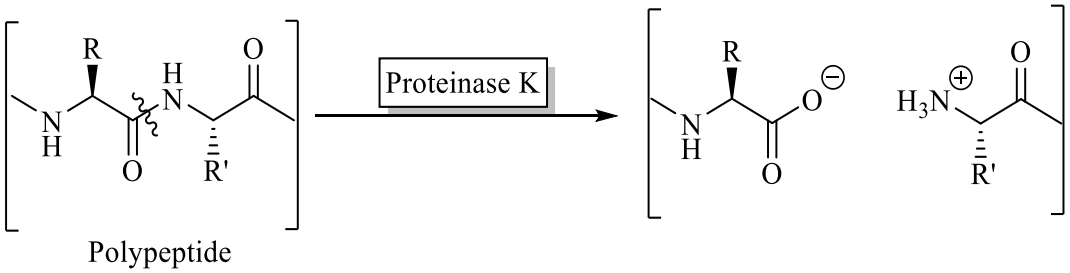

Polypeptide

Figure 3: Cleavage of protein peptide bonds by proteinase K.

DNase I (Deoxyribonuclease I) is a nuclease that hydrolyses DNA by the cleavage of phosphodiester bonds in the polynucleotide as shown in Figure 4. DNase I is a calcium-dependent enzyme (Moor, 1981), thus calcium chloride was added to DNase I solution at concentration = 1mM.

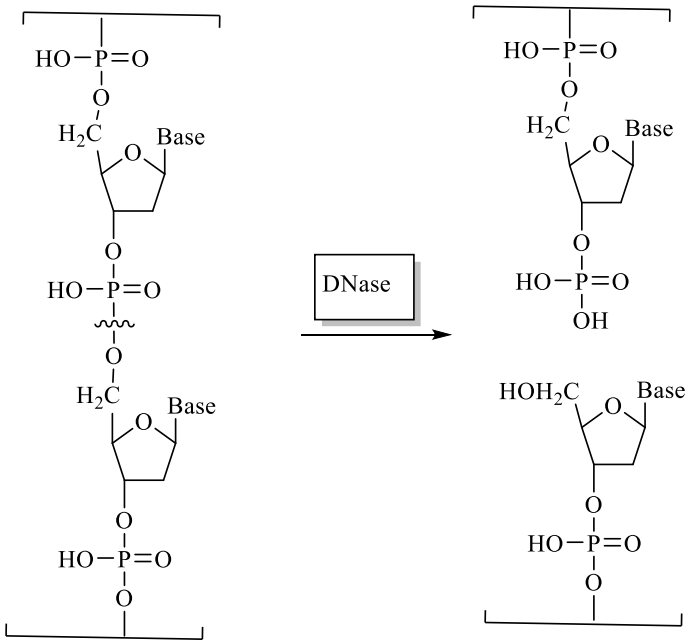

Figure 4: Cleavage of DNA by DNase I.

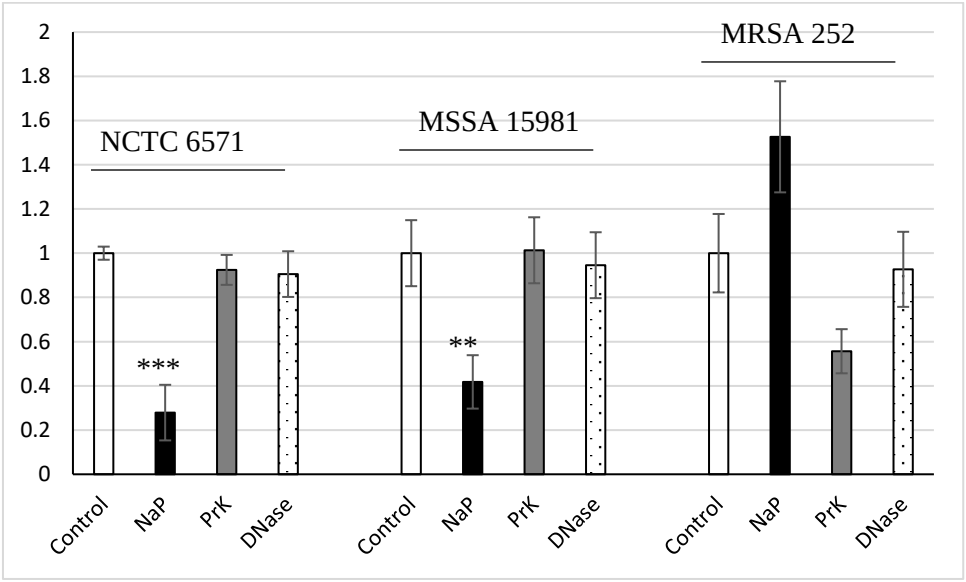

Figure 5: The effects of sodium metaperiodate (NaP), proteinase K (PrK), and DNase I on preformed biofilms in NCTC 6571, MSSA 15981, and MRSA 252 strains. The results are the average of three experiments, with each one replicated in 8 wells and normalised against Control (untreated bacteria). The error bars indicate the standard deviation. ** $p < 0.01$, *** $p < 0.001$. Crystal violet assay.

Figure 5 shows the ability of sodium periodate, proteinase K, and DNase I to disassemble preformed biofilms in the three chosen bacterial strains. This provides important molecular information about the composition of their biofilms.

MSSA 15981 and NCTC 6571 biofilms were both disrupted by sodium periodate, but not by proteinase K or DNase, indicating that the main component of the EPS in these biofilms is polysaccharide. MRSA 252 biofilm was disrupted by proteinase K (44%) and to a lesser extent by DNase (7%), but not by sodium periodate, thus the main component of the EPS in MRSA 252 biofilm is protein. Although the reduction in hydrolysis by proteinase K of MRSA 252 was not significant compared to the control, this strain is reported to be a protein-based biofilm (Phuong et al., 2017).

According to the polyamine SAR hypothesis in the retracted *Cell* paper (Kolodkin-Gal et al., 2012), introduced in chapter 1, the amino groups of norspermidine and norspermine will bind to the acidic groups of the extracellular polysaccharide component and break the hydrogen bonds that form bridges between polysaccharide chains. These hydrogen bonds give the biofilm its strength and three dimensional structure. By breaking these bonds, norspermidine and norspermine can disassemble polysaccharide-based biofilms. So, these polyamines are expected to be inactive against the protein-based strain MRSA 252 and active against the polysaccharide-based strains NCTC 6571 and MSSA 15981. However, they were only active against NCTC 6571, but not against MSSA 15981. Therefore, these two strains either have a different polysaccharide composition in which any acidic groups of the extracellular polysaccharides are not well aligned with the amino groups of the two polyamines, or polyamines target an entirely different biofilm component in NCTC 6571.

3.2.3 Effect of polyamines on dispersing existing biofilm

The activity of the four chosen polyamines (spermidine, spermine, norspermidine, and norspermine) to disperse preformed biofilms was measured on the three *S. aureus* strains: MRSA 252, NCTC 6571, and MSSA 15981.

Figure 6a shows the ability of the four chosen polyamines to disperse existing biofilm in MRSA 252. With the exception of norspermidine at concentration = 0.3 mM, all tested polyamines show no activity in MRSA 252 biofilms. However, norspermidine at concentration = 0.3 mM slightly increased biofilm mass. Figure 6b shows that tested polyamines have no activity to disperse existing biofilms in NCTC 6571. Figure 6c shows their lack of activity to disperse existing biofilms in MSSA 15981.

All four chosen polyamines show no ability to disperse preformed biofilms in the three strains regardless of their biofilm composition. Norspermidine and norspermine were able to prevent biofilm formation in NCTC 6571, but did not disperse existing biofilms of the same strain. This shows that these polyamines act on biofilm formation only and are not able to release cells from mature biofilms.

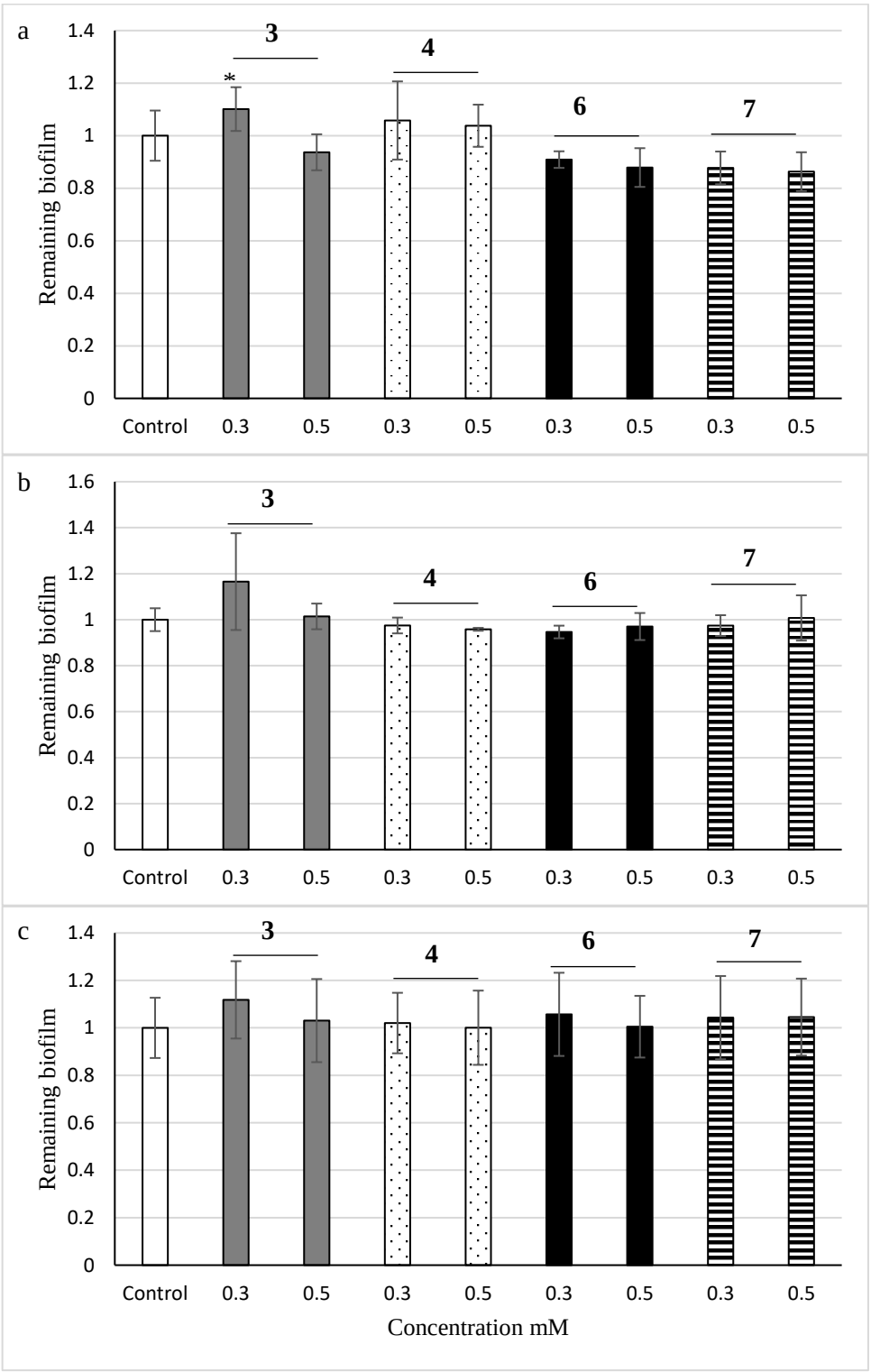

Figure 6: The effects of norspermidine **3**, spermidine **4**, norspermine **6**, and spermine **7** on dispersing existing biofilm in a) MRSA 252, b) NCTC 6571, c) MSSA 15981. The results are the average of three independent experiments, with each one replicated in 8 wells and normalised against Control (untreated bacteria). The error bars indicate the standard deviation. * $p < 0.05$. Crystal violet assay.

Norspermidine has been recently reported both to prevent biofilm formation and to disperse mature biofilms in *S. aureus* strains (Cardile et al., 2017). They showed that norspermidine reduces biofilm formation by about 80% and could disperse existing biofilms by 30%. However, they achieved these effects by using a very high concentration of norspermidine equal to 20 mM, which is 67-fold higher than the concentration we used which is 0.3 mM. However, the authors noted that norspermidine was toxic to *S.aureus* at 5 and 20 mM. A very recent study showed that such high concentrations of norspermidine and other polyamines inhibit planktonic growth of *S. aureus* strains (Li et al., 2018)

As set out in chapter 2, compounds **25**-**28** (Figure 7) were designed and synthesized from the four selected natural polyamines (spermidine, spermine, norspermidine, and norspermine) in order to test the biological effect of minimising or at least restricting conformational rotation, by means of selectively incorporating the two amines separated by three methylene chain in an easily formed and yet specifically stable hexahydropyrimidine ring (Chantrapromma and Ganem, 1980).

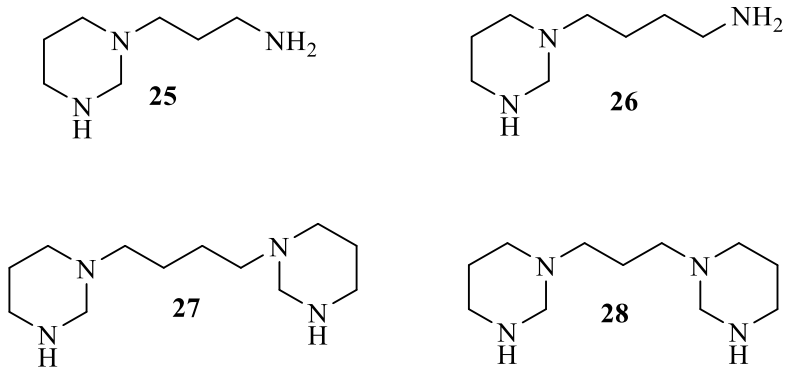

Figure 7: Hexahydropyrimidine derivatives tested for their activity against biofilms.

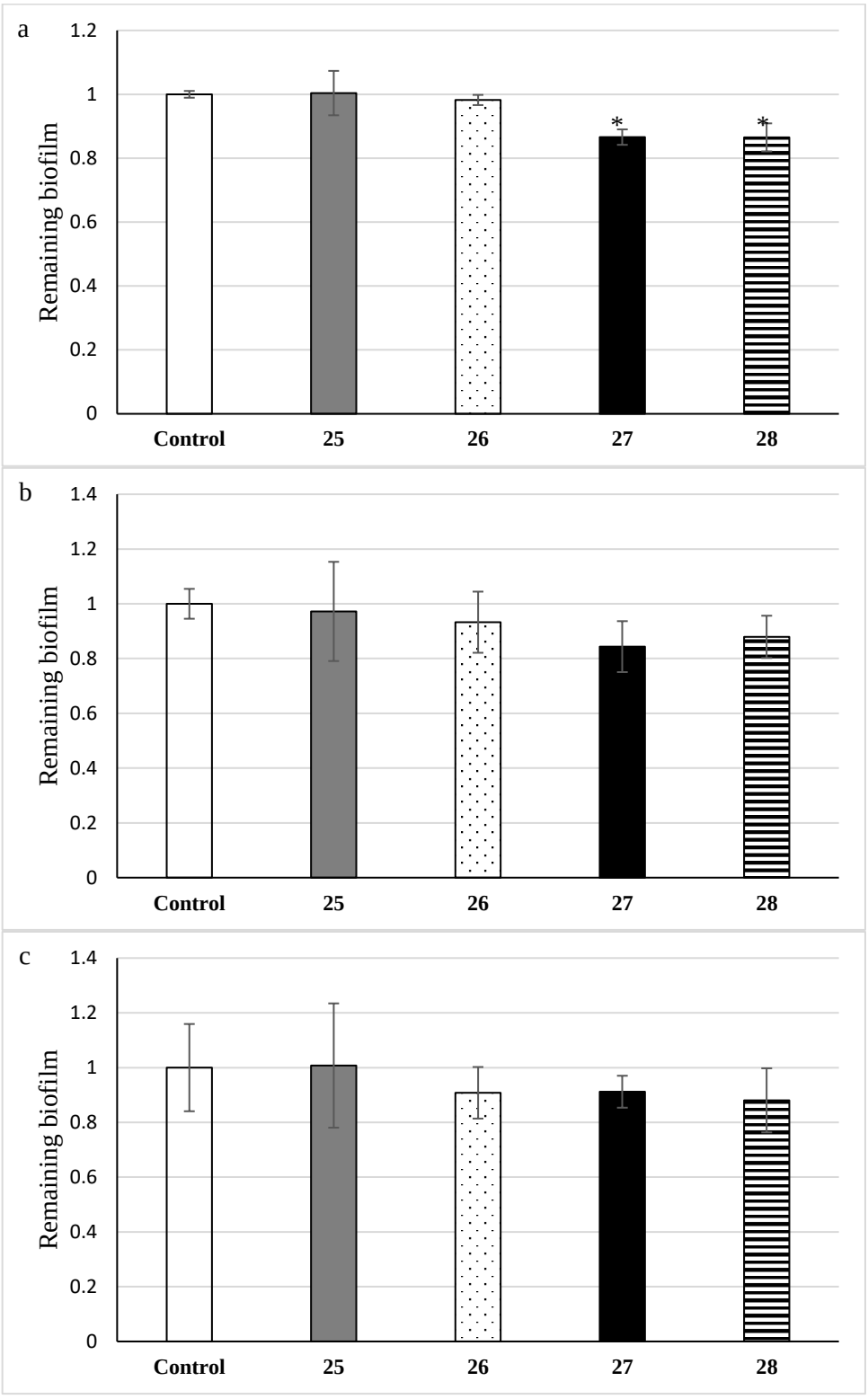

Figure 8: The effects of **25-28** on biofilm formation in a) MRSA 252, b) NCTC 6571, c) MSSA 15981 at concentration = 0.3 mM. The results are the average of three independent experiments, with each one replicated in 8 wells and normalised against Control (untreated bacteria). The error bars indicate the standard deviation. * $p < 0.05$. Crystal violet assay.

Figure 8a shows the activity of compounds **25-28** to prevent biofilm formation in MRSA 252. All tested polyamines showed low activity in MRSA 252 biofilms, the most active ones were **27** and **28** which only reduced biofilm by 15%. Figure 8b shows their activity to prevent biofilm formation in NCTC 6571. All tested polyamines show low activity in NCTC 6571 biofilms, the most active was **27** which reduced biofilm by 15%, but this reduction was not significant. Figure 8c shows their activity to prevent biofilm formation in MSSA 15981. All tested polyamines show low activity in MSSA 15981 biofilms, the most active was **28** which reduced biofilm by 12%, but this reduction was not significant.

Norspermidine and norspermine lose their activity against NCTC 6571 after cyclization. This could be due to the change in the distance between the amine groups (Figure 9), indicating that the three methylene spacer between the amines should be linear in order to achieve this kind of biological activity.

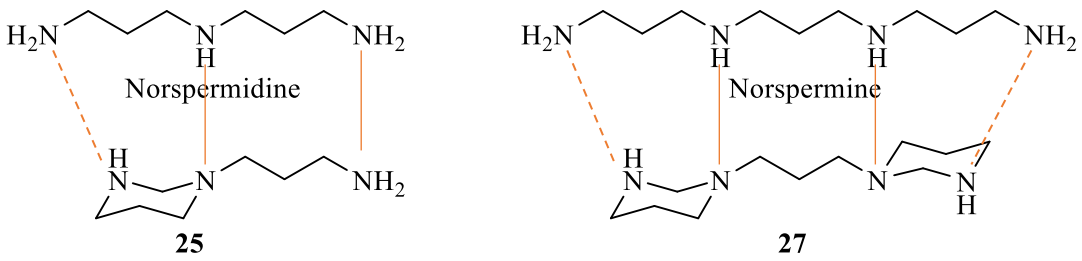

Figure 9: Norspermidine and norspermine lose the three-linear carbon atoms distance between amino groups after cyclization to **25** and **27**, respectively.

Compounds **33-36** (Figure 10) were designed and synthesised from compounds **25-28** respectively by the addition of two methylenes and a functional nitrile group to both free amines (secondary and primary) of the starting materials followed by reduction of both nitrile groups to their corresponding primary amines. Compounds **33-36** have two

additional amino groups separated by three methylene groups. Norspermidine and norspermine, which both have amino groups separated by three methylene groups from each other, show preventing biofilm formation activity in NCTC 6571 (Figure 1b). If this 3-carbon spacer is required for such microbiological activity, the final products (compounds **33**-**36**) are expected to prevent biofilm formation in this strain. Indeed, the addition of two more positive charges might increase the activity compared to compounds **25**-**28**, however, in reinforcing the 3.3 linear methylene pattern, biological activity might be mainly found in compound **33**.

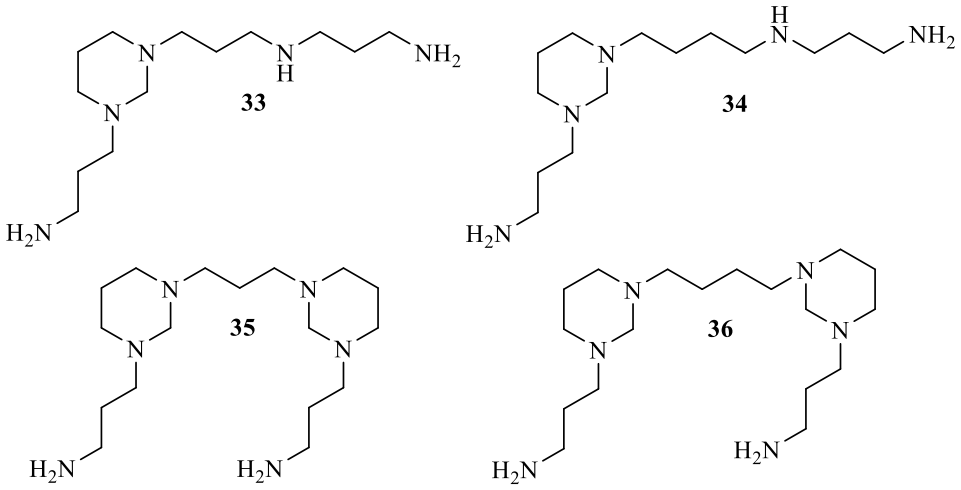

Figure 10: Extended polyamine analogues tested for their activity against biofilms.

Figure 11a shows the activity of compounds **33**-**36** to prevent biofilm formation in MRSA 252. All tested polyamines show low activity in MRSA 252 biofilms, the most active was **35** at concentration = 0.3 mM which reduced biofilm by 23% (Table 1). Figure 11b shows the activity of compounds **33**-**36** to prevent biofilm formation in NCTC 6571. All tested polyamines show activity to prevent biofilm formation in this strain. However, the activity of all compounds was less than norspermidine. The most active was **33** which reduced biofilm by 60% at concentration = 0.3 mM, and 46% at concentration = 0.5 mM, while norspermidine reduced biofilm by 85% at concentration = 0.5 mM (Tables 1, 2). The amine pattern of norspermidine is found

within **33**. However, **33** is still less active than norspermidine at concentration = 0.5 mM. Figure 11c shows the activity of compounds **33-36** to prevent biofilm formation in MSSA 15981 where all the tested polyamines showed low activity. The most active was **33** at concentration = 0.5 mM which reduced biofilm by 33% (Table 2). When compared with the previously discussed activity of compounds **25-28** in preventing biofilm formation in MSSA 15981 (Figure 8c), the addition of more amino groups separated by a three methylene spacer to compounds **25-28**, to make compounds **33-36**, respectively increased their activity to prevent biofilm formation in MSSA 15981.

Table 1: Percentage of biofilm reduction by polyamines (**3-7**, **25-28** and **33-36**) at concentration = 0.3 mM compared to negative bacteria control in MRSA 252, NCTC 6571 and MSSA 15981.

	3	**4**	**6**	**7**	**25**	**26**	**27**	**28**	**33**	**34**	**35**	**36**
MRSA 252	11	1	18	20	0	2	13	13	23	18	0	0
NCTC 6571	48	5	61	7	3	7	16	12	60	57	56	56
MSSA 15981	4	7	24	19	0	9	9	12	31	12	28	17

Table 2: Percentage of biofilm reduction by polyamines (**3-7** and **33-36**) at concentration = 0.5 mM compared to negative bacteria control in MRSA 252, NCTC 6571 and MSSA 15981.

	3	**4**	**6**	**7**	**33**	**34**	**35**	**36**
MRSA 252	15	15	17	17	2	7	0	6
NCTC 6571	85	8	61	9	46	49	52	56
MSSA 15981	14	10	27	16	33	14	23	18

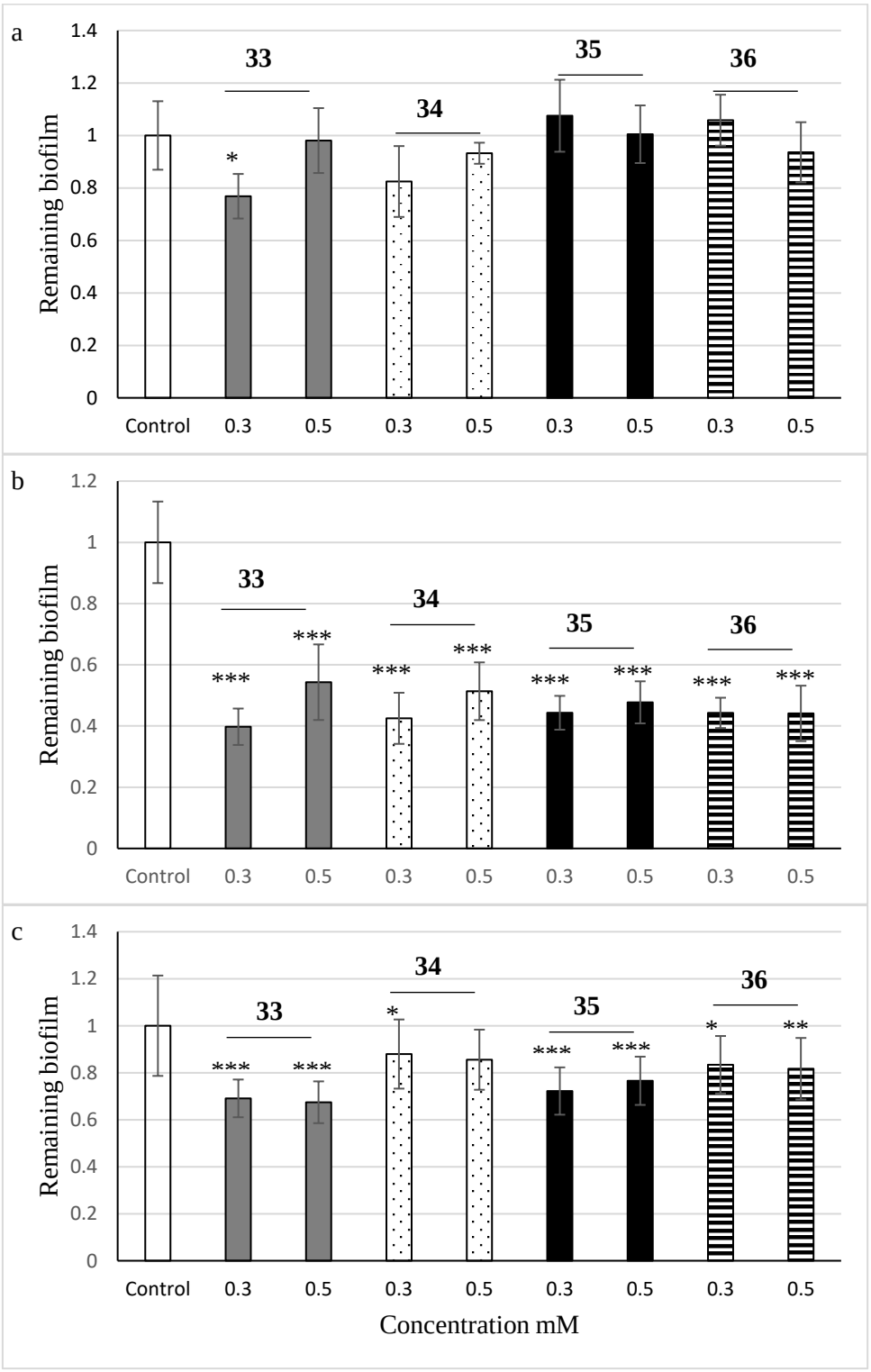

Figure 11: The effects of **33-36** on biofilm formation in a) MRSA 252, b) NCTC 6571, c) MSSA 15981. The results are the average of three independent experiments, with each one replicated in 8 wells and normalised against Control (untreated bacteria). The error bars indicate the standard deviation. * $p < 0.05$, ** $p < 0.01$, *** $p < 0.001$. Crystal violet assay.

The activity of **33**-**36** to prevent biofilm formation in the polysaccharide-based biofilm NCTC 6571 and MSSA 15981 strains (Figure 11b and c) was higher than the activity of their starting materials compounds **25**-**28**, respectively (Figure 8b and c). However, in the case of the protein-based biofilm MRSA 252 strain there was no general trend. Figure 8a shows low activity of **27** and **28** to prevent biofilm formation in MRSA 252 at concentration = 0.3 mM, but they lost their activity when converted into their analogues **35** and **36** (Figure 11a). In contrast, **25** showed no activity to prevent biofilm formation in MRSA 252 (Figure 8a), while its analogue **33** showed activity to prevent biofilm formation at concentration = 0.3 mM (Figure 11a). It could be that polyamines play some role in the production process of extracellular polysaccharides in NCTC 6571 and MSSA 15981. However, the activity of polyamines appears to be strain dependent.

Compounds **33**-**36** showed different activity to prevent biofilm formation in all three chosen strains, thus they were tested for their activity to disperse preformed biofilm in the same three bacterial strains (Figure 12). Figure 12a shows the activity of **33**-**36** to disperse existing biofilm in MRSA 252. All polyamines showed no significant reduction on biofilm mass. Figure 12b shows their total lack of activity to disperse existing biofilm in NCTC 6571. Figure 12c shows their low effect on biofilm mass in MSSA 15981.

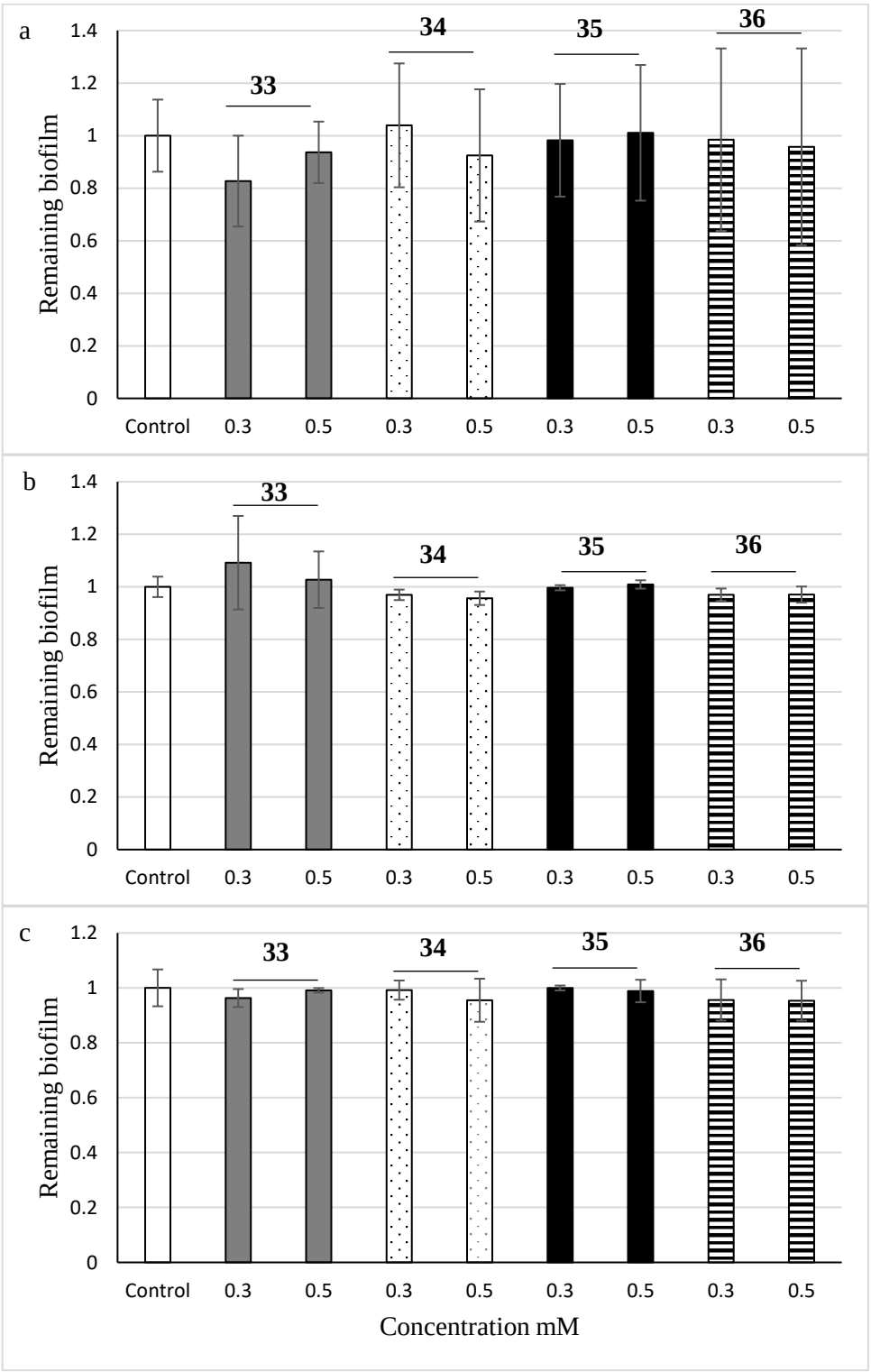

Figure 12: The effects **33-36** on dispersing existing biofilm in a) MRSA 252, b) NCTC 6571, c) MSSA 15981. The results are the average of three independent experiments, with each one replicated in 8 wells and normalised against Control (untreated bacteria). The error bars indicate the standard deviation. Crystal violet assay.

Compounds **46**-**49** (Figure 13) were designed and synthesised, in part, inspired by the recently published lipidic molecules showing activity against biofilms (Hoque et al., 2016; Wang et al., 2016). Compounds **46**-**49** were synthesised by the addition of two methylenes and a nitrile group to both ends of the starting diamine compounds to form **42**-**45** followed by reduction of nitrile groups to their corresponding primary amines. Lipidic compound **49** was insoluble in water unless it contained a small amount of ethanol as a co-solvent (0.85% ethanol in water v/v).

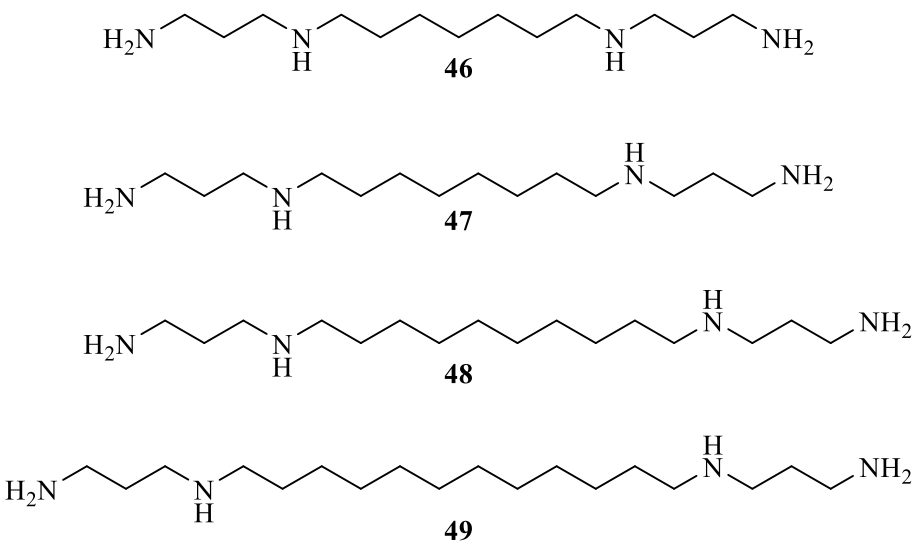

Figure 13: More lipidic polyamine analogues tested for their activity against biofilms.

Recently, quaternised cationic small molecules were reported to have antibacterial and anti-biofilm activity by targeting the bacterial cell membrane (Hoque et al., 2016). The chemical structures of these compounds contain long hydrophobic chains flanked by permanent positive charges (Figure 14). However, the disadvantage of these compounds is their cytotoxicity. By changing the length of the hydrophobic chain, the authors minimised the toxicity against mammalian cells without losing antibacterial and anti-biofilm activity. Compounds **50** and **51** have shorter carbon-chains with 6 and 8 carbons, respectively. These compounds show antibacterial and anti-biofilm activity.

By increasing the chain length to 10 and 12 carbons in **52** and **53**, respectively, the antibacterial and anti-biofilm activity increased and the toxicity decreased. The most active and least toxic compound was compound **53**, which incorporate a 12-carbon chain.

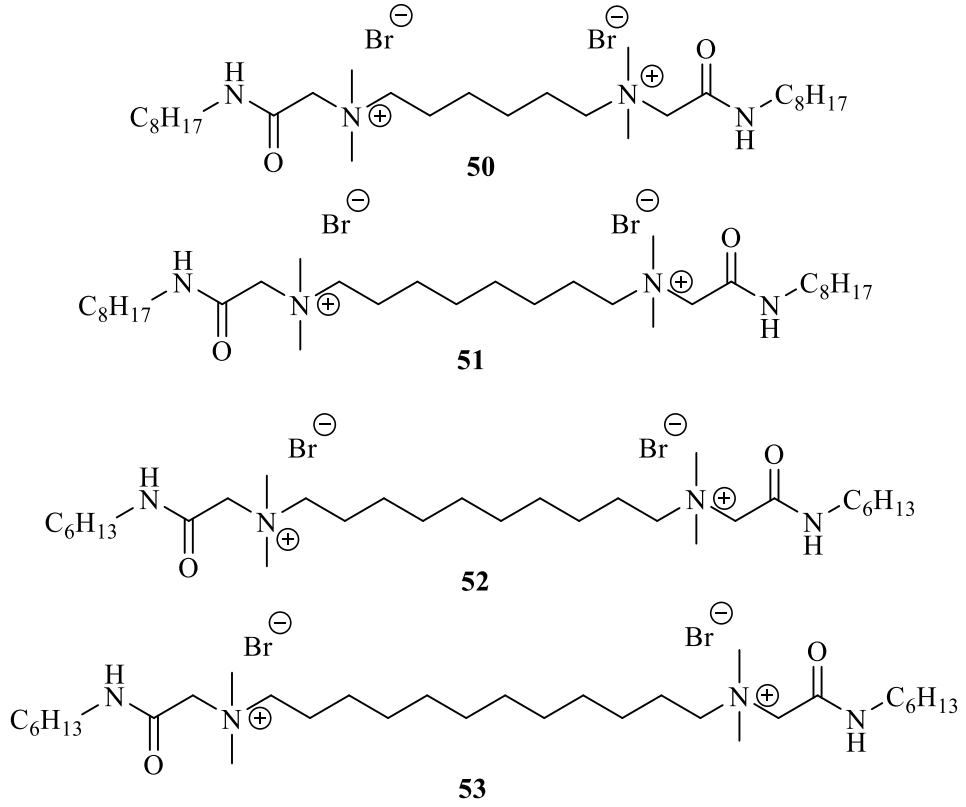

Figure 14: Polyamines analogues reported to have antibacterial and anti-biofilm activity.

Figure 15a shows the activity of compounds **46**-**48** to prevent biofilm formation in MRSA 252. Surprisingly, all tested polyamines show activity to increase biofilm formation in MRSA 252 biofilms, with the most active one being compound **48** at concentration = 0.5 mM which increased biofilm by 40%. This activity could be due to stress from these compounds on bacteria, which made the bacteria increase biofilm production to overcome this stress (Pöllänen et al., 2013).

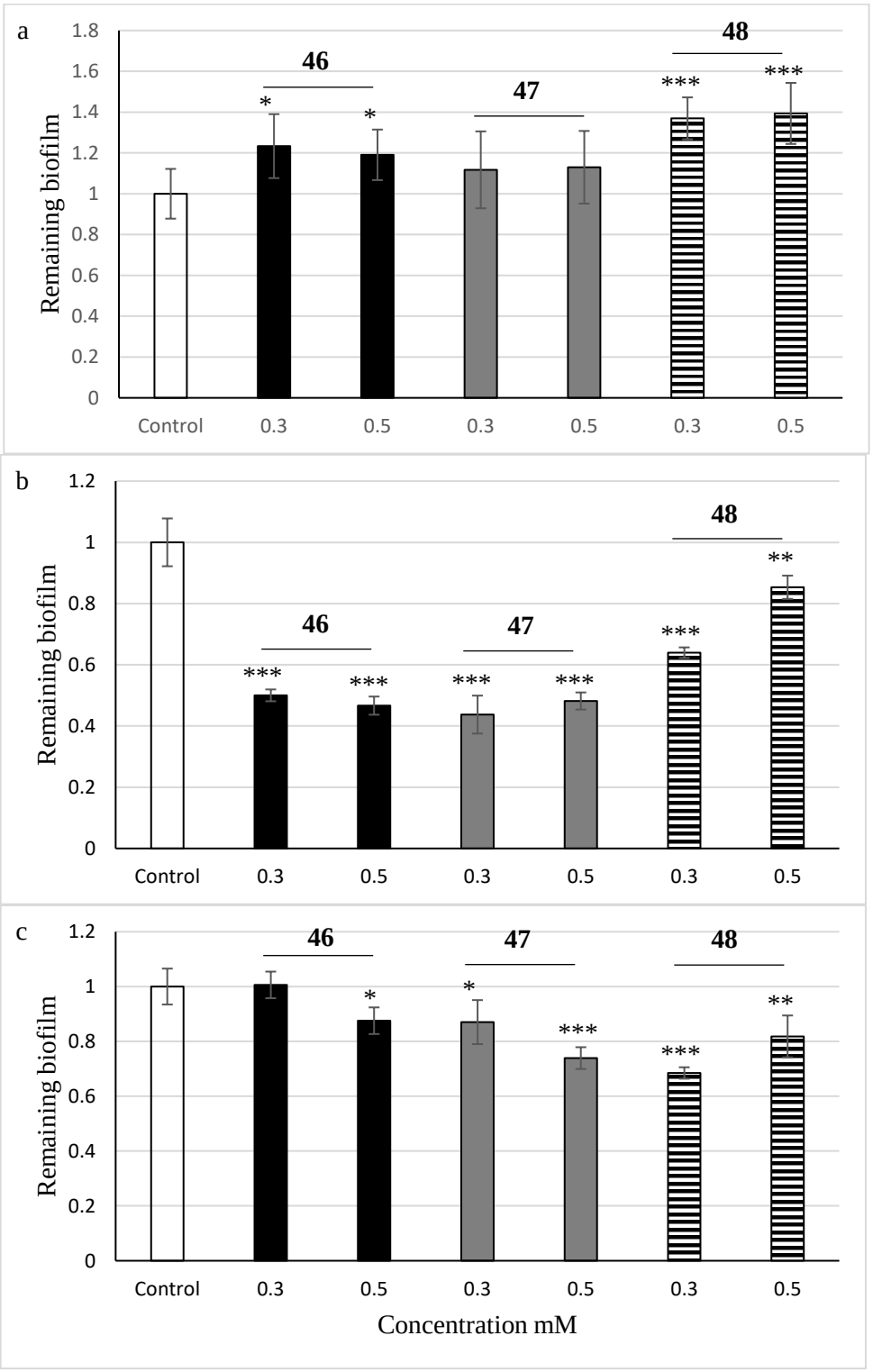

Figure 15: The effects of compounds **46**-**48** on biofilm formation in a) MRSA 252, b) NCTC 6571, c) MSSA 15981. The results are the average of three independent experiments, with each one replicated in 8 wells and normalised against Control (untreated bacteria). The error bars indicate the standard deviation. * $p < 0.05$, ** $p < 0.01$, *** $p < 0.001$. Crystal violet assay.

Figure 15b shows the activity of compounds **46**-**48** to prevent biofilm formation in NCTC 6571. Compound **48** showed low activity to prevent biofilm formation, the reduction of biofilm was 15% and 36% for concentrations 0.5 and 0.3 mM, respectively. Compounds **47** showed 52% and 56% reduction in biofilm formation for concentrations 0.5 and 0.3 mM, respectively. Compounds **46** showed 53% and 50% reduction in biofilm formation for concentrations 0.5 and 0.3 mM, respectively**.** Figure 15c shows the activity of compounds **46**-**48** to prevent biofilm formation in MSSA 15981. Compounds **46**-**48** show low activity in MSSA 15981 biofilms, the most active one was **48** at concentration = 0.3 mM which reduced biofilm by 32%.

As compound **49** is insoluble in water, it was dissolved in ethanolic aqueous solution (0.85% v/v). Figure 16a shows the activity of compound **49** to prevent biofilm formation in MRSA 252. Correspondingly, in each assay of this polyamine, a dilute aqueous solution of ethanol (0.85% v/v) was used as a positive control. Compound **49** prevented biofilm formation in MRSA 252 and showed ~99% reduction in biofilm mass. The presence of ethanol showed only a non-significant reduction in biofilm mass by 15%, which clearly indicated that the prevention of biofilm formation was due to compound **49**, not caused by ethanol at that low concentration

Figure 16b shows the activity of compound **49** to prevent biofilm formation in NCTC 6571 showing over 99% reduction in biofilm mass. The presence of ethanol showed a non-significant reduction in biofilm mass by 20%, which clearly indicated that the prevention of biofilm formation was again due to compound **49**, not ethanol.

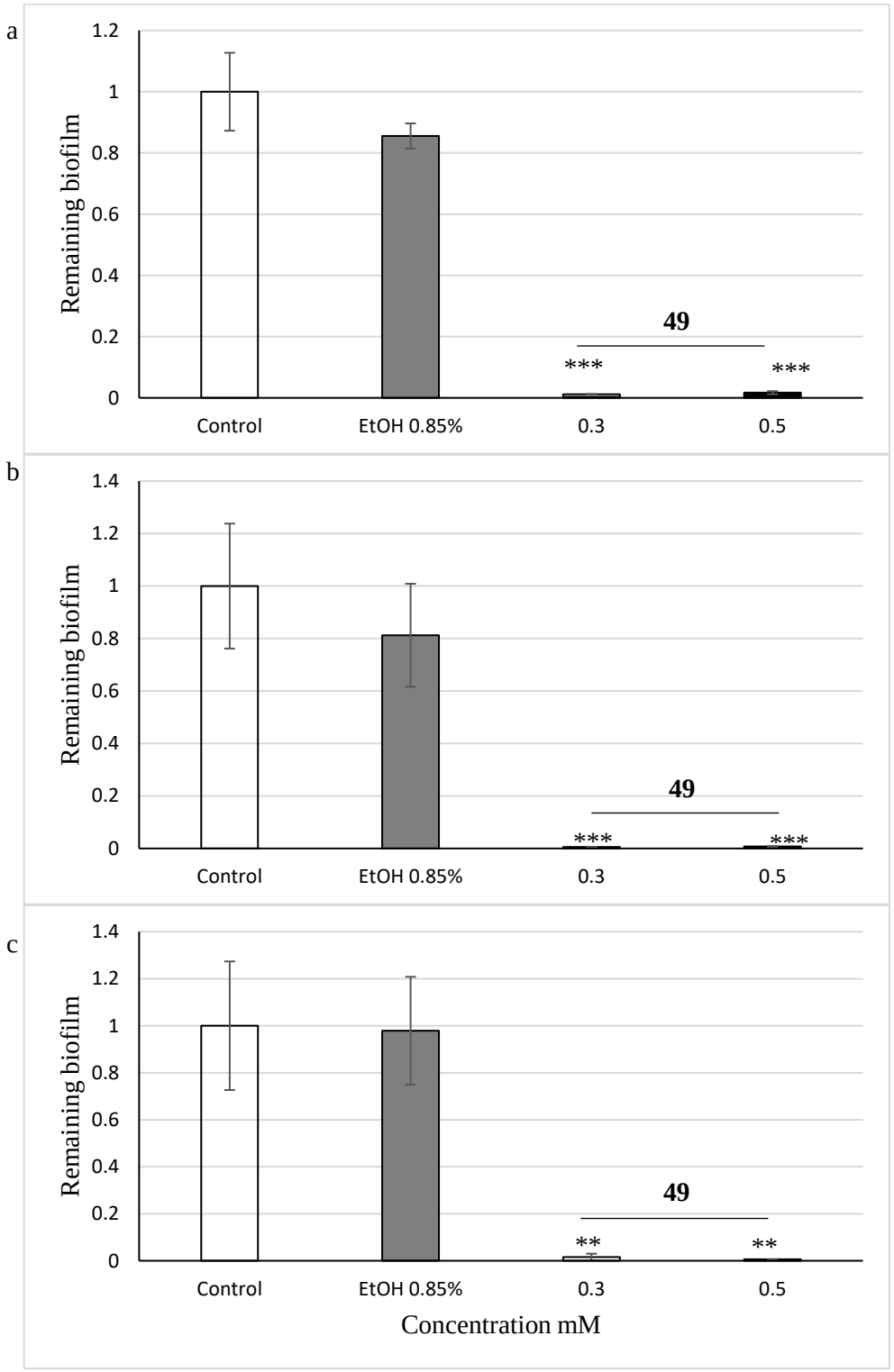

Figure 16: The effects of compound **49** on biofilm formation in a) MRSA 252, b) NCTC 6571, c) MSSA 15981. The results are the average of three independent experiments, with each one replicated in 8 wells and normalised against Control (untreated bacteria). The error bars indicate the standard deviation. Significance tests compared to control ** $p < 0.01$, *** $p < 0.001$. Crystal violet assay.

Figure 16c shows the activity of compound **49** to prevent biofilm formation in MSSA 15981 showing over 99% reduction in biofilm mass. The presence of such a low concentration of ethanol has almost no effect on biofilm mass, which clearly indicated that the prevention of biofilm formation was solely caused by compound **49**. Recalling certain published molecules (Figure 14), these molecules perform their activity by targeting bacterial cell membranes (Hoque et al., 2016), which explains their non-selective activity against bacteria. The structural resemblance between compound **49** and compound **53** and the non-selective activity against bacterial strains suggests that **49** may act by targeting bacterial cell membrane. Whereas compounds **33-36** are strain dependent and probably work by affecting QS or other toxicity mechanisms.

Compounds **46-48** were tested for their activity to disperse preformed biofilms in the three chosen bacterial strains. Figure 17a shows the activity of compounds **46-48** to disperse existing biofilm of MRSA 252. All tested polyamines show higher biofilm mass in MRSA 252 biofilms, the most active one was **48** at concentration = 0.5 mM which increased biofilm by 30%. The result of a higher biofilm mass was expected as these compounds showed activity to increase biofilm formation for this strain in the previous section (Figure 15a). Figure 17b shows the activity of compounds **46-48** to disperse existing biofilm in NCTC 6571. All three compounds tested showed no effect on preformed biofilms in NCTC 6571. Figure 17c shows the activity of compounds **46-48** to disperse preformed biofilm in MSSA 15981. All the tested polyamines show low activity in MSSA 15981 biofilms, the most active was **47** at concentration = 0.5 mM which reduced biofilm by 14%.

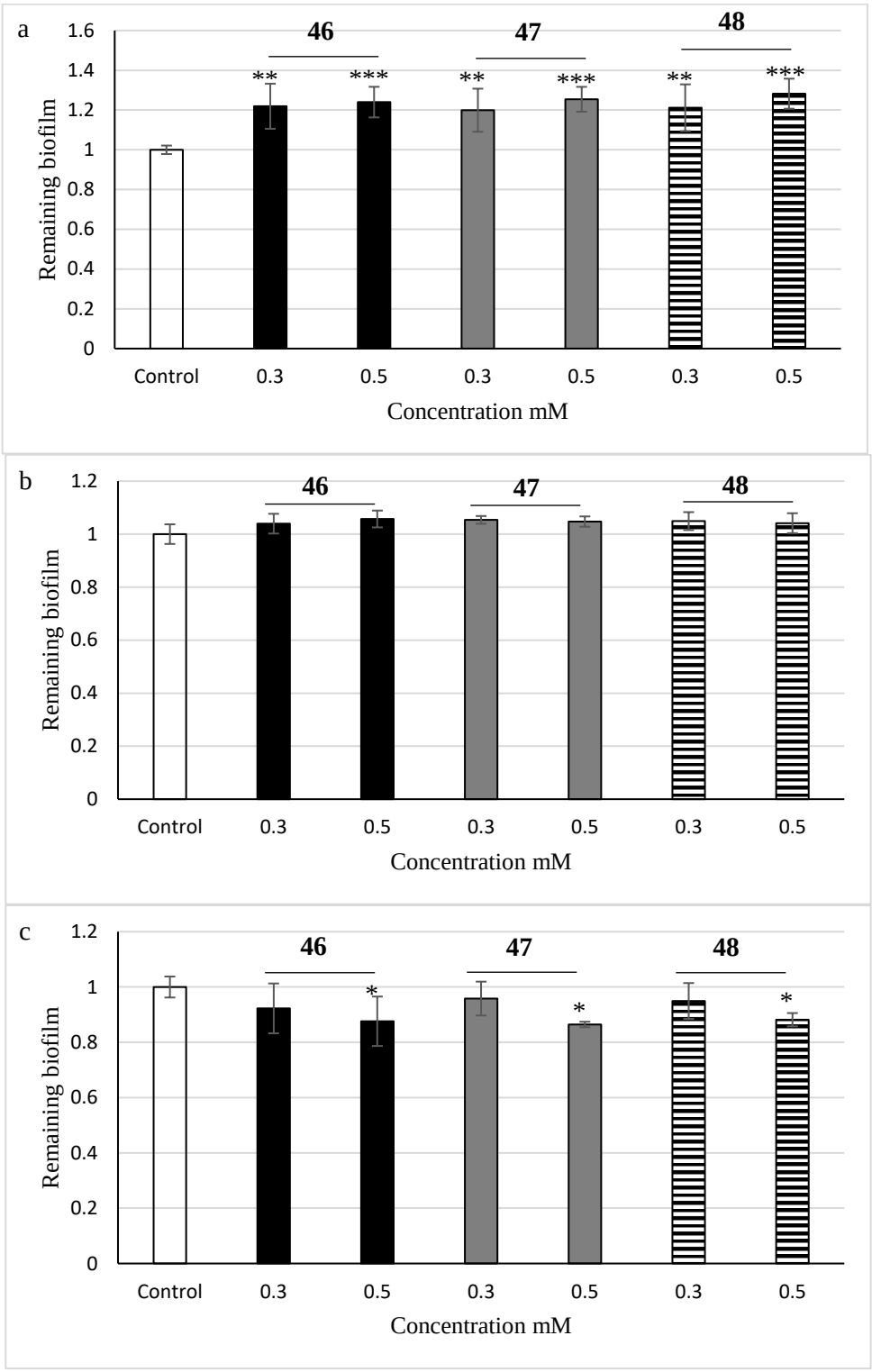

Figure 17: The effects of compounds **46**-**48** on dispersing existing biofilm in a) MRSA 252, b) NCTC 6571, c) MSSA 15981. The results are the average of three independent experiments, with each one replicated in 8 wells and normalised against Control (untreated bacteria). The error bars indicate the standard deviation. * $p < 0.05$, ** $p < 0.01$, *** $p < 0.001$. Crystal violet assay.

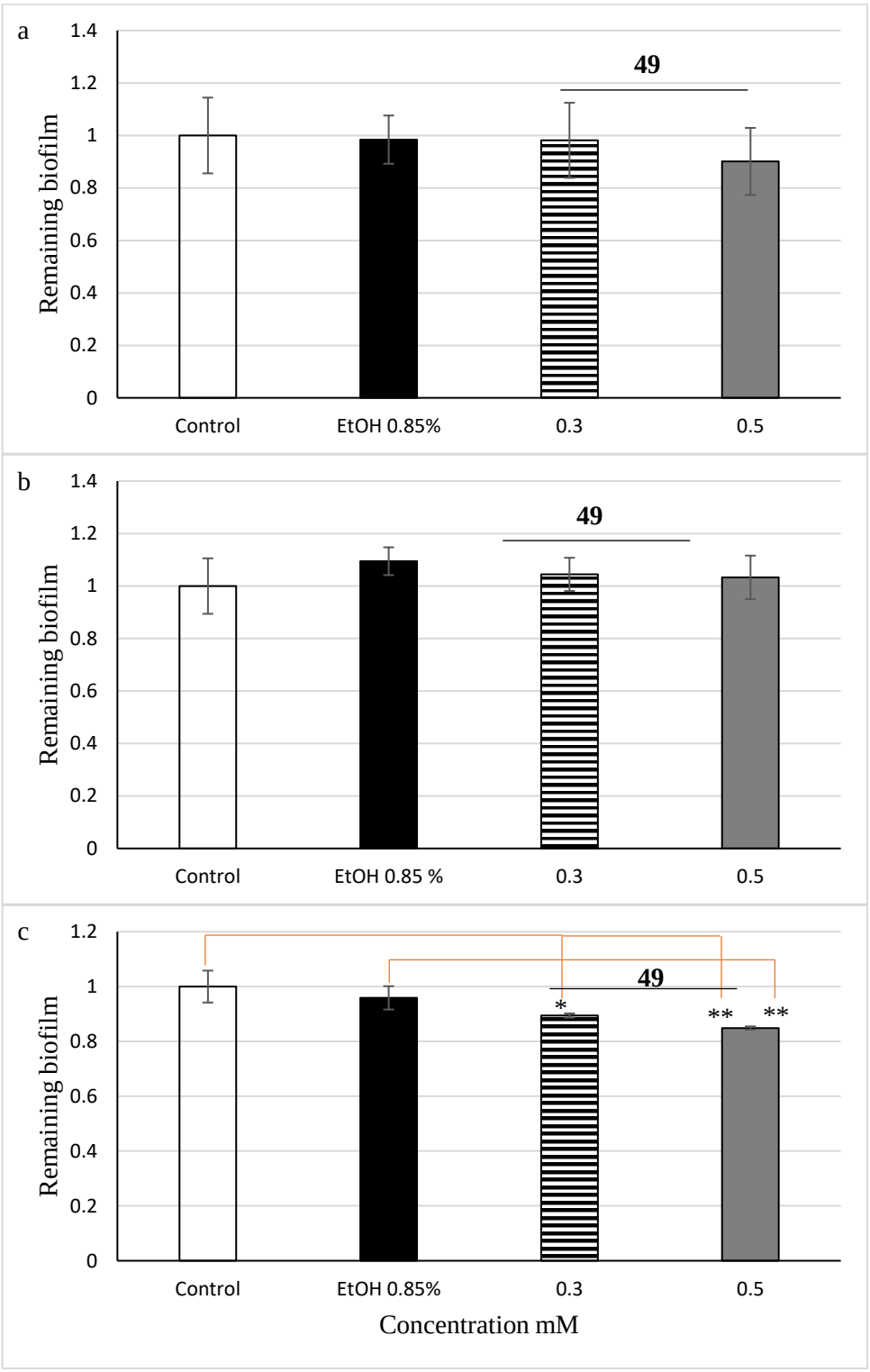

Figure 18: The effects of compound **49** on dispersing existing biofilm in a) MRSA 252, b) NCTC 6571, c) MSSA 15981. The results are the average of three independent experiments, with each one replicated in 8 wells and normalised against Control (untreated bacteria). The error bars indicate the standard deviation. Significance tests compared to control * $p < 0.05$, ** $p < 0.01$. Crystal violet assay.

As compound **49** is insoluble in water as mentioned in the previous section, a solution of ethanol in water (0.85% v/v) was therefore used as a positive control in each experiment. Compound **49** was dissolved in water solution containing a small amount of ethanol (0.85% v/v). Figure 18a shows the activity of compound **49** to disperse existing biofilm in MRSA 252. Figure 18b shows the activity of compound **49** to disperse existing biofilm in NCTC 6571. Compound **49** shows no activity to disperse preformed biofilms in either MRSA 252 or NCTC 6571.

Figure 18c shows the activity of compound **49** to disperse existing biofilm in MSSA 15981 where compound **49** shows low activity to disperse preformed biofilm in MSSA 15981, biofilm mass decreased by 15% at concentration = 0.5 mM. In this experiment, all biofilms were grown under the same conditions. After 24 h, polyamines were added for another 24 h, then biofilm mass was measured. The reduction in biofilm mass might be due to preventing full maturation of the biofilm on the second day.

3.2.4 Effect of polyamines on cellular viability

The crystal violet assay is a good technique to measure the biofilm mass. Crystal violet dyes can stain live and dead cells, and biofilm components as well. After dissolving this stain, the absorbance measured gives us an indication about the whole biofilm mass. However, lower biofilm mass does not necessarily mean lower viable count. Here we tested **33** and **35** for their ability to prevent biofilm formation using the Miles-Misra method by suspending the biofilm in PBS which was serially diluted and spotted on agar plates, incubated for 24 h, then colonies were counted. Figure 19 shows the relative number of colonies in biofilms treated with **33** and **35** to NCTC 6571 control. **33** and **35** reduce number of bacterial colonies by 70% and 69% respectively.

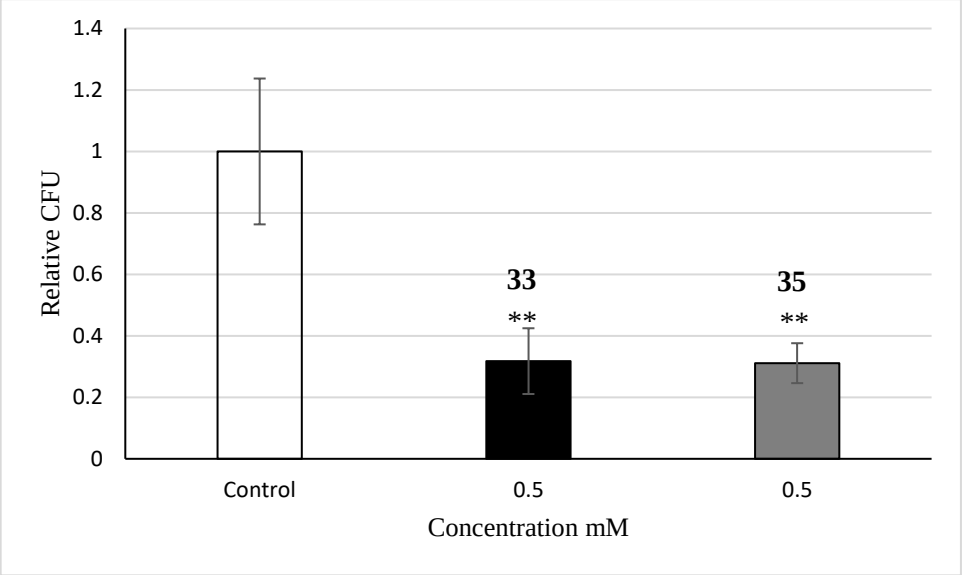

Figure 19: The effects of **33** and **35** on the number of live bacterial cells during biofilm formation in NCTC 6571. The number of colonies is the average of three independent experiments normalised against untreated bacteria control (1.5 X 10*7 CFU / mL). The error bars indicate the standard deviation. ** $p < 0.01$. Miles-Misra assay.

This result shows that the reduction in the number of colonies is not significantly different from the reduction of biofilm mass using the crystal violet assay previously discussed in this chapter (Figure 11b), where the reduction of biofilm mass were measured for the same compounds and the same concentration on NCTC 6571, and **33** and **35** reduced biofilm mass by 46% and 52% respectively (Table 3). This small non-significant variation in the reduction percentages may be indicative that some bacterial cells in polyamine treated biofilms either died and were trapped within the biofilm or were freed as cells with planktonic status and therefore potentially removed in the various washing steps. Under the conditions used, sonication to disperse cells in biofilms showed no detrimental effect on the viability of bacteria (Bolhuis, A., Personal communication, 17/01/19).

Table 3: The percentage reduction in mass and number of colonies in NCTC 6571 biofilms treated with **33** and **35** at concentration = 0.5 mM relative to NCTC 6571 control using crystal violet assay and Miles-Misra viable count assay.

	33	**35**
Reduction of the biofilm mass using the crystal violet assay	46 (±0.12)	52 (±0.07)
Reduction in the viable count in the biofilm using Miles-Misra assay	70 (±0.11)	69 (±0.06)

3.2.5 Preventing biofilm formation analysed using confocal microscopy

To investigate the ability of polyamines to prevent biofilm formation and disperse existing biofilms in a more qualitative technique, Live/Dead BacLight stains and confocal microscopy were used. Live/Dead BacLight stain contains two components: SYTO 9 that fluoresces green and propidium iodide that fluoresces red (Figure 20). These two dyes stain nucleic acids, however, SYTO 9 is able to penetrate both live and dead cells, but propidium iodide only penetrates dead cells (cells with a damaged membrane). When both dyes are added together, live cells appear green in colour, while dead cells, which contain both dyes, appear red in colour as propidium iodide is both a stronger fluorophore and has more affinity towards nucleic acids than SYTO 9.

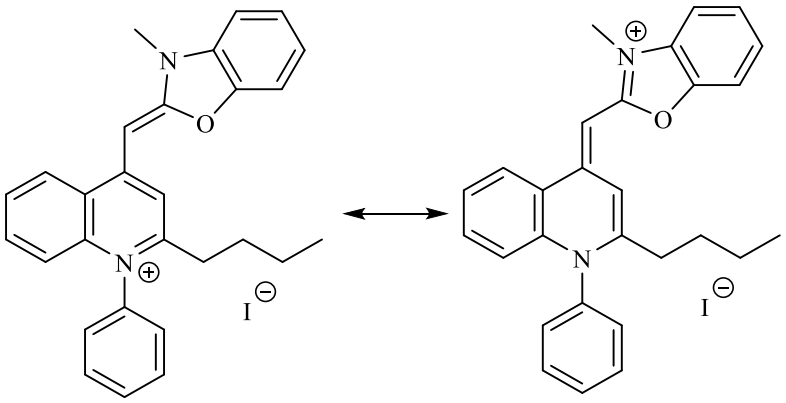

Resonance isomers of SYTO 9

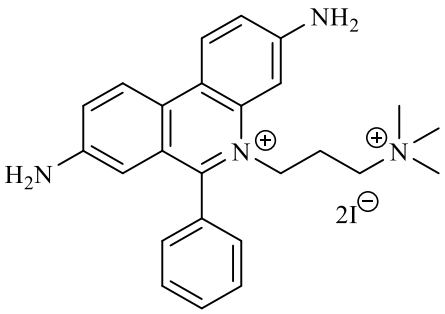

Propidium iodide

Figure 20: The chemical structure of SYTO 9 and propidium iodide dyes which present in BacLight stain.

Figure 21 shows confocal laser scanning microscopy (CLSM) images from which to analyse the activity of **33** or **35** to prevent biofilm formation in the NCTC 6571 strain. Biofilms were grown on plastic coverslips. Applying **33** and **35** at concentration = 0.5 mM resulted in lower biofilm thickness and reduced it by 46% and 48%, respectively.

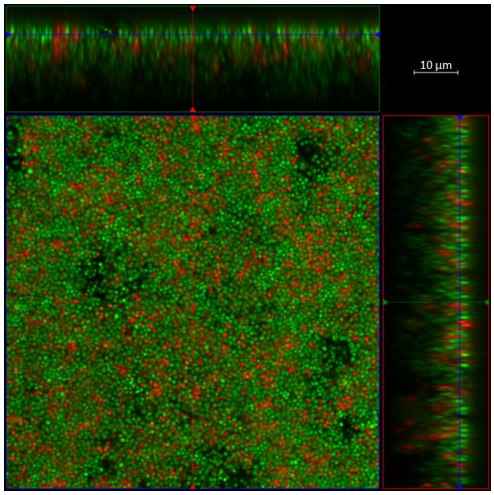

Control Thickness = 19.7 µm

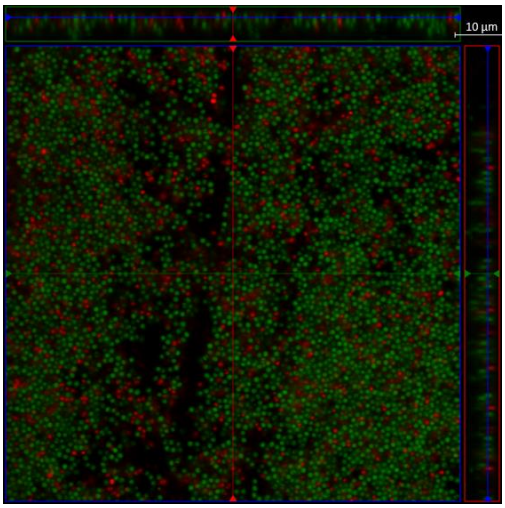

33 Thickness = 10.3 µm

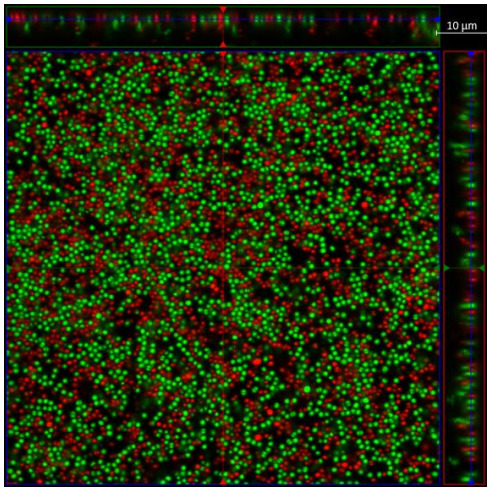

35 Thickness = 10.7 µm

Figure 21: Representative CLSM images showing the effects of **33** and **35** at concentration = 0.5 mM on the thickness of NCTC 6571 biofilms grown on plastic coverslips. Side views, XZ (top) and YZ (right) are sagittal sections of the biofilm. Scale Bar = 10 µm. Images analysed using ZEN lite program.

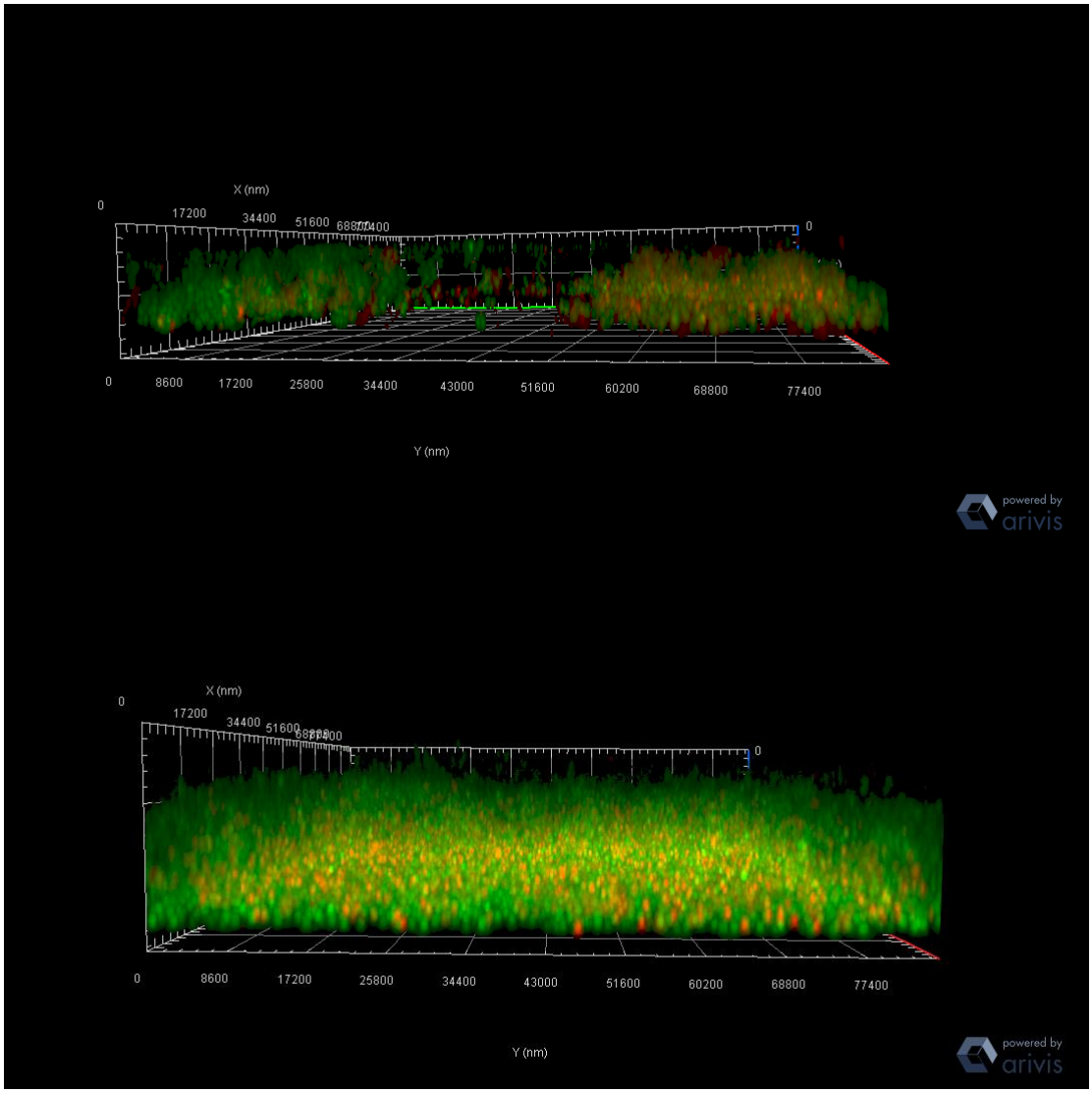

Figure 22: Representative CLSM 3D images showing the 3D distribution of 24-h control NCTC 6571 biofilm (lower) and **33** (concentration = 0.5 mM) treated biofilm (upper) grown on plastic coverslips. Images analysed using ZEN lite program.

The 3D structure of biofilms is not uniform, especially when polyamines are added. Figure 22 shows the 3D structure of control NCTC 6571 biofilm and **33** treated sample grown on plastic coverslips. The coverslips dimensions are 22 x 22 mm, image shown represents a 80 x 80 µm section of a random spot on the coverslip. Images show irregular shape of biofilm thickness in the **33** treated sample. This uneven distribution of biofilms resulted in unreliable measurements of biofilm thickness.

To quantify the ability of **33** and **35** to prevent biofilm formation statistically, biofilm thickness was measured in 5 previously determined random spots on coverslips. Figure 23 shows the average thickness of NCTC 6571 biofilm formed in the presence of **33** or **35** relative to NCTC 6571 control. **33** and **35** show lower biofilm thickness and reduce biofilm thickness by 46% and 48%, respectively.

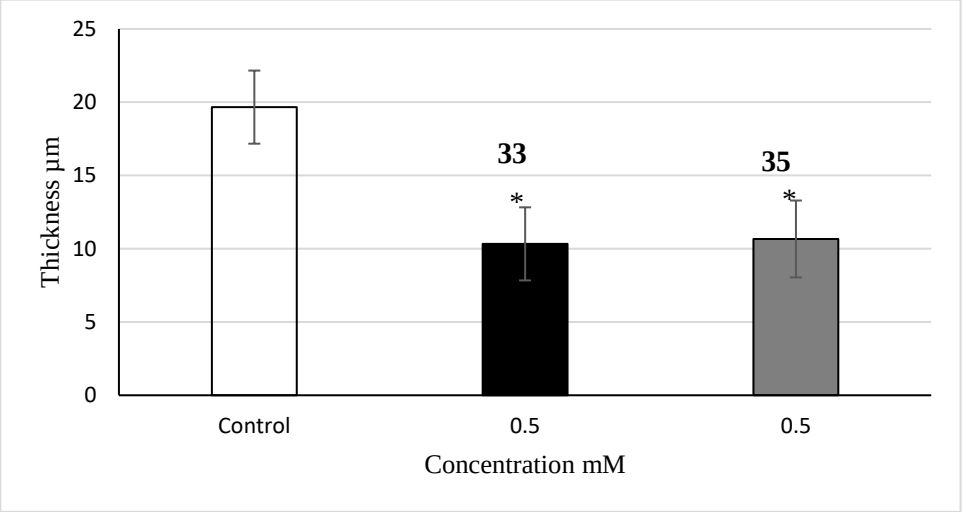

Figure 23: The effects of **33** and **35** on biofilm formation in NCTC 6571. The thickness is the average of three independent experiments, with each one measured in 5 random spots on each coverslip. The error bars indicate the standard deviation. * $p < 0.05$. Thickness was measured using confocal microscopy.

This result is close to the previously discussed result in this chapter (Figure 11b), where the reductions in biofilm mass was measured for the same compounds and at the same concentration on NCTC 6571 using the crystal violet assay. Compounds **33** and **35** reduced biofilm mass by 46% and 52% respectively (Table 4). However, the confidence in measuring biofilm mass by measuring thickness is limited by the variation of thickness from place to place on the coverslip, especially when treated with polyamines which makes the biofilm fragile with uneven distribution and irregular fragmentation after several washing steps. The modification of the surface on applying coverslips on the glass slides may induce different biofilm structures.

Table 4: The reduction percentage of mass and thickness of NCTC 6571 biofilms treated with **33** and **35** at concentration = 0.5 mM relative to NCTC 6571 control using crystal violet assay and confocal microscopy assay.

	33	**35**
Reduction of the biofilm mass using the crystal violet assay	46 (±0.12)	52 (±0.07)
Reduction in the biofilm thickness using confocal microscopy	48 (±0.13)	46 (±0.13)

In order to determine the effects of two chosen antibiotics, vancomycin and tetracycline, on the three bacterial strains, they were assayed using crystal violet which reports on the total mass of the biofilm not specifically on live or dead cells. The minimum inhibitory concentration (MIC) of vancomycin against MRSA 252 is 2 µg/mL. For both NCTC 6571 and MSSA 15981, the MIC is 4 µg/mL. For tetracycline, the MIC for MRSA 252 is 0.25 µg/mL, for NCTC 6571 the MIC is 0.5 µg/mL, and for MSSA 15981 the MIC is 4.0 µg/mL (Bolhuis, A., Personal communication, 04/06/18). Figure 24 shows the use of 10 X and 100 X MIC, but the results are all similar to controls. Therefore, CLSM was used rather than crystal violet to determine live/dead cells.

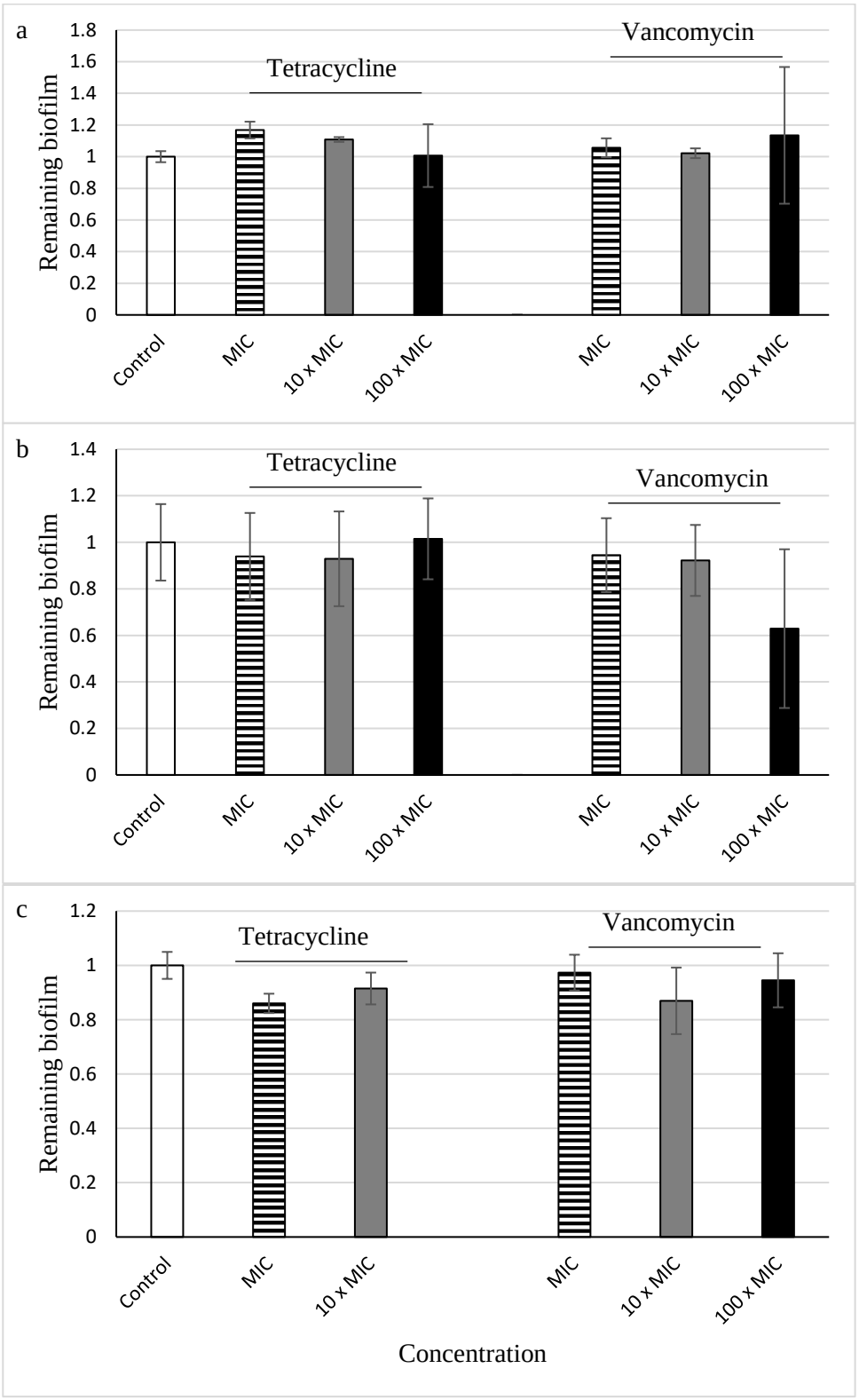

Figure 24: The effects of antibiotics vancomycin and tetracycline on dispersing existing biofilms in a) MRSA 252, b) NCTC 6571, c) MSSA 15981 strains, assayed using the crystal violet stain. The results are the average of three independent experiments, with each one replicated in 4 wells and normalised against Control (untreated bacteria). Crystal violet assay.

3.2.6 Dispersing existing biofilms analysed using confocal microscopy

The most active compounds **33**, **35**, and **49** were measured for their ability to disperse preformed biofilms in combination with vancomycin. Vancomycin was used at concentration = 40 µg/mL, which is 10 X the MIC of NCTC 6571. Figure 25 shows confocal images for the effect of these compounds (with/without vancomycin) on NCTC 6571 preformed biofilms. No significant reduction was noticed on the thickness compared to the control. However, all polyamines showed more dead cells when combined with vancomycin compared to NCTC 6571 control or vancomycin alone.

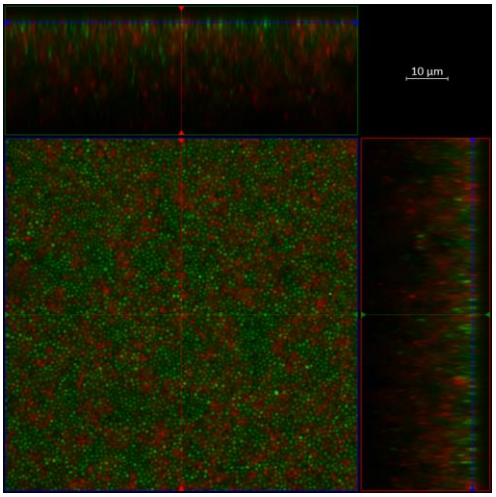

Control

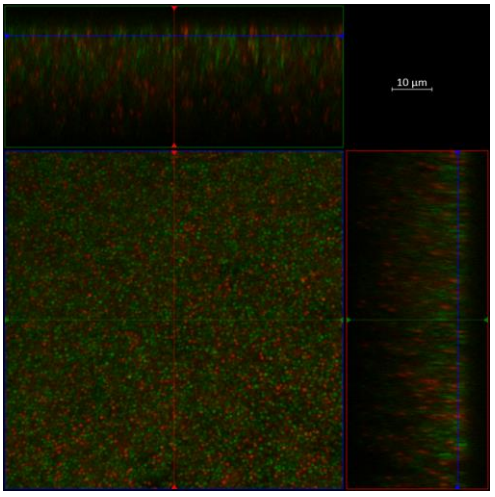

V

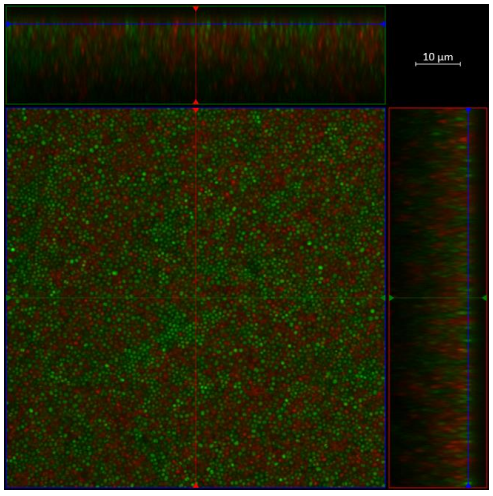

35

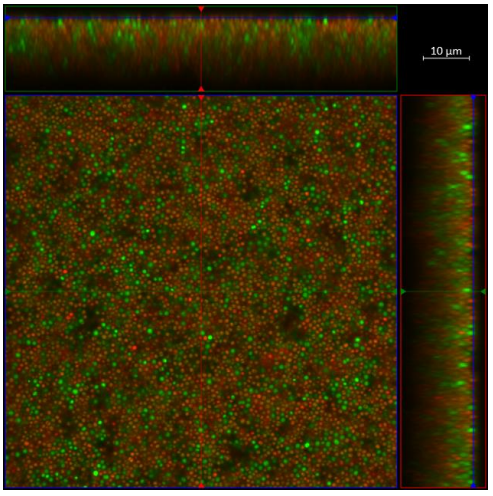

35 +V

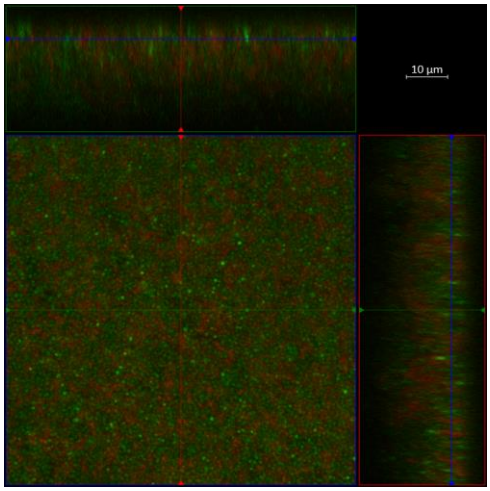

33

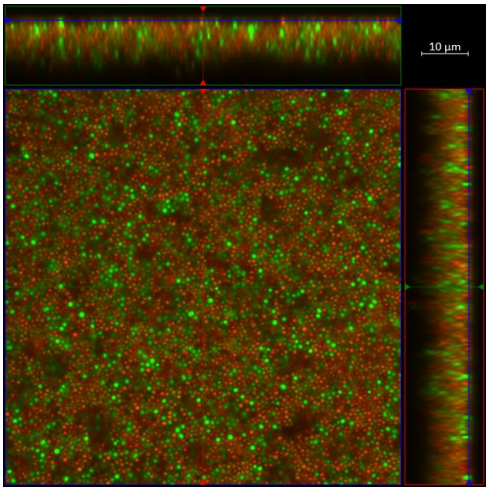

33 + V

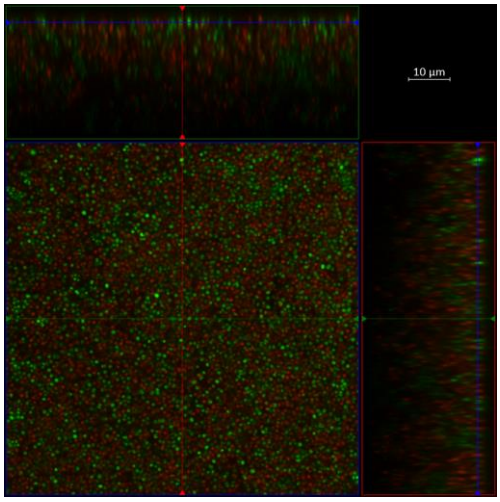

49

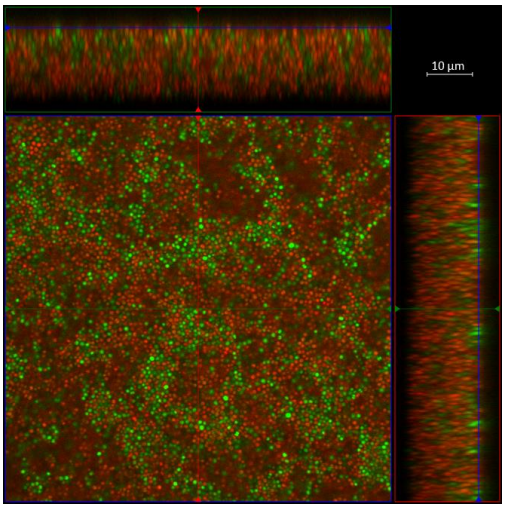

49 + V

Figure 25: Representative CLSM images showing the effect of **33**, **35**, and **49** at concentration = 0.5 mM in combination with vancomycin (40 µg/mL) on preformed biofilms of NCTC 6571 grown on plastic coverslips. Side views, XZ (top) and YZ (right) are sagittal sections of the biofilm. Scale Bar = 10 µm. Images analysed using ZEN lite program.

Compound **49** was more active, which showed a higher intensity of red fluorescence compared to control and, significantly, to vancomycin alone. This demonstrates the higher ability of this combination of compound **49** and vancomycin to kill bacteria. Still, there is no complete eradication of bacteria within the biofilm.

3.2.7 Preventing attachment

The mechanism of action of polyamines is not well-established yet. The previously discussed hypothesis in chapter 1 for the mechanism of action of polyamines (Kolodkin-Gal et al., 2012) suggested that norspermidine works by interaction with extracellular polysaccharides in the biofilm matrix. Recently, Ou and Ling suggested that norspermidine works by affecting QS (Cardile et al., 2017; Ou and Ling, 2017). We investigated whether polyamines prevent biofilm formation by affecting the EPS component of the biofilm after the maturation of the biofilm or if they act earlier in the initial adherence to surfaces. Figure 26 shows the effect of polyamines on the attachment of NCTC 6571 bacteria to the surface of 6-well plates. Tested polyamines were able to prevent adherence of cells in NCTC 6571, with compound **49** being the most active, and **48** the least active. With the exception of **48**, all compounds show more than 69% lower cells attached to the plate surfaces. **48** shows 18% lower number of cells attached to the plate surfaces, **48** has also the lowest activity to prevent biofilm formation in NCTC 6571 and lowered biofilm mass by 18% (Figure 15b). These results show that the mechanism of action of polyamines on NCTC 6571 happens primarily by inhibiting attachment to surfaces, which is the first step in biofilm formation.

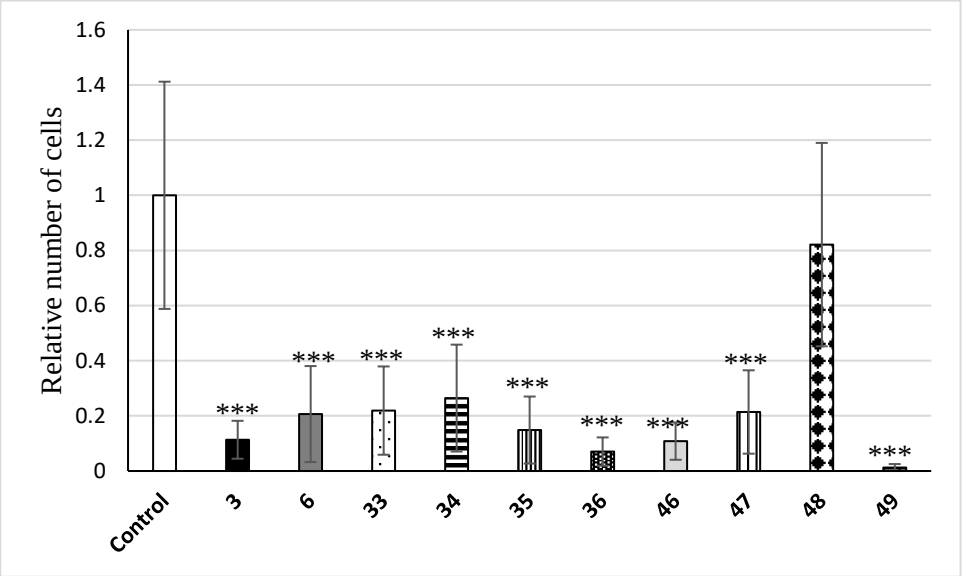

Figure 26: The effect of polyamines (norspermidine **3**, norspermine **6**, **33**-**36**, **46**- **49,** concentration = 0.5 mM) on the attachment of NCTC 6571 bacterial cells to 6-well plate polystyrene surface after 2 h of incubation. Attached bacterial cells were counted under microscope in 10 random spots on the plate surface (100 x, oil lens). The results are the average of 10 measurements in one experiment relative to control (40 attached cells). The error bars indicate the standard deviation. *** $p < 0.001$.

This result supports the hypothesis that polyamines work by affecting the QS system. QS plays an important role all the way in biofilm formation steps from the attachment to the late maturation stage (Tomlin et al., 2005). Via QS, bacteria can regulate the expression of various genes that affect the bacterial attachment in *S. aureus,* e.g. affecting the expression of surface proteins or extracellular polysaccharides, the latter affects cell-to-cell adhesion (Deep et al., 2011; Kong et al., 2006). Polyamines could prevent biofilm formation by affecting QS in both attachment and maturation steps.

3.2.8 Growth curves

The activity of polyamines on biofilm mass could not be only due to their effect on the formation of biofilm, but they might also be toxic for bacterial cells, which will result in a lower number of bacterial cells, and a lower biofilm mass as a result. Active compounds were tested for their effect on NCTC 6571 growth by measuring the optical density (O.D.) of the medium containing NCTC 6571 bacteria as a control or NCTC 6571 bacteria with one of the active polyamines every one hour for 13 hours. Figure 27 shows the effect of the most active compounds (norspermidine, norspermine, **33**-**36**, **46**-**48**, **49** (dissolved in 0.85% ethanol in water v/v), ethanol 0.85%)) on NCTC 6571 growth. With the exception of compound **49**, all compounds resulted in similar rate of growth for NCTC 6571, indicating that there is no toxic effect of these compounds on bacterial growth at the concentrations used and their activity is related to their effect on biofilms. However, compound **49** at concentration = 0.5 mM prevented bacterial growth. This reflects a toxic effect of this compound on NCTC 6571 strain.

This result, in addition to the previous results of the non-selective activity of **49** in preventing biofilm formation in all the three chosen strains, suggests that **49** which has a 12-methylene spacer kills bacteria, probably by targeting the cell wall in a similar way to the reported compound **53** discussed in Figure 14. Other polyamines with the shorter three-methylene spacers are strain selective and do not affect bacterial growth. These compounds might work by targeting QS.

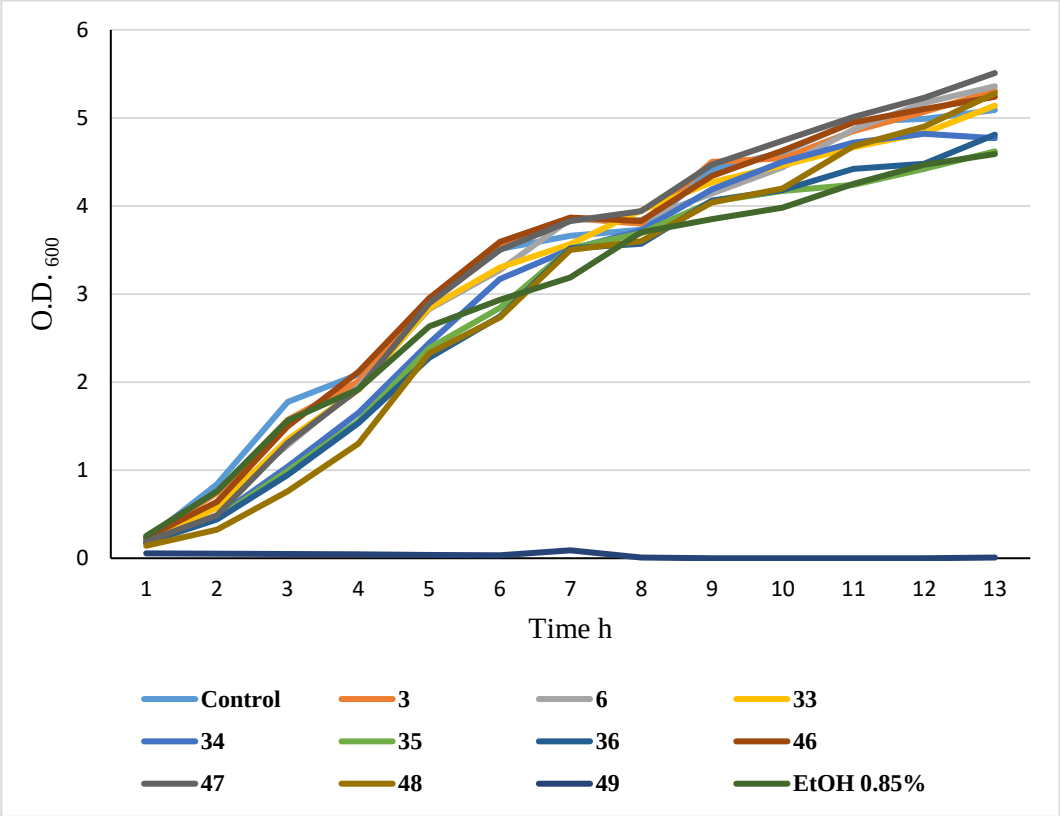

Figure 27: The effect of polyamines (norspermidine **3**, norspermine **6**, **33**-**36**, **44**-**48**, **49** dissolved in ethanol in water (0.85% v/v), and ethanol in water (0.85% v/v) as a solvent control for **49**) on the growth of NCTC 6571 cells at concentration = 0.5 mM. O.D. was measured at 600 nm. The results are for one experiment.

Following on from the interesting synergy result reported and discussed above (Figure 25), obtained from CLSM images, experiments were designed and carried out to investigate if this synergistic activity between polyamines and antibiotics with respect to eradicating existing biofilms can be quantified, e.g. using the Miles-Misra method. Vancomycin (40 µg/mL, 10 x MIC) alone and in combination with polyamines (**33**, **35**, or **49**, 0.5 mM) was added to biofilms of NCTC 6571, grown for 24 h in a 96-well plate format. After another 24 h, live bacterial cells were counted using the Miles-Misra method. However, with the exception of the negative bacteria control, all the tested biofilms showed no viable cells, a surprising result at only 10 X MIC and a result not in agreement with the results obtained by CLSM.

In the Miles-Misra counting method, the biofilm was removed by scraping the biofilm out of the well thoroughly with a tip, transferring in to a 1 mL Eppendorf tube with PBS. Finally, the cells were sonicated for 5 min to disperse the cells from the biofilm, converting them to planktonic cells for the required serial dilution in the chosen counting method. Possibly, therefore, an amount of vancomycin adsorbed on the biofilm killed the bacterial cells during the time between the scraping out, the sonication, and the dilution steps.

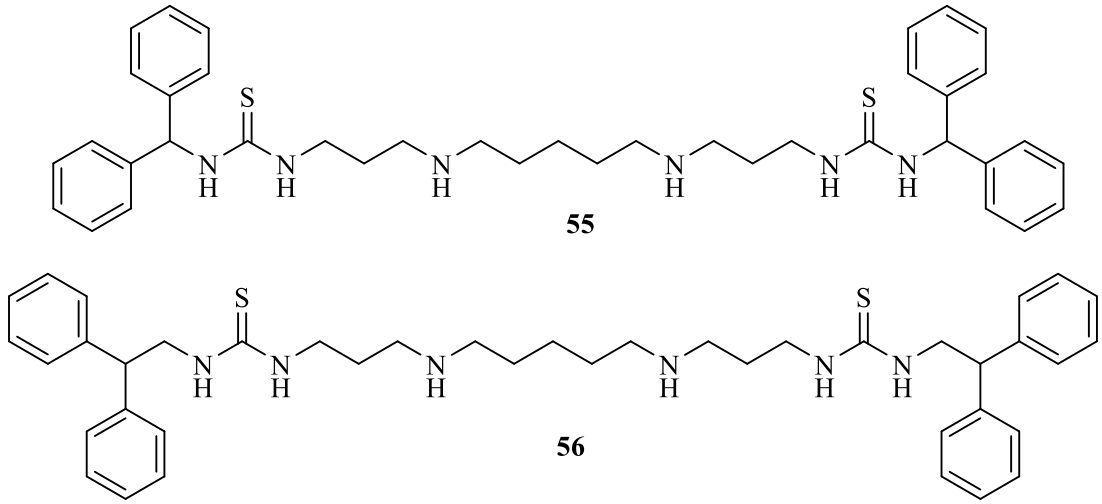

Figure 28: Polyamine analogues with antibacterial and anti-biofilm activity.

Polyamine-based analogues **55** and **56** were recently reported (Wang et al., 2016), where amino groups are separated by methylene groups and flanked by thioamides and hydrophobic moieties (Figure 28). These molecules reduce biofilm formation and disperse existing biofilms in *P. aeruginosa* by targeting bacterial membranes. Compound **56** was able to inhibit biofilm formation in *P. aeruginosa* at concentration = 64 µg/mL. Whilst the biofilms of *P. aeruginosa* have not been investigated in this thesis, the synthetic polyamine analogue **33** showed inhibition of *S. aureus* NCTC 6571 biofilm formation at concentration = 77 µg/mL (0.3 mM) and it reduced biofilm mass by 60%.

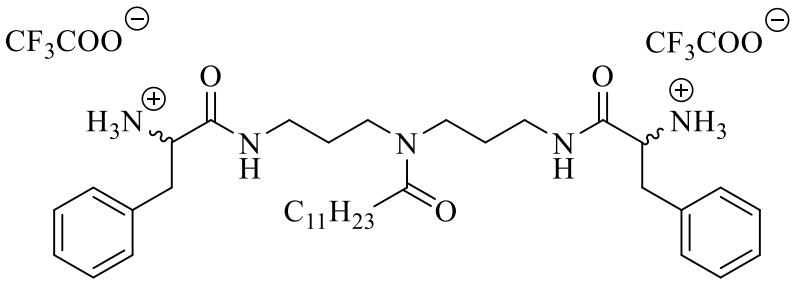

57

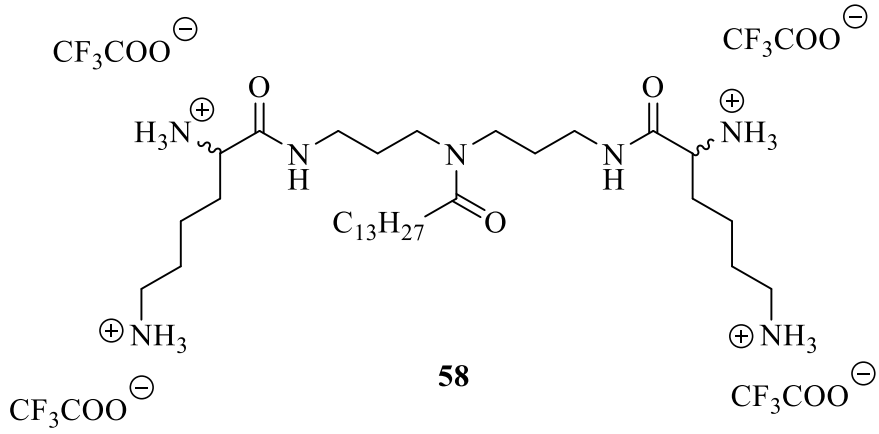

58

Figure 29: Lipidic polyamine analogues with antibacterial and anti-biofilm activity.

Norspermidine-di-amino acid designed analogues conjugated to long lipophilic chains (compounds **57** and **58**, Figure 29) have antibacterial activity (Konai et al., 2014; Konai and Haldar, 2015). Both compounds **57** and **58** were active against several Gram-positive and Gram-negative bacteria species including *S. aureus, E. faecium, E. coli,* and *K. pneumoniae*. Moreover, compound **58** showed biofilm disrupting activity in *S. aureus* MTCC 737 at concentration = 60 µg/mL by targeting bacterial cell membranes. Whilst compound **33** was unable to disrupt preformed biofilms, it inhibited biofilm formation of *S. aureus* NCTC 6571 at concentration = 77 µg/mL (0.3 mM).

These two analogues **57** and **58** are triamides with respect to the polyamine norspermidine moiety. Nevertheless, they each have four positive charges from the two Lysine amino acid substituents.

In addition to the above polyamine conjugates **55** and **56** and the tetracationic polyamine derived triamides **57** and **58** being recently reported, whilst these studies were ongoing, several other research groups have reported on the inhibition of biofilm formation using either relatively simple natural products or on the dispersal of biofilms using an antimicrobial polypeptide analogue which is comparable with the more active molecules reported herein as it also carries three positive charges and is hydrophobic. Recently, anthranilamide-amine and guanidine conjugates which display antibacterial and anti-biofilm activity have also been reported (Kuppusamy et al., 2018). They are antimicrobial peptide mimicking compounds that act by disrupting cell membranes. Therefore, the presence of a positive charge and a hydrophobic moiety, in this case a naphthyl region, makes them comparable with the lipopolyamines designed and synthesized above. The biological activity arising from these phytochemical natural products and their analogues is briefly discussed in the context of such lipid-substituted positively charged molecules.

The natural product ajoene **59**, extracted from antibacterial garlic, *Allium sativum*, inhibits QS in *P. aeruginosa* (Figure 30). Fong et al. screened 480 compounds, and following quantitative SAR QS inhibition studies on 25 disulfides, they established that the allyl group could be replaced with other substituents, e.g. benzothiazole (Fong et al., 2017). Analogue **60** containing the disulfide bridge of ajoene was the most active, inhibiting *P. aeruginosa* biofilm formation on a mouse implant infection model.

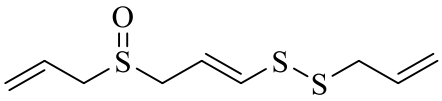

59

Ajoene

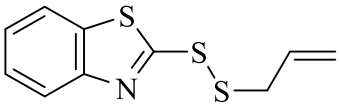

60

Figure 30: Disulfides with activity in preventing the formation of biofilms.

A synthetic analogue **61** of the antimicrobial linear lipopeptide paenipeptin has recently been reported to disperse existing biofilm in *S. aureus* TTCC 29213 at concentration = 40 µg/mL (Figure 31) (Moon et al., 2017). This compound carries three positive charges and hydrophobic residues; it acts by damaging cell membrane.

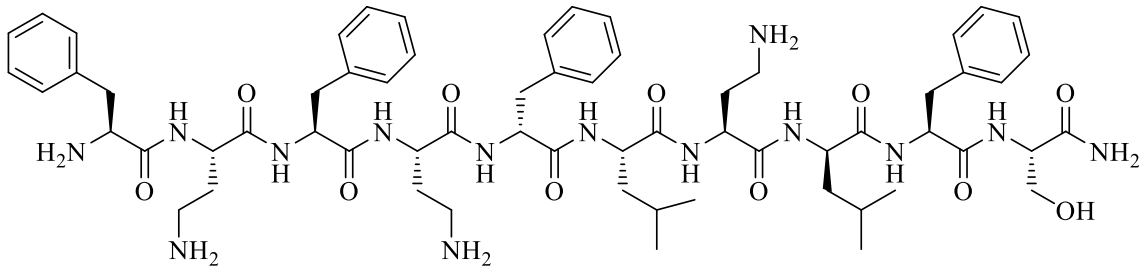

61

Figure 31: Antimicrobial polypeptide analogue which disperses existing biofilms.

In a very recent *Nature Communication*, iron oxide nanoparticles coated with carboxymethyl-dextran (Ferumoxytol), approved for the treatment of iron deficiency, have been reported to have biofilm disrupting activity by binding within the biofilm ultrastructure and generating free radicals from H_2O_2 that in situ kill bacteria by damaging their cell membrane and degrading the EPS matrix (Liu et al., 2018).

Biofilm disrupting activity for anthranilamides conjugated to a guanidine functional group, compounds **62** and **63** (Figure 32) has also recently been reported (Kuppusamy et al., 2018). They designed and prepared short peptidomimetics based on the anthranilic acid (2-aminobenzoic acid) moiety as their scaffold, terminating *N*-ethyl chains in primary amines, tertiary amines, *N*-trimethyl quaternised ammonium ions, and guanidines (Figure 32). The most active analogue fluoro-substituted **62** reduced preformed biofilms mass of *S. aureus* by 92% at concentration = 64 µM and bromo-substituted **63** reduced preformed biofilms mass of *S. aureus* by 83% at concentration = 62.4 µM (Kuppusamy et al., 2018). These guanidines, like triamine **61**, are antimicrobial peptide mimicking compounds that act by disrupting cell membranes.

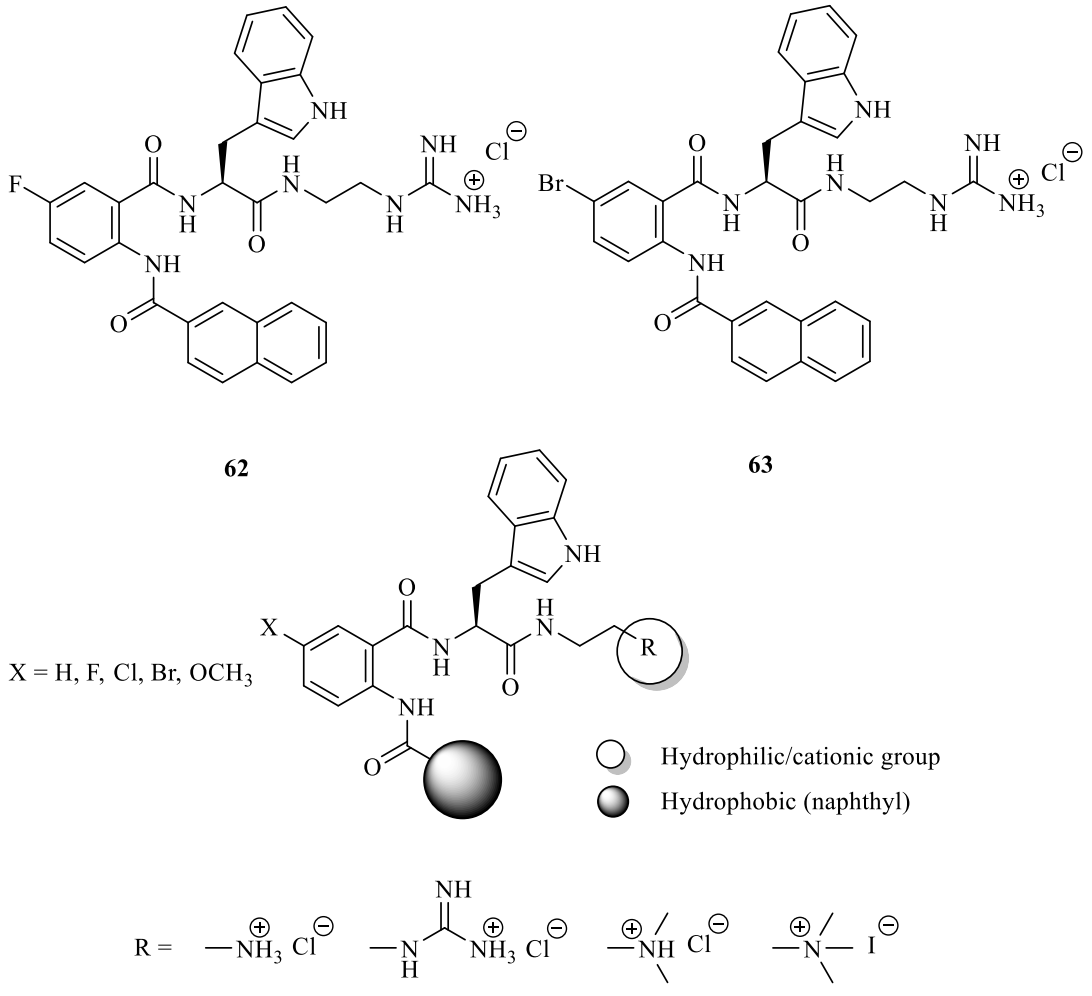

Figure 32: Anthranilamide-guanidine conjugates which display antibacterial and anti-biofilm activity.

A paper from Hoque and co-workers (Hoque et al., 2016) reports how lipid amide, quaternised polyamines **64**-**67** can prevent biofilm formation and even eradicate established biofilms. Some of their molecules are bactericidal. The compounds share a common structural feature of having amino groups separated by a hydrocarbon chain and flanked by positively charged moieties. Their most active molecules contain a hydrocarbon chain of 6 to 12 methylene spacers between amine groups.

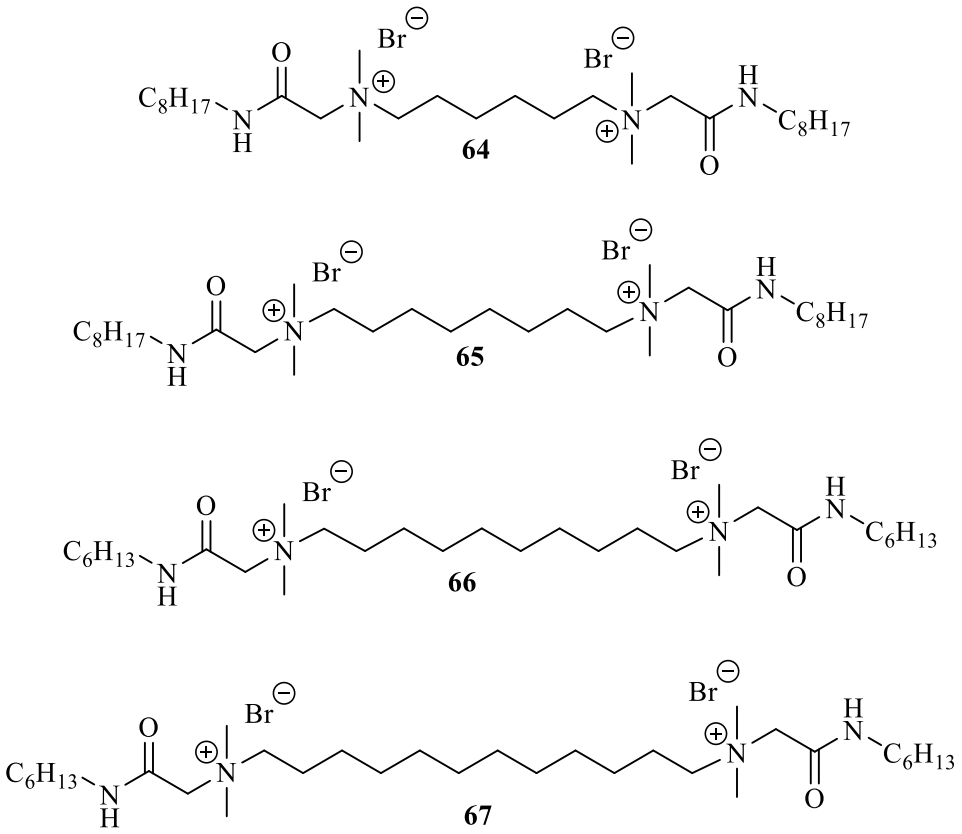

Figure 33: Cationic molecules **64**-**67** reported to have activity to prevent biofilm formation and eradicate established biofilms.

3.3 Conclusions

The microbiological activity of polyamines with controlled different spatial distances between the amino groups to prevent biofilm formation and disperse existing biofilms has been investigated. The presence of more amino groups separated by three methylene spacers in the chemical structure of the polyamines increased their activity in preventing biofilm formation in *S. aureus* NCTC 6571. However, this activity is strain dependent as these polyamines show low activity against MRSA 252 and MSSA 15981.

Most tested polyamines showed no activity to disperse preformed biofilms. The low activity of the polyamines that was observed may be due to the prevention of further biofilm formation in the second day of the preformed biofilm dispersion experiment. So, it can be realistically concluded that all tested polyamines are inactive in dispersing existing biofilms.

Vancomycin and tetracycline antibiotics showed no significant activity to disperse existing biofilms in the three chosen bacterial strains at concentrations up to the 100 X their MIC values against planktonic cells.

One polyamine, **49** did show high potency to prevent biofilm formation in all three *S. aureus* strains investigated in this thesis at concentration = 0.3 mM (94 µg/mL). Despite its low activity in dispersing existing biofilms, **49** (0.5 mM) showed activity to kill NCTC 6571 bacterial cells within preformed biofilms in combination with the antibiotic vancomycin (40 µg/mL).

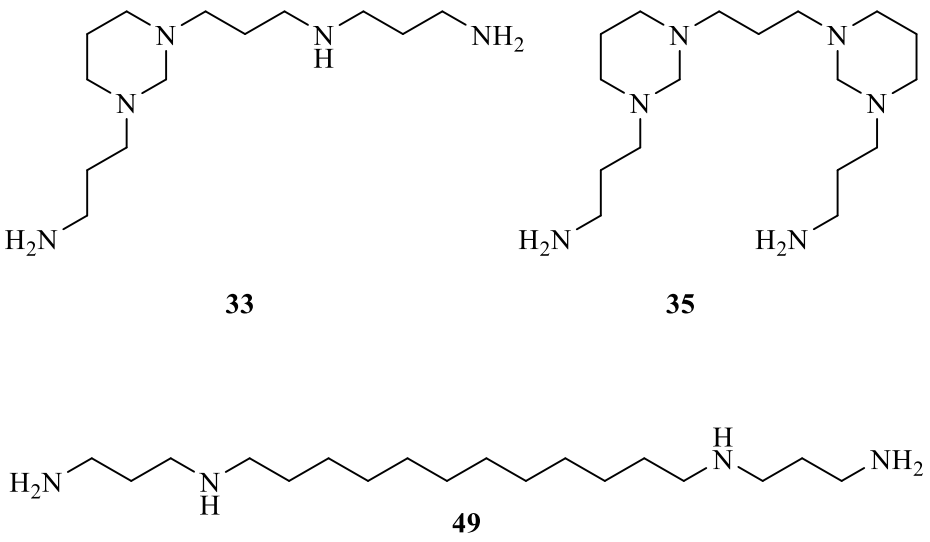

Figure 33: The most active polyamines discovered in this thesis.

In this thesis, the polyamine analogue **33** (Figure 33) showed inhibition of *S. aureus* NCTC 6571 biofilm formation at concentration = 77.2 µg/mL (0.3 mM) and reduced biofilm mass by 60%. Compound **35** also showed inhibition of *S. aureus* NCTC 6571 biofilm formation at concentration = 98.0 µg/mL (0.3 mM) and reduced biofilm mass by 56%. The analogue **49** showed inhibition of all three *S. aureus* strains biofilm formation at concentration = 94.4 µg/mL (0.3 mM) and reduced biofilm mass by 99%. Compound **49** did not show significant reduction in preformed biofilm, but showed activity to kill bacteria inside the biofilm at concentration = 157.2 µg/mL (0.5 mM).

3.4 Experimental

Materials and bacterial strains

Norspermidine, norspermine, spermidine and spermine, were purchased from Sigma-Aldrich. DNase I (bovine pancreas), proteinase K (*Tritirachiam album*), and sodium metaperiodate were purchased from Sigma-Aldrich. Ethanol and acetic acid were purchased from Fisher. Costar polystyrene 96-well plates (flat bottom, volume 0.36

mL, well diameter 7 mm) were purchased from Fisher. Tryptone Soya Broth (TSB) was purchased from Oxoid. Polyvinyl plastic coverslips (22 x 22 mm) were purchased from Electron Microscopy Science, Hatfield, UK. Crystal violet 1% was purchased from PRO-LAB Diagnostics. LIVE/DEAD BacLight was purchased from ThermoFisher. Ultraviolet-visible absorbance was measured at 595 nm using an FLUOstar Omega spectrophotometer (BMG Labtech, UK). Confocal images were obtained using a CLSM 880 (ZEISS, Germany). Bacterial strains *Staphylococcus aureus* MRSA 252 (Holden et al., 2004) MSSA 15981 (Pozzi et al., 2012), and NCTC 6571 were kindly provided by Dr A. Bolhuis, Department of Pharmacy and Pharmacology, University of Bath, Bath BA2 7AY, UK. For overnight cultures, bacterial strains were cultured in TSB medium for 15-18 h. For biofilm tests, bacterial strains were cultured in TSB medium supplemented with 0.5% glucose.

Effect of polyamines on biofilm formation

All polyamines were tested in eight wells in three independent experiments. Biofilms were grown as described previously (Alhusein et al., 2015) with modifications. Briefly, bacteria (200 µL of 1/1000 dilution of an overnight culture) were grown in 96-well plates at 37 °C in TSB medium containing 0.5% glucose for negative control and TSB medium containing 0.5% glucose, different concentrations (0.3 and 0.5 mM) of polyamines on a three dimensional plate rotator (40 rpm). After 24 h growth, the plates were washed carefully (twice with 200 µL PBS) to remove planktonic bacteria and then dried at 60 °C for 1 h. Wells were then stained with 0.1% crystal violet solution and after 15 min the plates were washed with lukewarm tap water. Acetic acid (30%, 200 µL) was added to dissolve the crystal violet and the visible absorbance was measured using a UV-visible plate reader at $\lambda = 595$ nm.

Biofilm composition studies

All strains were tested in eight wells in three independent experiments as described previously (Kogan et al., 2006; Wang et al., 2004) with modifications. Biofilms were grown as described above. After 24 h growth, the plates were washed carefully (twice with 200 µL PBS). After that, PBS (200 µL), sodium periodate (10 mM in PBS), proteinase K (0.1 mg/mL PBS), or DNase (0.1 mg/mL DNase solution containing 1 mM $CaCl_2$ and 150 mM NaCl in PBS) were added to the different wells. After 2 h, the plates were washed carefully (twice with 200 µL PBS) to remove planktonic bacteria and then dried at 60 °C for 1 h. Wells were then stained with crystal violet and the visible absorbance was measured as described above.

Effect of polyamines on dispersing existing biofilm

All polyamines were tested in eight wells in three independent experiments. Biofilms were grown as described above. After 24 h medium was replaced with TSB medium containing 0.5% glucose for control and TSB medium containing 0.5% glucose and different concentrations (0.3 and 0.5 mM) of polyamines on a three dimensional plate rotator (40 rpm). After 24 h growth, the plates were washed carefully (2 x with PBS) to remove planktonic bacteria and then dried at 60 °C for 1 h. Wells were then stained with crystal violet and the visible absorbance was measured as described above.

Effect of antibiotics on dispersing existing biofilm

Antibiotics vancomycin and tetracycline were tested in four wells in three independent experiments on each of the three chosen strains. Biofilms were grown as described above. After 24 h medium was replaced with TSB medium containing 0.5% glucose for control and TSB medium containing 0.5% glucose and different concentrations (MIC, 10 x MIC, or 100 x MIC) of the two antibiotics on a three dimensional plate

rotator (40 rpm). The minimum inhibitory concentration (MIC) of vancomycin against MRSA 252 is 2 μg/mL. For both NCTC 6571 and MSSA 15981, the MIC is 4 μg/mL. For tetracycline, the MIC for MRSA 252 is 0.25 μg/mL, for NCTC 6571 the MIC is 0.5 μg/mL, and for MSSA 15981 the MIC is 4.0 μg/mL. MIC values represent the minimum inhibitory concentration of these antibiotics against planktonic bacterial cells. After 24 h growth, the plates were washed carefully (2 x with PBS) to remove planktonic bacteria and then dried at 60 °C for 1 h. Wells were then stained with crystal violet and the visible absorbance was measured as described above.

Effect of polyamines on cellular viability

The experiment was carried out using the Miles-Misra (Miles et al., 1938) method as described previously (Alhusein et al., 2013) with modifications. Briefly, *S. aureus* NCTC 6571 biofims were grown as above with or without polyamines (**33** and **35** at concentration = 0.5 mM). After 24 h growth, the plates were washed carefully (2 x with PBS) to remove planktonic bacteria. The biofilm was removed by scraping the wells thoroughly with a tip and then transferred to a 1 mL Eppendorf tube with PBS and sonicated (Nickel electro Ltd, MU 1.5, 50-60 Hz, 20 °C) for 5 min to disperse the cells in the biofilm. The resulting suspension was then serially diluted to 10^{-6} in PBS. Ten microliters of each of 10^{-3}, 10^{-4}, 10^{-5}, and 10^{-6} dilutions were spotted on to TSB agar plates and grown at 37 °C. After 24 h, the numbers of CFU were counted using the following equation:

$$\text{CFU/well} = \text{CFU counted} \times \text{dilution factor} \times 100$$

Preventing biofilm formation analysed using confocal microscopy

The experiment was carried out as described previously (Alhusein et al., 2013) with modifications. Briefly, *S. aureus* NCTC 6571 (5 mL of 1/1000 dilution of an overnight

culture in TSB medium containing 0.5% glucose for control or TSB medium containing 0.5% glucose and 0.5 mM of polyamines **33** and **35**) were added to a 6-well plates. Polyvinyl plastic coverslips (22 x 22 mm), previously sterilized with ethanol (70%) and dried, were added to the wells and the well plates were incubated at 37 °C in static conditions. After 24 h, coverslips were washed with PBS (6 x) and stained with LIVE/DEAD BacLight mixture (500 µL, 50:50 v/v of each dye solution). The coverslips were kept in the dark for 15 min then washed with PBS (6 x) and mounted on glass slides with nail varnish. The stain was prepared from the manufacturer's kit by dissolving the powder of each stain (SYTO9 and propidium iodide) in filter-sterilized distilled water according to the manufacturer's instructions. The two solutions were mixed 1:1 and applied to the biofilm sample. The mixture was stored frozen at -20 ºC for future use. Images analysed using ZEN lite program supplied by the ZEISS Company.

Dispersing existing biofilms analysed using confocal microscopy

The experiment was carried out as described previously (Alhusein et al., 2013) with modifications. Briefly, *S. aureus* NCTC 6571 biofilms were grown on polyvinyl plastic coverslips as described above. After 24 h, medium was replaced with fresh TSB medium containing 0.5% glucose for control or TSB medium containing 0.5% glucose and 0.5 mM of polyamines (**33**, **35**, and **49**) with/without vancomycin (40 µg/mL, 10 x MIC) and grown at 37 °C in static conditions. After 24 h, coverslips were washed and stained as described above. The MIC values represent the minimum inhibitory concentration of vancomycin against planktonic bacterial cells. Images analysed using ZEN lite program supplied by the ZEISS Company.

Preventing attachment

S. aureus NCTC 6571 (200 µL of 1/1000 dilution of an overnight culture) cells were grown in 6-well plates at 37 °C in TSB medium containing 0.5% glucose for control and TSB medium containing 0.5% glucose with 0.5 mM of polyamines (norspermidine, norspermine, **33**-**36**, and **46**-**49,** concentration = 0.5 mM) on a three dimensional plate rotator (40 rpm). After 2 h growth, the plates were washed carefully (2 x with PBS) to remove planktonic bacteria and then dried at 60 °C for 1 h. Wells were then stained with 0.1% crystal violet solution and, after 15 min, the plates were washed with lukewarm water. The number of attached cells was counted under a light microscope in 10 random spots on the plate surface (100 x, oil lens).

Growth curve

S. aureus NCTC 6571 (15 mL of 1/100 dilution of an overnight culture in TSB medium for control or TSB medium containing 0.5 mM of polyamines (norspermidine (NSD), norspermine (NS), **33**-**36**, **44**-**48**, and **49** dissolved in aqueous ethanol (0.85% v/v), and ethanol in water (0.85% v/v) as a positive control for **49**) were added to a 50 mL universal tube. The O.D. was measured at 600 nm every hour for 13 h. The O.D. was plotted versus time (h).

Statistical analysis

Statistical analysis was performed using one-way ANOVA with a Dunnett post hoc test, where all groups compared to the untreated control group. * $p < 0.05$, ** $p < 0.01$, *** $p < 0.001$.

References

Alhusein, N., Blagbrough, I. S., Beeton, M. L., Bolhuis, A., De Bank, P. A., 2015. Electrospun zein/PCL fibrous matrices release tetracycline in a controlled manner, killing *Staphylococcus aureus* both in biofilms and *ex vivo* on pig skin, and are compatible with human skin cells. Pharm. Res. 33, 237-246.

Alhusein, N., De Bank, P. A., Blagbrough, I. S., Bolhuis, A., 2013. Killing bacteria within biofilms by sustained release of tetracycline from triple-layered electrospun micro/nanofibre matrices of polycaprolactone and poly(ethylene-co-vinyl acetate). Drug Deliv. Transl. Res. 3, 531-541.

Blagbrough, I. S., Metwally, A. A., Geall, A. J., 2011. Measurement of polyamine pK_a values. In: Pegg, A. E., Casero, R. A., Jr. (Eds.), Polyamines: Methods and Protocols. Humana Press, Totowa, NJ, pp. 493-503.

Booth, I. R., 1985. Regulation of cytoplasmic pH in bacteria. Microbiol. Rev. 49, 359-378.

Cardile, A. P., Woodbury, R. L., Sanchez, C. J., Jr., Becerra, S. C., Garcia, R. A., Mende, K., Wenke, J. C., Akers, K. S., 2017. Activity of norspermidine on bacterial biofilms of multidrug-resistant clinical isolates associated with persistent extremity wound infections. Adv. Exp. Med. Biol. 973, 53-70.

Chantrapromma, K., Ganem, B., 1980. The chemistry of naturally-occurring polyamines .A. Total synthesis of thermospermine. Tetrahedron Lett. 21, 2475-2476.

Cohen, S. S., 1998. A guide to the polyamines. Chapter 22, pp 481-511. Oxford University Press, New York.

Deep, A., Chaudhary, U., Gupta, V., 2011. Quorum sensing and bacterial pathogenicity: From molecules to disease. J. Lab. Physicians 3, 4-11.

Doll, K., Jongsthaphongpun K. L., Stumpp, N. S., Winkel, A., Stiesch, M., 2016. Quantifying implant-associated biofilms: Comparison of microscopic, microbiologic and biochemical methods. J. Microbiol. Methods.130, 61-68

Fong, J., Yuan, M., Jakobsen, T. H., Mortensen, K. T., Delos Santos, M. M., Chua, S. L., Yang, L., Tan, C. H., Nielsen, T. E., Givskov, M., 2017. Disulfide bond-containing ajoene analogues as novel quorum sensing inhibitors of *Pseudomonas aeruginosa*. J. Med. Chem. 60, 215-227.

Hoiby, N., Bjarnsholt, T., Givskov, M., Molin, S., Ciofu, O., 2010. Antibiotic resistance of bacterial biofilms. Int. J. Antimicrob. Agents 35, 322-332.

Holden, M. T. G., Feil, E. J., Lindsay, J. A., Peacock, S. J., Day, N. P. J., Enright, M. C., Foster, T. J., Moore, C. E., Hurst, L., Atkin, R., Barron, A., Bason, N., Bentley, S. D., Chillingworth, C., Chillingworth, T., Churcher, C., Clark, L., Corton, C., Cronin, A., Doggett, J., Dowd, L., Feltwell, T., Hance, Z., Harris, B., Hauser, H., Holroyd, S., Jagels, K., James, K. D., Lennard, N., Line, A., Mayes, R., Moule, S., Mungall, K., Ormond, D., Quail, M. A., Rabbinowitsch, E., Rutherford, K., Sanders, M., Sharp, S., Simmonds, M., Stevens, K., Whitehead, S., Barrell, B. G., Spratt, B. G., Parkhill, J., 2004. Complete genomes of two clinical *Staphylococcus aureus* strains: Evidence for the rapid evolution of virulence and drug resistance. Proc. Natl. Acad. Sci. U. S. A. 101, 9786-9791.

Heatley, N. G., 1944. A method for the assay of penicillin. Biochem. J. 38, 61–65.

Hoque, J., Konai, M. M., Sequeira, S. S., Samaddar, S., Haldar, J., 2016. Antibacterial and antibiofilm activity of cationic small molecules with spatial positioning of hydrophobicity: An in vitro and in vivo evaluation. J. Med. Chem. 59, 10750-10762.

Kogan, G., Sadovskaya, I., Chaignon, P., Chokr, A., Jabbouri, S., 2006. Biofilms of clinical strains of *Staphylococcus* that do not contain polysaccharide intercellular adhesin. FEMS Microbiol. Lett. 255, 11-16.

Kolodkin-Gal, I., Cao, S., Chai, L., Bottcher, T., Kolter, R., Clardy, J., Losick, R., 2012. A self-produced trigger for biofilm disassembly that targets exopolysaccharide. Cell 149, 684-692.

Konai, M. M., Ghosh, C., Yarlagadda, V., Samaddar, S., Haldar, J., 2014. Membrane active phenylalanine conjugated lipophilic norspermidine derivatives with selective antibacterial activity. J. Med. Chem. 57, 9409-9423.

Konai, M. M., Haldar, J., 2015. Lysine-based small molecules that disrupt biofilms and kill both actively growing planktonic and nondividing stationary phase bacteria. ACS Infect. Dis. 1, 469-478.

Kong, K. F., Vuong, C., Otto, M., 2006. *Staphylococcus* quorum sensing in biofilm formation and infection. Int. J. Med. Microbiol. 296, 133-139.

Kuppusamy, R., Yasir, M., Yee, E., Willcox, M., Black, D. S., Kumar, N., 2018. Guanidine functionalized anthranilamides as effective antibacterials with biofilm disruption activity. Org. Biomol. Chem. 16, 5871-5888.

Li, B., Maezato, Y., Kim, S. H., Kurihara, S., Liang, J., Michael, A. J., 2018. Polyamine-independent growth and biofilm formation, and functional spermidine/spermine N-acetyltransferases in *Staphylococcus aureus* and *Enterococcus faecalis*. in press Mol. Microbiol. [preprint]. doi:10.1111/mmi.14145.

Liu, Y., Naha, P. C., Hwang, G., Kim, D., Huang, Y., Simon-Soro, A., Jung, H.-I., Ren, Z., Li, Y., Gubara, S., Alawi, F., Zero, D., Hara, A. T., Cormode, D. P., Koo, H., 2018. Topical ferumoxytol nanoparticles disrupt biofilms and prevent tooth decay in vivo via intrinsic catalytic activity. Nat. Commun. 9, 2920.

Miles, A. A., Misra, S. S., Irwin, J. O., 1938. The estimation of the bactericidal power of the blood. J. hyg. (Lond). 38, 732-749.

Moon, S. H., Zhang, X., Zheng, G., Meeker, D. G., Smeltzer, M. S., Huang, E., 2017. Novel linear lipopeptide paenipeptins with potential for eradicating biofilms and sensitizing gram-negative bacteria to rifampicin and clarithromycin. J. Med. Chem. 60, 9630-9640.

Moore, S. 1981. Pancreatic DNase. In *The Enzymes* (eds. P.D. Boyer et al.), 3rd edn. 14, 281-296. Academic Press, New York.

Morihara, K., Tsuzuki, H., 1975. Specificity of proteinase K from *Tritirachium album* limber for synthetic peptides. Agric. Biol. Chem. 39, 1489-1492.

Ou, M. Z., Ling, J. Q., 2017. Norspermidine changes the basic structure of *S. mutans* biofilm. Mol. Med. Rep. 15, 210-220.

Phuong, N. T. M., Van Quang, N., Mai, T. T., Anh, N. V., Kuhakarn, C., Reutrakul, V., Bolhuis, A., 2017. Antibiofilm activity of α-mangostin extracted from *Garcinia mangostana L*. against *Staphylococcus aureus*. Asian Pac. J. Trop. Med. 10, 1154-1160.

Pöllänen, M. T., Paino, A., Ihalin, R., 2013. Environmental stimuli shape biofilm formation and the virulence of periodontal pathogens. Int. J. Mol. Sci. 14, 17221-17237.

Pozzi, C., Waters, E. M., Rudkin, J. K., Schaeffer, C. R., Lohan, A. J., Tong, P., Loftus, B. J., Pier, G. B., Fey, P. D., Massey, R. C., O'Gara, J. P., 2012. Methicillin resistance alters the biofilm phenotype and attenuates virulence in *Staphylococcus aureus* device-associated infections. PLoS Pathog. 8, e1002626.

Tomlin, K. L., Malott, R. J., Ramage, G., Storey, D. G., Sokol, P. A., Ceri, H., 2005. Quorum-sensing mutations affect attachment and stability of *Burkholderia cenocepacia* biofilms. Appl. Environ. Microbiol. 71, 5208-5218.

Xiu, A. H., Kong, Y., Zhou, M. Y., Zhu, B., Wang, S. M., Zhang, J. F. 2010. The chemical and digestive properties of a soluble glucan from Agrobacterium sp ZX09. Carbohydr. Polym. 82, 623-628

Wang, B., Pachaiyappan, B., Gruber, J. D., Schmidt, M. G., Zhang, Y. M., Woster, P. M., 2016. Antibacterial diamines targeting bacterial membranes. J. Med. Chem. 59, 3140-3151.

Wang, X., Preston, J. F., Romeo, T., 2004. The pgaabcd locus of *Escherichia coli* promotes the synthesis of a polysaccharide adhesin required for biofilm formation. J. Bacteriol. 186, 2724-2734.

Worthington, R. J., Richards, J. J., Melander, C., 2012. Small molecule control of bacterial biofilms. Org. Biomol. Chem. 10, 7457-7474.

Yang, H., Zhai, C., Yu, X., Li, Z., Tang, W., Liu, Y., Ma, X., Zhong, X., Li, G., Wu, D., Ma, L., 2016. High-level expression of proteinase K from *Tritirachium album limber* in *Pichia pastoris* using multi-copy expression strains. Protein. Expr. Purif. 122, 38-44.

General Conclusions

Biofilm formation represents a significant mechanism by which pathogens are able to evade the human body immune system and antimicrobial treatments. Here we demonstrate the synthesis of linear and novel cyclic polyamines containing different spatial distances between the amino groups and investigate their effects to prevent biofilm formation and to disperse existing biofilms. Different techniques have been used to evaluate the anti-biofilm activity of the synthesised compounds including: crystal violet assay, confocal microscopy with Live/Dead BacLight stains, and utilising the Miles-Misra method for viable cell counting.

A variety of solution methods have been used to synthesise the designed final products. Analogues were designed on the basis of the chemical structures of norspermidine, norspermine, spermidine, and spermine polyamines, which have been reported to have preventing biofilm formation and dispersing preformed biofilm activities on different bacterial strains.

The very high polarity of polyamines represents a defining feature in the synthesis, extraction, and purification of final products. However, large scale synthesis of polyamines facilitates the extraction of more pure final products. Different synthetic methods have been investigated in detail to reduce nitrile groups to primary amines, but they failed either due to incomplete reduction of the nitrile groups or it was hard to extract the final products from the reaction medium. It was determined experimentally that the complete reduction of aliphatic nitrile groups to primary amines can be performed via catalytic hydrogenation using Raney nickel catalyst under 1 atm pressure of hydrogen and in a basic medium, which resulted in a pure

product in high yield. However, the high polarity of polyamines still remains a challenge to extract the final product from the reaction mixture in an efficient manner.

The spectral data of synthesised compounds that have not been fully assigned or have been mis-assigned in literature were unambiguously assigned. The assignments were performed using MS and 1D and 2D NMR spectroscopic data supported by the theoretically calculated values of the ^{13}C chemical shifts of these compounds.

The activity of polyamines tested in this thesis to prevent biofilm formation with the exception of compound **49** is strain dependent. Their activity to prevent biofilm formation is performed by preventing bacterial attachment to surfaces, the first step of biofilm formation. That polyamines interfere with bacterial attachment to surfaces supports the hypothesis that polyamines act by affecting QS system which is involved in the attachment process.

All the tested polyamines have low activity to disperse preformed biofilms. This low activity occurred mostly because of the inhibition of further growth of biofilm more than dispersing existing biofilms. Two novel polyamines **33** and **35** show activity to prevent biofilm formation in NCTC 6571 and MSSA 15981 strains. The combination of these polyamines with vancomycin shows higher activity to kill bacteria inside preformed biofilms than vancomycin alone in the NCTC 6571 strain. Compound **49** shows antibacterial activity and prevents biofilm formation in all three *S. aureus* strains used in this thesis and shows high activity to kill bacterial cells within preformed NCTC 6571 biofilm in a combination with vancomycin.

In future chemical work, further modifications could be made to the two lead polyamines, the mono-hexahydropyrimidine **33** and the di-hexahydropyrimidine **35**. These could be converted into open-chain (linear) polyamines which would still carry a similar positive charge at physiological pH. Their biological activity could be further investigated to go beyond MRSA252 , NCTC 6571, and MSSA 15981 strains in order to investigate bacterial strain dependence. Linear polyamine **49**, which shows antibacterial activity and prevents biofilm formation in the above strains, could be converted to its di-guanidine adduct and extended on both termini with acrylonitrile (followed by reduction) to see if such modifications enhance its biological activity.

Based on the results of this thesis, polyamines could be useful in preparing surface coatings of medical devices to prevent the formation of biofilms. This will be of great interest in reducing the spreading of bacterial infections for regularly used medical devices. In addition, polyamines could be useful in the topical treatment of bacterial skin infections which protect themselves by the formation of biofilms. This potential use is especially important when combined with the application of antibiotics. The presence of polyamines in combination with antibiotics may decrease the required dose of antibiotics and thus decrease the risk of resistance that follows from the usage of high antibiotic doses.

A combination of polyamines with other antibacterial agents, e.g. silver ions, could potentially be used to prevent pipe blockage in water distribution system.

The evaluation of the impact following these proposed applications of the novel polyamines discovered in this work requires further research.

Appendix

Outputs from this research

The 12th International Conference and Workshop on Biological Barriers, Saarbrucken, Germany. 27-29/8/2018. Novel polyamines prevent biofilm formation in *Staphylococcus aureus* NCTC 6571 strain (poster presentation).

The 19th SCI/RSC Medicinal chemistry symposium, Cambridge, UK. 10-13/9/2017. Biofilm disruption by polyamines and their analogues (poster presentation).

The 8th APS International PharmSci conference, Hatfield, UK. 5-7/9/2017. Biofilm disruption by polyamines and their analogues (poster presentation).

The 25th GP2A medicinal chemistry conference, Liverpool, UK. 31/8-1/9/2017. Biofilm disruption by polyamines and their analogues (poster presentation).

The 24th Young Research Fellow Meeting in Medicinal Chemistry, Paris, France. 8-10/2/2017. Biofilm disruption by natural polyamines and their analogues (flash and poster presentation).

Plugging the Antibiotics Gap: A Medicinal Chemist's Perspective, Manchester, UK. 16/11/2016. Biofilm disruption by natural polyamines and their analogues (poster presentation).

The 7th Academy of Pharmaceutical Sciences (APS) International Pharmaceutical Science Conference, Glasgow, UK. 5-7/09/2016. Biofilm disruption by natural polyamines and their analogues (oral and poster presentation).

Plugging the Antibiotics Gap: A Medicinal Chemist's Perspective

Biofilm disruption by natural polyamines and their analogues

Rami Alnajadat, Albert Bolhuis, and Ian S. Blagbrough
University of Bath
Bath BA2 7AY, UK

The growth in antibiotic resistance in bacteria creates an ever more significant challenge to global health. One important driver of resistance is the formation of biofilms, in which cells may be 100-1000-fold more resistant to antibiotics as compared to free floating planktonic bacteria.[1] This research project is aimed at developing novel compounds that prevent or disrupt biofilm formation and thereby can restore or enhance the activity of co-administered antibiotics.

We are investigating the effects of natural polyamines and their analogues in preventing biofilm formation in *Staphylococcus aureus* strains which produce biofilms of significantly different composition. The designed polyamine analogues are based on the naturally occurring polyamines spermidine, spermine, norspermidine, and norspermine. Some of these and their synthetic analogues contain two three-carbon spacers between amino groups, e.g. norspermidine and norspermine.

Polyamines are thought to be active by targeting the exopolysaccharide component of the extracellular polymeric substance (EPS) in the biofilm matrix.[2] However, the composition of the EPS varies greatly between *S. aureus* strains, and we therefore investigated the effects of polyamines on three different *S. aureus* strains. Of those three strains, two strains has a polysaccharide-based biofilm, whereas the third had a protein-based biofilm. Surprisingly, norspermidine and norspermine, each containing two 3-carbon spacers, were active against only one strain of the two polysaccharide-based strains. This suggests that certain polyamines may disrupt biofilms by targeting specific polysaccharides of specific bacterial strains, or that polyamines have an entirely different target and their mechanism of action is not related to interaction with exopolysaccharides. Corroborating earlier reports, spermidine and spermine, which have asymmetrically spaced polyamines, were not active against any strain, indicating that the distance between the amine groups in polyamines is a key factor in the SAR of polyamines. As expected, no activity was of polyamines was found against a biofilm that contained mainly protein in the EPS. Further investigation is required to determine the true target of polyamines, and to investigate whether polyamines may have clinical use.

Acknowledgment

We thank Al Isra University, Amman, Jordan, for the financial support of this research by a scholarship to RA.

References

1. Hoiby N, Bjarnsholt T, Givskov M, Molin S, Ciofu O. Antibiotic resistance of bacterial biofilms. *International journal of antimicrobial agents*. **2010**, 35, 322-332.
2. Bottcher T, Kolodkin-Gal I, Kolter R, Losick R, Clardy J. Synthesis and activity of biomimetic biofilm disruptors. *Journal of the American Chemical Society*. **2013**, 135, 2927-2930.

Number to be inserted by organisers

Biofilm disruption by polyamines and their analogues

Rami M. Alnajadat, Albert Bolhuis, and Ian S. Blagbrough
Department of Pharmacy and Pharmacology, University of Bath
Bath BA2 7AY, UK

I do wish to be to be considered for a flash oral presentation [single slide].

Summary

The growth in antibiotic resistance in bacteria creates an ever more significant challenge to global health. One important driver of resistance is the formation of biofilms, in which cells may be 100-1000-fold more resistant to antibiotics as compared to free floating planktonic bacteria.[1] Polyamines are thought to be active by targeting the exopolysaccharide component of the extracellular polymeric substance (EPS) in the biofilm matrix.[2] We are investigating the effects of polyamines and their analogues on three different *S. aureus* strains. Of those three strains, two strains have a polysaccharide-based biofilm, whereas the third has a protein-based biofilm. Surprisingly, norspermidine and norspermine, each containing two 3-carbon spacers, were active against only one strain of the two polysaccharide-based strains (Fig. 1). Norspermine cyclic analogue NS1 show high activity to prevent biofilm formation in NCTC 6571, while other cyclic and acrylonitrilic analogues show low activity in preventing biofilm formation (Fig. 1). The amine properties of nitrogen, the distance between the amine groups and the symmetry in polyamines is a key factor in the SAR of polyamines disrupting biofilms. However, the mechanism of action of polyamines is still unclear.

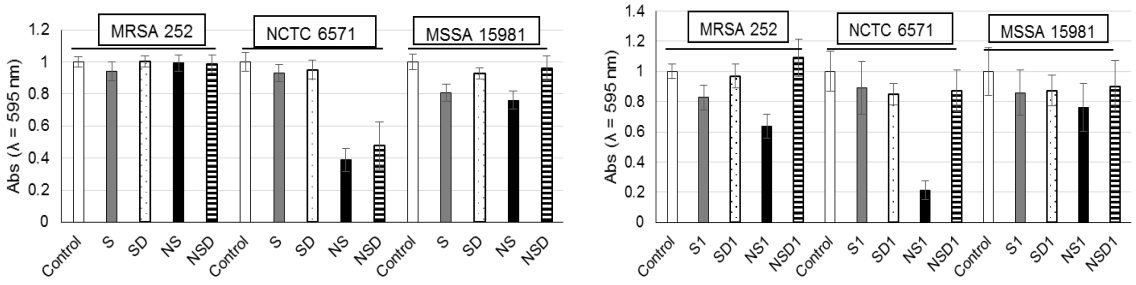

Figure 1. The effects of four polyamines (left): spermine (S), Spermidine (SD), norspermine (NS), and norspermidine (NSD), and their cyclic analogues (right): spermine (S1), spermidine (SD1), norspermine (NS1) and norspermidine (NSD1) on biofilm formation in MRSA 252, NCTC 6571 and MSSA 15981. Concentration = 0.3 mM.

Acknowledgement: We thank Al Isra University, Amman, Jordan, for the financial support of this research by a scholarship to RA.

References

1. Hoiby, N. ; Bjarnsholt T. ; Givskov M. ; Molin S. ; Ciofu O. Int. J. Antimicrob. Agents **2010**, 35, 322-332.
2. Bottcher, T. ; Kolodkin-Gal I. ; Kolter R. ; Losick R. ; Clardy J. J. Am. Chem. Soc. **2013**, 135, 2927-2930.

12th International Conference and Workshop on BIOLOGICAL BARRIERS

Novel polyamines prevent biofilm formation in *Staphylococcus aureus* NCTC 6571 strain

*Alnajadat R. M.; Bolhuis A.; and Blagbrough I. S.**
Department of Pharmacy and Pharmacology, University of Bath, Bath BA2 7AY, UK

Keywords: bacterial resistance, biofilm, *Staphylococcus aureus*, polyamine

Aims: We are investigating the effects of natural polyamines and their analogues in preventing biofilm formation in *Staphylococcus aureus* strains which produce biofilms of significantly different composition.

Introduction: The growth in antibiotic resistance in bacteria creates an ever more significant challenge to global health. One important driver of resistance is the formation of biofilms biological barriers, whereby cells may become 100-1000-fold more resistant to antibiotics as compared to free-floating planktonic bacteria.

Methods: The polyamine analogues were designed by the addition of further amine functional groups, each with a 3-carbon spacer attached, on to naturally occurring polyamines. They were synthesized, purified, characterized, and tested against biofilm formation and preformed biofilms using a crystal violet assay on three *S. aureus* strains, MRSA 252, NCTC 6571, and MSSA 15981. Polyamines were also tested for activity in dispersing existing biofilms in combination with vancomycin using confocal microscopy and Live/Dead staining.

Results: The designed polyamine analogues are based on the naturally occurring polyamines spermidine, spermine, norspermidine, and norspermine. The latter two compounds, each containing two 3-carbon spacers, were active in preventing biofilm formation in the NCTC 6571 strain. These polyamines were not active against the other strains. Twenty polyamine analogues were synthesised of which four novel compounds showed activity in preventing biofilm formation in the NCTC 6571 strain. The most active compound reduced the biofilm mass by more than 65% at a concentration of 0.5 mM. In dispersing exicting biofilms, the most active compound reduced biofilm mass by more than 25 % at a concentration of 0.3 mM. However, there was no synergy with vancomycin (Figure 1).

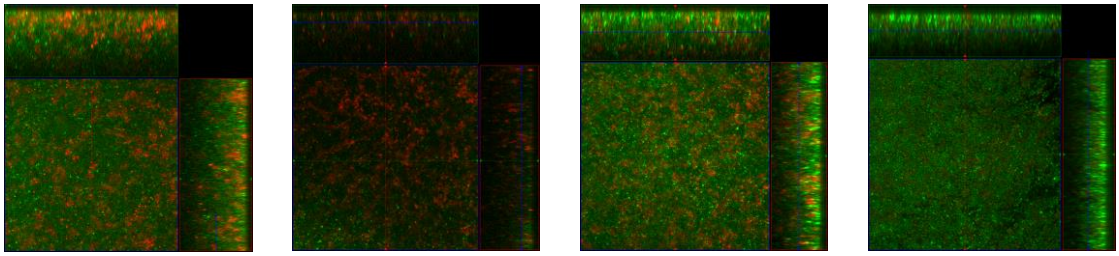

Control	Vancomycin	NSD1	NSD1 + Vancomycin
Thickness = 36 µM	Thickness = 26 µM	Thickness = 25 µM	Thickness = 23 µM

Fig. 1. Confocal microscopy images showing NSD1 disperses preformed biofilms in combination with vancomycin.

Conclusions: The distance between the amine groups and the symmetry in polyamines is a key factor in the structure-activity relationship (SAR) of polyamines disrupting biofilms. This activity against these clinically important biological barriers was also shown to be strain dependent. The mechanism of action of polyamines is still unclear but they act on carbohydrate-rich biofilms much more effeciently than on DNA- or proteine-rich biofilms .

Acknowledgments: We thank Al Isra University for financial support.

Biofilm disruption by natural polyamines and their analogues

Rami Alnajadat, Albert Bolhuis, Ian Blagbrough.

University of Bath, Bath, BA2 7AY.

The growth in antibiotic resistance in bacteria creates an ever more significant challenge to global health. One important driver of resistance is the formation of biofilms, in which cells may be 100-1000-fold more resistant to antibiotics as compared to free floating planktonic bacteria.[a] We are investigating the effects of natural polyamines and their analogues in preventing biofilm formation in *Staphylococcus aureus* strains which produce biofilms of significantly different composition. The designed polyamine analogues are based on the naturally occurring polyamines spermidine, spermine, norspermidine, and norspermine. Some of these and their synthetic analogues contain two three-methylene spacers between amino groups, e.g. norspermidine and norspermine.

Polyamines are thought to be active by targeting the exopolysaccharide component of the extracellular polymeric substance (EPS) in the biofilm matrix.[b] However, the composition of the EPS varies greatly between *S. aureus* strains, and we therefore investigated the effects of polyamines on three different *S. aureus* strains. Of those three strains, two strains have a polysaccharide-based biofilm, whereas the third has a protein-based biofilm. Surprisingly, norspermidine and norspermine, each containing two 3-carbon spacers, were active against only one strain of the two polysaccharide-based strains. This suggests that certain polyamines may disrupt biofilms by targeting specific polysaccharides of specific bacterial strains, or that polyamines have an entirely different target and their mechanism of action is not related to interaction with exopolysaccharides. Corroborating earlier reports, spermidine and spermine, which have asymmetrically spaced polyamines, were not active against any strain, indicating that the distance between the amine groups in polyamines is a key factor in the SAR of polyamines. As expected, no activity of polyamines was found against a biofilm that contained mainly protein in the EPS. Therefore, polyamines may interact with certain polysaccharides.

Cyclic analogues of the four primary polyamines were tested and show almost no activity in preventing biofilm formation. Cyclization decreases the activity of the active polyamines in preventing biofilm formation. Further investigation is required to determine the true target of polyamines, and to investigate whether polyamines may have clinical use.

We thank Al Isra University, Amman, Jordan, for the financial support of this research by a scholarship to RA.

Bibliographic references:

(a) Hoiby N, Bjarnsholt T, Givskov M, Molin S, Ciofu O. Antibiotic resistance of bacterial biofilms. *Int. J. Antimicrob. Agents*. 2010, 35, 322-332.
(b) Bottcher T, Kolodkin-Gal I, Kolter R, Losick R, Clardy J. Synthesis and activity of biomimetic biofilm disruptors. *J. Am. Chem. Soc*. 2013, 135, 2927-2930.

* Correspondence: I.S.Blagbrough@bath.ac.uk

Biofilm disruption by polyamines and their analogues

Rami M. Alnajadat, Albert Bolhuis, and Ian S. Blagbrough

Department of Pharmacy and Pharmacology, University of Bath, Bath BA2 7AY, UK
E-mail: prsisb@bath.ac.uk

The growth in antibiotic resistance in bacteria creates an ever more significant challenge to global health. One important driver of resistance is the formation of biofilms, in which cells may be 100-1000-fold more resistant to antibiotics as compared to free floating planktonic bacteria.[1] Polyamines are thought to be active by targeting the exopolysaccharide component of the extracellular polymeric substance (EPS) in the biofilm matrix.[2] We are investigating the effects of polyamines and their analogues on three different *S. aureus* strains. Of those three strains, two strains have a polysaccharide-based biofilm, whereas the third has a protein-based biofilm. Surprisingly, norspermidine and norspermine, each containing two 3-carbon spacers, were active against only one strain of the two polysaccharide-based strains (Fig. 1). Norspermine cyclic analogue NS1 show high activity to prevent biofilm formation in NCTC 6571, while other cyclic and acrylonitrilic analogues show low activity in preventing biofilm formation (Fig. 1). The amine properties of nitrogen, the distance between the amine groups and the symmetry in polyamines is a key factor in the SAR of polyamines disrupting biofilms. However, the mechanism of action of polyamines is still unclear.

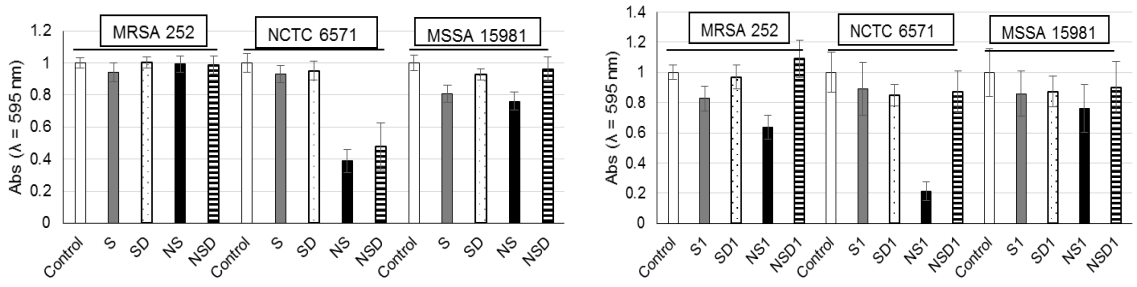

Figure 1. The effects of four polyamines (left): spermine (S), Spermidine (SD), norspermine (NS), and norspermidine (NSD), and their cyclic analogues (right): spermine (S1), spermidine (SD1), norspermine (NS1) and norspermidine (NSD1) on biofilm formation in MRSA 252, NCTC 6571 and MSSA 15981. Concentration = 0.3 mM.

Acknowledgement: We thank Al Isra University, Amman, Jordan, for the financial support of this research by a scholarship to RA.

References

1. Hoiby, N. ; Bjarnsholt T. ; Givskov M. ; Molin S. ; Ciofu O. Int. J. Antimicrob. Agents **2010**, 35, 322-332.
2. Bottcher, T. ; Kolodkin-Gal I. ; Kolter R. ; Losick R. ; Clardy J. J. Am. Chem. Soc. **2013**, 135, 2927-2930.

Biofilm disruption by polyamines and their analogues

Rami Alnajadat, Albert Bolhuis, Ian Blagbrough*
Department of Pharmacy and Pharmacology, University of Bath, Bath BA2 7AY, UK

ARTICLE INFO

*Corresponding author.
Tel.: +44 1225 386795
Fax: +44 1225 386114
E-mail:
i.s.blagbrough@bath.ac.uk

KEYWORDS: Antimicrobial resistance, biofilm, polyamines, exopolysaccharides

SUMMARY

We are investigating the effects of natural polyamines and their analogues in preventing biofilm formation in three *Staphylococcus aureus* strains which express biofilms of significantly different composition. The designed polyamine analogues contain two three-carbon spacers between amino groups and this is apparently a requirement for biological activity. This activity differs depending upon the bacterial target and is not obviously related to polysaccharide biofilm composition.

INTRODUCTION

The growth in antibiotic resistance in bacteria creates an ever more significant challenge to global health. One important driver of resistance is the formation of biofilms (Fig. 1), in which cells may be 100-1000-fold more resistant to antibiotics as compared to free floating planktonic bacteria Hoiby (2010).

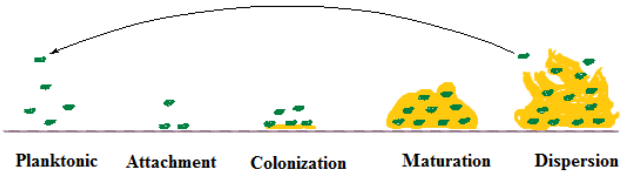

Fig. 1. *Biofilm formation stages: 1. Attachment of free planktonic cells to a surface. 2. Bacterial cells start to anchor to each other under the effect of quorum sensing, forming small colonies. These colonies start to secrete extracellular polymeric substances which form the biofilm. 3. The biofilm matures by cell growth and division. 4. Triggered by e.g. nutrient depletion, cells in the biofilm disperse allowing the formation of new colonies elsewhere.*

We are investigating the effects of natural polyamines and their analogues in preventing biofilm formation in *Staphylococcus aureus* strains which produce biofilms of significantly different composition. The designed polyamine analogues are based on the naturally occurring polyamines spermidine, spermine, norspermidine, and norspermine. Some of these and their synthetic analogues contain two three-methylene spacers between amino groups, e.g. norspermidine and norspermine.

MATERIALS AND METHODS

1) Analogue synthesis (Fig. 2): Each polyamine (1 g each of spermidine, spermine, norspermidine, or norspermine) was dissolved in distilled water (30 mL). The aqueous solution was then cooled to 5 °C and paraformaldehyde (1 or 2 eq.) was added. The mixture was stirred for 1 h at 20 °C and then thoroughly extracted with chloroform.

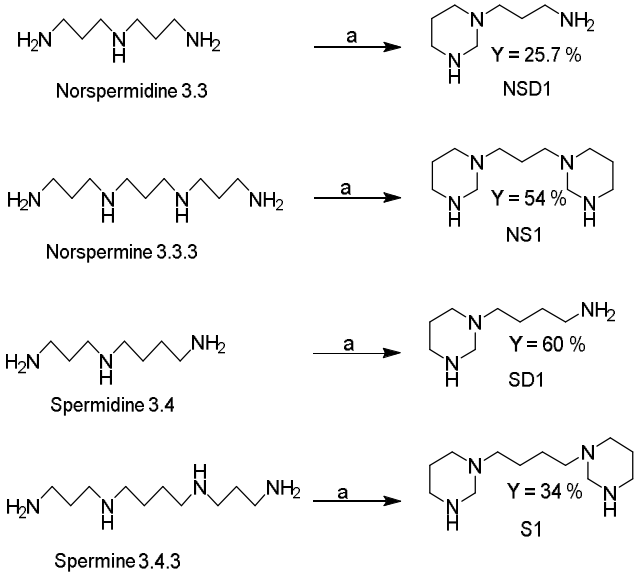

Fig. 2. *Synthetic schemes based on the four primary polyamines. Reagents and conditions: (a) (i) H_2O, 5°C, (ii) paraformaldehyde, 1 h.*

2) Biofilm assay: Bacteria (200 µL) were grown in 96-well plates at 37 °C in TSB medium containing 0.5 % glucose and different concentrations of polyamines. After 24 h growth, the plates were washed (3 x with 200 µL 0.9 % aq. NaCl per well) to

remove planktonic bacteria, and then dried at 60 °C (1 h). Wells were then stained with 0.1% aq. crystal violet solution (200 µL) and after 15 min the plates were washed by immersing in warm water (3 x). Acetic acid (30%, 200 µL) was then added to each well and the visible absorbance was measured using a UV-visible plate reader at λ = 595 nm.

RESULTS AND DISCUSSION

Polyamines are thought to be active by targeting the exopolysaccharide component of the extracellular polymeric substance (EPS) in the biofilm matrix Bottcher (2013). However, the composition of the EPS varies greatly between *S. aureus* strains, and we therefore investigated the effects of polyamines and their analogues (Fig. 2) on three different *S. aureus* strains. Of those three strains, two strains have a polysaccharide-based biofilm, whereas the third has a protein-based biofilm. Surprisingly, norspermidine (NSD) and norspermine (NS), each containing two 3-carbon spacers, were active against only one strain of the two polysaccharide-based strains (Fig. 3).

The, norspermine cyclic analogue NS1 (with two hexahydropyrimidine rings) shows potent activity to prevent biofilm formation in NCTC 6571 cells, while other analogues show only low activity in preventing biofilm formation (Fig. 4).

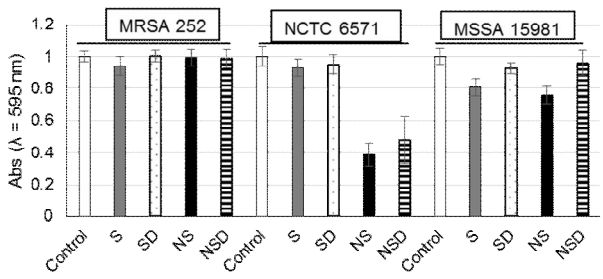

Fig. 3. *The effects of polyamines: spermine (S), spermidine (SD), norspermine (NS), and norspermidine (NSD) on biofilm formation in MRSA 252, NCTC 6571 and MSSA 15981 cells. Concentration = 0.3 mM.*

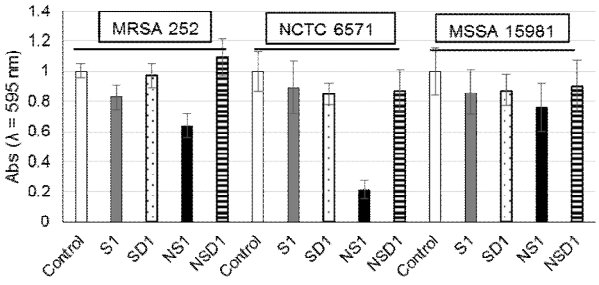

Fig. 4. *The effects of polyamine analogues: spermine (S1), spermidine (SD1), norspermine (NS1), and norspermidine (NSD1) on biofilm formation in MRSA 252, NCTC 6571 and MSSA 15981 cells. Concentration = 0.3 mM.*

CONCLUSIONS

The distance between the amine groups and the symmetry in polyamines is a key factor in the SAR of polyamines disrupting biofilms. However, the mechanism of action of polyamines is still unclear.

ACKNOWLEDGEMENTS

We thank Al Isra University, Amman, Jordan, for the financial support of this research (scholarship to RA).

REFERENCES

Bottcher, T., Kolodkin-Gal, I., Kolter, R., Losick, R., Clardy, J., 2013. Synthesis and activity of biomimetic biofilm disruptors. J. Am. Chem. Soc., 135, 2927-2930.

Hoiby, N., Bjarnsholt, T., Givskov, M., Molin, S., Ciofu, O., 2010. Antibiotic resistance of bacterial biofilms. Int. J. Antimicrob. Agents, 35, 322-332.

Biofilm disruption by natural polyamines and their analogues

Rami Alnajadat, Albert Bolhuis, and Ian S. Blagbrough
Department of Pharmacy and Pharmacology, University of Bath, Bath BA2 7AY, U.K.

Abstract – **We are investigating the effects of natural polyamines and their analogues in preventing biofilm formation in three *Staphylococcus aureus* strains which express biofilms of significantly different composition. The designed polyamine analogues contain two three-carbon spacers between amino groups and this is apparently a requirement for biological activity. The biological activity differs depending upon the bacterial target and is not obviously related to polysaccharide biofilm composition.**

INTRODUCTION

The growth in bacterial resistance due to biofilms creates an ever more significant challenge to global health. Bacterial biofilms are up to 100-1000-fold more resistant to antibiotics in comparison to free floating planktonic bacteria [1]. Norspermidine can display biofilm disrupting activity [2]. This activity is thought to be by interacting with polysaccharides [2]. This research project is aimed at developing novel polyamines that prevent biofilm formation and ultimately we hope to restore or enhance the activity of co-administered conventional antibiotics.

MATERIALS AND METHODS

Analogue synthesis:

Each polyamine (1 g each of spermidine, spermine, norspermidine, and norspermine) was dissolved in a sufficient amount of water. The aqueous solution was then cooled to 5 °C and paraformaldehyde (1 eq.) was added. The mixture was stirred for 1 h at 20 °C and then thoroughly extracted with chloroform. The resulting formaldehyde adducts were dissolved in anhydrous methanol followed by the dropwise addition of acrylonitrile with stirring under N_2. After 15 h, more acrylonitrile was added and stirring was continued for a further 9 h. The acrylonitrile adducts were dissolved in ethanol. Pd/C catalyst (10% w/w of reactant) was added and the mixture was reduced under H_2 (16 h) to afford the desired target primary amines.

Biofilm assay:

Bacteria (200 µL) were grown in 96-well plates at 37 °C in TSB medium containing 0.5 % glucose and different concentrations of polyamines. After 24 h growth, the plates were washed (3x with 0.9 % aq. NaCl) to remove planktonic bacteria and then dried at 60 °C for 1 h. Wells were then stained with 0.1% crystal violet solution and after 15 min the plates were washed with warm water. Acetic acid (30%, 200 µL) was added and the visible absorbance was measured using a UV-visible plate reader at λ = 595 nm.

To determine the composition of bacterial biofilms, bacteria were grown in 96-well plates at 37 °C in TSB medium with 0.5 % glucose. After 24 h growth, the plates were washed 3x with 0.9 % NaCl to remove planktonic bacteria. Sodium periodate, proteinase K, and DNase were added to wells and incubated for 4 h. The biofilm mass was then measured using the above crystal violet assay.

RESULTS AND DISCUSSION

Three bacterial strains were used: MRSA 252, NCTC 6571, and MSSA 15981. Sodium periodate, proteinase K, and DNase, which disrupt biofilms containing polysaccharide, protein, or DNA, respectively, were used to determine the composition of bacterial biofilms. MRSA 252 biofilms were only affected by proteinase K, indicating that these are protein-based biofilms. In contrast, NCTC 6571 and MSSA 15981 showed polysaccharide-based biofilms as they were affected by sodium periodate, but neither by proteinase K nor by DNase. All the polyamines tested were inactive against the MRSA 252 biofilm. Spermine was inactive against NCTC 6571 and MSSA 15981. Norspermidine and norspermine, each containing two 3-carbon spacers, were active against NCTC 6571, but not against MSSA 15981. Both the NCTC 6571 and MSSA 15981 are polysaccharide-based biofilms, but only NCTC 6571 was affected by norspermidine and norspermine. Therefore, from these results, there is either the possibility that certain polyamines disrupt biofilms by targeting specific polysaccharides of specific bacterial strains, or that polyamines have a different target and their mechanism of action is not related to exopolysaccharides in the first place.

CONCLUSIONS

The distance between the amine groups in polyamines is a key factor in the SAR of polyamines. Polyamines may disrupt biofilms by interacting with certain polysaccharides.

ACKNOWLEDGEMENTS

We thank Al Isra University, Amman, Jordan, for the financial support of this research by a scholarship to RA.

REFERENCES

[1] H. Anwar and J.W. Costerton, Enhanced activity of combination of tobramycin and piperacillin for eradication of sessile biofilm cells of *Pseudomonas aeruginosa Antimicrob Agents Chemother*., **34** (1990) 1666-1671.

[2] T. Böttcher, I. Kolodkin-Gal, R. Kolter, R. Losick and J. Clardy, Synthesis and activity of biomimetic biofilm disruptors, *J. Am. Chem. Soc*., **135** (2013) 2927-2930.